The position of ureteric budding and its relationship to vesico-ureteric reflux and kidney defects in mice

By

Inga Jadwiga Murawski

Department of Human Genetics
McGill University, Montreal, Canada
May 2009

A thesis submitted to McGill University in partial fulfillment of
the requirements of the degree of Doctor of Philosophy

To my parents, with love

TABLE OF CONTENTS

ABSTRACT

Vesico-ureteric reflux (VUR) is a congenital urinary tract defect that results in the retrograde flow of urine from the bladder to the kidneys. It is caused by a defect in the formation of the uretero-vesical junction such that the ureter does not insert properly into the bladder. VUR affects up to 1% of the population and patients are at increased risk of developing recurrent urinary tract infections, hypertension, and end-stage renal disease. Patients with VUR frequently have malformed kidneys and short intravesical ureters, one component of the uretero-vesical junction. The co-occurrence of these defects suggests that they arise from a common developmental mechanism, notably, abnormal formation of the ureteric bud. The ureteric bud is an outgrowth of the mesonephric duct and develops into both the kidney and the urinary tract. We hypothesize that proper ureteric bud development is critical for the formation of a normal kidney and an intact uretero-vesical junction. We further hypothesize that VUR is associated with mutations in genes that direct early formation of the ureteric bud. Our objective is to identify mouse models of VUR to determine if an abnormal ureteric bud precedes the development of small or malformed kidneys and a refluxing urinary tract.

We identified VUR in two mouse lines at birth: the *Pax2*$^{1Neu+/-}$ mouse and the inbred C3H/HeJ mouse. At postnatal day 1, *Pax2*$^{1Neu+/-}$ and C3H/HeJ mice had a 32% and 100% incidence of VUR, respectively. Control mice (CD1 and C57BL/6J) had a 6.25% and 0% incidence of VUR, respectively. We measured kidney size in all mice tested for VUR and *Pax2*$^{1Neu+/-}$ mice had small malformed kidneys while C3H/HeJ mice had small but no malformed kidneys at birth when compared to controls. To identify a specific urinary tract abnormality, we measured the length of the intravesical ureter. Both refluxing mouse models had significantly shorter intravesical ureters compared to controls, providing evidence for a defective uretero-vesical junction. Lastly, to understand the embryonic origin of VUR, we characterized the position of the ureteric bud along the mesonephric duct. At embryonic day 10.5, both *Pax2*$^{1Neu+/-}$ and C3H/HeJ embryos had ureteric buds that exited from a more caudal position along the mesonephric duct compared to controls. Furthermore, detailed analysis of the kidney and urinary tracts throughout development revealed that both *Pax2*$^{1Neu+/-}$ and C3H/HeJ embryos had urinary tracts that were severely delayed in their development such that the ureters achieved an

independent insertion into the bladder later than in controls. Our data suggest that a caudal origin of the ureteric bud is associated with a delay in urinary tract development, a short intravesical ureter, and the development of VUR.

Since VUR is associated with a malformed kidney in *Pax2*$^{1Neu+/-}$ mice, but a normal kidney in C3H/HeJ mice, we characterized the kidney phenotype in C3H/HeJ mice by assessing for VUR and kidney size at adulthood. Surprisingly, C3H/HeJ mice continued to reflux, but now had larger kidneys than C57BL/6J mice. We hypothesized that this change in kidney size was caused by a reduction in nephron number at birth and subsequent renal hypertrophy by adulthood. Nephrons are the functional units of the kidney and reduced nephron number leads to reduced renal function and can predispose to hypertension, renal disease, and compensatory renal hypertrophy. We therefore counted the number of nephrons in newborn and adult C3H/HeJ and C57BL/6J kidneys. Our results demonstrated that C3H/HeJ mice had the same number of nephrons as C57BL/6J at birth and at adulthood. Furthermore, nephron number did not correlate with kidney size or body weight at birth or during adulthood in either mouse strain. These results suggest that in these inbred mice, nephron number appears to be independent of kidney size. Our results also demonstrate that C3H/HeJ mice are actually a model of VUR and normal kidneys.

From human studies, VUR can be a genetic disorder. To identify the gene(s) that cause(s) VUR in the C3H/HeJ mouse, we performed genetic studies on backcross and intercross progeny derived from a cross between C3H/HeJ and C57BL/6J mice. We identified a 24Mb genomic region on chromosome 12, VUR1, which is linked to the VUR phenotype (LOD=7.8, p=0.001). We hypothesize that the candidate gene(s) within VUR1 will be expressed either by the ureteric bud or by the surrounding mesenchyme and will be critical for establishing proper kidney and urinary tract development. We believe that the candidate gene(s) responsible for VUR in the C3H/HeJ mouse will be important to consider in human studies of VUR.

RESUME

Le reflux vésico-rénal est un défaut de l'appareil urinaire. Chez les patients atteints de cette pathologie, l'urine remonte anormalement depuis la vessie vers les reins. Le reflux est causé par un défaut dans la formation de la jonction entre la vessie et l'uretère, ce dernier ne s'insérant pas correctement dans la vessie. Le reflux vésico-rénal est une anomalie génétique humaine très fréquente, affectant près de 1% de la population. Les patients sont susceptibles de développer des infections urinaires, de l'hypertension, et de la néphropathie. Ils sont aussi sujets à des malformations rénales et peuvent présenter des anomalies au niveau de la jonction entre la vessie et l'uretère (uretères intravésicaux courts). Étant donné que ces malformations se manifestent ensemble, il a été suggéré qu'elles résultent toutes d'un mécanisme commun qui a lieu au cours du développement embryonnaire. Les reins et l'appareil urinaire se développent tous les deux à partir du bourgeon urétéral. Dans notre hypothèse de travail, nous présumons que le développement normal du bourgeon urétéral est très important pour la formation adéquate aussi bien du rein que de la jonction entre la vessie et l'uretère. De plus, nous présageons que des mutations touchant des gènes impliqués dans la formation du bourgeon urétéral seraient à l'origine du reflux vésico-rénal. Afin de déterminer une éventuelle relation entre la présence d'un bourgeon urétéral anormal et le développement de reins malformés et/ou de reflux vésico-rénal, nous avons essayé, dans un premier temps, de trouver un modèle animal développant un reflux vésico-rénal.

Deux lignées de souris atteintes de reflux vésico-rénal ont été identifiées: la souris *Pax2*$^{1Neu+/-}$ et la souris consanguine C3H/HeJ. Le reflux vésico-rénal a été mis en évidence par l'injection de bleu de méthylène dans les vessies des souris et l'observation du retour du colorant de la vessie vers les reins. À la naissance, les souris *Pax2*$^{1Neu+/-}$ et C3H/HeJ avaient une incidence de reflux vésico-rénal, respectivement, de 32% et 100%. Les souris qui servaient de contrôle (CD1 et C57BL/6J) avaient, respectivement, une incidence de 6.25% et 0%. Lorsque nous avons mesuré la taille des reins pour toutes les souris, nous nous sommes aperçus que les souris *Pax2*$^{1Neu+/-}$ et C3H/HeJ avaient des reins plus petits comparativement aux contrôles. Elles avaient aussi des uretères intravésicaux plus courts que ceux des contrôles, ce qui confirme la présence d'un défaut dans la formation de la jonction entre la vessie et l'uretère. Nous avons également caractérisé la

position du bourgeon urétéral par une hybridation *in situ*. Au stade embryonnaire 10.5, les bourgeons urétéraux des souris *Pax2*$^{1Neu+/-}$ et C3H/HeJ se formaient à une position plus postérieure que celle des contrôles. Nos données suggèrent que le déplacement du bourgeon urétéral, à une position plus postérieure, est associé au reflux vésico-rénal et que la formation normale du bourgeon urétéral est nécessaire pour que la jonction entre la vessie et l'uretère soit bien établie.

Nous avons supposé que la taille réduite des reins chez les nouveau-nés des souris C3H/HeJ serait associée à une diminution dans le nombre de néphrons et que le nombre de néphrons serait relié à la taille des reins. Les néphrons sont les unités fonctionnelles des reins et une réduction dans le nombre de néphrons est associée à de l'hypertension. Lorsque nous avons caractérisés les souris C3H/HeJ adultes (taille des reins et nombre de néphrons), elles avaient des reins plus grands mais un nombre équivalent de néphrons comparativement aux souris C57BL/6J. Ainsi, la taille réduite des reins chez les nouveau-nés n'a pas d'influence sur la quantité de néphrons à la naissance ou à l'âge adulte. De plus, le nombre de néphrons n'a pas de corrélation avec la taille des reins ni avec le poids du corps à la naissance ni à l'âge adulte. Nos résultats suggèrent que chez les souris consanguines, normales, le nombre de néphrons est indépendant de la taille des reins et que la souris C3H/HeJ est un modèle du reflux vésico-rénal avec des reins normaux.

Le reflux vésico-rénal affecte souvent plusieurs membres d'une même famille et plusieurs gènes et loci ont déjà été identifiés. Pour identifier les gènes qui causent le reflux vésico-rénal chez la souris C3H/HeJ, nous avons réalisé des études génétiques sur des souris issues d'inter-croisements et de croisements en retour entre les lignées C3H/HeJ et C57BL/6J. Nous avons identifié une région génomique de 24Mb sur le chromosome 12, nommée VUR1, qui est associée avec le phénotype du reflux vésico-rénal (LOD=7.8, p=0.001). Nous émettons l'hypothèse que des gènes de la région de VUR1 exprimés par le bourgeon urétéral ou par le mésenchyme seraient de bons candidats dans l'étude du développement des reins et de l'appareil urinaire. Nous croyons que les gènes candidats dans VUR1 seraient aussi importants pour les études chez les humains.

ACKNOWLEDGEMENTS

I am indebted and grateful to my supervisor, Dr. Indra Gupta, who has inspired me and encouraged me throughout my graduate studies. She has played an enormous role in my growth as a scientist and as a teacher. She always made the extra effort to explain things to me and gave me lots of great advice, whether it was for experimental design or for public speaking. Throughout my thesis writing, her encouragement and support made this thesis what it is. It is because of her personality and great sense of humor that my graduate experience has been this memorable.

I was fortunate enough to work in a creative and collaborative environment. I thank my supervisory committee, Dr. Roman Jednak, Dr. Danielle Malo, and Dr. Paul Goodyer, who provided countless insights into my project. I would also like to thank the MCH Research Institute, FRSQ, and CIHR for my fellowships and travel grants that have supported me during my many years of research. And a special thanks to my mice, I am indebted to each and every one of you.

To all those that I have worked with over the last few years, I will forever cherish the moments we shared. Thanks to the past members of the Gupta lab, including Oriana Yu who took me under her wing when I first started, Tristan Alie, my fellow bench mate who made life in the lab extremely interesting, and of course Dave Myburgh who helped me earn some respect and understanding of computers. Thanks to the present members of the Gupta Lab, Nicholas Haddad who wants me to describe him as "cool and funny", Rita Maina, an entertaining friend who made nephron counting and genotyping more exciting. My graduate experience isn't complete without mention of all the members of the Goodyer and Ryan labs who were always there to lend reagents, equipment, and insight into problem solving and life in general.

My journey as a graduate student wouldn't have been complete without my husband William Nahorniak who is by far the best friend I have ever had. He has encouraged me since the beginning, helped me practice for oral presentations, and was always able to put a positive spin on things. I promised him that once I graduated, I would get a real job. Lastly, and most importantly, I wish to thank my parents, Adam Murawski and Grażyna Herlig Murawski who have supported me my entire life with constant encouragement and love. I dedicate this thesis to them.

PREFACE

This thesis is written in accordance with the guidelines of the Faculty of Graduate Studies at McGill University. This thesis is comprised of five chapters and four appendices. Chapter I is a detailed introduction to the field of kidney development, vesico-ureteric reflux, nephron number, and gene mapping. Chapter I also includes a description of the rationale for the research. Many of the figures and background information were drawn from three reviews that were published by Ms. Inga Murawski and Dr. Indra Gupta (see appendix D). Chapters II, III, and IV are data chapters. Chapter II has been published in the *American Journal of Physiology: Renal Physiology* and is reproduced in this thesis with permission. Chapters III and IV are in the form in which they will be submitted for publication. Connecting texts between Chapters I and II, II and III, and III and IV provide a linking text between the different manuscripts and were written in accordance with the Guidelines for Submitting a Doctoral Thesis in the manuscript-based format. Chapter V is a detailed discussion of all the results presented in this thesis and includes future studies.

Human and mouse gene and protein nomenclatures were assigned following the guidelines provided by the HUGO Gene Nomenclature Committee (www.genenames.org) and Mouse Genome Informatics (www.informatics.jax.org).

CONTRIBUTION OF AUTHORS

The research reported in this thesis was carried out by Ms. Inga Murawski under the supervision of Dr. Indra Gupta. All of the figures presented in the thesis were generated from her results or were designed with the help of Mr. David Myburgh. Members of Ms. Inga Murawski's supervisory committee, Dr. Paul Goodyer, Dr. Roman Jednak, and Dr. Danielle Malo, provided guidance and discussion for all of the experiments. The following authors have contributed to the experimental work presented in this thesis:

Ms. Inga Murawski performed the animal breeding and actively participated in the design of the experiments. Ms. Inga Murawski was responsible for carrying out all experiments, along with the analysis of the data. Ms. Inga Murawski wrote the first draft of each of the manuscripts and actively participated in the revision process. For Chapter I, Mr. David Myburgh assisted with the VUR experiments and the design of the figures. Dr. Jack Favor identified the *Pax2*$^{1Neu+/-}$ mouse model in Germany and provided the lab with this mouse. For Chapter II, Ms. Rita Maina collected serial sections from countless mouse kidneys and assisted with H&E staining and data collection. For Chapter III, Ms. Rita Maina assisted with the VUR and intravesical ureter experiments as well as with genotyping. Dr. Indra Gupta's perseverance in the belief that we can study the development and the genetics of VUR using the mouse was the inspiration behind this research. She provided supervision and insight. Dr. Indra Gupta helped design the experiment for all three Chapters and helped edit the many versions of each of the manuscripts.

ABBREVIATIONS

ACE: angiotensin I converting enzyme
AGTR1/2: angiotensin II receptor
APOB: apolipoprotein B
ASKL2: additional sec-combs like
ATAD2B: ATPase family
B6: C57BL/6J inbred mouse strain
BXH: B6/C3H recombinant inbred mice
BMP4: bone morphogenetic protein
BOR: Branchio-oto-renal syndrome
C3H: C3H/HeJ inbred mouse strain
CAKUT: congenital anomalies of the kidney and urinary tract
CPH: congenital progressive hydronephrosis
CRE: Cre recombinase
DLGH1: discs large homolog
DMSA: dimercaptosuccinic acid
E: embryonic day
EFNB2: ephrin
EMX2: empty spiracles homeobox
EYA1: eyes absent homolog
F1: first generation hybrid
F2: intercross
FGF8: fibroblast growth factor
FGFR1/2: fibroblast growth factor receptor
FMTC: familial medullary thyroid carcinoma
FOXC1/C2: forkhead transcription factor
GATA3: GATA binding protein
GDNF: glial cell derived neurotrophic factor
GFP: green fluorescent protein
GFRα1: GDNF family receptor alpha
HDR: Hypoparathyroidism, sensorineural deafness, and renal dysplasia
HLA: human leukocyte antigen
HOXB7/11: homeobox
ING1: inhibitor of growth family member
KAL1: anosmin
KRD: kidney and retinal defects
LIM1: lim homeobox protein
MB: megabase
MEN2A/B: multiple endocrine neoplasia
MWF: Munich Wistar Frömter rat
N2: backcross
NAIP: neuronal apoptosis inhibitory protein
NN: nephron number
NTC5C1B: 5'-nucleotidase, cytosolic
OS: Oligosyndactylism mutation
OSR1: odd-skipped related
P: postnatal day
PAX2/3/5/6/8/9: paired-box gene
PCR: polymerase chain reaction
POMC1: pro-opiomelanocortin-alpha
PTC1: patched
PTPRF/S: protein tyrosine phosphatase receptor
QTL: quantitative trait locus
RALDH2: retinaldehyde dehydrogenase
RARα/β/γ: retinoic acid receptor
RCS: Renal-coloboma syndrome
RDH5/14/16: retinol dehydrogenase
RET: rearranged during transfection
ROBO2: roundabout
SALL1: sal-like
SE: standard error
SFRP2: secreted frizzled-related protein
SHH: sonic hedgehog
SHR: spontaneously hypertensive rat
SIX1: SIX homeobox
SLIT2: slit homolog
SNP: single nucleotide polymorphism
SPRY1: sprouty homolog
SRY: sex determining region Y
TBX18: T-box
TGFβ: transforming growth factor
UPJ: uretero-pelvic junction
UPK2/3: uroplakin
UTR: untranslated region
UVJ: uretero-vesical junction
VCUG: voiding cystourethrogram
VEGF: vascular endothelial growth factor
VUR: vesico-ureteric reflux
WNT4/8b/9b: wingless-type MMTV integration site family
WT1: wilms' tumor suppressor gene

LIST OF FIGURES

LIST OF TABLES

CHAPTER I

INTRODUCTION

1.1 Overview and rationale for the research

The kidney and the urinary tract are among the most common sites for congenital malformations and account for 20-30% of all malformations identified in the prenatal period (1, 2). Among the urinary tract malformations, vesico-ureteric reflux (VUR) is one of the most common defects observed and results in the retrograde flow of urine from the bladder to the kidneys (3-5). As many as 1% of children suffer from VUR and are at increased risk of developing recurrent urinary tract infections, hypertension, and end-stage renal disease (6-8).

VUR is caused by abnormal formation of the uretero-vesical junction (UVJ), the anatomical junction between the ureter and the bladder (9). Components of the UVJ include the intravesical ureter, the portion of the ureter that passes through the bladder wall, and the bladder musculature that compresses the intravesical ureter (10, 11). Clinical studies have demonstrated that patients with VUR frequently have short intravesical ureters (10, 12, 13). It is hypothesized that a short intravesical ureter cannot be properly compressed by the bladder as it fills with urine and thus allows for the backflow of urine into the ureters (10, 14). Patients with VUR also frequently have renal malformations present at birth (15). This co-occurrence of kidney and urinary tract defects suggests that these defects may arise from a common developmental mechanism: the formation of the ureteric bud.

During kidney development, the ureteric bud is an outgrowth of the mesonephric duct and develops into the kidney and the urinary tract (16). The proximal portion of the ureteric bud, which is attached to the mesonephric duct, elongates into the ureter, while the distal portion of the ureteric bud grows into the collecting ducts of the kidney (17-19). Later kidney development involves the continued branching of the ureteric bud and the induction of the surrounding metanephric mesenchyme to epithelialize into nephrons, the functional units of the kidney that filter blood and actively excrete and absorb solutes (20).

It has been hypothesized that abnormalities in the formation of the ureteric bud give rise to abnormalities of the kidney and the urinary tract (21-23). This is supported by mouse studies in which mutations in genes expressed by the ureteric bud or the surrounding metanephric mesenchyme cause abnormalities of both the kidney and the

urinary tract (24-28). Many of the phenotypes observed in these mutant mice include: the absence of kidneys or small malformed kidneys, dilated ureters, and duplicated ureters and kidneys. It is hypothesized that the small kidneys arise from impaired signaling between the ureteric bud and metanephric mesenchyme, resulting in reduced branching morphogenesis and/or the development of fewer nephrons. The dilated ureters are an indication of a urinary tract defect, and the mice often show evidence of either ureter obstruction or VUR. These observations suggest that the proper formation of the ureteric bud is crucial for the formation of an intact UVJ and a normal kidney that has an adequate amount of nephrons.

Genetic studies in humans have identified multiple loci and genes associated with VUR, demonstrating that VUR is a multigenic disorder (29-32). Of the genes that have been identified, many are expressed during ureteric bud development (32). However, the developmental mechanisms that lead to VUR remain unknown. The mouse has therefore become an important model to study both the development and the genetics of VUR. We have identified several mouse models of VUR and have examined them to determine whether abnormal formation of the ureteric bud is associated with a defective UVJ that refluxes and renal malformations. We hypothesize that mutations in genes important for ureteric bud development lead to its abnormal formation and are directly responsible for combined kidney and urinary defects.

1.2 Patterning of the embryo

Embryologists and developmental biologists have examined the embryo to understand the molecular, cellular, and developmental processes that lead to congenital diseases (4). The following sections describe kidney and urinary tract development in the mouse in detail such that the co-occurrence of kidney and urinary tract defects can be appreciated.

Proper patterning of the early embryo is critical for the establishment of the different tissues that will make up the mature organism. After fertilization, the embryo undergoes a number of cell divisions to form a blastocyst, which has all of the necessary cells to form the extra-embryonic and embryonic tissues (33). At embryonic day (E) 6.5, cell rearrangements occur during gastrulation to form the three germ layers of the

embryo: the ectoderm, the endoderm, and the mesoderm (33). Each of these germ layers differentiates into the different cell types of the body. The ectoderm differentiates into the epidermis, the neural crest, and the neural tube (33). The endoderm differentiates into the gut, bladder, liver, respiratory tract, tonsils, and pancreas (33). Within the mesoderm, the lateral plate and paraxial mesoderm give rise to the head, the somites, and the circulatory system, and the intermediate mesoderm gives rise to the urogenital system. The urogenital system will be described in the next section and is comprised of the urinary system and the reproductive system (4, 16, 34).

1.2.1 Overview of the urogenital system

At E8.5 in the mouse, the intermediate mesoderm extends along the anterior-posterior axis adjacent to the somites and differentiates into the urogenital system (4, 16, 34). Differentiation of the intermediate mesoderm into the tubular epithelial tissue of the kidney and the gonad occurs via a process known as mesenchymal to epithelial transition (35, 36). These two cell types are distinct: mesenchymal cells are unconnected and form loose aggregates while epithelial cells form organized layers, adhere to each other, and are polarized (36). Mesenchymal to epithelial conversion is a recurrent theme throughout kidney and urinary tract development (36). The mesonephric duct (also known as the nephric or Wolffian duct) is the first epithelial tube to form from the intermediate mesoderm (34, 36). It is a tubular structure that develops in an anterior-posterior direction and is situated adjacent to the somites (16, 37). It remains unknown whether the mesonephric duct extends caudally by inducing mesodermal cells to epithelialize, or whether the duct grows by proliferation and extension (38). It is this mesonephric duct that will give rise to both the urinary system and the reproductive system. While a brief review of the development of the reproductive system will be described, the major focus will be on the development of the urinary system.

Development of the reproductive system occurs when the mesonephric duct induces the surrounding mesenchyme to proliferate and form a band of mesenchymal cells called the genital ridge, which will differentiate into the future gonads (4). At E11, the genital ridge proliferates into primitive sex cords and the Müllerian ducts epithelialize adjacent to the mesonephric ducts (4, 34). During this time, and depending on the

karyotype of the embryo, the primitive sex cords differentiate into the testis or the ovary (34). In males, the mesonephric ducts differentiate into the vas deferens and seminal vesicles while in females, the mesonephric ducts degenerate and the Müllerian ducts develop into the fallopian tubes (4, 34).

The urinary system consists of the upper and the lower urinary tract (Figure 1.1A) (4, 16, 34). The upper urinary tract is derived from the intermediate mesoderm and encompasses the kidney and the ureter, while the lower urinary tract develops from the endoderm and encompasses the bladder and the urethra (34). Although these two structures develop from two different primordial tissues, a functional urinary system depends on the proper connection of these two structures such that the ureters enter into the bladder to allow for the passage of urine.

The kidneys main function is to filter blood to excrete toxic waste products and to maintain homeostasis by regulating salt and water re-absorption (16, 39, 40). The kidney obtains its blood supply from the renal arteries, which arise from the aorta (40). Not much is known about how the kidney receives its blood supply during development, but it has been hypothesized that it occurs through a combination of vasculogenesis, in which new vessels are made from endothelial progenitors in the kidney, and angiogenesis, in which already existing vessels infiltrate the kidney (37, 41).

The functional units of the kidney are nephrons, which filter the blood at the glomerulus and selectively re-absorb solutes along the tubule (16). The kidney also functions to produce various hormones: it makes renin that is involved in regulating blood pressure, erythropoietin that stimulates red blood cell production, and converts vitamin D to its active form (16, 39, 40). The final filtrate, urine, is transported down the ureter, stored in the bladder, and excreted via the urethra. The ureter is a muscular tube that propels urine towards the bladder using peristalsis (40). Both the bladder and the urethra have smooth muscle layers that contract to expel the urine from the body (4).

1.2.2 Pronephros and mesonephros development

In mammals and other amniotes (birds and reptiles), three serial kidneys develop from the mesonephric duct as it extends posteriorly: the pronephros, the mesonephros, and the metanephros (Figure 1.1B-C) (16, 20, 36). Each serial kidney is formed when the

mesonephric duct induces the surrounding mesenchyme to differentiate in an anterior-posterior sequence into epithelial tubules that function as filtrating units (36, 37). The pronephros is the functional kidney in most fish and amphibians (37, 39). The mesonephros is functional in adult lampreys, and in some fish and amphibians (37, 39, 42). In amniotes, the pronephros and mesonephros exist only during embryogenesis and degenerate for the final metanephric kidney to be functional (4, 33, 39).

Xenopus is an amphibian with a single pronephric nephron and is an important genetic model for the study of tissue patterning during kidney development. A number of transcription factors have been shown to be critical for *Xenopus* pronephros development, including: *XLim1* (lim homeobox protein 1), *XPax2* (paired-box gene 2), and *XWt1* (wilms' tumor suppressor gene 1) (43). Importantly, many of the transcription factors and signaling pathways involved in the patterning of the pronephric nephron are also involved in mesonephros and metanephros formation in higher vertebrates (43). In the mouse, the first transcription factors expressed at E8.5 in the intermediate mesoderm that are critical for its differentiation are: *Osr1* (odd-skipped related 1), *Lim1*, *Wt1*, *Pax2* and *Pax8* (44-47). This demonstrates that similar genetic pathways have evolved and have been conserved for the development of the three serial kidneys.

During the time in which the intermediate mesoderm differentiates in mice, expression of the aforementioned genes becomes restricted to either the mesenchymal or epithelial compartments of the developing pronephros/mesonephros. Both *Osr1* and *Wt1* expression becomes restricted to the mesenchyme while *Lim1* expression becomes restricted to the mesonephric duct (44-47). Mice that lack these genes further demonstrate the importance of these transcription factors for intermediate mesoderm differentiation. Mice that lack *Osr1* and *Wt1* only form the most anterior mesonephric tubules demonstrating that these two genes are required for the formation of posterior mesonephric tubules (45, 48). Although the roles of anterior versus posterior mesonephric tubules are not well characterized, the anterior tubules connect to the mesonephric duct and are important for gonad differentiation (specifically, they become the epididymal ducts in males, and degenerate in females), while the posterior tubules do not connect to the mesonephric duct (48, 49). Lastly, mice that lack *Lim1* have defective extension of the mesonephric duct such that it is unable to extend posteriorly (46).

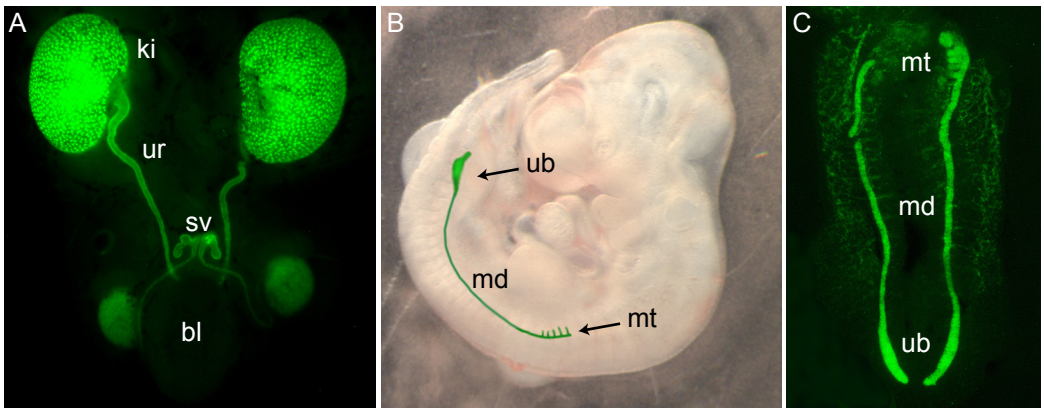

Figure 1.1: The urogenital system and the development of the mouse kidney
(A) *Hoxb7/GFP* mice express green-fluorescent protein throughout the developing kidney and urinary tract. The kidneys and urinary tract from an E17 embryo are shown. The kidneys (ki) are paired organs that connect to the bladder (bl) with the ureter (ur). The bladder does not express GFP. When the bladder is filled with urine, urine is expelled through the urethra. In males, the remnant mesonephric duct differentiates into the vas deferens and seminal vesicles (sv) while in females, it degenerates. **(B)** A lateral view of an E10.5 mouse embryo. In mice, three serial kidneys develop along the anterior-posterior axis of the embryo from the mesonephric duct (md). The pronephros degenerates at E9. The mesonephros develops at the level of the forelimb at E9.5 and mesonephric tubules (mt) are visible. The final metanephric kidney develops at E10.5 at the level of the hindlimb from an outgrowth of the mesonephric duct called the ureteric bud (ub). **(C)** Ventral view of paired mesonephric ducts dissected from an E10 mouse. At the anterior end, mesonephric tubules are visible. At the posterior end, a swelling of the mesonephric duct is visible. This is the site at which the ureteric bud will emerge and develop into the metanephric kidney.

Pax2 and *Pax8* are also required for the formation of the mesonephric duct (42). They are first expressed in the mesonephric duct at the level of the pronephros, and by E9.5, their expression is detected in the mesonephros (42, 50, 51). *Pax8*$^{-/-}$ mice develop normal kidneys, however, *Pax2*$^{-/-}$ mice fail to form mesonephric tubules and their mesonephric ducts degenerate (42, 52). Mice lacking both *Pax2* and *Pax8* never form a pronephros and their mesonephric ducts fail to develop (42). Compound heterozygous *Pax2*$^{+/-}$/*Pax8*$^{+/-}$ mice develop malformed kidneys but have a more severe renal phenotype than *Pax2*$^{+/-}$ mice alone demonstrating that there is synergism between *Pax2* and *Pax8* and that the two transcription factors work together to pattern the intermediate mesoderm (42, 53). Each of the transcription factors described above is necessary for regulating gene expression in the different segments of the intermediate mesoderm and for setting up the patterning of the pronephros, the mesonephros, and as will be described below, the metanephros.

1.3 Metanephric kidney and urinary tract development

The function of the metanephros differs from the pro/mesonephros in that it can concentrate urine (20). This is critical for land-dwelling animals as they are therefore able to conserve fluids during periods of low water intake. The development of the metanephros also differs from that of the pro/mesonephros. Instead of the mesonephric duct inducing tubule formation from the adjacent mesenchyme, the metanephros develops through induction and branching morphogenesis of the ureteric bud as it interacts with the surrounding mesenchyme to form nephrons. The theme of branching morphogenesis is common in organogenesis and is seen in the development of the lungs, the mammary gland, the salivary gland, and the pancreas (54).

1.3.1 Induction of the ureteric bud

Induction of the ureteric bud occurs by reciprocal interactions between the epithelial mesonephric duct and the adjacent metanephric mesenchyme. At the level of the hindlimb, the most caudal (posterior) end of the mesonephric duct swells to form the ureteric bud at E10.5 (Figure 1.2) (16, 17). Once the ureteric bud is formed, the proximal portion of the ureteric bud, which is still attached to the mesonephric duct, extends and

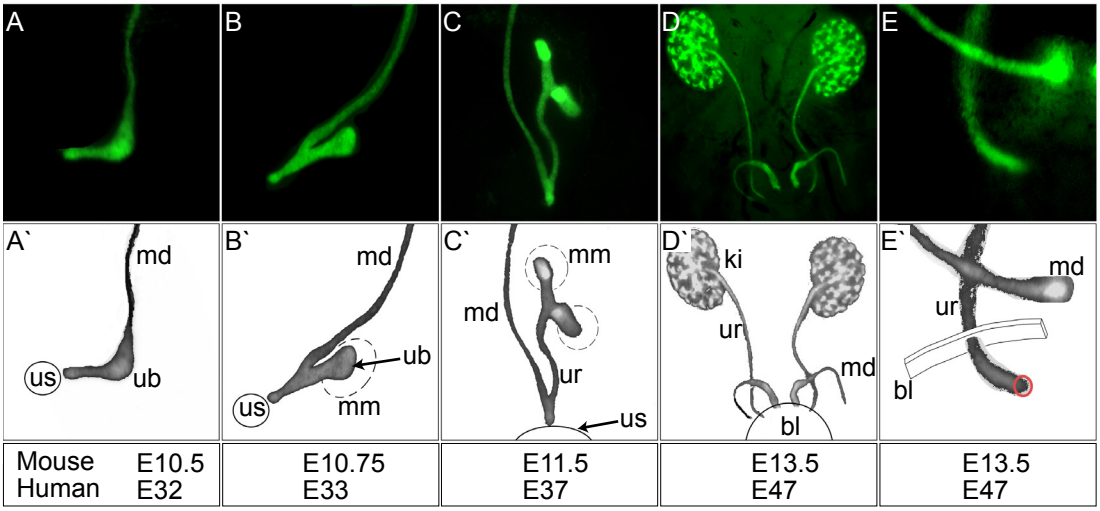

Figure 1.2: Mouse embryonic kidney and urinary tract development
(A-E) Images of *Hoxb7/GFP* embryos dissected at various stages of kidney and urinary tract development and corresponding schematic representations **(A'-E')** are shown. Equivalent human and mouse developmental stages are shown below each image. **(A)** At E10.5, a lateral view of a mesonephric duct (md) and emerging ureteric bud (ub) is shown. The caudal end of the mesonephric duct is situated near the urogenital sinus (us), which will differentiate into the bladder. **(B)** At E10.75, a lateral view of the ureteric bud as it grows into the surrounding metanephric mesenchyme (mm). The metanephric mesenchyme is located within the dashed circle. **(C)** At E11.5, a lateral view shows the distal end of the ureteric bud has branched once. The surrounding metanephric mesenchyme will differentiate to become nephrons. The proximal end of the ureteric bud remains attached to the mesonephric duct and elongates into the ureter (ur) that will connect the kidney to the bladder. **(D)** At E13.5, a frontal view of the two kidneys (ki) and ureters. The ureteric bud has branched multiple times to form the collecting ducts of the kidney while the ureter has elongated, separated from the mesonephric duct, and contacted the bladder (bl). **(E)** An enlarged view of the embryo shown in (D) showing one of the ureters after it has separated from the mesonephric duct and inserted into the bladder. The ureter passes through the bladder wall at an oblique angle and forms the ureteral orifice, indicated by the circle. (adapted from Murawski, 2006)

elongates into the ureter, while the distal portion of the ureteric bud undergoes branching morphogenesis to form the collecting ducts of the kidney (Figure 1.2) (17-19).

In 1953, Grobstein, a researcher who was interested in kidney organogenesis, was the first to demonstrate that the ureteric bud and the adjacent metanephric mesenchyme needed to be in contact to form a kidney (55). He showed that embryonic kidney explants could be cultured *in vitro* and he performed tissue recombination experiments that demonstrated that the ureteric bud and mesenchyme failed to differentiate when in isolation (55). As will become evident in this thesis, the induction of the ureteric bud is a critical step and abnormalities in its development give rise to combined kidney and urinary tract defects.

A multitude of transcription factors and receptor-ligand pairs are expressed by either the ureteric bud or the metanephric mesenchyme and are critical for the induction and branching of the ureteric bud (56, 57). Many of these genes will be described in more detail in section 1.4; however, the *Gdnf/Ret* pathway is one signaling pathway that is critical for the induction of the ureteric bud. GDNF (glial cell derived neurotrophic factor) is a ligand that binds to RET (rearranged during transfection), a receptor tyrosine kinase, together with the GFRα1 co-receptor (GDNF family receptor alpha) (58, 59). Prior to ureteric bud induction, *Gdnf* is expressed in the mesenchyme along the length of the mesonephric duct (58). By E10-E10.5, its domain of expression resembles that of a teardrop with its widest domain of expression in the region where the ureteric bud will form (Figure 1.3A) (58). By E10.5-E11, *Gdnf* becomes restricted to the metanephric mesenchyme directly surrounding the ureteric bud (Figure 1.3B) (26). *Ret* is expressed in the mesonephric duct along with *Gfrα1*, and when bound to GDNF, this receptor-ligand complex promotes the outgrowth of the ureteric bud (Figure 1.3C) (60, 61). During branching morphogenesis, the ureteric bud bifurcates and trifurcates and *Ret* expression becomes restricted to the tips of the ureteric buds, where it continues to interact with GDNF to promote cell migration, cell differentiation, and cell survival within the kidney (Figure 1.3D) (60, 62, 63).

Gdnf/Ret signaling is sufficient to promote ureteric bud induction (64). Experiments with GDNF-soaked agarose beads demonstrate that when the beads are placed next to mesonephric ducts in culture, they promote the emergence of ectopic

ureteric buds and induce increased branching morphogenesis of the kidney (Figure 1.3E-F) (64, 65). GDNF also acts as a chemoattractant for cells that express *Ret* (66). Experiments in *axolotl* embryos, an amphibian, show that the pronephric duct migrates along a GDNF gradient (67). A similar GDNF gradient is believed to exist in mammals and is represented by the tear-dropped shape of *Gdnf* expression seen in E10.5 embryos (Figure 1.3A). The ureteric bud emerges at the widest domain of *Gdnf* expression, which is believed to represent the largest GDNF concentration (Figure 1.3A) (68).

The deletion of *Ret*, *Gdnf*, or *Gfrα1* in mice results in either the development of extremely small kidneys (hypoplasia), malformed kidneys (dysplasia), or the absence of kidneys altogether (renal agenesis) (59, 60, 69). In the absence of proper epithelial to mesenchyme signaling, the metanephric mesenchyme undergoes apoptosis and kidney development halts (70).

1.3.2 Differentiation of the metanephric mesenchyme and nephrogenesis

The mesenchyme that directly surrounds each ureteric bud tip is induced to condense and epithelialize into a nephron during a process called nephrogenesis (41, 71). In addition to the mesenchyme that is fated to form a nephron, the remaining un-induced mesenchyme either proliferates to maintain a stromal cell population or undergoes apoptosis (36, 47, 72-75). This stromal cell population is essential for the regeneration of mesenchyme that is required for nephrogenesis and is also needed for the formation of the interstitial cells of the kidney (36, 75).

As the ureteric bud undergoes multiple rounds of bifurcation and trifurcation, the ureteric bud forms the collecting ducts of the kidney and each ureteric bud tip induces the formation of approximately four nephrons (19, 76). The collecting ducts of the kidney connect each nephron with the ureter (16, 20). The extent of branching morphogenesis is therefore directly related to the number of nephrons that are formed. Section 1.9 describes the importance of nephron number in more detail and is the main focus of chapter III of this thesis.

Nephrogenesis is divided into distinct morphological stages (Figure 1.4A-E) (20, 77). The initial induction of the mesenchyme by the ureteric bud causes it to condense into a vesicle and aggregate around the growing ureteric bud tip (Figure 1.4B) (16, 20).

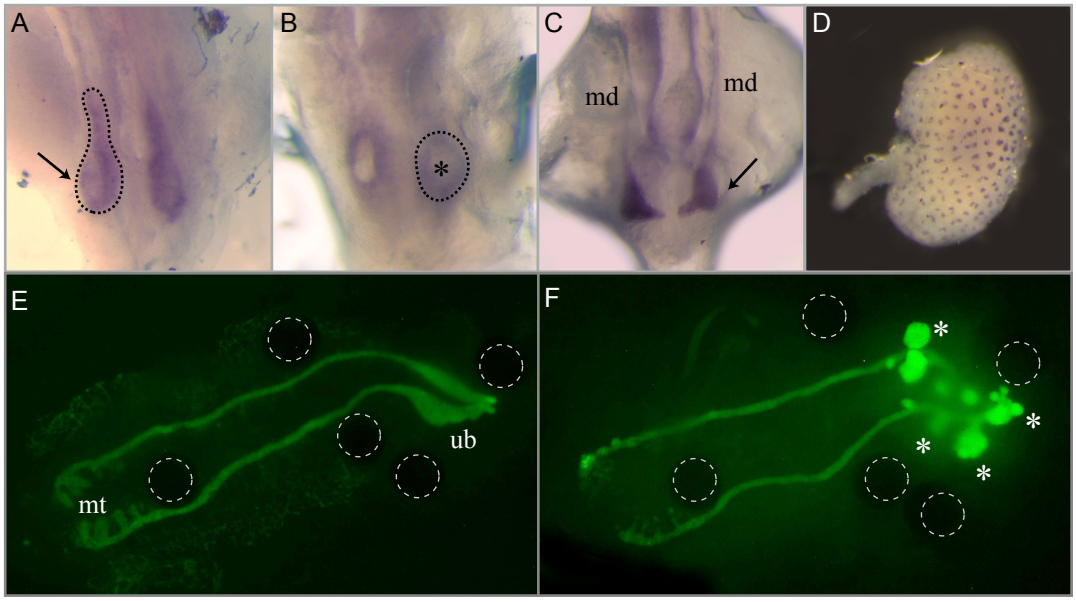

Figure 1.3: *Ret* and *Gdnf* expression in the mouse embryo

(A-D) Whole-mount *in situ* hybridization for *Gdnf* or *Ret*. **(A)** Ventral view of an E10.25 embryo at the level of the hindlimb. At the start of ureteric bud induction, *Gdnf* is expressed in the mesenchyme along the length of the mesonephric duct and its expression domain resembles that of a tear-drop (dotted line). The ureteric bud is believed to emerge at the site of the widest *Gdnf* expression domain (arrow). **(B)** Ventral view of an E10.5 embryo at the level of the hindlimb. Once the ureteric bud has invaded the metanephric mesenchyme, the expression domain of *Gdnf* becomes restricted to the metanephric mesenchyme (dotted line) directly surrounding the ureteric bud (star). **(C)** Ventral view of an E10.5 embryo. *Ret* is expressed in the mesonephric duct (md) and the emerging ureteric bud (arrow). **(D)** An E13.5 mouse kidney and ureter. Once the ureteric bud has branched, *Ret* expression becomes restricted to the tips of the branching ureteric bud. The developing kidney therefore has a spotted appearance. **(E)** Ventral view of an E10.5 mesonephric duct that has been removed from the embryo and cultured *in vitro*. At the anterior end, mesonephric tubules (mt) are visible, and at the posterior end, the mesonephric duct is beginning to swell at the site of the future ureteric bud (ub). The circles outline the positions of GDNF-soaked beads. **(F)** After 72 hours in culture, the GDNF-soaked beads promote the emergence of ectopic ureteric buds (stars). The posterior end of the mesonephric duct is more competent in forming ectopic ureteric buds than the anterior end.

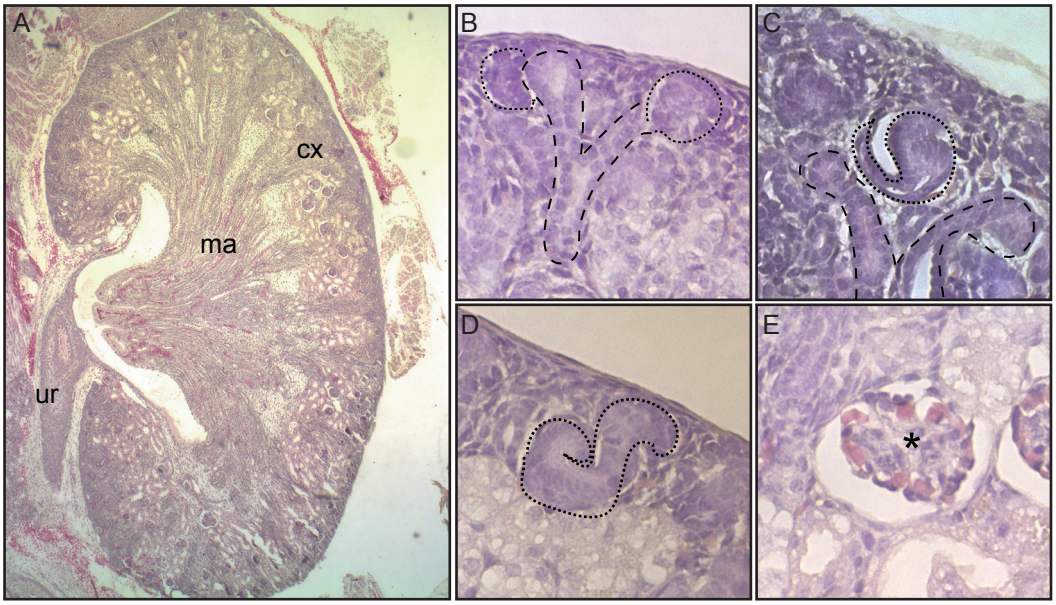

Figure 1.4: The metanephric kidney and nephrogenesis

(A) A sagittal section through the pelvis of a newborn kidney that was stained with hematoxylin and eosin. The kidney is organized into distinct regions. The cortex (cx) is situated at the periphery of the kidney and contains nephrons and glomeruli. The medulla (ma) is situated towards the center of the kidney and consists of ureteric bud derivatives that form the collecting duct network of the mature kidney that drain into the ureter (ur). **(B-E)** The four major steps of nephrogenesis are shown. Nephrogenesis is the process of forming nephrons, the functional units of the kidney. **(B)** Initially, mesenchymal cells (dotted line) aggregate surrounding the branching ureteric bud (dashed line). **(C)** Next, the mesenchymal aggregates begin to epithelialize such that a comma-shaped body (dotted line) is formed adjacent to the ureteric bud (dashed line). **(D)** The comma-shaped body continues to change morphology into an S-shaped body (dashed line). The S-shaped structure becomes compartmentalized to form the different segments of a nephron. **(E)** At the tip of the nephron furthest from the ureteric bud, the glomerulus (star) develops which is a complex capillary tuft that filters blood. The white space surrounding the glomerulus is the urinary space and is surrounded by an epithelial layer known as the Bowman's capsule.

After this condensation of mesenchyme, the cells begin to epithelialize and the vesicle changes morphology to become a comma-shaped structure and then an S-shaped structure (Figure 1.4C-D) (16). The S-shaped structure then becomes compartmentalized to form the different segments of a nephron (71). Closest to the ureteric bud tip, the distal convoluted tubule, the loop-of-Henle, and the proximal convoluted tubule form (71). Each of these segments selectively absorbs and secretes solutes (16, 78). Furthest from the ureteric bud tip, the glomerulus forms, which is a complex capillary tuft that actively filters blood by allowing water, solutes, and selective proteins to traverse the glomerular filtration barrier (Figure 1.4E) (36, 71).

Lauri Saxén was a developmental biologist who studied the kidney and extensively characterized the interaction of the ureteric bud with the surrounding mesenchyme and the induction of nephron formation (20). He performed recombination experiments by culturing the metanephric mesenchyme with other candidate inducers, including salivary mesenchyme and embryonic spinal cord (20). He noticed that the spinal cord, and not the salivary mesenchyme, could reproduce the role of the ureteric bud by inducing tubule formation in the metanephric mesenchyme. Years later, it was determined that the inductive effect of the ureteric bud and spinal cord was due to a family of secreted proteins known as WNTs (wingless-type MMTV integration site family) (79). When metanephric mesenchyme was cultured with different WNT proteins, certain ones were able to induce epithelialization and tubule formation and mimic the action of the ureteric bud (79).

WNTs belong to a large family of secreted glycoproteins that signal through the frizzled family of transmembrane receptors (77). Recombination experiments using cell lines that express different WNT proteins combined with metanephric mesenchyme have revealed that a number of WNTs, including WNT4, are capable of inducing tubule formation (79). *Wnt4* is expressed in early mesenchyme condensates (80), is maintained in comma-shaped structures, but becomes downregulated in S-shaped bodies (79). Homozygous knockout *Wnt4* mice fail to form kidneys because their mesenchyme remains undifferentiated and does not undergo epithelialization (80). *Wnt9b* is another WNT family member expressed by the mesonephric duct that acts on the surrounding mesenchyme (81). *Wnt9b* is believed to be one of the earliest inducers of the metanephric

mesenchyme, and *Wnt9b*$^{-/-}$ mutants have mesenchyme that fails to aggregate, therefore, epithelialization fails to occur and mesonephric and metanephric tubules never develop (81).

1.3.3 Ureter development

The ureter, which develops from the proximal ureteric bud, is initially a simple epithelial tube surrounded by mesenchymal cells (17, 82). As development proceeds, the ureter differentiates into three distinct layers shown in Figure 1.5A (40). The inner epithelial layer is an impermeable urothelium, the middle lamina propria layer contains connective tissues and collagen, and the outer layer contains smooth muscle that is needed for peristalsis of urine towards the bladder (4, 40).

Up until approximately E12-E14 in the mouse, the ureter and the mesonephric duct are connected via the common nephric duct (Figure 1.6) (17, 18). In order for the ureter to acquire an independent insertion site into the bladder, the ureter must separate from the mesonephric duct (Figure 1.6) (17, 18). Studies in mice have shown that complex rearrangements of the ureter and mesonephric duct occur so that the ureter can enter through the bladder wall (18). The ureter first undergoes vertical displacement such that it moves along the mesonephric duct towards the future bladder (Figure 1.6) (18). The ureter next undergoes lateral displacement, which allows for the ureter and mesonephric duct to separate (18). Apoptosis of the common nephric duct removes the cells that connect the ureter and the mesonephric duct, thereby allowing the ureter to enter through the bladder to form the uretero-vesical junction, UVJ (ureter-bladder junction) (Figure 1.6) (18, 83). The UVJ is a junction that ensures the unidirectional flow of urine from the kidneys into the bladder (10).

As well as the *Ret/Gdnf* pathway being involved in ureteric bud induction, expression of *Ret*, *Gdnf*, and *Gfrα1* has also been shown in the urogenital sinus, the embryonic structure that gives rise to the bladder (18). This expression data suggests that this new domain of *Ret/Gdnf* signaling in the future bladder may influence ureter maturation and UVJ formation (18). A number of other genes are involved in ureter maturation, including, *Rarα/β2*, two retinoic acid receptors, and *Raldh2* (retinaldehyde dehydrogenase 2), an enzyme required for retinoic acid synthesis. Vitamin A derivatives

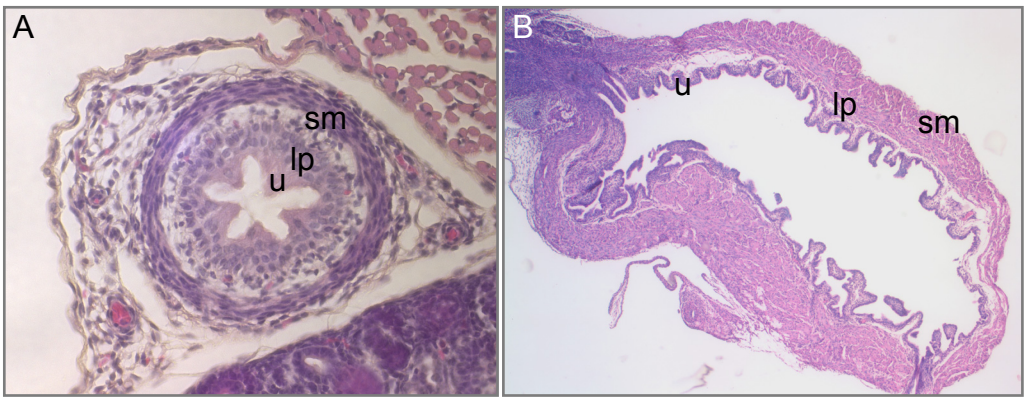

Figure 1.5: Histology of the mouse ureter and bladder

(A) Transverse section through a newborn mouse ureter at the level of the renal pelvis that is stained with hematoxylin and eosin. The inner lumen of the ureter is lined by a specialized epithelium, the urothelium (u), which is impermeable to urine. The ureter lumen resembles a star when it is in the relaxed state. The middle layer of the ureter contains a collagenous lamina propria (lp). The outer-most layer contains smooth muscle (sm). Surrounding the muscular layer of the ureter, there are blood vessels and nerves. **(B)** Transverse section through a newborn mouse bladder that is stained with hematoxylin and eosin. The bladder is similar in histology to that of the ureter. The inner urothelium is seen as having many folds in the relaxed state. The middle lamina propria contains connective tissue, and the outer layer is a smooth muscle layer.

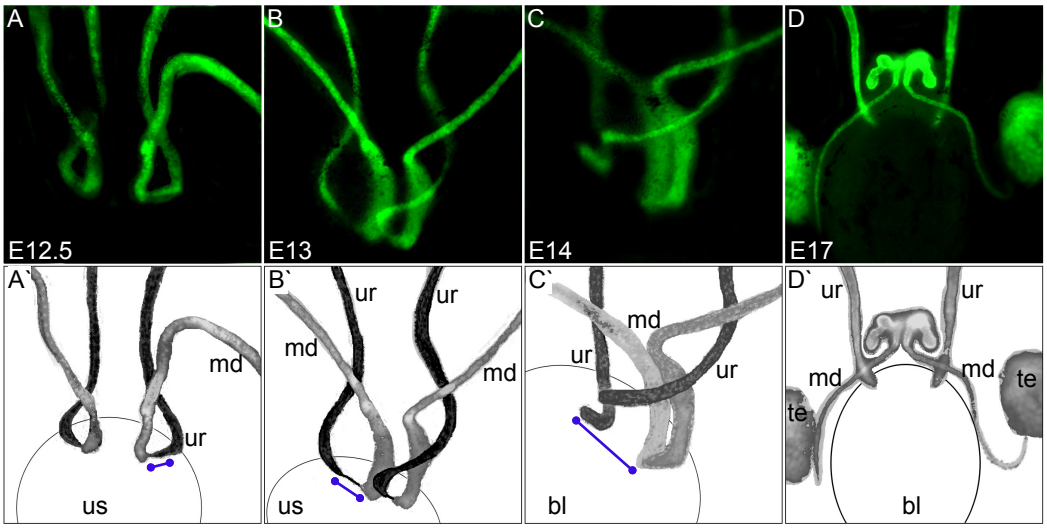

Figure 1.6: The maturation of the ureter to form the uretero-vesical junction
The ureter remains attached to the mesonephric duct until it reaches the bladder. Apoptosis of the segment of mesonephric duct that lies between the ureter and the urogenital sinus (common nephric duct) is required to permit the ureter to begin its insertion into the bladder. **(A-D)** Images of *Hoxb7/GFP* urogenital tracts with corresponding schematic representations **(A'-D')**. The lines in **(A'-C')** outline the separation of the ureter from the mesonephric duct. **(A)** At E12.5, a frontal view shows that upon contact with the urogenital sinus (us), the ureters (ur) begin to separate from the mesonephric ducts (md). **(B)** At E13, a frontal view shows that the ureter continues to separate from the mesonephric duct. Expansion and differentiation of surrounding bladder tissue causes the ureter to move away from the mesonephric duct. **(C)** At E14, a lateral view shows that the ureter has completely separated from the mesonephric duct to obtain an independent opening in the bladder (bl). **(D)** At E17, the ureters have inserted into the bladder wall and are components of the uretero-vesical junction. In females, the remnant mesonephric ducts degenerate, and in males, they form the vas deferens and seminal vesicles. This image shows a male embryo with testes (te) on either side of the bladder. (adapted from Murawski, 2006)

signal through these retinoic acid receptors to maintain high levels of *Ret* in the branching ureteric bud (18, 83). Mice deficient in either *Ret*, *Rarα/β2*, or *Raldh2* have abnormalities in both branching morphogenesis and ureter maturation: in males, the ureters remain attached to the mesonephric duct, and in females, the ureters insert into the uterus resulting in obstructed and dilated ureters (18, 83). These studies demonstrate that *Ret* signaling and the regulation of *Ret* signaling by Vitamin A is important for ureter maturation. When the ureter fails to separate from the mesonephric duct, the UVJ never forms.

Genes have also been implicated in the proper induction and maintenance of the smooth muscle layer of the ureter (84). Development of the ureter is achieved through cross talk between the ureteral epithelium and the ureteral mesenchyme. *Dlgh1* (discs large homolog 1) is a scaffolding protein expressed in the ureter epithelium that is required for this cross talk and is involved in protein-protein interactions (85). *Dlgh1*$^{-/-}$ mutants have abnormal smooth muscle formation in the ureter, have impaired peristalsis, and develop hydronephrosis (dilated kidneys) (85, 86). *Tbx18* (T-box 18) encodes a transcription factor expressed in the ureter mesenchyme that is required to maintain *Shh* (sonic hedgehog) expression in the ureter epithelium (87). *Shh* is a secreted signaling protein that promotes mesenchymal smooth muscle proliferation and mice deficient in either *Tbx18* or *Shh* have impaired smooth muscle differentiation in the ureter and develop hydroureter (dilated ureters) and hydronephrosis (82, 87).

These animal models demonstrate that when the ureter does not form properly, urine is not transported properly from the kidney to the bladder resulting in dilated ureters and a dilated kidney. We can hypothesize that this dilation is caused either by incomplete or absent formation of the UVJ that results in obstruction, or by defective peristalsis of the ureter from a smooth muscle deficiency.

1.3.4 Bladder development

In contrast to the kidney and the ureter, which are mesodermal in origin, the bladder is endodermal in origin (88, 89). Although the bladder originates from a different tissue, its final structure is similar to that of the ureter: it has an inner epithelium that

forms an impermeable barrier, a middle lamina propria layer, and an outer smooth muscle layer (Figure 1.5B) (40).

The bladder develops from a primordial structure called the cloaca, which is situated at the posterior end of the mesonephric duct (4, 39). When the ureteric bud emerges from the mesonephric duct, the mesonephric duct comes into contact with the cloaca (18, 90). The ingrowth of the mesoderm into the cloaca causes the cloaca to separate into the rectum and urogenital sinus (33, 39, 91). The urogenital sinus then differentiates into the bladder and the urethra (33).

Little is known about the signaling pathways that regulate cloacal development, but one important molecule that has been characterized is *Shh*. *Shh* is expressed not only during ureter development, but also in the cloacal epithelium and the epithelial lining of the bladder (92). SHH signals to its receptor, PTC1 (patched 1), which is expressed in the cloacal mesenchyme (92). *Shh* and *Ptc1* signaling is required for epithelial to mesenchymal interactions to promote mesenchymal smooth muscle differentiation in the bladder (92). This smooth muscle differentiation is an integral process that leads to the formation of the detrusor muscle, which allows the bladder to stretch when filled with urine and to contract to expel urine from the urethra (4).

Lining the bladder wall, the ureters, and the renal pelvis is a specialized urothelium that acts as a permeability barrier to protect surrounding tissues from urine (93). This urothelium is made up of membrane proteins called uroplakins (UPK) that form specialized epithelial plaques that maintain the impermeable barrier (93, 94). The maintenance of an intact urothelium is critical to the formation of the bladder. Mice deficient in *Upk2* or *Upk3* develop bladders that leak through their urothelium, hydronephrosis and have dilated ureteral orifices, which is evidence of a defective UVJ (93, 94).

1.3.5 The uretero-vesical junction and the trigone

Our understanding of how the ureter inserts into the bladder dates to the time of Galen during the second century and Leonardo da Vinci during the Renaissance (4, 95). Both discovered that each ureter had an oblique angle of entry into the bladder. This was required to ensure that the ureter connected to the bladder properly to form a competent

UVJ to allow the urine to pass freely into the bladder but also to prevent the backflow of urine from the bladder back into the ureters. The UVJ is not a sphincter, but rather a functional valve that becomes compressed during bladder filling (10). It is composed of the intravesical ureter, the portion of the ureter that passes through the bladder wall, and the surrounding musculature (10, 96, 97).

The trigone describes the bladder detrusor that triangulates between the two ureters and the urethra (98). As the bladder fills, the trigone stretches and compresses the UVJ to prevent the backflow of urine. Descriptions of the trigone are largely based on studies in animals and from human autopsies, which have hypothesized that the trigone develops from the mesonephric duct and is a direct continuation of the ureter (4, 88, 96). Only recently has it been shown that the trigone does not develop from the ureter, and that the trigone muscle develops separately from that of the ureter muscle (89). These two muscle populations actually intercalate at the UVJ but remain as distinct muscle types. The muscle fibers of the ureter differentiate from the ureteral mesenchyme and extend into the bladder muscle, but do not contribute to the muscle fibers of the trigone (89). The competence of the UVJ is therefore dependent on its relationship with the trigone and how the muscle layers of the intravesical ureter and bladder act together to compress the UVJ.

1.4 Genes involved in kidney and urinary tract development

Over 300 genes including a multitude of transcription factors and at least 80 ligand-receptor pairs are expressed by the ureteric bud and the adjacent metanephric mesenchyme (56, 57). Even with this plethora of genes, the majority of the molecules that have been implicated in the formation of the ureteric bud appear to function by regulating two critical genes: *Ret* and *Gdnf* (99).

1.4.1 Genes that regulate *Ret*

A number of transcription factors and signaling pathways regulate *Ret*. One of these transcription factors is *Gata3* (GATA binding protein 3), which is expressed by the mesonephric duct and ureteric bud and is required for the differentiation of the metanephric mesenchyme (100). *Gata3*$^{-/-}$ deficient embryos fail to express *Ret* in the

mesonephric duct and as a result have guidance defects such that the mesonephric ducts fail to reach the cloaca and instead grow aberrantly towards the ectoderm (101). This guidance defect may be caused by the loss of *Gdnf/Ret* signaling in the mesonephric duct such that the duct is unable to respond to GDNF in the mesenchyme and grows towards the cloaca (67). Interestingly, *Gata3* is a target of PAX2, another transcription factor important for kidney development (101).

The Vitamin A pathway is also critical for regulating *Ret* expression and is needed for maintaining *Ret* in the branching ureteric bud (102). Vitamin A is oxidized to retinoic acid, which signals through retinoic acid receptors RARα and RARβ2 (103). These retinoic acid receptors are nuclear transcription factors expressed in the peripheral mesenchyme of the growing kidney (104). They induce unknown downstream targets that signal to the branching ureteric bud to induce *Ret* expression and branching morphogenesis (102, 104). Deficiencies in Vitamin A therefore have an impact not only on branching morphogenesis, but also on nephron number (105, 106). Pregnant mice and rats that are maintained on Vitamin A deficient diets have offspring with malformed kidneys that show downregulated *Ret* expression and fewer nephrons (102, 105). Similarly, when embryonic kidney explants are cultured *in vitro* in the absence of retinoic acid, the ureteric bud tips fail to express *Ret* and show impaired branching morphogenesis (102). *Rarαβ2*$^{-/-}$ double knockout mice that lack both retinoic acid receptors also demonstrate a similar phenotype to the aforementioned experiments: they develop smaller kidneys that have downregulated *Ret* expression (102). To further demonstrate *Ret* is regulated by Vitamin A signaling, *Rarαβ2*$^{-/-}$ mice were crossed with mice that overexpress *Ret* (102). The offspring from this cross develop normal kidneys, demonstrating that the defect in branching morphogenesis could be rescued by restoring *Ret* expression (102).

Not only is the Vitamin A pathway critical for regulating *Ret* expression in the kidney, but it is also important for regulating *Ret* expression during ureter maturation. As was described in section 1.3.3, *Ret*, *Rarα/β2*, and *Raldh2* (an enzyme required for retinoic acid synthesis) mutant mice have abnormalities in ureter maturation such that their ureters fail to join the bladder. This demonstrates that the regulation of *Ret* by

Vitamin A is needed not only for branching morphogenesis but also for separation of the ureter from the mesonephric duct and formation of the UVJ (18, 83).

1.4.2 Genes that positively regulate *Gdnf*

A cascade of transcription factors, including PAX2, EYA1 (eyes absent homolog 1), SIX1 (six homeobox 1), SALL1 (sal-like 1), and HOX11 (homeobox 11), all positively regulate *Gdnf* expression and are expressed by the metanephric mesenchyme.

Pax2, which is expressed throughout the mesonephric duct, the ureteric bud, and in induced metanephric mesenchyme, is critical for kidney development (107). It binds to upstream regulatory elements within the *Gdnf* promoter and regulates *Gdnf* expression (107). Although *Pax2*$^{-/-}$ embryos show patchy *Ret* expression in the mesonephric duct, they do not express *Gdnf* and therefore a ureteric bud never forms (107). When *Pax2*$^{-/-}$ mesonephric duct explants are cultured with GDNF-soaked beads, the ducts remain unresponsive and never form ectopic ureteric buds, likely due to the loss of *Gdnf/Ret* signaling (107).

Pax2, *Eya1*, and *Six1* belong to the *Pax/Eya/Six* signaling network that is evolutionarily conserved throughout *Drosophila* eye as well as mammalian kidney development (108). This network works together to regulate *Gdnf* (108). *Eya1* appears to be at the top of this signaling network as mice mutant for *Eya1* never express *Gdnf* and completely lack ureteric bud outgrowth (109) (73). Mice mutant for *Six1* have reduced *Gdnf* expression and their ureteric buds fail to invade the metanephric mesenchyme (110). Furthermore, *Sall1* deficient mice have reduced *Gdnf*, are able to develop a ureteric bud, but the ureteric bud is unable to properly invade the metanephric mesenchyme and branch (111). The *Hox11* paralogs (*Hoxa11*, *Hoxc11*, *Hoxd11*) also regulate *Gdnf*. These three genes appear to be functionally redundant during kidney development and triple knockout mice fail to form a ureteric bud and cannot maintain normal *Gdnf* expression (112, 113).

All of the aforementioned transcription factors act together in a cascade to either directly induce *Gdnf* expression (like *Pax2* and *Eya1*), or maintain *Gdnf* expression (like *Six1*, *Sall1* and *Hox11*) in the mesenchyme. These knockout mouse models demonstrate

that proper induction of the ureteric bud, and maintenance of signals between the mesenchyme and the ureteric bud are critical for normal kidney development.

In addition to these knockout phenotypes, haploinsufficiency for these transcription factors is sufficient to produce a kidney and/or a urinary tract phenotype. Heterozygous *Eya1*, *Six1*, and *Pax2* mice all show a range of phenotypes, from renal agenesis and renal hypoplasia to duplex collecting systems (73, 109, 110, 114). Compound heterozygotes have even more severe defects, demonstrating that these genes interact within the same signaling network (109). It is still not known why haploinsufficiency would produce a phenotype. However, it has been hypothesized that haploinsufficiency of a transcription factor affects the regulation of downstream target genes (115). It appears that there may be a critical threshold level for transcription factors, either because they have to compete with other transcription factors or because a certain amount is needed to form a transcriptional regulatory complex (115). With half of the protein product, normal regulation of downstream target genes fails to occur. Interestingly, mutations in *EYA1*, *SIX1*, and *PAX2* have also been implicated in human syndromes that have combined kidney and urinary tract defects, including renal agenesis, renal hypoplasia, and duplex collecting systems. This will be further discussed in section 1.10.

1.4.3 Genes that negatively regulate *Gdnf*

From studies on experimental mouse models, it has become evident that normal kidney and urinary tract development not only requires factors to promote growth of the ureteric bud, but also requires factors that inhibit growth of the ureteric bud. A number of signaling molecules and transcription factors negatively regulate *Gdnf* expression to ensure that only a single ureteric bud emerges from the mesonephric duct.

One of these factors is BMP4 (bone morphogenetic protein 4), which belongs to the TGFβ (transforming growth factor) signaling molecule family and is expressed in the mesenchyme surrounding the mesonephric duct and the ureter (25). BMP4 inhibits the ability of GDNF to induce ureteric budding (107). When mice lack *Bmp4*, multiple ureteric buds arise, which leads to the formation of duplex collecting systems that have dilated ureters and malformed kidneys (25).

The FOXC1/FOXC2 (forkhead transcription factor c1/c2) set of transcription factors is initially expressed in the metanephric mesenchyme and later in the stroma of the kidney (28). FOXC1 and FOXC2 work together to regulate the expression domain of *Gdnf* (28). When either *Foxc1* or *Foxc2* are knocked out, mice develop supernumerary ureteric buds because of an expanded domain of *Gdnf* expression around the mesonephric duct (28). Instead of *Gdnf* becoming restricted around the ureteric bud, its expression domain extends anteriorly and is sufficient to induce ectopic ureteric bud formation.

The receptor-ligand complex of ROBO2 (roundabout 2) in the metanephric mesenchyme and SLIT2 (slit homolog 2) in the ureteric bud functions in a similar fashion to FOXC1 and FOXC2 (26). In both *Slit2*$^{-/-}$ and *Robo2*$^{-/-}$ mutant embryos, the *Gdnf* expression domain becomes expanded anteriorly, resulting in supernumerary ureteric buds that develop into multiple dilated ureters with multiple kidneys and collecting systems (26). It is important to note that the ureteric buds that are more anterior (cranial) along the mesonephric duct fail to separate from the mesonephric duct and never insert into the bladder resulting in obstruction and dilated ureters (26).

Spry1$^{-/-}$ (sprouty 1) mice also behave in a similar fashion (27). *Spry1* is a receptor tyrosine kinase antagonist expressed in the ureteric bud that negatively regulates the *Gdnf/Ret* signaling pathway (27, 116). *Spry1*$^{-/-}$ embryos develop supernumerary ureteric buds that develop into multiple ureters and malformed kidneys (27). Interestingly, the *Gdnf* expression domain is not expanded in *Spry1*$^{-/-}$ embryos, as was observed in *Foxc1/Foxc2*$^{-/-}$, *Slit2*$^{-/-}$, and *Robo2*$^{-/-}$ embryos. Although it is still not known whether SPRY1 directly acts upon *Ret*, it has been shown that *Spry1*$^{-/-}$ mesonephric ducts are more sensitive to GDNF protein (27). As a result, normal levels of GDNF are sufficient to induce ectopic ureteric budding (27). Since both the dose and domain of expression of GDNF appears to be critical for normal kidney and urinary tract development, when either the *Slit2*$^{-/-}$*/Robo2*$^{-/-}$ or the *Spry1*$^{-/-}$ mutant mice are crossed with heterozygous *Gdnf*$^{+/-}$ mice, the reduction in GDNF dose is sufficient to rescue the kidney and urinary tract phenotype (26, 27).

One additional gene, *Agtr2*, is expressed in the metanephric mesenchyme and is known to regulate ureteric budding. *Agtr2* encodes the angiotensin type II receptor, which is a component of the renin-angiotensin system that regulates blood pressure (117).

Although its interaction with *Gdnf* has never been examined, it is known to prevent ectopic ureteric budding. *Agtr2*$^{-/-}$ mice develop double ureteric buds, duplicated ureters, hypoplastic kidneys, and dilated ureters (117, 118). These phenotypes may be a result of either an expanded *Gdnf* expression domain or increased sensitivity of the mesonephric duct to GDNF protein.

1.5 Congenital anomalies of the kidney and urinary tract

Congenital anomalies of the kidney and urinary tract, widely known as CAKUT, are extremely common in humans and account for 20-30% of all malformations identified in the newborn period (71). CAKUT can cause death from renal failure in the newborn period in 1/2000 infants (119) and is identified in up to 46% of all patients with end-stage renal disease (119, 120). The following is a list of phenotypes associated with CAKUT, their incidence, and a brief description of their genetics if it is known. Many of these phenotypes are observed in the mutant mouse models described in the previous sections. Importantly, more than one of the phenotypes described below can be observed in the same individual (71, 121, 122) demonstrating that CAKUT encompasses a spectrum of defects that may include any combination of the following entities:

1. *Renal agenesis*: This lesion affects between 1/400 and 1/5000 births depending if it describes the absence of one or both kidneys, respectively (123-125). Renal agenesis arises because the ureteric bud fails to develop or because the kidney undergoes apoptosis (Figure 1.7A) (16). Bilateral renal agenesis is incompatible with postnatal life while unilateral renal agenesis is compatible with postnatal life (123). The absence of one kidney greatly reduces the total filtration surface area because half of the nephrons are missing (126). Therefore, patients with renal agenesis are at increased risk of developing proteinuria, hypertension, and renal insufficiency (121, 126). The remaining kidney, in response to the increased workload, undergoes compensatory hypertrophy (127). Renal agenesis has been shown to be inherited within families (128-130) and is associated with a number of syndromes (131-133). It is hypothesized to be inherited as an autosomal dominant trait with incomplete penetrance (129, 134). One human linkage study

demonstrated that a locus on chromosome 1 is associated with renal agenesis in some families, but the underlying genes have not yet been identified (135).

2. *Renal hypoplasia and renal dysplasia*: Renal hypoplasia describes a congenitally small kidney that has fewer nephrons, while renal dysplasia describes a congenitally small kidney that shows evidence of maldifferentiated tissues including cartilage, smooth muscle, and cysts (2). Renal hypoplasia is hypothesized to arise from reduced branching morphogenesis and/or impaired ureteric bud to mesenchyme signaling (Figure 1.7B) (136, 137). The true incidence of renal hypo/dysplasia is not known because this is a pathological lesion and tissue is rarely obtained for diagnosis (138). Renal hypo/dysplasia can also have a familial occurrence, and one human linkage study demonstrated that a region on chromosome 1 is associated with renal hypo/dysplasia in certain families, but the underlying genes have not yet been identified (135).

3. *Obstruction*: This is also known as obstructive uropathy and refers to an obstruction in the flow of urine along the ureter (4). Obstruction can occur at the junction of the ureter and the renal pelvis (uretero-pelvic junction, UPJ, obstruction) or at the junction of the ureter and the bladder (UVJ obstruction). Above the site of the obstruction, dilation occurs, and can result in a dilated ureter (hydroureter) and/or a dilated kidney (hydronephrosis) (Figure 1.7C). There is evidence that obstruction can have a genetic origin: there are reports of a familial occurrence of unilateral UPJ obstruction (139). A mouse model of autosomal recessive UPJ obstruction exists: the *cph* mouse that has congenital progressive hydronephrosis as a result of bilateral UPJ obstruction (140). Genetic mapping in *cph* mice identified a region on the distal end of chromosome 15 that is associated with the phenotype, but the gene has not yet been identified (140).

4. *Ureterocele*: This is a cystic dilation of the ureter that often forms within the intravesical ureter (4). Ureteroceles affect up to 1/4000 live births (141) and in severe cases, they can cause obstruction of the ureter (4). One mouse model of ureterocele exists and is a double mutant for *Ptprs* and *Ptprf*, two tyrosine phosphatase receptors that

belong to the leukocyte antigen-related family that are hypothesized to influence RET phosphorylation (142). *Ptprs* is expressed in the epithelial and mesenchymal cells of the common nephric duct and cloaca, while *Ptprf* is restricted to the epithelial cells of the common nephric duct and cloacal epithelium. Mice homozygous mutant for both *Ptprs* and *Ptprf* develop hydronephrosis, hydroureter, duplicated ureters and kidneys, and ureteroceles. It was shown that reduced apoptosis of the common nephric duct affected ureter maturation and the insertion of the ureter within the bladder wall such that upon the initiation of urine production, the distal ureter swells to form an ureterocele (142).

5. *Duplex systems*: From autopsy studies, the estimated incidence of bifid or duplicated ureters/kidneys is between 0.8-5% (39, 125). A duplex kidney has two separate pelvic systems, each draining into their respective ureter (4). The ureters can either be bifid, if they join below the uretero-pelvic junction (UPJ), or they can be duplex if each ureter has its own independent insertion into the bladder (4). A bifid ureter is hypothesized to arise from a single ureteric bud that then bifurcates during development (Figure 1.7D). A completely duplex system is hypothesized to arise from two ureteric buds (Figure 1.7E). The Weigert-Meyer Principle applies to duplex systems (4). The upper renal pole usually drains into the bladder through an orifice that is lower than normal within the bladder wall (i.e. closer to the urethra), while the lower renal pole usually drains into the bladder through an orifice that is higher than normal (4). It has therefore been hypothesized that the upper renal pole develops from the more cranial ureteric bud and the lower renal pole develops from the more caudal ureteric bud (22, 23). Duplex systems have also been reported to run in families and appear to have an autosomal dominant inheritance (30, 130, 143-145).

6. *Ectopic ureters*: From autopsies, the incidence is estimated at 1/1900. Ectopic ureters describe any ureter whose orifice (opening into the bladder) terminates outside of the trigone (4). The ureter can insert closer or further away from the bladder neck and be considered in an ectopic position. The ureter can also insert outside of the bladder wall and insert into the urethra or the genital tract. In over 80% of cases, ectopic orifices are associated with duplex systems and affect more females than males (4). An ectopic ureter

is believed to arise from abnormal ureter maturation that results in a ureter that does not connect to the bladder at the proper location (Figure 1.7E) (17, 18).

7. *Vesico-ureteric reflux*: (OMIM #193000) VUR is one of the most common urinary tract defects encountered by clinicians with a reported incidence of 1% (4, 121, 146-150). It is defined as the retrograde flow of urine from the bladder to the kidney and is caused by an abnormal UVJ (Figure 1.7F) (4). It can be associated with a dilated ureter and renal malformations (151-154). Up to 37% of patients with unilateral renal agenesis have VUR in the contralateral kidney (124) and between 8-42% of children with duplex systems have VUR (4, 155). VUR is the major focus of this thesis and will be described in section 1.6.

1.5.1 Ureteric bud theory

Over 30 years ago, Mackie and Stephens proposed the ureteric bud theory based on observations of autopsies from infants with duplex systems (21, 156). They made a correlation between the position of the ureteric orifice within the bladder and the degree of renal hypo/dysplasia in duplex systems: the more displaced the ureteric orifice, the more severe the kidney malformation (21). They believed that the site of ureteric budding was critical and would determine both the final position of the ureteral orifice within the bladder wall and the severity of the kidney malformation in the duplex system.

When a ureteric bud emerges from the mesonephric duct too cranial (high) or too caudal (low) in position, it is hypothesized to encounter a population of mesenchymal cells that cannot differentiate properly to support normal growth of the kidney (23, 156, 157). This results in the development of either hypoplastic or dysplastic kidneys (157). In addition, the growth of the ureter is hypothesized to be disturbed. A cranial ureteric bud is believed to elongate into a ureter that takes longer to separate from the mesonephric duct and then contacts the bladder later than usual, such that the final position of the ureteric orifice is more medial (i.e. closer to the urethra or bladder neck) than normal and the ureter is at risk for obstruction (22, 23). Conversely, a caudal ureteric bud is believed to elongate into a ureter that reaches the bladder earlier than expected, giving the ureter

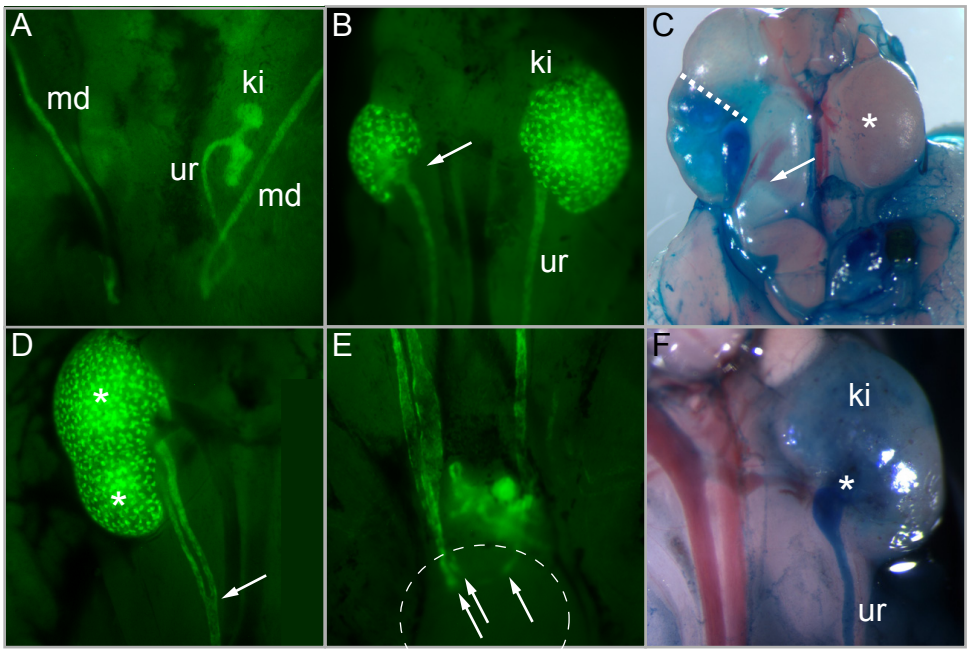

Figure 1.7: Phenotypes observed in CAKUT

(A) Unilateral renal agenesis. Ventral view of a developing E11.5 kidney (ki) whose ureter (ur) is still attached to the mesonephric duct (md). The left kidney has undergone one branching event. The right kidney is missing, either due to the failure of the ureteric bud to develop or because the kidney has undergone apoptosis. **(B)** Renal hypoplasia. Ventral view of a developing E17 kidney. The right kidney is hypoplastic (arrow) compared to the left kidney. **(C)** Obstruction at the uretero-vesical junction. Ventral view of newborn kidneys that have been tested for VUR. The left kidney is normal (star). The right kidney is duplex (separation at the dashed line) in which the upper kidney pole has a ureter that is obstructed at the level of the bladder. The result is a tortuous and dilated ureter (arrow). **(D)** Duplex system. Ventral view of a developing E17 kidney that is duplex with a bifid ureter. Two kidney poles are visible (stars) with two ureters that fuse midway to the bladder (arrow). **(E)** Duplex ureter with ectopic ureter. Ventral view of E17 ureters that insert into the bladder (circle). A single left ureter inserts into the bladder (arrow). There are two right ureters that insert into the bladder independently of each other. The two right ureteral orifices are visible (arrows). **(F)** Vesico-ureteric reflux. Ventral view of a left newborn kidney that has VUR. Methylene blue dye is seen flowing retrogradely up the ureter into the pelvis (star) of the kidney.

more time to move laterally along the bladder wall resulting in an abnormally formed UVJ that refluxes (Figure 1.8) (22, 23).

The goal of researchers has been to understand the pathogenesis of CAKUT by discovering the underlying gene mutations and by characterizing the cellular events that lead to it. Although the ureteric bud theory attempts to explain the relationship between renal dysplasia and VUR or obstruction, it does not explain how an abnormality in ureteric bud development leads to the spectrum of defects observed in CAKUT. What we know is that many of these defects can arise from abnormalities in the formation of the ureteric bud: from its absence to an alteration in its position or a delay in its development. A number of genes are critical for normal ureteric bud formation; therefore, it is not entirely unexpected that the coordinated action of many, if not all, of these genes is needed for normal kidney and urinary tract development. It is possible that a spectrum of defects could arise because of the nature of the genetic mutation, such that mutations in different genes affect the spatial and temporal regulation of ureteric bud development differently. Alternatively, individuals with the same mutation could exhibit phenotypic differences because of modifier genes and/or environmental factors that influence ureteric bud formation.

To date, the ureteric bud theory has never been proven. Even with the availability of numerous mouse models of double and/or supernumerary ureteric buds, detailed descriptions of the consequence of an abnormally positioned ureteric bud on ureter maturation have not been described. We are the first to examine the ureteric bud theory in detail to determine if a caudally positioned ureteric bud is associated with a refluxing urinary tract and a malformed kidney. This work will be presented in chapters II and IV.

1.6 Vesico-ureteric reflux

VUR was first described in man in 1893 (158). By 1897, experiments on cadavers showed that bladders could be distended without inducing VUR, suggesting that the UVJ functions as a one-way valve (3). This suggested that the normal physiological function of the ureter was to propel urine from the kidneys to the bladder and to prevent urine from passing retrogradely towards the kidneys.

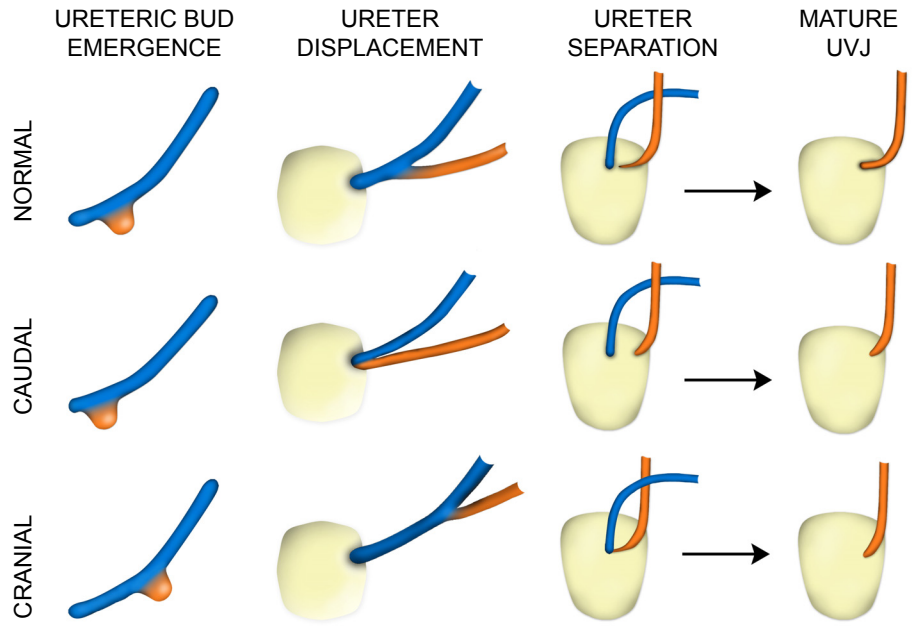

Figure 1.8: The ureteric bud theory

From left to right the images depict two lateral and two ventral views of the developing urinary tract. NORMAL: During normal ureteric bud development, the ureteric bud emerges from the mesonephric duct. The distal end branches to form the collecting ducts of the kidney while the proximal end forms the ureter. Vertical displacement of the ureter leads to separation of the ureter from the mesonephric duct within the developing bladder (yellow). Once the ureter has achieved an independent opening into the bladder, the length of the intravesical ureter and its angle of entry into the bladder wall are important components of the uretero-vesical junction (UVJ). CAUDAL: The ureteric bud theory predicts that a caudal ureteric bud will cause quicker ureter displacement and early separation of the ureter from the mesonephric duct, resulting in increased migration of the ureter within the bladder wall. This leads to an abnormally positioned ureteral orifice and a short intravesical ureter that refluxes. CRANIAL: The ureteric bud theory predicts that a cranial ureteric bud will cause ureter displacement to take longer such that there is late separation of the ureter from the mesonephric duct, resulting in decreased migration of the ureter within the bladder wall. This leads to an abnormally positioned ureteral orifice and obstruction.

The UVJ consists of several components that are essential to prevent VUR (Figure 1.9). These include: an adequate length of the intravesical ureter, an oblique angle of entry of the ureter into the bladder wall, a well-formed trigone that can compress the ureteral orifices during voiding, and correctly positioned ureteric orifices within the trigone (14). Early evidence supporting the importance of the intravesical ureter came from studies performed by Gruber in 1929 (159). He tested a variety of animal species for VUR. Those species with the highest incidences of VUR were those with the shortest intravesical ureters. Similar findings have been found in humans: patients with VUR often have short intravesical ureters and large dilated ureteric orifices that are ectopically placed within the trigone (22, 160).

1.6.1 Incidence of VUR

VUR is reported to affect 0.1-1% of all children (149, 150). However, the true incidence of VUR in the general population is not known, largely due to the fact that it is not feasible to screen the population at large for VUR. One study reviewed approximately 15 independent reports that attempted to determine the frequency of VUR in "normal" children (161). Surprisingly, the results vary greatly and estimate the incidence of VUR from 0-30% (161). This huge variation may arise from differences in the study population, including ethnicity and age. It is therefore believed that the widely reported VUR incidence of 1% is almost certainly an underestimate (161).

1.6.2 Diagnosis and natural history of VUR

VUR is diagnosed by voiding cystourethrogram (VCUG), an invasive test that requires catheterization by the urethra to fill the bladder with a radio-opaque contrast solution (162). Immediately after voiding, X-ray images of the urinary tract are obtained and if the contrast solution is observed flowing retrogradely from the bladder to the ureter or renal pelvis, a diagnosis of VUR is made (Figure 1.10).

There can be differences in the severity of VUR and whether VUR is present in one ureter (unilateral) or both (bilateral) (163). International guidelines have been established to classify VUR from grades I-V (164, 165). Grade I VUR only extends into the ureter. Grade II VUR extends into the renal pelvis, but there is no evidence of ureter

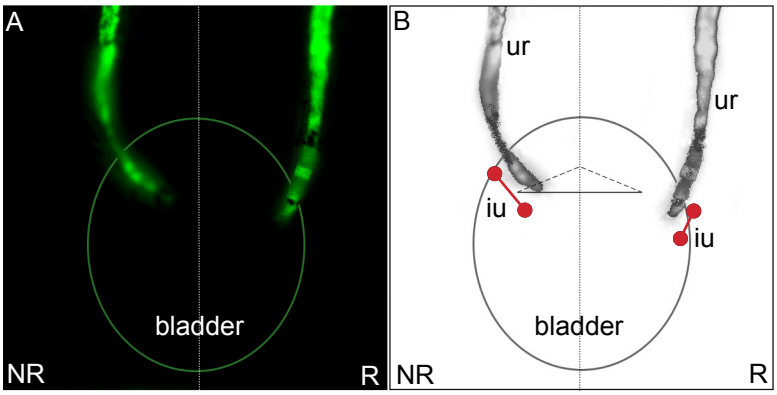

Figure 1.9: The components of the uretero-vesical junction in refluxing and non-refluxing mice

Mouse embryos that contain the *Hoxb7/GFP* transgene express green fluorescent protein throughout the ureteric bud and its derivatives and are used to demonstrate ureter insertion in the bladder at E17. **(A)** A composite view of the uretero-vesical junction from a non-refluxing (NR) and a refluxing (R) mouse strain is shown. The ureters are visualized by their GFP expression and the bladder is outlined by the line. **(B)** A schematic representation of the photograph in (A). The non-refluxing ureter (ur) enters the bladder at an oblique angle within the trigone (indicated by triangle). The non-refluxing mouse also has a long intravesical ureter (iu), as delineated by the red line, which is able to form a competent uretero-vesical junction. The refluxing ureter does not enter the bladder at an oblique angle, is positioned more laterally along the bladder wall, and consequently has a shorter intravesical ureter. In the trigone, the solid line represents the portion of the trigone that connects the two ureters and the dotted lines represent the remainder of the trigone as it funnels towards the bladder neck, which is in a plane perpendicular to the page. (Murawski, 2006)

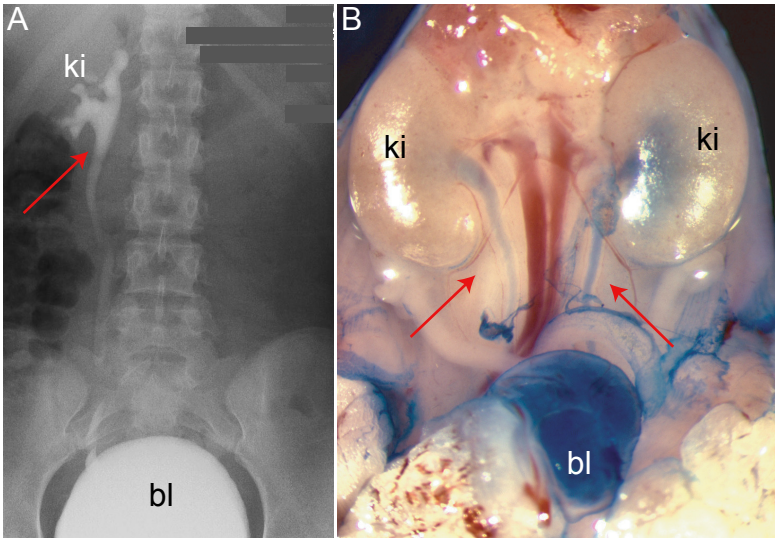

Figure 1.10: Voiding cystourethrogram in humans and in mice
(A) VUR is diagnosed by VCUG (voiding cystourethrogram) in humans. This test requires catheterization by the urethra to fill the bladder (bl) with a radio-opaque contrast solution. Upon voiding, an X-ray of the urinary tract is taken and if the contrast solution is observed in the ureter or the kidney pelvis (ki), a diagnosis of VUR is made. This patient has unilateral reflux in the right ureter and kidney (arrow). **(B)** We perform a similar assay in our mice to test for VUR. Methylene blue dye is injected into the bladder of newborn mice. The column of dye is raised at specific intervals and the rate of dye flowing into the bladder is determined by the pressure exerted on the column of dye. When VUR is present, the dye can be seen flowing up the ureters and into the renal pelvis. This mouse has bilateral VUR (arrows). (adapted from Murawski, 2007)

dilation. Grade III VUR has mild ureter dilation. Grade IV VUR has moderate dilation of the ureter accompanied by dilation of the renal pelvis. Grade V VUR has gross dilation of the ureter and gross dilation of the renal pelvis.

The natural history of VUR is that it will frequently resolve with time (166-168). This is hypothesized to occur because of normal growth and maturation of the intravesical ureter with age (169). For children with mild grades of VUR (grades I-II), VUR can spontaneously resolve in more that 71% of cases (167). Higher grades of VUR (grades III-V) are more likely to persist, although they usually become less severe with time (167, 168, 170). Furthermore, there are gender differences. VUR is more common in boys at a young age (171), while most females with VUR are identified after they present with urinary tract infections (167). The presence of VUR may also change from one VCUG to the next; it has been known to be detected on one exam but missed on the next (172). And, alternating bilateral and unilateral VUR has been observed on follow-up VCUGs (163).

1.6.3 How patients with VUR come to clinical attention

There are four ways by which patients with VUR are identified. The first two describe patients that present with symptoms associated with VUR. The last two encompass patients that are identified through screening.

The majority of individuals with VUR are identified after they present either with their first urinary tract infection or with a history of recurrent urinary tract infections (group 1) (9, 171, 173, 174). The occurrence of a urinary tract infection is frequently the first sign that there may be a urinary tract defect (175), and therefore, VUR is diagnosed in as many as 30-40% of patients that present with urinary tract infections (176). More rarely, patients with VUR are identified after they present with complications of VUR, such as hypertension and/or renal failure (group 2) (4, 177, 178). The risk for renal damage in patients with VUR will be further described in the following section.

Another group (group 3) of patients with VUR is identified in the newborn period after an antenatal ultrasound detects hydronephrosis (179, 180). These patients never present with clinical symptoms of VUR and are screened for VUR postnatally by VCUG. Up to 80% of children with evidence of antenatal hydronephrosis are subsequently found

to have VUR when a VCUG is performed (175). The last group (group 4) is identified as part of family-based screening after an index case with VUR is identified. The prevalence of VUR among first-degree relatives is much higher compared to the prevalence in the general population (181, 182). The risk of VUR if the parents have VUR is between 31-65%, and the risk of VUR if a sibling has VUR is between 27-64% (183-186). In the last decade these latter two groups of patients have changed the epidemiology of VUR and raised many questions about their diagnosis and their management as they are detected before any symptoms of VUR arise.

While all four groups of patients have VUR, it is hypothesized that they may actually represent distinct phenotypes of VUR and therefore may warrant different management strategies (178). It is important to know that as many as 46% of patients with VUR never develop urinary tract infections and/or renal damage (187). Although we are currently not able to do this, it is extremely important to distinguish the subset of patients that are and are not at risk of developing urinary tract infections and/or renal damage.

1.6.4 VUR and the risk for renal damage and end-stage renal disease

VUR is reported to account for up to 25% of all cases of end-stage renal disease and is associated with the development of severe hypertension and reflux-induced scarring/nephropathy (188); however, its relationship with each of these entities is poorly understood. Hypertension is considered to be a late complication of VUR and is believed to arise secondary to renal scars acquired from recurrent urinary tract infections (189). The risk of hypertension increases as renal function deteriorates and may accelerate the progression to renal failure (189, 190).

In 1960, Hodson and Edwards were the first to demonstrate the association between VUR and renal scarring (6). The term reflux nephropathy was then coined to describe the pathophysiological changes that occur in the kidney, including chronic inflammation, fibrosis, tubular dilation, and atrophy (6, 191). It is believed that much of the damage to the kidney is acquired from reflux of infected urine into the kidney, which leads to the infiltration of inflammatory cells and the deposition of collagen (191). Damage to the kidney can also be caused by the hydrodynamic effect of intra-renal reflux

on the collecting duct system (192). The majority of renal scars occur at the poles of the kidney where the anatomy of the human papilla favors the backflow of urine into the collecting ducts (193). Using a pig model of VUR, it was demonstrated that the reflux of urine, whether it was infected or sterile, led to the pathological changes consistent with reflux nephropathy (193). Importantly, infected urine was not essential for scar formation, but it did increase the severity of scar formation (194). This was the first experimental evidence that VUR can cause reflux nephropathy.

The risk of renal damage from severe grades of VUR is six times greater than for mild grades of VUR (195). Despite this observation, a staggering 85% of children with VUR show evidence of renal damage at the time of diagnosis (196). Renal scars are diagnosed with a DMSA scan, which measures the uptake of technetium 99m dimercaptosuccinic acid (^{99m}Tc-DMSA), an isotope, by the kidney (138). Regions of decreased isotope uptake are indicative of areas with renal scars (179, 197). However, it is not clear whether these scars are acquired because of reflux or whether these are regions of renal dysplasia arising from a congenitally malformed kidney. While renal scars are more prevalent in the kidney that has VUR, the contralateral non-refluxing kidney can also show evidence of decreased isotope uptake (198). This has provoked a new hypothesis: that reflux nephropathy may actually be congenital in origin and not solely due to damage caused by urinary tract infections.

There are numerous cases in the literature in which decreased isotope uptake is evident but there is no history of urinary tract infections, suggesting that these scars actually represent regions of dysplasia and not acquired scars (178, 199-201). It has also been hypothesized that since patients with VUR have congenitally small and malformed kidneys, then any region with decreased isotope uptake is likely a region of dysplasia (15). These observations are consistent with the hypothesis that congenital maldevelopment of the kidney causes the formation of a dysplastic kidney that is at risk of developing reflux nephropathy. However, in reality, any lesions of decreased isotope uptake are probably a combination of acquired and congenital damage. It is now a common belief that early detection of VUR is important to either treat patients that already have renal damage or to treat patients early enough to prevent renal damage from occurring.

It is important to recognize that while some patients with VUR have hypo/dysplastic kidneys that are easily identified as malformed on ultrasound or after DMSA scan, between 20-67% of patients with VUR have kidneys that appear morphologically normal (202-206). It is presumed that this subset of VUR patients is also at risk of developing reflux nephropathy (207). What we lack the ability to do is detect those patients that are at greatest risk for developing reflux nephropathy. We need a better understanding of the relationship between VUR and the renal phenotype to be able to improve prognosis and to avoid end-stage renal disease.

1.6.5 Treatment of VUR

Medical management of VUR has focused on prophylactic treatment with prolonged low-dose antibiotics to prevent recurrent urinary tract infections (208, 209). Surgical management of VUR has focused on ureter re-implantation to correct the UVJ defect or endoscopic injection of a viscous gel within the intravesical ureter to narrow the UVJ and to prevent VUR (208-210).

Both surgical and medical management of VUR has been the gold-standard treatments for VUR (211). However, despite these treatments, the incidence of renal damage and end-stage renal disease secondary to reflux nephropathy has remained the same over the past 40 years (212). Studies have found that ureter re-implantation does not always reduce the appearance of renal scars or prevent further loss of renal function post-operatively (213, 214). Another study demonstrated that despite prolonged antibiotic prophylaxis, 50% of patients have breakthrough urinary tract infections, further questioning the benefit of this treatment (215).

It is important to understand that while certain patients with VUR do progress to reflux nephropathy and end-stage renal disease, many patients never develop these phenotypes (120, 188, 214). It is therefore extremely important to develop new strategies to identify the patients that are at risk for hypertension, reflux nephropathy, and end-stage renal disease, to provide them with appropriate care, and to avoid the un-necessary treatment of those patients who will not develop any complications.

1.7 Mouse models of vesico-ureteric reflux

Our understanding of VUR has come a long way (Figure 1.11). Centuries ago, the first observations describing the importance of the UVJ were made (4, 95). More recently, mouse models with mutations in genes expressed by the developing kidney and urinary tract have provided us with a wealth of information about the development of CAKUT. Five mutant mouse models have been identified that have VUR and kidney malformations: the transgenic *Hoxb7/Ret*$^{+/-}$ mouse, the conditional *Lim1*$^{-/-}$ mouse, the *Agtr2*$^{-/-}$ mouse, and the *Upk2*$^{-/-}$ and *Upk3*$^{-/-}$ mice (24, 46, 93, 94, 216). These mouse models of VUR exhibit many of the same phenotypes observed in humans, including renal hypoplasia, renal dysplasia, duplex systems, hydronephrosis, and hydroureter. Chapter II of this thesis describes the sixth mouse model of VUR and malformed kidneys, the *Pax2*$^{1Neu+/-}$ mouse (68).

1. Hoxb7/Ret$^{+/-}$: The *Hoxb7/Ret*$^{+/-}$ transgenic mouse is a misexpression model in which *Ret* is constitutively expressed throughout the ureter and collecting ducts instead of becoming restricted to the ureteric bud tips (217). *Hoxb7* encodes one of the many HOX transcription factors that specify positional identity along the anterior-posterior axis of the embryo (218). *Hoxb7* is expressed in the intermediate mesoderm, the mesonephros, the mesonephric duct, and the ureteric bud, but unlike *Ret*, expression persists throughout development in the ureter and in the branching collecting ducts (63, 217, 219, 220).

Hoxb7/Ret$^{+/-}$ mice develop small cystic kidneys that have grossly reduced ureteric bud branching, which results in the formation of fewer nephrons (24, 217). It was hypothesized that the kidney defect arises from a decrease in *Gdnf/Ret* signaling. The misexpressed RET protein throughout the ureteric bud would quench GDNF away from the ureteric bud tips such that GDNF would be less available to promote normal branching morphogenesis (217). This hypothesis was proven to be true: *Hoxb7/Ret*$^{+/-}$ embryonic kidney explants that are cultured with GDNF show a significant improvement in their growth and their ability to branch (217). This demonstrates that restoring GDNF to the ureteric bud tips is sufficient to rescue the kidney phenotype.

Our Laboratory acquired the *Hoxb7/Ret*$^{+/-}$ mouse from Dr. F. Costantini at Columbia University (217). Because *Ret* is expressed in the ureteric bud and is required

100AD	Galen noted the importance of a competent junction could not induce VUR in live or dead animals called this one-way junction “Nature’s Artistic Skill”
1487-1513	Leonardo da Vinci saw the importance of the one-way UVJ
1812	Oblique course of the ureter described by Charles Bell
1883	VUR demonstrated in rabbits and dogs
1893	First case of human VUR reported
1896	Importance of ureteric bud position demonstrated
1903	Demonstrated ureters enter bladder at an oblique angle
1912	Observed ureteric budding, ureter migration, and trigone
1920	Trigone muscle described in detail
1929	Importance of intravesical ureter length and bladder musculature from studies by Gruber on different animals
1952	Association between VUR and chronic urinary tract infections
1966	VUR was rare in Black Americans but 1% of Caucasians affected: believed this could only be explained by a genetic pool
1972	Intravesical ureter length is a strong predictor of VUR
2000+	Discovery of mouse models of VUR and genetics of VUR

Figure 1.11: The history of VUR

This figure demonstrates the history of VUR reported over the centuries, from early observations of the uretero-vesical junction to ureteric budding and modern genetic analysis.

for its formation, we hypothesized that *Hoxb7/Ret*$^{+/-}$ mice would have a urinary tract defect in addition to renal malformations. A previous graduate student in the lab tested newborn *Hoxb7/Ret*$^{+/-}$ mice for the presence of VUR and noted that *Hoxb7/Ret*$^{+/-}$ mice have an increased incidence of VUR when compared to wildtype littermates (24). I confirmed these results and found that *Hoxb7/Ret*$^{+/-}$ mice have a 42% incidence of VUR when compared to CD1 controls that have a 4% incidence of VUR (24).

Humans with VUR have been reported to have short intravesical ureters (10); therefore one of my objectives was to develop a method to measure the length of the intravesical ureter in mice. The UVJ and the intravesical ureter cannot be easily visualized in postnatal (P) day 1 mice, therefore, I injected dye into the pelvis of a P1 kidney until it flowed down the ureter and exited into the bladder through the ureteral orifice (24). The distance between the insertion of the extravesical ureter into the bladder and the exit of dye from the ureteral orifice inside the bladder corresponds to the intravesical ureter and can then be easily measured. I found that *Hoxb7/Ret*$^{+/-}$ mice have shorter intravesical ureters than their wildtype littermates, thus predisposing them to VUR (24). To determine if the ureteric bud theory proposed by Mackie and Stephens over thirty years ago is correct (21), I examined the position of the ureteric bud relative to the end of the mesonephric duct by *in situ* hybridization. I found that ureteric buds from E10.5 *Hoxb7/Ret*$^{+/-}$ embryos develop from a more caudal position along the mesonephric duct, consistent with the ureteric bud theory (24). My work on the *Hoxb7/Ret*$^{+/-}$ mouse model appears in a second-author publication (24) and established important methods that I used to characterize additional mouse models of VUR described in chapters II and IV.

2. Conditional Lim1$^{-/-}$: Another gene that regulates ureteric bud formation and causes VUR when deleted is *Lim1*. *Lim1* encodes a homeobox transcription factor expressed in the mesonephric duct and is necessary for the extension of the duct and the formation of the ureteric bud (46). *Lim1*$^{-/-}$ knockout mice die at E10 from abnormalities of the head thus preventing the assessment of metanephric kidney development. Therefore, conditional knockout *Lim1*^{lacZ}*;Pax2-Cre* mice were created (46). The *Pax2* promoter was used to drive *Cre* expression and to selectively knockout *Lim1* in the

mesonephric duct and ureteric bud. The conditional knockout mice exhibit a range of phenotypes, including unilateral renal agenesis, renal hypoplasia, and duplex systems with bifid ureters (46). In some mice, the ureters fail to separate from the mesonephric duct causing severe hydroureter and hydronephrosis. In the mice whose ureters did connect to the bladder, VUR was often observed demonstrating that the UVJ did not develop properly. Analysis of young mutant embryos demonstrated that at E9.5, some mesonephric ducts did not reach the cloaca and at E11, ureteric buds were often smaller, suggesting that they were either delayed or abnormal in their development (46). This mouse model shows that *Lim1*, which is required for the specification of the intermediate mesoderm, is also required for extension of the mesonephric duct, induction of the ureteric bud, and separation of the ureter from the mesonephric duct (46).

3. Agtr2$^{-/-}$: *Agtr2* encodes the angiotensin type II receptor that is important during kidney and urinary tract development. It is expressed in the metanephric mesenchyme at the start of kidney development and later it is expressed in the undifferentiated mesenchyme surrounding the ureter (118, 216). One important role of *Agtr2* is to promote apoptosis of mesenchyme that has not been induced by the ureteric bud (216). Consequently, *Agtr2*$^{-/-}$ mutant mice have reduced apoptosis surrounding the ureter and have a higher density of undifferentiated mesenchyme cells in their ureters (216). *Agtr2*$^{-/-}$ mice exhibit a range of phenotypes including double ureteric buds that are more cranial than normal, renal agenesis, renal hypoplasia, duplex systems, VUR, obstruction, and hydroureter (117, 118, 216). These phenotypes may be a result of either an expanded *Gdnf* expression domain or increased sensitivity of the mesonephric duct to GDNF protein.

4 and 5. Upk2$^{-/-}$ *and Upk3*$^{-/-}$: Uroplakins are proteins that make up the urothelium, a specialized impermeable barrier that lines the bladder, ureter, and renal pelvis and comes in contact with urine (93). Four major uroplakins herterodimerize to form specialized epithelial plaques on the surface of the urothelium (93). Their expression and function during development has not been reported, although both *Upk2* and *Upk3* knockout mice develop small epithelial plaques, hydronephrosis, VUR, obstruction, and

renal failure (93, 94). *Upk3*$^{-/-}$ mice also develop an urothelium that is leaky and ureteric orifices that are enlarged (93). These large ureteric orifices are an indication of an abnormal UVJ. It is not known whether the urothelium provides some sort of structural integrity to the UVJ once it is formed, or whether the presence of the urothelium impacts on how the ureter separates from the mesonephric duct and inserts into the bladder.

These mouse models provide the first direct evidence that VUR has a developmental origin. The ureteric bud is abnormal in three of the mouse models: it is caudally shifted in *Hoxb7/Ret*$^{+/-}$ embryos, it is duplicated and cranially shifted in *Agtr2*$^{-/-}$ embryos, and it is smaller in *Lim1*$^{-/-}$ embryos. The genes disrupted in these mice are also expressed during kidney and urinary tract development. *Ret* and *Lim1* are expressed in the mesonephric duct and ureteric bud (46, 63), *Agtr2* is expressed in the surrounding metanephric mesenchyme (118), and uroplakins are expressed in the urothelium from E15 onward (89). These mouse models demonstrate that the disruption of genes that are important for normal kidney and urinary tract development can lead to the many features of CAKUT, including VUR and malformed kidneys. Interestingly, all of these genes, with the exception of *Lim1*, have been associated with VUR in humans (216, 221-223). This will be further discussed in section 1.10. Identifying and studying mouse models of VUR will therefore provide insights into the developmental mechanisms that lead to VUR in humans.

1.8 *Pax2*

PAX2 is a paired-box transcription factor that belongs to the *Pax* gene family (51). It is expressed in the three serial kidneys, the urinary tract, the genital tract, the central nervous system, the ear, and the eyes, and is critical for the development of each of these structures (51, 224-227). During kidney development, *Pax2* is expressed in the mesonephric duct, the ureteric bud, and in the mesenchyme that is induced to epithelialize into a nephron (51, 228, 229). The role of *Pax2* during kidney development has been extensively studied (107, 114, 230), but the role of *Pax2* during urinary tract development has never been described. Chapter II of this thesis describes the urinary tract defects observed in heterozygous *Pax2* mice (68).

The *PAX2* gene is located on human chromosome 10q24 (mouse chromosome 19) and has 12 exons that encode a paired-box domain, an octapeptide domain, a partial homeodomain, and a transactivation domain (51, 53, 231). The paired-box domain is a DNA-binding domain that is evolutionarily conserved between zebrafish, fruit flies, chicks, quails, mice, rats, and humans (224, 232). The homeodomain encodes a second DNA-binding domain while the function of the octapeptide is not clear (233). The octapeptide is presumed to bind to other proteins that are part of the PAX2 transcriptional complex (233). The transactivation domain, located at the C-terminus of the protein, is responsible for carrying out the transcriptional regulation of target genes (233).

1.8.1 *Pax* gene family

Pax2 belongs to a family of nine *Pax* genes that are expressed in a distinct spatio-temporal expression pattern and are involved in anterior-posterior segmentation during development (51, 234). The nine *PAX* genes arose from a series of duplications that occurred during vertebrate evolution (235). They are organized into 4 distinct groups based on their structural similarities and whether they contain an octapeptide domain and/or a complete homeodomain (53). Group I includes *Pax1/9*. Group II includes *Pax2/5/8*. Group III includes *Pax3/7*. Group IV includes *Pax4/6*. Of the nine genes, *Pax2*, *Pax8*, and *Pax3* are expressed during kidney development. Both *Pax2* and *Pax8* are expressed by the developing mesonephric duct and ureteric bud and are required for the development of these structures (42, 53). *Pax3* is expressed in the metanephric mesenchyme and the mesenchyme surrounding the ureter, although its function during development is still unknown (236, 237).

Five of the nine *PAX* genes have been shown to cause rare autosomal dominant developmental disorders in humans: *PAX2*, *PAX3*, *PAX6*, *PAX8,* and *PAX9* (238). *PAX2* will be described below and in Chapter II. *PAX3* mutations have been associated with Waardenburg syndrome, which is characterized by pigmentation defects (e.g. white patches of hair) and hearing loss (239, 240). Mouse studies have demonstrated that *Pax3* is expressed in neural crest cells and melanocytes (53). *Pax3* deficient mice have severe neural tube defects and have white spotting on their abdomen, tail, and feet due to abnormal migration of neural crest cells (241). Although *Pax3* is expressed in the

developing kidney, no renal malformations have yet been reported in humans or in mice. *PAX6* mutations cause aniridia, which is characterized by severe hypoplasia of the iris and the retina and cataracts (115, 242). Mouse studies have demonstrated that *Pax6* is expressed in the developing visual system and while homozygous *Pax6*$^{-/-}$ mice never develop eyes, heterozygous mice have iris hypoplasia and cataracts (115, 243). *PAX8* mutations have been associated with congenital hypothyroidism (244). Mouse studies have demonstrated that *Pax8* is expressed in the thyroid and in the developing kidney (235). Although *Pax8*$^{-/-}$ mice exhibit thyroid gland hypoplasia, they do not exhibit a renal phenotype, which is hypothesized to occur because *Pax2* compensates for the loss of *Pax8* in the kidney (235). *PAX9* is involved in the development of the tooth bud and mutations in *PAX9* have been identified in patients with oligodontia, or tooth agenesis (245).

Although each of these aforementioned disorders is caused by mutations in a different *PAX* gene, one thing is certain: the amount of PAX protein is critical for development. Each of these disorders is caused by haploinsufficiency of a PAX protein, demonstrating that expression from both alleles is required for normal development to occur. Studies using *Pax6* transgenic mice have demonstrated the importance of *Pax* gene dosage (115). Increasing the *Pax6* gene dosage to almost 10-times the normal level causes eye abnormalities similar to those observed during *Pax6* haploinsufficiency (115). Furthermore, decreasing the dosage of *Pax6* to be in between that of heterozygous and wildtype mice causes an intermediate phenotype of eye abnormalities: instead of developing small eyes and cataracts, these transgenic mice only exhibited iris hypoplasia (115). A similar situation has been observed in humans (115). A patient with a mutation in the C-terminal end transactivation domain of *PAX6* lost only 10% of the protein's transactivation capacity and developed a mild form of Aniridia that did not include iris hypoplasia. These studies demonstrate that there is a critical level of PAX transcription factor that is required for normal development to occur. It is hypothesized that when these transcription factor levels are too low or too high, proper regulation of downstream target genes fails to occur thereby affecting normal development (115).

1.8.2 *PAX2* mutations and Renal-coloboma syndrome

Renal-coloboma syndrome (RCS) is a rare autosomal dominant condition caused by heterozygous mutations in *PAX2* (246, 247). The exact incidence of RCS is not known, but only a few dozen patients have been reported (233). Homozygous *PAX2* mutations have never been reported in humans and are presumed to be embryonic lethal. Patients with RCS present with a range of phenotypes that include: malformations of the optic nerve (optic nerve coloboma), dysplastic or hypoplastic kidneys, uretero-pelvic junction obstruction, VUR, hearing defects, genital abnormalities, and central nervous system abnormalities (246, 248, 249). Patients are also at increased risk of developing hypertension and/or renal failure (247). Phenotypic variation is extremely common such that different patients with RCS can exhibit a wide range of phenotypes, and not all exhibit extra-renal defects (230, 250). Approximately 25% of RCS patients are reported to have VUR, demonstrating that only a subset of patients develop urinary tract abnormalities (233).

The majority of mutations identified in patients with RCS are present in the 5'-end of the *PAX2* gene (N-terminal end of the protein) (251). Many of the *PAX2* mutations and sequence variants that have been identified are recorded in an online database (251). The majority of these mutations occurs in the paired-box domain and are deletions or insertions that result in frameshift mutations (250-252). Other mutations include missense mutations and nonsense mutations, but all are predicted to result in either decay of the mutant mRNA or a non-functional PAX2 protein that is truncated or unable to bind DNA and transactivate target genes (251). Despite the identification of these mutations, the clinical outcome of RCS cannot be predicted, as there is no evident correlation between *PAX2* genotype and RCS phenotype. Figure 1.12A illustrates some of the most common *PAX2* mutations that are associated with RCS (251).

1.8.3 *Pax2* mouse models

Three *Pax2* loss-of-function mutants exist: the *Pax2* knockout mouse (52), the *Krd* mouse (253), and the $Pax2^{1Neu}$ mouse (114). All three of these mouse models exhibit kidney and eye defects in the heterozygous state that resemble RCS.

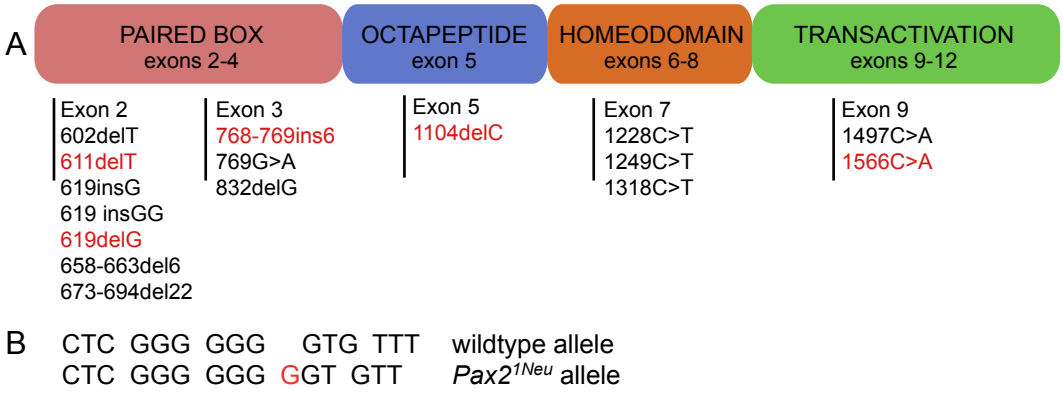

Figure 1.12: *PAX2* gene structure and mutations

(A) The PAX2 protein is encoded by 12 exons and has a paired box domain, an octapeptide domain, a partial homeodomain, and a transactivation domain. The majority of mutations identified in the *PAX2* gene occur in the paired-box DNA-binding domain. The most common mutation is the 619insG that occurs in a homonucleotide tract of 7 Gs that results in a frameshift mutation and a premature stop codon. The majority of the mutations are deletions or insertions, with a few missense and nonsense mutations. All known disease-causing mutations occur in exons and are predicted to result in non-functional proteins. The missense mutation 1497C>A in exon 9 is associated with isolated renal hypoplasia and does not have any of the extra-renal features of Renal-coloboma syndrome (RCS). Interestingly, the occurrence of VUR is not associated with any specific PAX2 mutation. The mutations that have been identified in patients with VUR are shown in red. **(B)** The *Pax2*^{1Neu} mouse model most closely represents RCS. It has the same mutation that is found in approximately 30% of RCS patients (619insG): a one base-pair guanine (G) insertion in exon 2 that results in a frameshift mutation and a premature stop codon.

1. Pax2 knockout: The knockout mouse was created with a neomycin cassette that disrupts the DNA-binding paired-box domain (52). Heterozygous *Pax2*$^{+/-}$ mice exhibit renal hypoplasia and have abnormalities of the eyes, ears, and central nervous system, similar to the defects identified in RCS (52, 226). Homozygous *Pax2*$^{-/-}$ mutants completely lack the development of kidneys, ureters, and genital tracts because the mesonephric ducts degenerate and a ureteric bud never forms (42, 52, 107). These phenotypes are not unexpected as *Pax2* is required for the differentiation of the intermediate mesoderm (52). *Pax2*$^{-/-}$ mice survive during development because the placenta regulates excretion of wastes and maintains body homeostasis during embryogenesis, but die shortly after birth. Homozygous mutants completely lack *Gdnf* expression in the metanephric mesenchyme and have reduced *Ret* expression (107). *Pax2*$^{-/-}$ mesonephric duct explants that are cultured with GDNF-soaked beads are unable to respond to GDNF and are unable to form a ureteric bud, likely due to the reduced *Ret* expression (52, 107).

2. The Krd mouse: The *Krd* mouse, which stands for kidney and retinal defects, has the entire *Pax2* gene and flanking DNA (~7cM) lost because of the insertion of a transgene (253). Heterozygous *Krd* mice develop renal agenesis, renal hypoplasia, hydroureter, cysts, and retinal defects. In contrast to *Pax2*$^{-/-}$ mice, homozygous *Krd* fertilized oocytes die prior to implantation, likely due to the deletion of a number of genes within the 7cM, including *Wnt8b*, *Hox11*, and *Fgf8* (fibroblast growth factor), which are important for regulating development (253).

3. The Pax2^{1Neu} *mouse:* The *Pax2*^{1Neu} mouse has the same mutation that is found in approximately 30% of RCS patients: a one base-pair guanine (G) insertion in exon 2 that results in a frameshift mutation and a premature stop codon (Figure 1.12B) (114). This insertion occurs in a region of seven conserved G residues that is believed to be a mutation hotspot caused by *de novo* polymerase slippage allowing for the insertion of an extra G. The mice, and humans with this same mutation, form a protein with a truncated paired-box domain, no homeodomain, and no DNA binding activity (114). *Pax2*$^{1Neu+/-}$

mice have unilateral renal agenesis, hypoplastic kidneys, fewer nephrons, and renal cysts (230, 254).

1.8.4 *Pax2* and its role during kidney development

Pax2 has been shown to be important for branching morphogenesis by preventing apoptosis in the ureteric bud (254). When cells derived from the inner collecting ducts of mice are grown *in vitro*, they normally exhibit branching morphogenesis (254). When these same cells are transfected with an anti-sense sequence to *Pax2*, the cells undergo apoptosis and tubule formation is impaired (254). Similarly, $Pax2^{1Neu+/-}$ kidneys show increased apoptosis in the collecting ducts, demonstrating that PAX2 is involved in preventing apoptosis of ureteric bud-derived cells (254). To further demonstrate that apoptosis has an important role during kidney development, mice expressing a pro-apoptotic gene under the control of the *Pax2* promoter were generated (255). These mice exhibit a similar phenotype to $Pax2^{1Neu+/-}$ mice: they have retinal defects and reduced branching morphogenesis that results in hypoplastic kidneys with fewer nephrons (255). These studies have shown that the survival of the ureteric bud is dependent on the dose of PAX2. Similarly, having too much PAX2 also causes a phenotype. Mice that constitutively express *Pax2* develop dilated proximal tubules and multiple cysts in their kidneys (256).

The role of PAX2 as a transcription factor is to regulate the transcription of target genes, however, only a handful are known, including *Gdnf*, *Ret*, *Gata3*, *Wt1*, *Wnt4*, *Sfrp2* (secreted frizzled-related protein 2), and *Naip* (neuronal apoptosis inhibitory protein) (101, 107, 257-261). Because the amount of PAX2 protein is hypothesized to be critical in determining affinity of PAX2 to its target genes (115), it is not surprising that haploinsufficiency causes such a severe phenotype. Abnormal kidney development may be a manifestation of how PAX2 regulates the expression of each of these downstream targets, which have their own important roles during kidney development.

1.9 Nephron number

I have already introduced the idea that while many patients with VUR have malformed kidneys, as many as 20-67% of patients with VUR have kidneys that appear

normal on ultrasound or DMSA scan (167, 202-205, 262-264). These "normal" kidneys may be completely normal or they may be mildly hypoplastic with a nephron deficit in the absence of an obvious renal malformation (137, 230, 265). This latter group of patients is of great interest because it is presumed that they too are at risk of developing hypertension and/or end-stage renal disease. From autopsy studies, we know that individuals with fewer nephrons are at an increased risk of developing hypertension and chronic renal failure (266-268). Since patients with VUR/reflux nephropathy can also develop hypertension and/or chronic kidney disease (7, 8), we speculate that patients with VUR and renal hypoplasia are those that are at greatest risk of developing these complications later in life.

From animal studies, we know that abnormal development of the ureteric bud can lead to the formation of hypo/dysplastic kidneys with fewer nephrons in addition to a urinary tract defect (24, 46, 68, 118). Hypoplastic kidneys can arise either because the metanephric mesenchyme cannot support nephrogenesis or because the ureteric bud does not undergo normal branching morphogenesis to induce a sufficient amount of nephrons (76, 157). A review of the literature that describes the importance of nephron number in humans and in rodents is presented below. The study of nephron number in inbred mice will be the focus of chapter III of this thesis.

1.9.1 Nephron number variation in humans

Nephron number varies considerably in humans such that a single "normal" kidney can have anywhere from 200,000 to over 1 million nephrons (269, 270). Although this range in nephron number is often referenced, the data for these nephron estimates actually comes from kidneys from autopsies of individuals with a wide range of ethnicities and ages. It is currently not possible to estimate nephron number in living individuals, since nephron counts can only be obtained from kidneys after autopsy or nephrectomy (271). It is therefore unclear if this variation represents the "normal" human population or whether individuals with undiagnosed renal disease are also represented. It has been hypothesized that individuals on the lower end of this nephron number spectrum are at increased risk of developing hypertension and chronic kidney disease (266, 267, 272).

From studies on fetal autopsy specimens, it has been estimated that nephrogenesis in humans ends by 36 weeks of gestation (273). No new nephrons are able to develop postnatally, therefore, the number of nephrons an individual is born with is the most nephrons an individual will have for life (273). However, nephron number does decrease with age, suggesting that nephrons are lost either due to aging and/or disease (274, 275). It is still unclear whether the large variation in nephron number in humans is a reflection of normal human variation, or whether it is a result of a congenital nephron deficit arising *in utero* (268).

1.9.1.1 Correlation between nephron number and hypertension

In the 1980s, results from epidemiological studies suggested that individuals with low birth weight are at increased risk of developing hypertension later in life (276). More recently, it has been demonstrated that infants below the 10^{th} percentile in birth weight have smaller kidneys and fewer nephrons (277). Together, these results suggest that there is a congenital origin to both nephron number and disease susceptibility; infants with low birth weight are at increased risk of developing hypoplastic kidneys with fewer nephrons and therefore are at increased risk of developing hypertension later in life. It has therefore been hypothesized that impaired kidney development links reduced nephron number and the risk of acquiring renal disease (e.g. hypertension).

Other evidence supporting the hypothesis that reduced nephron number is associated with hypertension comes from observations of patients with unilateral renal agenesis and/or patients that have had a kidney removed following a nephrectomy (126). The 50% reduction in nephron number is associated with a higher incidence of hypertension in this group of patients (126). The correlation between low nephron number and adult-onset hypertension has also been studied in Caucasians and shows that hypertensive Caucasians have on average 46% fewer nephrons than normotensive controls (266). However, in this latter study, it is not known if the nephron deficit is congenital in origin or acquired secondary to hypertension.

1.9.1.2 Low nephron number and glomerular/cortical hypertrophy

The total filtration surface area of the kidney is dependent not only on the number of nephrons, but also on the size of the glomeruli as they are the sites of filtration (78). The kidney filters a human's blood volume as many as 300 times a day (40). The fewer nephrons an individual has, the less efficient the kidney is at excreting and absorbing solutes. Because the kidney is unable to regenerate new nephrons, the remaining glomeruli increase their filtration rate and undergo hyperfiltration. In response to hyperfiltration, hypertrophy of the remaining glomeruli occurs to compensate for the loss in filtration surface area and to maintain the filtration capacity of the kidney (278).

Hypertrophy can be deleterious as enlarged glomeruli are more susceptible to sclerosis (glomerulosclerosis), which is characterized by the thickening or scarring of glomeruli (275). Not only can the remaining glomeruli increase in volume by as much as 50%, but the total kidney can increases in weight by as much as 50% as well (78, 278). This increase in kidney size is commonly seen in cases of unilateral renal agenesis in which the remaining kidney increases its renal mass (127).

Clinically, hyperfiltration of glomeruli manifests as proteinuria, in which proteins such as albumin are detected in the urine (138). Interestingly, abnormal urinary protein excretion is common in individuals with hypertension, and this may be a manifestation of reduced nephron number (138). A kidney with fewer nephrons that undergo hypertrophy may be unable to adapt to hyperfiltration such that the nephrons become limited in their ability to efficiently excrete solutes (138). One example of this is the regulation of sodium; during hyperfiltration, sodium excretion should increase, but this may be impaired with significant nephron loss such that sodium accumulates in the body and in turn causes salt-induced hypertension (78, 279).

1.9.1.3 Markers for nephron number

Counting nephrons is technically demanding and currently, all estimates of nephron number rely on examination of postmortem kidneys (271). In order to predict nephron number in living individuals, nephron number has been correlated with a number of factors. Positive linear relationships have been demonstrated between nephron number

and birth weight (269, 280), height or body surface area in adults (267), and kidney weight or volume (274). In addition, correlations have been demonstrated between kidney volume and body surface area or body weight at birth (272), as well as between kidney weight and body surface area in both children and adults (275, 281). Inverse relationships have also been demonstrated between glomerular volume and birth weight (280), as well as between glomerular volume and nephron number (269, 275, 281), suggesting that increased glomerular volume is a marker for low nephron number.

Although these aforementioned studies each test a different relationship, together they suggest that larger birth weights or body surface areas are associated with larger kidneys that have more nephrons. Because each of the factors that have been correlated with nephron number is easier to obtain than nephron number itself, investigators have used these factors as markers for nephron number. Furthermore, markers for nephron number, such as birth weight, have been found to correlate with diseases like hypertension and chronic renal failure, suggesting that nephron number either is associated with these diseases or is a risk factor predisposing to these diseases (276, 282, 283).

We must keep in mind that while these studies are interesting, they also have their limitations. They include data from children and adults, the study populations are often of different ethnicities, and only a limited number of these studies have actually estimated nephron number. Most have made correlations using kidney weight and kidney volume, have assumed that smaller kidneys have fewer nephrons, and have ignored the possibility that some kidneys may actually be hypertrophied.

Despite these "positive" associations, other reports have shown that there is no relationship between nephron number and susceptibility to hypertension or chronic renal failure (275, 283). Studies have also shown that there is no correlation between nephron number and kidney weight, body weight, or adult height (269, 281), or between nephron number and body surface area in adults despite the fact that body surface area correlates with kidney weight (274, 275). Reports have also failed to demonstrate an inverse correlation between nephron number and glomerular volume (274, 281). This leads us to question whether using these markers as surrogates for nephron number is appropriate and whether nephron number is truly a risk factor for renal diseases.

1.9.1.4 Genetic and environmental influences on nephron number

Certain ethnic groups have high incidences of chronic kidney disease and/or hypertension (267, 272, 281); therefore, these groups have been investigated to determine if reduced nephron number is a risk factor for developing these diseases. Australian Aboriginals have higher rates of proteinuria, hypertension, and end-stage renal disease compared with Australian non-Aboriginals (267). African Americans and the Senegalese population also have a higher incidence of hypertension and chronic kidney disease compared to White Americans or control populations, respectively (281, 283). When kidneys from autopsy were examined for nephron number, Australian Aboriginal had 30% fewer nephrons and glomerular volumes that were 27% larger (267, 272). However, both the African American and Senegalese groups did not have fewer nephrons compared to controls (269, 281, 283). Although reduced nephron number appears to be a risk factor for hypertension in White Americans (266) and Australian Aboriginals, the results obtained for the other ethnic groups suggest that nephron number may not be the only factor predisposing to hypertension and kidney disease. It is therefore possible that there are differences in the pathogenesis of hypertension and kidney disease in different ethnic groups.

An unfavorable intrauterine environment has also been shown to affect kidney development and nephron number (284). Environmental factors that influence nephron number *in utero* include: exposure to glucocorticoids, insufficient Vitamin A, and protein malnutrition (284). Infants that have died within the first year of life from intrauterine growth retardation have up to 35% fewer nephrons than controls (285). Populations known to be Vitamin A deficient, such as the Indian population, have a high incidence of hypertension (106). A pilot study on this population showed that low levels of maternal Vitamin A are associated with a decrease in kidney volume (106). This suggests that Vitamin A deficiency may be a risk factor for subtle renal hypoplasia and low nephron number, thereby increasing an individual's risk of developing hypertension. From rodent studies, we know that Vitamin A directly regulates the *Gdnf/Ret* signaling pathway and branching morphogenesis (102, 286). It is therefore likely that many of these

environmental factors may impact kidney development by modifying the regulation and/or expression of developmental genes.

1.9.2 Nephron number variation in rodents

Nephrogenesis in rats and mice differs from humans in that it is not complete prenatally, but continues postnatally until a few days or few weeks after birth (287, 288). Despite this difference, rodent models have been used to examine the relationship between a reduction in nephron number and the development of renal damage, hypertension, and/or chronic renal disease. In one rat model, a 20% decrease in nephron number is sufficient to induce glomerular hypertrophy and proteinuria (289). Rodent models can also be examined during development to determine whether impaired nephrogenesis or impaired branching morphogenesis contributes to a reduction in nephron number and renal hypo/dysplasia. To give an example of the impact of branching morphogenesis on nephron development, a 2% decrease in ureteric bud branching in a mouse kidney can reduce nephron number by a drastic 50% (290).

1.9.2.1 Rodent models of low nephron number and hypertension

Experiments in rats have demonstrated that the removal of one kidney and 2/3 of the remaining kidney (5/6th nephrectomy) results in hypertension and compensatory hypertrophy of the remaining glomeruli because of hyperfiltration and glomerulosclerosis (291, 292). Similarly, rats that have undergone a uninephrectomy, which is a less drastic loss of kidney tissue, also develop hypertension by 8 weeks of age and glomerulosclerosis by 20 weeks of age (293). These studies demonstrate that a large loss of nephrons in rats is sufficient to result in hyperfiltration and hypertension.

Rat models that develop hypertension without the removal of kidney tissue have also been studied. The spontaneously hypertensive rat (SHR) is a strain of rat that develops hypertension within the first few months of age (294). It was shown that the SHR strain has 14% fewer nephrons by 3 months of age when compared to a normotensive rat strain, suggesting that the nephron deficit is associated with hypertension (294). Interestingly, despite the nephron deficit, the SHR strain did not show evidence of glomerular hypertrophy, and the reason for this remains unknown

(294). A follow-up study crossed the SHR rat with a normotensive rat to generate intercross progeny to determine whether nephron number and hypertension segregated together as phenotypes in the offspring from this cross (295). Interestingly, the intercross progeny with reduced nephron number were not those that developed hypertension (295). This demonstrates that nephron number is not associated with the onset of hypertension in the SHR strain and that the mechanisms that lead to low nephron number and hypertension may actually be different. This also suggests that the lack of glomerular hypertrophy in the SHR strain may not be entirely unexpected as the nephron deficit is not sufficient to induce hyperfiltration in the SHR rat.

The Munich Wistar Frömter (MWF) rat is another model of low nephron number that exhibits a 30-50% reduction in nephron number in addition to hypertension, proteinuria, and glomerulosclerosis (296). Genetic studies on the MWF rat identified two loci on chromosomes 6 and 8 that are significantly associated with early onset-proteinuria (297, 298). As for the SHR rat studies, if a nephron deficit is responsible for the onset of proteinuria, then the two phenotypes should segregate together. A chromosome substitution strain was therefore created such that chromosome 8 from the SHR strain was inserted into the MWF rat genome (299). In contrast to what was expected, the chromosome substitution strain did not exhibit proteinuria, although it retained its nephron deficit, suggesting that the nephron deficit is not associated with the development of proteinuria in MWF rats (299).

The SHR and MWF rats demonstrate that although a reduction in nephron number may appear associated with hypertension or proteinuria at first, further genetic studies on these rats have clearly shown that the nephron deficit and the onset of kidney disease phenotypes are actually caused by different genetic mechanisms. The advantage of using rodent models of low nephron number is that they can be bred to generate these experimental crosses to determine if nephron number really is a risk factor for kidney disease, something that cannot be done in humans. Although a nephron deficit is associated with hypertension in some humans and rats, specifically those with a solitary kidney or after nephrectomy, it appears that this may not always be the case (126, 291, 293). Both the SHR and MWF rat studies correlate with the results obtained from the African American and Senegalese populations that have a high incidence of hypertension

and chronic renal failure, but no decrease in nephron number (269, 281, 283). Additional studies need to continue to examine the relationship between nephron number, hypertension, and chronic kidney disease to better understand the role of nephron number on disease onset and progression.

1.9.2.2 Genetic and environmental influences on nephron number

Much of our understanding of the molecular mechanisms that lead to low nephron number has come from animal models with mutations in genes that are expressed during kidney development. Mice with mutations in *Fgfr2* (fibroblast growth factor receptor 2), *Pax2*, and *Gdnf* all exhibit impaired branching morphogenesis that leads to renal hypoplasia and a nephron deficit (292, 300, 301). Mice heterozygous for $Gdnf^{+/-}$ have kidneys that are 25% smaller with 30% fewer nephrons. By adulthood, the mice develop glomerular hypertrophy and hypertension (292, 302). Heterozygous $Pax2^{1Neu+/-}$ mice have kidneys that are 20% smaller with 40% fewer nephrons, and have reduced renal function as measured by increased serum Cystatin C levels (230, 300). Conditional knockouts mice that delete *Fgfr2* specifically in the ureteric bud have kidneys that are 35% smaller with 24% fewer nephrons, and also develop hypertension (301, 303). These mouse models demonstrate that genes that regulate kidney growth and nephron formation are important in determining nephron number, kidney size, and possibly risk of hypertension.

Environmental influences, including maternal diet and the intrauterine environment, can further impact kidney and nephron development in rodents. Exogenous administration of retinoic acid to rat kidney explants increases nephron formation in a dose-dependent manner by increasing branching morphogenesis (304). Pregnant rats injected with supplemental retinoic acid deliver pups that have on average 21% more nephrons (105). Conversely, Vitamin A deficiency during pregnancy in rats causes a decrease in *Ret* expression, kidneys that are 30% smaller, and a 20% reduction in nephron number (105). The administration of gentamicin, an antibiotic, to pregnant mice inhibits normal branching morphogenesis, thereby reducing nephron formation (305). Intrauterine growth retardation induced by partial uterine artery ligation or by feeding pregnant rats a low protein diet causes a 40% and 52% reduction in kidney weight, and a 37% and 19%

reduction in nephron number, respectively in the pups (287, 289, 306, 307). Lastly, one rat model of naturally occurring low birth weight develops a 20% decrease in nephron number, glomerular hypertrophy, and proteinuria (289).

In addition to environmental influences that impact kidney development and nephron number, the combination of genetic and environment appears to be equally important. Evidence from inbred mouse strains reveals that some strains, like C57BL/6J, are more susceptible to developing smaller kidneys caused by maternal dietary restriction when compared to other strains, like A/J (308). Although nephron number was not estimated in this study, it is hypothesized that the smaller kidneys develop fewer nephrons because of impaired kidney development. This demonstrates that different genetic modifiers make certain mouse strains more sensitive to nutrient restriction and this can impact kidney development and nephron formation.

The genetic background of a mouse strain has also been shown to be important in determining whether a nephron deficit will lead to glomerulosclerosis or not. Because glomerulosclerosis occurs in response to glomerular hypertrophy (275), it is hypothesized that a nephron deficit is sufficient to predispose to glomerulosclerosis. The oligosyndactylism (*Os*) mouse is a radiation-induced mutant that has oligosyndactyly, renal hypoplasia, a 50% reduction in nephron number, and develops glomerular hypertrophy and glomerulosclerosis by three months of age (309, 310). However, when the *Os* mutation is bred on different mouse genetic backgrounds, the pathological lesion of glomerulosclerosis only develops on a ROP genetic background but not a C57BL/6J genetic background (309, 310). This suggests that the C57BL/6J mouse genome has a modifier gene(s) that protects against the development of glomerulosclerosis despite the severe nephron deficit.

1.9.3 Methods to estimate nephron number

Marcello Malpighi, a doctor in the late 17th century who was interested in physiology and anatomy, was the first to discover glomeruli (311). He described Malpighian tubules, the primary excretory tubules of insects that function like a nephron, and he also described human glomeruli, although he only speculated about their function (311). By the early 19th century, many investigators were interested in postnatal growth

of the kidney and in the number of glomeruli (288). In 1917, serial sections from a whole rat kidney were made and each glomerulus was exhaustively tracked such that one of the first absolute nephron counts for an adult rat kidney was obtained (and estimated at 30,000 glomeruli per kidney) (288). After this, it became evident that nephron counting was extremely technically demanding; it is time-consuming and limited by the availability of whole kidney samples. Therefore, methods to estimate total nephron number from a sub-sampling were developed. These methods count glomeruli because they are large, are easy to identify, and are easy to isolate physically (311). Using these estimation methods, a single kidney from a mouse has anywhere from 10,000-30,000 nephrons, a rat kidney has 25,000-45,000 nephrons, while a human kidney has 200,000 to over 1 million nephrons (277, 312-314).

One method to estimate nephron number is the acid-maceration technique (277, 311). This method is based on the principle that the Bowman's capsule, an epithelial layer that surrounds the glomerulus, is resistant to acid (277). Mechanical disruption of kidney tissue by maceration in acid causes the kidney to dissolve, but the glomeruli are preserved in solution. The glomeruli can then be counted in aliquots of known volume, and an estimate of nephron number can be made. One limitation of the acid-maceration technique is that it assumes that all glomeruli survive the maceration equally, but the technique can be biased depending on the extent of mechanical injury (311). A more precise technique was developed that isolates individual glomeruli with the help of magnetic beads (313). The magnetic beads are perfused into mouse hearts and become trapped in glomeruli. The kidney tissue is then digested and the individual glomeruli are isolated for counting with the help of a magnet (313). It is estimated that this technique is able to isolate 97% of all glomeruli in a kidney.

The most widely used method to estimate nephron number is the physical disector/fractionator method (311, 315). It is based on stereology, a mathematical method that allows 3-dimensional objects, like glomeruli, to be counted in a 2-dimensional setting (311, 315). For this method, a whole kidney or a known fraction of a kidney is paraffin embedded and serially sectioned. Adjacent section pairs are compared at regular intervals (e.g. every ten sections) so that glomeruli that appear on one section, but not the other, are counted (311, 312). This method is based on the principle that if the number of

glomeruli in a fraction is known, then the total number of glomeruli in the original sample can be estimated (312). The following formula estimates total nephron number: Nglom= f x 0.5 x NN; where f is the fraction of the kidney that is sampled, 0.5 is a correction factor that takes into account the fact that adjacent section pairs are compared, and NN is the number of nephrons (glomeruli) physically counted on the section pairs. The advantage of the disector/fractionator method is that it is not biased by glomerular size, shape, or frequency (273, 315). However, this method also has its limitations. Two projecting microscopes are required to be able to compare adjacent section pairs, a set-up that is often not available. Furthermore, sections obtained from paraffin-embedded kidneys may have compressed glomeruli and Bowman's capsules, making the visual identification of glomeruli difficult. This can bias the identification of glomeruli depending upon the observer. I have developed and validated a simplified version of the disector/fractionator method that does not rely on the comparison of adjacent section pairs. This method is described in Chapter III of this thesis.

1.9.4 Link between nephron number and VUR

Renal hypoplasia is associated with VUR (154) and patients with VUR are at increased risk of developing hypertension, reflux-induced scarring/nephropathy, and end-stage renal disease (7, 8, 177, 316). It has therefore been hypothesized that VUR-associated renal disease may arise from congenital renal hypo/dysplasia, injury from urinary tract infection, injury from hypertension, or injury form hyperfiltration. From nephrectomy specimens from patients with VUR and hypoplastic kidneys, over half of the kidneys demonstrate >25% nephron loss (265). However, it is not clear whether this nephron loss is congenital or acquired and whether it is associated with disease susceptibility.

One study thus far examined whether nephron number is a prognostic factor for the development of reflux nephropathy (317). Biopsy specimens from patients with VUR and reflux nephropathy were evaluated for the number of nephrons. Biopsy specimens with fewer nephrons were associated with glomerular hypertrophy, decreased renal function measured as increased proteinuria, and more severe renal scarring (317). However, what is not evident from this study is whether the patients were born with a

nephron deficit, or whether the nephron deficit was acquired subsequent to renal scarring. Nonetheless, this study suggests that low nephron number may be associated with the development of hypertension and reflux nephropathy in patients with VUR.

1.10 Genetics of vesico-ureteric reflux

I have already illustrated that congenital anomalies of the kidney and the urinary tract, including renal hypo/dysplasia and VUR, are associated with the development of hypertension and end-stage renal disease (4, 7, 8). However, the incidence of end-stage renal disease secondary to reflux nephropathy has not decreased since both medical and surgical management of VUR began in the 1960s (212, 318). Therefore, new hypotheses need to be generated to explain disease progression in patients with VUR.

Epidemiological evidence and studies on patients with VUR demonstrate that VUR can be genetic (17, 29, 32, 150, 178). It is hypothesized that if we understand the genetics of VUR, we will understand the biology behind VUR and disease progression. The discovery of genes that cause VUR may facilitate early diagnosis and identification of patients with VUR and those at risk of reflux nephropathy. As will become evident from the following sections, VUR is extremely genetically heterogeneous: mutations in a number of different genes have been associated with VUR. Chapter IV of this thesis describes the identification of a novel genetic locus that is associated with VUR in inbred mice. We hypothesize that this locus will also be important in human VUR.

1.10.1 Genetic epidemiology of VUR

The first evidence that VUR could be genetic came from case reports of affected monozygotic (identical) twins. Stephens, a doctor, described the first set of monozygotic twins with VUR and hydroureter in 1955 (319). He also described a set of dizygotic twins, in which one twin had VUR and the other twin was normal (319). From this, he hypothesized that the occurrence of VUR in monozygotic twins could be caused by a genetic determinant that affects the formation of the uretero-vesical junction (319). Subsequent reports have added to the list of monozygotic twins affected with VUR (320-323). A study of 46 twin pairs provides the strongest evidence for a genetic origin to VUR: at birth, monozygotic twins were 100% concordant for VUR while dizygotic twins

were 50% concordant (324). When older twins were examined, monozygotic and dizygotic twin concordances dropped to 80% and 35%, respectively (324). This drop in concordance may reflect the fact that VUR resolves with time. Nonetheless, the higher concordance of VUR among monozygotic than dizygotic twins supports a genetic basis to VUR.

Evidence that VUR can be genetic also comes from observations that VUR affects 1% of White American children, but 10-fold fewer Black American children (325). This suggests that ethnic differences, which may be due to genetic differences, affect susceptibility to VUR. Additional evidence that favors a genetic predisposition to VUR comes from observations of familial clustering of VUR (149, 182, 326-329). Many large, multigenerational families have been identified that are affected by VUR and/or reflux nephropathy (29, 330). From family studies, a range of inheritance patterns have been reported, including autosomal dominant with incomplete penetrance (150, 331), sex-linked (332), autosomal recessive (128, 333), and even complex (149, 182, 327). There is also an increased risk of VUR among first-degree relatives of an index patient with VUR (182, 183). Siblings of affected patients and offspring of affected parents have a 50% chance of also being affected with VUR (334, 335).

1.10.2 Complex segregation analysis of VUR

Complex segregation analysis applies statistical modeling to determine the inheritance of a trait and to estimate gene frequency for a genetic disease (336). In 1985, complex segregation analysis was performed on data from 88 families in which at least one person was affected with VUR (150). Results of the analysis concluded that VUR was most likely a complex trait. It would be caused by one major gene with autosomal dominant inheritance that would be affected by random environmental effects and would show incomplete penetrance. It was predicted that the gene would have a gene frequency of 0.16% in the population, and that 45% of gene carriers would develop VUR and/or reflux nephropathy, while 15% would be at risk of developing renal failure. This study provided the first evidence for a major susceptibility locus for VUR. Subsequent studies have attempted to identify the VUR-causing gene and are described below.

1.10.3 Strategies to identify human VUR-causing genes

To be able to identify VUR-causing genes, the VUR phenotype must be clearly defined. From human studies of VUR, VUR is phenotypically heterogeneous (29, 178, 330). As described previously, there are different ways in which patients with VUR come to clinical attention; either they present with urinary tract infections, hypertension, or reflux nephropathy, or they are identified through screening (178). Furthermore, VUR can be isolated or part of CAKUT. Many patients have two or more urinary tract abnormalities, including the co-occurrence of VUR with duplex kidneys, hypo/dysplastic kidneys, and/or renal agenesis (121, 124, 154, 331, 337-339). However, many patients with VUR have normally sized kidneys that do not show evidence of renal scarring or dysplasia. Depending on the study, as many as 20-67% of humans with VUR have normal-looking kidneys on ultrasound or DMSA scan (167, 203, 204, 262-264). It remains unknown whether these kidneys are actually normal or whether they have a subtle nephron deficit, given the limitations in determining nephron number. It is also assumed that patients with VUR and "normal" kidneys are at risk of developing hypertension, reflux nephropathy, and end-stage renal disease later in life, but this has not been well documented.

Defining VUR as a phenotypic trait is further complicated by the fact that VUR frequently resolves with time (166, 169, 340). When large multi-generational families are collected for genetic studies, older family members may never know if they had VUR as children because they were never tested for it and/or it has subsequently resolved. Furthermore, family members may have had a history of urinary tract infections, but may never have undergone a VCUG to confirm the diagnosis. Complete family histories are therefore very difficult to obtain for families with VUR and may affect the power of genetic studies (29, 31, 144).

Despite the limitations in defining VUR as a phenotypic trait, four major strategies have been used to search for VUR-causing genes in humans. The first strategy is a candidate gene approach that screens for mutations in genes that are involved in kidney and urinary tract development, genes that have been identified from mouse models of VUR, or genes that have been implicated in the pathogenesis of VUR (221, 341-346). The second strategy has taken advantage of the coincidental finding of

chromosomal abnormalities in patients with VUR. Some of these chromosomal abnormalities have been genetically characterized and have helped identify new VUR-causing gene candidates (347-350). The third approach has identified VUR-causing genes from the study of rare syndromes that have VUR in addition to many other congenital abnormalities (246, 351-354). The last approach has used whole-genome mapping as a method to search for novel loci in affected patients and families with VUR and/or reflux nephropathy (29-31, 144, 330). Together, these approaches have led to the discovery of at least 14 genes and 10 potentially interesting loci, demonstrating that VUR is an extremely genetically heterogeneous disorder.

1.10.3.1 Candidate gene approaches

Genes that have been implicated in kidney and urinary tract development, including those that are relevant in mouse models of VUR, are also important for VUR in humans.

1. AGTR2 and ACE: *AGTR2* encodes the angiotensin type II receptor, which is a component of the renin-angiotensin system that regulates vascular tone and fluid volume (355). Angiotensin is converted to angiotensin I by renin, and angiotensin I is converted to angiotensin II by ACE (angiotensin converting enzyme) (355). Angiotensin II exerts multiple physiological effects and regulates blood pressure and fluid and electrolyte balance by binding to two different receptors, AGTR1 and AGTR2 (355-357). *Agtr2*$^{-/-}$ mice have CAKUT, including VUR (118, 216), and *Ace*$^{-/-}$ mice are unable to concentrate urine and have hypoplastic kidneys with fewer nephrons and hydronephrosis (358). A number of common polymorphisms have been identified in *ACE* and *AGTR2* that are predicted to alter either mRNA stability or protein activity, including the *ACE* DD (deletion) and the *AGTR2* A1332G polymorphism (216, 359, 360). Studies have tested the association between these polymorphisms and VUR and have shown that polymorphisms in both genes occur more frequently in patients with VUR and/or reflux nephropathy than controls (216, 359, 360). These studies conclude that these polymorphisms are risk factors for the development of hypoplastic kidneys, VUR, and

reflux nephropathy (216, 359, 360). However, other studies have failed to find an association between these polymorphisms in *ACE* and *AGTR2* with VUR (361-365).

2. RET and GDNF: *RET* is a receptor tyrosine kinase important for the development of the kidney and the enteric nervous system (366). Mutations in *RET* and *GDNF* are most often associated with Hirschsprung's disease or multiple endocrine neoplasias (MEN2). Hirschsprung's disease is characterized by the absence of innervation of the lower gastrointestinal tract and is caused by a loss of RET function (367). MEN2 is often caused by ligand (GDNF)-independent constitutive activation of RET (367). There are 3 different subtypes of MEN2: familial medullary thyroid carcinoma (FMTC), MEN2A, and MEN2B (62, 367-369). Each of these subtypes is classified based on the severity of the symptoms, from least to most severe, such that patients with FMTC develop only medullary thyroid carcinomas, patients with MEN2A develop medullary thyroid carcinoma and tumors of the adrenal gland or parathyroid, while patients with MEN2B develop tumors in addition to muscle, joint, spinal, and digestive problems (62, 367-369).

Despite the importance of GDNF/RET signaling during kidney development, kidney abnormalities associated with either constitutive or loss of function *RET* mutations are not commonly reported in humans. Only one family with FMTC is reported to also have unilateral renal agenesis (368). Therefore, one study examined the prevalence of CAKUT in patients with Hirschsprung's disease and found that approximately 25% of Hirschsprung's patients have associated CAKUT (including hydronephrosis, hypoplasia, duplex kidneys, and VUR) and mutations in *RET* or *GDNF* (370). This suggests that kidney and urinary tract phenotypes associated with *RET* or *GDNF* mutations are more common than initially perceived.

Evidence from the mouse clearly indicates the importance of *Ret* during the development of the kidney, the ureter, and the UVJ (18, 24); therefore, studies have also examined if mutations in *RET* are associated with isolated CAKUT in humans (221, 371). A large cohort of French-Canadian families with VUR was tested for mutations in *RET* and a rare SNP (rs1799939G>A) was found to occur more frequently in patients with VUR than in controls (221). This SNP causes a non-synonymous polymorphism that is

predicted to create a novel phosphorylation site that disrupts RET's kinase activity, and likely impacts distal ureter maturation and the formation of the UVJ. Another study screened DNA from stillborn fetuses with unilateral or bilateral renal agenesis for mutations in *RET*, *GDNF*, and *GFRα1* (371). Up to 37% of the fetuses had mutations in *RET*, which were predicted to either abolish or constitutively activate RET phosphorylation (371). These studies support our findings on the *Hoxb7/Ret*$^{+/-}$ mouse that also develops kidney abnormalities and VUR and demonstrate that mutations in *RET* can be associated with urinary tract defects and kidney abnormalities in humans (24).

3. UPK2 and UPK3: Uroplakins are proteins that make up the urothelium that lines the ureter and the bladder (93, 94). From studies on mice, *Upk2*$^{-/-}$ and *Upk3*$^{-/-}$ knockout mice develop VUR demonstrating that uroplakins are important in either UVJ function or formation (93, 94). Subsequent studies have identified heterozygous mutations in *UPK2* and *UPK3* in humans with VUR, renal malformations, and renal failure (222, 223). However, like the *AGTR2* studies, other reports have failed to replicate these findings and demonstrate that uroplakins are not major gene candidates for VUR (341, 372-374).

4. HLA: Patients with VUR are at increased risk of developing urinary tract infections, hypertension, and reflux nephropathy (188, 189, 375). Therefore, candidate genes implicated in these processes have also been examined. The human leukocyte antigens (HLA) refers to a set of cell-surface antigens that confer host-specific immune responses to infections and other inflammatory processes, and confer susceptibility to various diseases (343, 376). HLA haplotypes have been associated with increased susceptibility to urinary tract infections, VUR, or reflux nephropathy (164, 343, 376, 377). Interestingly, each VUR family often has its own unique HLA haplotype, suggesting that these HLA haplotypes might not be causally associated with VUR, but instead might be in linkage disequilibrium with a gene that confers susceptibility to urinary tract infections and reflux nephropathy (343).

5. TGFβ1 and VEGF: Two growth factors, vascular endothelial growth factor (VEGF) and transforming growth factor β1 (TGFβ1), have been reported to have roles in the progression of a number of renal diseases. Increased VEGF protein levels have been observed in the urine of patients with reflux nephropathy (378) and elevated tissue levels of TGFβ1 have been implicated in renal fibrosis (379). Several different common polymorphisms in both *VEGF* and *TGFβ1* have been identified and the association between these polymorphisms and recurrent urinary tract infections, VUR, and reflux nephropathy was studied (345). Results showed that polymorphisms in both genes are associated with an increased incidence of urinary tract infections, VUR, and subsequent renal scarring in children (345). It was hypothesized that polymorphisms in these genes could affect protein function and subsequently have important roles in the pathogenesis or progression of VUR.

1.10.3.2 Chromosome abnormalities in patients with VUR

Chromosome abnormalities in patients with VUR have helped to identify a number of chromosome locations and candidate genes that are involved in VUR. Following karyotyping and chromosome banding analysis on patients with VUR, a number of different deletions have been identified on the following chromosomes: 11q (348), 10q26 (347, 380), 22q11 (381, 382), and 13q33-34 (349). In addition to VUR, many of the patients have other anomalies including facial dysmorphic features, low birth weights, growth retardation, developmental delays, and sometimes neurodevelopment delays (349, 380, 382). This demonstrates that in addition to the genes that are important for urinary tract development, a number of other developmental genes are deleted. On chromosome 10q26, although the gene responsible for VUR has not yet been identified, the breakpoint is adjacent to *PAX2*, *GFRα1*, *FGFR2*, and *EMX2* (empty spiracles homeobox 2), four genes that are important for ureteric bud development (347). Chromosome 22q11 is reported to contain a number of genes expressed in the ureteric bud and the developing kidney, but the specific genes have not been reported (381). Chromosome 13q33-34 has multiple genes that are expressed by the bladder and the kidney, including *EFNB2* (ephrin B2), a receptor tyrosine kinase, and *ING1* (inhibitor of growth family member 1), a growth factor, although the significance of these genes in the

development of VUR are not yet known (349). The genes within these chromosomal deletions are therefore excellent candidates for further investigation and to understand the biology of VUR.

A translocation between the Y chromosome and chromosome 3, t(Y;3)(p11;p12), was identified in a patient with high-grade VUR (350). Subsequent mapping of the breakpoint region found that the *ROBO2* gene, the gene that encodes the receptor for the SLIT2 ligand, was disrupted (350). From mouse studies, *Slit2/Robo2* signaling regulates the site of ureteric budding by inhibiting *Gdnf* such that only a single ureteric bud emerges (26). Homozygous mutant mice for either *Slit2* or *Robo2* have an expanded domain of *Gdnf* expression, which results in the formation of supernumerary ureteric buds that develop into multiple kidneys and ureters (26). The kidney and urinary tract phenotype of $Slit^{-/-}$ and $Robo2^{-/-}$ mice includes dysplastic kidneys, cysts, hydroureter, and hydronephrosis (26, 350). Heterozygous $Robo2^{+/-}$ mice exhibit a less severe phenotype, but also exhibit CAKUT including hydronephrosis, hydroureter, and a dilated UVJ (350). Although $Robo2^{+/-}$ mice have never been tested for VUR, they do develop dilated ureters that insert more laterally within the bladder wall, suggesting that the UVJ is not formed properly (350). Since *Robo2* is important for kidney and urinary tract development and is disrupted in a patient with VUR, *ROBO2* mutations were examined in a cohort of families with VUR (350). Two families with VUR, hypoplasia, and duplex kidneys were found to have novel missense mutations in *ROBO2* that were predicted to alter the ability of SLIT2 to bind to the ROBO2 receptor (350). These results demonstrate that candidate genes identified in patients with chromosome abnormalities can have roles in isolated VUR.

1.10.3.3 Rare multi-organ syndromes that include VUR

VUR in combination with other organ defects frequently co-occur as part of a syndrome. At least 29 human syndromes have been reported to include congenital abnormalities of the kidney and/or the urinary tract (17, 383, 384). Several of these syndromic forms of VUR have been informative in understanding the genetics and pathogenesis of VUR, including Renal-coloboma syndrome (RCS, which was described

previously), Branchio-oto-renal syndrome (BOR), Hypoparathyroidism, sensorineural deafness, and renal malformations syndrome (HDR), and Kallmann syndrome.

BOR is a rare autosomal dominant syndrome with an incidence of approximately 1:40,000 (352). Patients with BOR have hearing loss due to structural malformations of the outer, middle, and inner ear, branchial cysts, renal malformations that include renal hypoplasia, duplex systems, and renal agenesis, and urinary tract malformations that include VUR and obstruction (132, 352). BOR has been associated with mutations in *EYA1*, *SIX1*, or *SALL1*, which encode transcription factors expressed in the metanephric mesenchyme (351-353). As was described in section 1.4.2, EYA1, SIX1, and SALL1 work together with PAX2, which is mutated in RCS, in a common molecular network that regulates ureteric bud outgrowth (108).

HDR is an autosomal dominant syndrome associated with a number of kidney and urinary tract abnormalities, including renal hypo/dysplasia, renal agenesis, hydronephrosis, and VUR (385). The exact incidence of HDR is unknown, but only a few dozen patients have been described in the literature (354, 385-389). Haploinsufficiency of the *GATA3* gene has been shown to cause HDR (354, 385). From mouse studies, we know that *GATA3* is a genetic target of PAX2 and encodes a transcription factor that is expressed by the mesonephric duct and ureteric bud (101). This demonstrates that *GATA3* is essential for normal embryonic development of the kidney and the urinary tract.

Mice that have mutations in the genes that cause BOR and HDR display similar renal malformations as described in humans. Mice heterozygous for $Eya^{+/-}$ develop duplex systems, renal hypo/dysplasia, and renal agenesis (73). Mice homozygous for $Sall1^{-/-}$, $Six1^{-/-}$, and $Gata3^{-/-}$ develop renal agenesis because the ureteric bud is unable to develop into a kidney and ureter (101, 110, 390). Unfortunately, none of these mouse models have been tested for VUR, and the kidney and urinary tract phenotypes for heterozygous $Sall1^{+/-}$, $Six1^{+/-}$, and $Gata3^{+/-}$ mice have not yet been reported or studied. However, we can hypothesize that mice heterozygous for these genes will have urinary tract abnormalities that may include VUR.

Kallmann syndrome is another rare syndrome that affects less than 1:70,000 people in which patients have an inability to smell (anosmia), hearing loss, and optic nerve colobomas in addition to duplex kidneys and ureters, renal agenesis, and VUR

(391, 392). Kallmann syndrome has been shown to be either X-linked or autosomal dominant (133, 391). The X-linked form is caused by mutations in *KAL1* (anosmin 1), an extracellular protein expressed in the kidney and brain, while the autosomal dominant form is caused by mutations in *FGFR1*, a tyrosine kinase receptor expressed in the metanephric mesenchyme (133, 391).

Taken together, although these syndromes are rare, they demonstrate that VUR can arise from mutations in genes that are expressed during ureteric bud development. There appears to be a common molecular network, which includes the coordinated action of a number of transcription factors including *PAX2*, *EYA1*, *SIX1*, *SALL1*, and *GATA3* that regulate kidney and urinary tract development. Disruption of any of the genes in this network results in the abnormal formation of the kidney and the urinary tract and the development of VUR.

1.10.3.4 Whole-genome mapping studies of VUR

The strategy of whole-genome mapping has been powerful in identifying novel genetic loci that are associated with VUR. It is an exploratory approach that relies on identifying loci in the genome that occur more frequently in individuals with VUR versus those without VUR. The first genome-wide search for VUR-causing loci studied seven large multigenerational European families affected with VUR and reflux nephropathy (29). While some of the families showed suggestive linkage to chromosome 1p13, 12 additional loci were identified, including a region on chromosome 3 that encompasses the *ROBO2* gene. These results imply that other regions of the genome are important in conferring susceptibility to VUR in different families. Subsequently, two groups attempted to replicate these findings, but were unsuccessful in reproducing these loci, further emphasizing the genetic heterogeneity of VUR (144, 330).

The second genome-wide study examined a large cohort of Italian families with VUR, recurrent urinary tract infections, and reflux nephropathy, and demonstrated suggestive linkage to four loci on chromosomes 1p34-36, 3p12-3q24, 4q26, and 22q11-12 (31). This study was unable to replicate the linkage to the chromosome 1p13 locus, but did identify another locus on this chromosome. The locus on chromosome 3 is known to contain *ROBO2*, however, no *ROBO2* mutations were identified in these families.

The largest family study conducted thus far examined 129 Irish families with VUR and identified a novel locus on ch2q37 that reached genome-wide significance (30). Suggestive linkage was also observed at 11 additional regions, including three loci that overlap with the loci identified in the first study on chromosomes 1q, 3q, and 20p (29), and two loci on chromosomes 10q26 and 13q33 which correspond to the deleted regions that have been reported in patients with VUR and renal malformations (347, 349).

These studies are encouraging in understanding the heterogeneity of VUR since novel loci continue to be identified and some of these loci are being replicated in different studies. However, these studies also demonstrate that VUR is extremely genetically heterogeneous and that different loci/genes are likely responsible for VUR in different families. Future studies must concentrate on the genetic characterization of these loci to identify the specific genes that cause VUR. By identifying the genes within these loci, new mechanistic insight into the biology of VUR and its complications will be generated. Figure 1.13 illustrates many of the genes and the loci that have been identified from human and mouse studies.

1.11 Introduction to genetic mapping using the mouse

1.11.1 The advantage of using the mouse for genetic studies

Diseases show two main inheritance patterns: Mendelian or complex (336). Mendelian diseases are caused by mutations in a single gene and are relatively rare, such as the multi-organ syndromes, RCS, BOR, and HDR, which were described in section 1.10.3 (336, 393-395). In contrast, the majority of human diseases such as obesity, diabetes, hypertension, and chronic kidney disease actually show complex inheritance and account for a significant amount of morbidity and mortality in the population (395, 396). Importantly, mice are excellent models of complex human diseases, and mouse models of obesity, diabetes, hypertension, and chronic kidney disease have been described and studied (397-400). The mouse has therefore become a model system in which to identify and study the genes responsible for these complex diseases.

Genetics has had a major impact on our understanding of human disease as it has aimed to link genes to the biology of the disease. Unfortunately, mapping of complex diseases has been challenging; numerous susceptibility loci, or quantitative trait loci

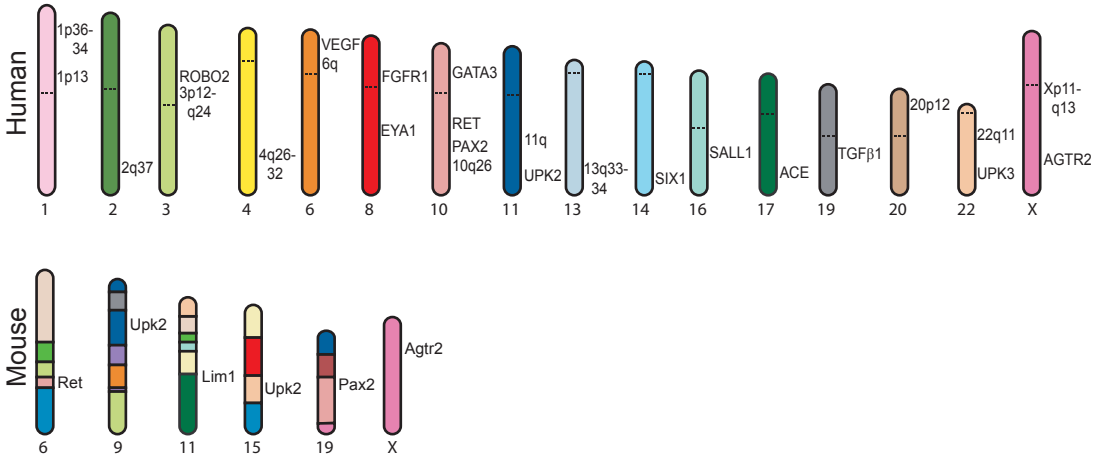

Figure 1.13: Genes and loci that are associated with vesico-ureteric reflux in humans and in mice

This figure summarizes the locations of genomic loci and of genes that have been associated with VUR in mice and humans. The upper panel shows human chromosomes while the lower panel shows mouse chromosomes. Blocks of genes that have been conserved between the human and the mouse are shown by color coding. The approximate regions of relevant genes and loci that are associated with VUR are indicated to the right of each chromosome. Of the six genes that have been associated with VUR in mice, only *Lim1* has not been associated with VUR in humans. (adapted from Murawski, 2006)

(QTL), have been found for the same disease, but the underlying genes have been difficult to identify (401). Mapping strategies in humans are limited because, not only can a disease be caused by more than one gene, but the human population is extremely genetically heterogeneous and ancestral haplotypes or mutations can cause individual studies to be influenced by the population being studied (393, 394, 396). Furthermore, many complex diseases are not only caused by common genetic variants, but are also greatly influenced by rare allele variants at multiple genetic loci, in addition to the environment (336, 396). These rare variants are not always easy to identify because current mapping techniques lack sufficient power. Because of these limitations, few genes underlying susceptibility to common complex diseases have actually been identified.

The same is true for VUR. Whole-genome mapping strategies on humans with VUR have identified many causative loci, but most of the underlying genes have not yet been discovered (32). We have therefore turned to the mouse as a model organism for mapping complex traits. Approximately 150 chromosomal rearrangements, including duplications and the formation of pseudogenes, have occurred in the mouse since it diverged from humans over 75 million years ago (402, 403). Despite this divergence, there are strong homologies between the human and mouse genomes and both species share approximately 99% of their genes (Figure 1.14) (404). In addition to the genetic similarities between humans and mice, the mouse is well suited for genetic analysis. It is a small mammal that can be housed in cages, it has a short generation time of approximately 6-8 weeks from the time the mouse is born to when it is ready to reproduce, and a single female can generate 5-10 pups per litter (405). Furthermore, large samples of genetically homogeneous populations can be examined, it can be bred to generate specific genetic crosses, and the environment in which it is raised can be controlled (394, 405).

Chapter IV describes the first report of a whole-genome mapping approach in mice with the objective to identify VUR-causing loci.

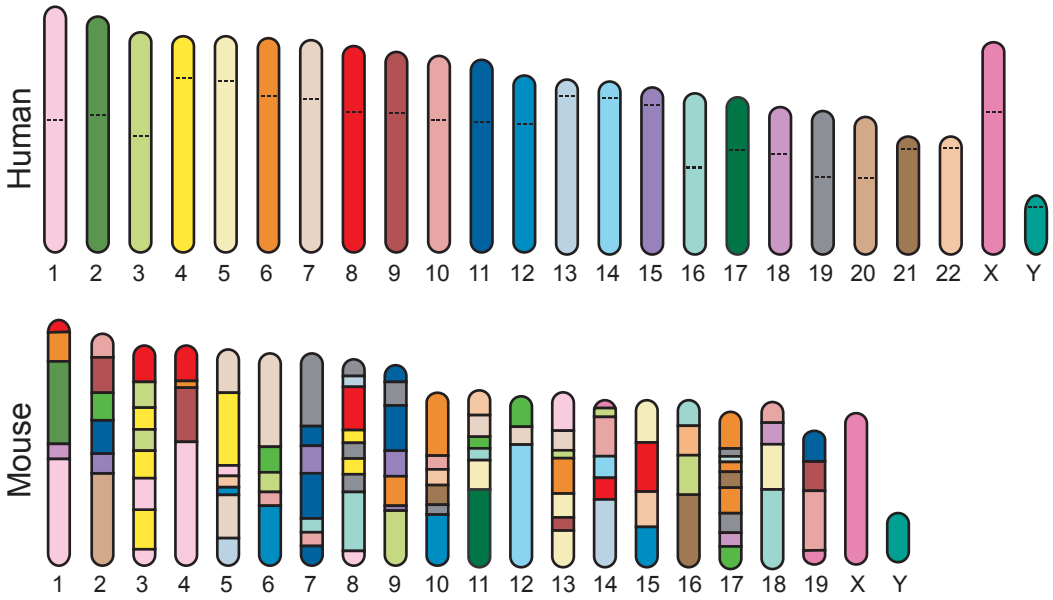

Figure 1.14: Human-mouse homology

During the evolution of the human and mouse genomes, multiple rearrangements have placed blocks of genes in different combinations within the mouse compared with the human. Approximately 150 chromosomal rearrangements, including duplications and the formation of pseudogenes, have occurred in the mouse since mice diverged from humans over 75 million years ago. The upper panel shows the human chromosomes while the lower panel shows the rearranged chromosomes in the mouse. There are strong homologies between the human and mouse genomes and both species share approximately 99% of their genes. Human and mouse homology relationships were obtained from the National Center for Biotechnology Information.

1.11.2 Inbred mouse strains are models of human diseases

Mouse genetics dates back to the eighteenth century when Japanese mice were collected for their different traits, including coat color and behavioral traits, and descriptions of the matings and the inheritance patterns of these traits were recorded in detail (406). Modern mouse genetics began in the early twentieth century when the importance of inbred mouse lines was recognized, and the breeding of the first inbred strain, DBA, began (405). Inbred mouse strains are generated by at least 20 generations of brother-sister matings until all alleles are homozygous (407). The classical inbred mouse strains used for research were developed from a limited founder population and do not represent any mouse found in the wild (405, 408). The inbred mouse strains used as laboratory mice are actually mosaics from three distinct species: *Mus musculus* (Asia), *Mus domesticus* (Europe), with a minor contribution from *Mus castaneous* (Southeast Asian) (408, 409). The first inbred mouse strain created was the DBA strain in 1909, which had the different coat color alleles, dilute (d), brown, (b), and non-agouti (a) (405, 407). Over the next decade, many of the classical inbred mouse strains that are still used in research today were created, including C57BL, C3H, CBA, and BALB/c (405, 407). To date, over 450 inbred mouse strains exist and between these different inbred strains there is a considerable amount of genetic and phenotypic heterogeneity (407, 410, 411).

Different inbred strains can vary considerably in disease susceptibility such that some strains are resistant, while others are susceptible, to developing the same diseases found in humans (400, 402, 404, 412). It has been shown that by analyzing approximately 40 different inbred mouse strains, they can exhibit the same range of phenotypic variability that is found in the human population (413). By crossing inbred strains that are phenotypically different, the genes predisposing to the underlying disease can be mapped (404). By identifying the genes that cause these diseases in mice, it is believed that the same genes, or genes in the same genetic pathway, will also confer susceptibility to the same diseases in humans (400, 402).

The phenotypic variation in inbred mouse strains is caused by the underlying genotypic variation produced by mutations that arose during the divergence of the different inbred lines (414, 415). Sequencing of the mouse genome has identified a number of polymorphisms, including microsatellites (small tandem repeats of DNA such

as dinucleotide repeats) and single nucleotide polymorphisms (SNPs) that can be genotyped (336, 403). Mapping in the mouse is therefore easily achieved, and polymorphisms that associate more frequently than expected with a disease phenotype can identify a region of the genome, or a locus, that likely contains a disease-causing gene.

In addition to inbred mouse strains, outbred mouse strains exist that are not homozygous at each locus (416). Outbred strains are often referred to as "stocks" rather than strains because they are a closed population of mice that are bred to maintain genetic variability (417). These outbred stocks are not derived from any known inbred strain but are important in animal research because they are large, easy to breed, and can produce multiple large litters compared to inbred strains (417). The CD1 mouse is an example of an outbred mouse that is commonly used because it shows more genetic and phenotypic variation than an inbred mouse (417). It is hypothesized that these outbred stocks of mice can closely resemble a genetically heterogeneous human population (416). In Chapter II of this thesis, we crossed the *Pax2*^{1Neu} mutation on a CD1 outbred background so that the *Pax2* mutation could be maintained on a genetically heterogeneous background.

Once a candidate gene is identified, the mouse allows for functional studies. The creation of transgenic and/or knockout mice can provide insight into gene function (405, 414). In summary, mice are invaluable tools that can be used to identify the underlying genetic, molecular, and developmental pathways that lead to complex genetic diseases.

1.11.3 Inbred mouse models of VUR

The first 5 mouse models of VUR that I described in section 1.7 all have mutations in genes involved in development. These mouse models provide the first direct evidence that VUR has a developmental origin. However, the first mouse model of VUR described is actually the inbred DDD mouse. This mouse model of VUR differs from the others because its gene defect has yet to be characterized, its development has not been described, and it does not have severe renal malformations. The DDD mouse is derived from the outbred dd mouse (418, 419). DDD mice were initially identified for their high incidence of hydronephrosis and were subsequently found to also exhibit VUR. Scanning electron microscopy revealed that the ureteral orifice in DDD mice is significantly larger

than control B6 mice, providing evidence for a defective uretero-vesical junction. Chapter IV describes the identification of four additional inbred mouse models of VUR.

1.11.4 Strategies to map genes using the mouse

There are a number of different genetic mapping strategies that are used in mice. The following section describes some of the strategies that are used to identify candidate QTLs and genes.

1. *Backcross and intercross*: To locate genetic loci that control a trait in inbred mice, either backcross or intercross mice are generated (405). Initially, two inbred mouse strains that are phenotypically distinct (i.e. susceptible and resistant to VUR) are crossed to create an F1 hybrid. All F1 hybrids are genetically identical as they carry one copy of a chromosome from one inbred mouse strain and the other copy from the other inbred mouse strain. These F1 hybrids are then either backcrossed to a parental strain to derive backcross mice (N2) or intercrossed with an F1 littermate to derive intercross mice (F2). N2 and F2 mice are all genetically distinct because recombination events that occur during meiosis create progeny that are mosaics of the two parental inbred strains. The analysis of genotypes derived from backcross mice is more straightforward, because these mice have only one recombinant chromosome and therefore two possible genotypes at each allele (recombinant or homozygous for one of the parental strains) (Figure 1.15) (414). In contrast, intercross mice have two recombinant chromosomes and therefore three possible genotypes at each allele (recombinant or homozygous for either of the parental strains) (Figure 1.15) (420).

Several hundred N2 or F2 progeny can be tested/screened for the phenotype of interest and genotyped genome-wide using SNPs, microsatellites, or some other genetic marker. The markers that associate more frequently than expected with a disease phenotype identify loci that harbor potential disease-causing genes (405). This is the process of determining linkage to a locus. For backcross mice, because there are two possible genotypes (recombinant and parental), a deviation from the expected 50:50 ratio of either genotype is indicative of linkage (405). Backcross and intercross mice are useful for coarse mapping and can identify a chromosome or chromosomal segment that is

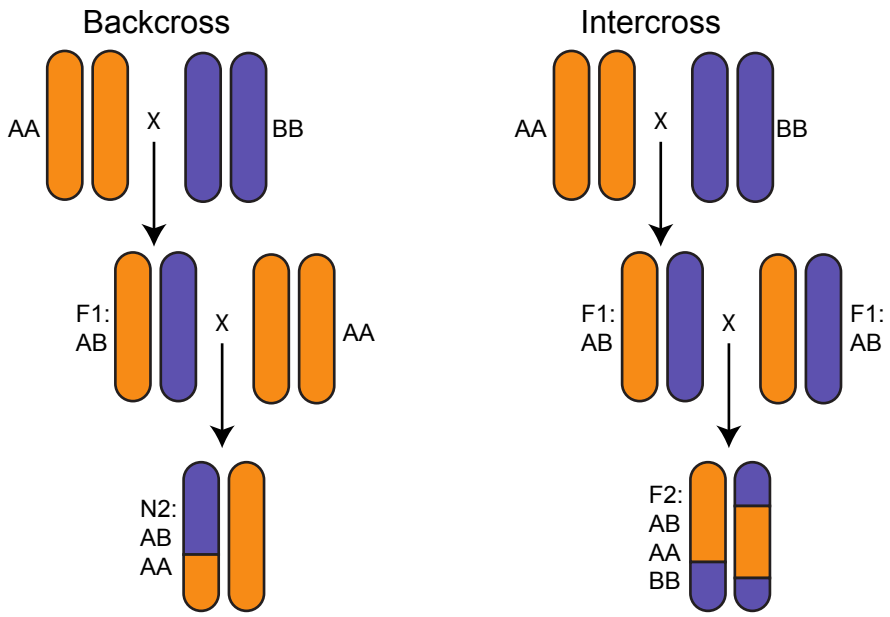

Figure 1.15: The generation of backcross and intercross mice

The breeding scheme used to generate backcross and intercross mice is shown. Two inbred mouse strains that are phenotypically distinct are crossed to create an F1 hybrid. The orange strain is homozygous AA and has the phenotype of interest (e.g. VUR). The blue strain is homozygous BB and is the strain that does not show the phenotype of interest (e.g. no VUR). All F1 hybrids are genetically identical as they carry one copy of the A chromosome and one copy of the B chromosome. To create backcross mice (N2), the F1 hybrids are backcrossed to one of the parental strains. To create intercross mice (F2), two F1 hybrids are intercrossed. Recombination events in the F1 hybrids create a chromosome that is a mosaic of the two parental inbred strains. Backcross mice have only one recombinant chromosome and therefore two possible genotypes at each allele (AA homozygous or AB recombinant). In contrast, intercross mice have two recombinant chromosomes and therefore three possible genotypes at each allele (AA homozygous, BB homozygous, or AB recombinant).

associated with a disease (399). After the initial coarse mapping reveals a locus of interest, further characterization of the locus is needed and is performed using the following crosses or methods:

2. *Recombinant inbred strains*: To narrow a large quantitative trait locus, recombinant inbred strains can be useful. They are created from an F1 intercross and subsequent brother-sister matings for 20 generations (405) (Figure 1.16A). The result is an inbred line whose genome is a random mosaic of the two parental inbred strains from which it was derived (400). Genotyping of these recombinant inbred strains reveals the regions at which recombination events have occurred. Phenotyping approximately 20 recombinant inbred strains for the disease of interest can narrow the initial locus identified (405). These recombinant inbred lines are further important because they permit a larger number of genetically identical animals to be studied indefinitely. Chapter IV analyzes the phenotypes of 10 BXH lines derived from a C3H/HeJ and C57BL/6J cross (Figure 1.16B).

3. *Recombinant congenic strains*: Recombinant congenic strains are inbred strains created by a specific breeding strategy to fix a defined chromosome segment from one inbred strain, the donor, onto the genetic background of another inbred strain, the recipient (405, 421). Recombinant congenic strains are useful because if multiple loci are responsible for a trait, each locus can be separated and the individual gene effects examined (422). To create recombinant congenic strains, an F1 hybrid between the donor and recipient strains is repeatedly backcrossed to the recipient strain (405). After only two generations of backcrossing, 12.5% of the donor genome becomes introgressed onto the recipient background, and after 10 generations of backcrossing, the donor genome is on a 99.8% recipient background (405). The creation of recombinant congenic strains can be expedited with the help of marker-assisted breeding (423). At each generation of backcrossing, the locus of interest is genotyped for informative markers for the inbred mouse strain of interest. Animals that are positive for the donor genotype are chosen for backcrossing to the recipient mouse strain.

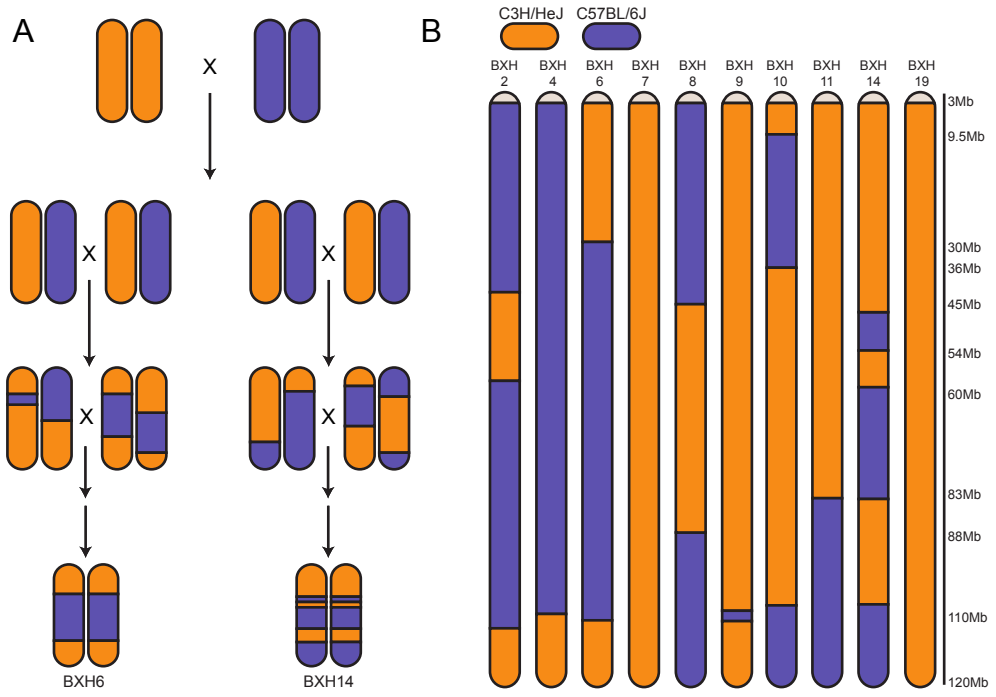

Figure 1.16: BXH recombinant inbred strains

(A) Recombinant inbred strains are created from an F1 intercross and subsequent brother-sister matings for 20 generations such that an inbred line is created whose genome is a random mosaic of the two parental inbred strains from which it was derived. Brother-sister matings ensure that all alleles are fixed to homozygosity in each line. An example breeding scheme for two recombinant inbred strains is shown. **(B)** Ten different BXH recombinant inbred strains were created by crossing C3H/HeJ and C57BL/6J mice. This figure demonstrates the mosaic structure of chromosome 12 for ten BXH recombinant inbred lines. Only one chromosome from each line is shown. Chromosome segments in blue are derived from the C57BL/6J parental strain while segments in orange are derived from the C3H/HeJ parental strain. On the right, the megabase position along chromosome 12 is shown.

4. *Chromosome substitution strains*: Chromosome substitution strains are also known as consomic strains and contain one entire chromosome from one strain on the background genome of a different strain (400). In order to cover the entire mouse genome, 21 chromosome substitution strains need to be made, 19 for each autosome, and 2 for the sex chromosomes (424). Once these chromosome substitution strains are generated, they provide a powerful yet quick method to detect the chromosomal location of a QTL (400, 405, 424).

5. *In silico approaches*: A QTL can be narrowed with the help of *in silico* mapping such that phenotypic and genotypic information is analyzed on the computer to predict chromosomal regions that regulate a disease trait (404, 409). After a QTL is identified in the mouse, the first approach is to compare this QTL with other QTLs that may have been identified in other mouse studies or even in different species like humans and rats (409). By performing comparative genomics, common regions of overlap between the QTLs will not only strengthen the association of a particular QTL with a disease, but can also narrow the QTL interval (404, 409, 425).

Another *in silico* mapping approach is to perform haplotype analysis to identify chromosomal regions that are common between inbred strains that have similar phenotypes (or chromosomal regions that differ between inbred strains that have contrasting phenotypes) (404, 409). Because inbred mouse strains are derived from a restricted number of progenitors, it is hypothesized that most inbred strains share a common ancestor (421, 426). Therefore, regions of the genome that have similar genotypes are considered as haplotypes (409). If two inbred mouse strains share a similar trait, then regions of the genome that share haplotypes are likely to contain a disease-causing gene. If a large QTL is identified, haplotype analysis can also narrow the QTL interval (409).

There are numerous online databases available that document sequence polymorphisms between inbred strains, including the Mouse SNP Miner (427) and the Mouse Phenome Database (http://www.jax.org/phenome). Sequence comparisons can identify non-synonymous sequence polymorphisms (polymorphisms that change the amino acid in a protein) (409). Genes that have documented non-synonymous sequence

polymorphisms may lead to changes in protein function. However, these databases can have errors and may be incomplete (409). Therefore, this type of *in silico* approach should help prioritize gene candidates, but it cannot rule out the involvement of other genes that do not have documented non-synonymous SNPs.

1.12 Summary of objectives

It has been hypothesized that an abnormally positioned ureteric bud along the mesonephric duct is responsible for the development of a malformed kidney and a malformed urinary tract (21, 23, 156). The objective of my research is to determine if a caudally positioned ureteric bud is associated with the development of VUR and renal malformations in mice. Since the kidney and the urinary tract both develop from the ureteric bud, we hypothesize that mutations in genes expressed by the ureteric bud or the surrounding metanephric mesenchyme can cause the ureteric bud to emerge from an abnormal location. This in turn is directly responsible for the combined kidney and urinary tract defects observed in humans and in mice.

This thesis contains three manuscript-based chapters. The first chapter describes how haploinsufficiency for *Pax2* in the $Pax2^{1Neu+/-}$ mouse leads to a caudally shifted ureteric bud, a short intravesical ureter, VUR, and a malformed kidney. $Pax2^{1Neu+/-}$ embryos also exhibit a delay in urinary tract maturation such that the ureters separate from the mesonephric duct at a later time than in wildtype embryos. The second chapter describes the identification of two inbred mouse strains, C3H/HeJ and C57BL/6J, which have contrasting kidney and urinary tract phenotypes. Initially, eleven inbred mouse strains were screened for the presence of VUR and for kidney size. Of these mice, C3H/HeJ mice have a 100% incidence of VUR and small kidneys at birth while C57BL/6J mice have no VUR and larger kidneys. The kidney phenotype was characterized in depth for these two inbred strains. The number of nephrons was counted at birth and at adulthood to determine if a smaller kidney at birth is associated with fewer nephrons and to determine if there is a relationship between nephron number and kidney size. The third chapter focuses on the genetic characterization of the C3H/HeJ inbred mouse. The C3H/HeJ mouse is a new model of VUR that has a caudally shifted ureteric bud but normal kidneys that are not malformed like in the $Pax2^{1Neu+/-}$ mouse. C3H/HeJ

mice also exhibit a delay in urinary tract maturation and have short intravesical ureters when compared to the non-refluxing C57BL/6J mouse. We present evidence demonstrating that a locus on chromosome 12 is associated with the VUR phenotype in the C3H/HeJ mouse.

Connecting text for Chapters I and II

The *Pax2*$^{1Neu+/-}$ mouse was identified in Neuherberg, Germany as part of a screen to identify mouse strains with eye defects (114). Linkage analysis identified a region on chromosome 19 that was significantly associated with the ocular phenotype of optic disc hypoplasia and optic nerve colobomas (114). Sequencing identified a mutation in *Pax2*: an insertion of a nucleotide that results in a frameshift mutation and a premature stop-codon (114). This mutation is identical to a mutation that is found in the majority of patients with RCS (114). Further phenotypic analysis of the *Pax2*$^{1Neu+/-}$ mouse revealed a number of developmental defects of the inner ear, the mid-hindbrain, and the kidney (114). The kidney phenotype has been extensively studied and is characterized by renal hypo/dysplasia and a nephron deficit as a result of reduced ureteric bud branching (230, 254, 300).

The *Pax2*$^{1Neu+/-}$ mouse has never been examined for urinary tract defects. Since *Pax2* is expressed in the mesonephric duct and ureteric bud early during development and humans with RCS have VUR, we hypothesized that the *Pax2*$^{1Neu+/-}$ mouse would reproduce the urinary tract defect observed in RCS and be a model of VUR. We demonstrate that the *Pax2*$^{1Neu+/-}$ mouse does have VUR. We further examined the *Pax2*$^{1Neu+/-}$ mouse to determine how the refluxing ureter arises during urinary tract development. We also examined this model with the objective of testing the ureteric bud theory proposed by Mackie and Stephens over 30 years ago to determine whether a caudally positioned ureteric bud is associated with VUR and renal dysplasia (21). We demonstrate that a caudally positioned ureteric bud is associated with malformed kidneys, VUR, a short intravesical ureter, a delay in urinary tract maturation, and a refluxing urinary tract. The *Pax2*$^{1Neu+/-}$ mouse is the 6th mouse model of VUR to be discovered (68).

CHAPTER II

Vesico-ureteric reflux and urinary tract development in the *Pax2*$^{1Neu+/-}$ mouse

Inga Murawski, David Myburgh, Jack Favor, and Indra Gupta

American Journal of Physiology: Renal Physiology (2007) 293(5): F1736-45

used with permisson

2.1 ABSTRACT

Vesico-ureteric reflux is a urinary tract abnormality that affects roughly 1/3rd of patients with Renal-coloboma syndrome, an autosomal dominant condition caused by a mutation in *PAX2*. Here we report that a mouse model with an identical mutation, the *Pax2*$^{1Neu+/-}$ mouse, has a 30% incidence of vesico-ureteric reflux. In vesico-ureteric reflux, urine flows retrogradely from the bladder to the ureter and is associated with urinary tract infections, hypertension and renal failure. The propensity to reflux in the *Pax2*$^{1Neu+/-}$ mouse is correlated with a shortened intravesical ureter that has lost its oblique angle of entry into the bladder wall compared to wildtype mice. Normally, the kidney and urinary tract develop from the ureteric bud, which grows from a pre-determined position on the mesonephric duct. In *Pax2*$^{1Neu+/-}$ mice, this position is shifted caudally while surrounding metanephric mesenchyme markers remain unaffected. Mutant offspring from crosses between *Pax2*$^{1Neu+/-}$ and *Hoxb7/GFP*$^{+/-}$ mice have delayed union of the ureter with the bladder and delayed separation of the ureter from the mesonephric duct. These events are not caused by a change in apoptosis within the developing urinary tract. Our results provide the first evidence that vesico-ureteric reflux may arise from a delay in urinary tract maturation and an explanation for the clinical observation that vesico-ureteric reflux resolves over time in some affected children.

2.2 INTRODUCTION

During kidney and urinary tract development, reciprocal signaling between the mesonephric duct and the adjacent metanephric mesenchyme induces the formation of an epithelial structure known as the ureteric bud. The distal portion of the ureteric bud branches to form the kidney, while the proximal portion elongates to become the ureter. Initially, the mesonephric duct and ureter are connected via a segment of tissue known as the common nephric duct. Later in development, the common nephric duct undergoes apoptosis, which permits the ureter to contact the urogenital sinus, the future bladder (83). Extensive remodeling of the lower ureter then occurs such that it develops an independent site of entry into the muscular layer of the bladder known as the trigone (14).

Many of the genes that regulate ureteric budding and branching are also important for ureter maturation. One such gene is *Pax2*, a paired-box transcription factor expressed in a wide variety of developing tissues and organs including the optic/otic vesicles, meso/metanephric kidneys, the spinal cord, and the midbrain/hindbrain. Humans with heterozygous *PAX2* mutations develop Renal-coloboma syndrome (RCS), a rare autosomal dominant disorder in which affected individuals have optic nerve colobomas, hearing problems, kidney abnormalities, and vesico-ureteric reflux (VUR). During kidney and urinary tract development, *Pax2* is expressed in the mesonephric duct, the ureteric bud, the ureter, and in mesenchymal condensates (428). *Pax2* homozygous mutant mice (*$Pax2^{-/-}$*) lack kidneys, ureters and genital tracts and have eye and ear defects. They die in the newborn period from renal failure (52). In 1996, the *$Pax2^{1Neu+/-}$* mouse was discovered to carry an identical mutation as humans with RCS: a G base insertion in exon 2 resulting in a truncated, non-functional protein that lacks DNA-binding activity (114). The kidney phenotype in the *$Pax2^{1Neu+/-}$* mouse includes small kidneys with increased ureteric bud apoptosis, decreased ureteric bud branching, and decreased nephron number (230). Although patients with RCS have been reported to have urinary tract abnormalities including VUR, urinary tract development has thus far not been examined in the *$Pax2^{1Neu+/-}$* mouse.

VUR is a congenital defect of the urinary tract caused by the abnormal insertion of the ureter into the bladder leading to the retrograde flow of urine from the bladder to the ureters (429). It affects 0.1-1% of all children and is associated with recurrent urinary

tract infections, hypertension and renal failure (149). The uretero-vesical junction is the anatomical connection between the ureter and the bladder. The junction, composed of the intravesical ureter, the portion of the ureter within the bladder wall, and the surrounding bladder mucosa, is compressed and pulled closed when the bladder fills to form a physiologic valve. This prevents the retrograde flow of urine into the ureters (430). Detailed descriptions of the uretero-vesical junction date back to 1903 when the oblique angle of ureteral entry into the bladder wall was first identified as an important component that prevents VUR (431). In the 1960's, cystoscopies were frequently performed and showed that humans with VUR had shortened intravesical ureters and widely separated and dilated ureteral orifices (12).

In humans, VUR is often associated with small dysplastic kidneys (6). In 1975, Mackie and Stephens examined autopsies from infants with duplex kidneys and ureters and observed a relationship between the position of the ureteral orifice within the bladder and the degree of renal hypo/dysplasia: the more displaced the ureteral orifice, the more severe the kidney malformation (21). This observation was the basis for the "ureteric bud" theory in which they proposed that an abnormal site of ureteric budding leads to combined urinary tract and kidney defects. They hypothesized that VUR, dysplastic kidneys, and laterally displaced ureteral orifices could all arise from a ureteric bud that develops from a more caudal location along the mesonephric duct. In addition, the mesenchyme adjacent to the caudally shifted ureteric bud would be incompetent to respond to inductive signals and result in a malformed kidney.

The ureteric bud theory has prevailed in the literature for many years, but has not been formally tested because of the paucity of genetic mouse models with both urinary tract and renal malformations. Here, we report that the *Pax2*$^{1Neu+/-}$ mouse has a congenital urinary tract defect, VUR, in addition to its eye and renal malformations. We have examined this model to determine whether the *Pax2*$^{1Neu+/-}$ mouse has a caudally positioned ureteric bud and whether this outcome is associated with VUR and renal dysplasia.

2.3 MATERIALS AND METHODS

2.3.1 *Pax2*$^{1Neu+/-}$ and *Hoxb7/GFP*$^{+/-}$ mouse colonies

Heterozygous *Pax2*$^{1Neu+/-}$ mice (114) were crossed to *Hoxb7/GFP*$^{+/-}$ transgenic mice that express green fluorescent protein throughout the mesonephric duct and its derivatives (432). All mice were maintained on a CD1 background. Embryos were generated by performing timed two-hour early morning matings and genotyped by PCR from either tail-clip or head DNA using previously described primers for *Pax2*, *GFP* (432, 433) and *Sry* (5'-CCTCATCGGAGGGCTAAAGT-3') and (5'-TCATGGAACTGCTAGCTTC TG-3'). The visualization of a vaginal plug was recorded as embryonic day (E) 0. All embryos were staged using Theiler's criteria and crown-rump lengths were measured to confirm the age of the embryos. Embryos collected between E10 and E17 were dissected using fluorescent microscopy in order to image mesonephric duct, ureteric bud, ureter, and kidney development. Studies were performed in accordance with the rules and regulations of the Canadian Council of Animal Care (CCAC).

2.3.2 Vesico-ureteric reflux and intravesical ureter lengths

Postnatal (P) day 1 mice were tested for VUR as described by needling the bladder and injecting methylene blue dye (24). VUR was identified by the retrograde passage of methylene blue dye into the ureters. Whole-mount planar surface area measurements (434) for each kidney were obtained using SPOT RT software (v4.0, Diagnostic Instruments). The kidneys attached to their ureters were fixed and embedded in paraffin. Serial transverse sections were obtained at 10μm thickness and stained with hematoxylin and eosin (Sigma). The length of the intravesical ureter was measured as described by injecting 1% fast green dye into the renal pelvis of each kidney using a microinjector (Microinjector IM 300, Narishige) (24). The dye was photographed moving through the ureters into the bladder and the distance between the bladder periphery and the site of dye exit was defined as the intravesical ureteral length and measured using SPOT RT. Bladders were cut to allow the dye to exit more freely.

2.3.3 Whole-mount *in situ* hybridization

In situ hybridization was performed (435) on timed whole embryos that were partially eviscerated to ensure adequate probe penetration. A DIG-labelled UTP (Roche) *c-Ret* probe was used to visualize the mesonephric duct and the ureteric bud in E10.5 embryos. The position of the ureteric bud was determined by measuring the distance between the caudal edge of the mesonephric duct and the start of the ureteric bud (24). *In situ* hybridization using *Gdnf* and *Robo2* cDNA probes (26) was performed on E10.25 embryos. To compare gene expression in wildtype and $Pax2^{1Neu+/-}$ embryos, whole mount images were taken and four measurements were obtained: the anterior limit of gene expression was compared to the midline of the hindlimb, the posterior limit of gene expression was compared to the caudal edge of the hindlimb, the anterior-posterior length of gene expression was measured, and the total area of gene expression was measured. These measurements were taken by one observer who was blinded to the genotype of the embryonic tissue.

2.3.4 Detection of apoptosis

Sagittal cryosections were obtained at 10μm thickness from timed E11 embryos generated from $Pax2^{1Neu+/-}$/$Hoxb7/GFP^{+/-}$ crosses. Sections were preblocked with 0.3% Triton X-100 and 10% horse serum in PBS in a humidified chamber. Immunostaining was performed as previously described using a rabbit polyclonal antibody to activated Caspase-3 (83). Staining of dorsal root ganglia was used as a positive control for apoptosis.

2.3.5 Statistical analyses

Statistical analysis was performed using Chi squared test of two proportions or Student's t-test. Statistical significance was set at a p value<0.05.

2.4 **RESULTS**

2.4.1 *Pax2*$^{1Neu+/-}$ mice have VUR, dilated ureters, and duplicated urinary tracts

Mice were tested for VUR by injecting methylene blue into the bladder and observing whether the dye refluxed up the ureter. At postnatal day (P) 1, only 6.25% (n=48) of wildtype mice had VUR compared to 31.4% (n=51) of *Pax2*$^{1Neu+/-}$ mice ($p<0.05$, chi squared=10.06, Figure 2.1A-C). Both unilateral and bilateral VUR was observed in *Pax2*$^{1Neu+/-}$ mice, however left-sided VUR was more frequently seen ($p<0.05$. Figure 2.1F), consistent with at least one report in children (170). Infants affected with VUR are more likely to be male, while in older children, there is a slight female predominance (195, 436). Among the mutant mice, 45% of the males had VUR compared to only 12% of the females ($p<0.05$). Transverse sections from paraffin-embedded tissues at the level of the kidney demonstrated that refluxing *Pax2*$^{1Neu+/-}$ ureters were dilated compared to littermate controls (Figure 2.1D-E). The smooth muscle layer was intact in mutant embryos and there were no gross malformations of any of the ureteral layers. In addition to hydroureters, bifid ureters and duplicated urinary tracts were observed in 27.6% of mutant mice between E11 and E17 and occasionally at P1 (Figure 2.1G-I), as reported in humans with VUR (4). Interestingly, in one mouse with a duplicated urinary tract, VUR was present in both ureters extending to the upper and lower pole of the duplex kidney. *Pax2*$^{1Neu+/-}$ mice were crossed to *Hoxb7/GFP*$^{+/-}$ mice to obtain offspring in which the ureteric bud and its derivatives were labelled by green fluorescent protein. Kidneys in the mutant offspring had markedly reduced branching compared to their wildtype counterparts (Figure 2.1J,K), as previously demonstrated (230). The kidneys of mutant mice were also significantly smaller than those of wildtype mice at P1 ($p<0.05$, Figure 2.1L-N). Mean kidney planar surface area ± SE in wildtype mice: 5.094 mm^2 ± 0.082, n=98, compared to *Pax2*$^{1Neu+/-}$ mice: 2.901 mm^2 ± 0.106, n=124 ($p<0.05$, Student's t-test).

2.4.2 *Pax2*$^{1Neu+/-}$ mice have short intravesical ureters that correlate with kidney size

The length of the intravesical ureter, the portion of the ureter within the bladder wall, was measured in wildtype and *Pax2*$^{1Neu+/-}$ mice by injecting 1% fast green dye into the renal pelvis and observing its exit from the ureteral orifice. At P1, *Pax2*$^{1Neu+/-}$ mice

had significantly shorter left ($p<0.05$, Student's t-test) and right ($p<0.05$, Student's t-test) intravesical ureters than their wildtype littermates (Figure 2.2). Mean lengths of the intravesical ureter ± SE in the mutant mice were: 0.261 mm ± 0.013, n=16 (left ureter), and 0.256 mm ± 0.022, n=9 (right ureter), and of the wildtype mice were: 0.351 mm ± 0.01, n=21 (left ureter), and 0.348 mm ± 0.013, n=15 (right ureter). Both the kidney and the ureter develop from the ureteric bud, so we determined whether there was a relationship between kidney size and intravesical ureter length. In *Pax2*$^{1Neu+/-}$ mice, mean kidney planar surface area ± SE positively correlated with intravesical ureter length ($y=0.02x+0.16$, $R^2=0.4$, $p<0.05$, 4.324 mm^2 ± 0.314, n=20), while in wildtype mice, there was no relationship, likely because they had very little variation in kidney size ($y=0.006x+0.305$, $R^2=0.05$, $p>0.05$, 5.918 mm^2 ± 0.131, n=32). We also examined whether refluxing *Pax2*$^{1Neu+/-}$ mice had smaller kidneys than their non-refluxing mutant littermates, but were unable to show a correlation ($p>0.05$, data not shown). This may have been due to variability in the *Pax2*$^{1Neu+/-}$ kidney phenotype due to haploinsufficiency (115) and/or the possibility that additional factors predispose to VUR.

2.4.3 *Pax2*$^{1Neu+/-}$ mice have more caudally positioned ureteric buds

An altered position of ureteric budding has been postulated to cause maldevelopment of both the kidney and the urinary tract (21). To determine if the renal dysplasia and VUR observed in the *Pax2*$^{1Neu+/-}$ mouse was due to an abnormality in the site of ureteric budding, we used whole mount *in situ* hybridization to detect *Ret* transcripts within the mesonephric duct and the emerging ureteric bud. At E10.5, the ureteric bud was visible as an outgrowth extending dorsally from the mesonephric duct. The distance from the end of the mesonephric duct to the edge of the ureteric bud was determined to be significantly shorter in *Pax2*$^{1Neu+/-}$ mice compared to wildtype littermates, consistent with a more caudally positioned ureteric bud ($p<0.05$, Student's t-test, Figure 2.3). Mean lengths of the distance from the end of the mesonephric duct to the ureteric bud ± SE in the *Pax2*$^{1Neu+/-}$ mice were left: 0.095 mm ± 0.003, n=15 and right: 0.099 mm ± 0.005, n=15 compared to left: 0.142 ± 0.008, n=10 and right: 0.149 mm ± 0.010, n=10 in the wildtype mice.

2.4.4 *Pax2*$^{1Neu+/-}$ mice do not exhibit altered *Gdnf* or *Robo2* gene expression

Genes expressed by the mesonephric duct and the adjacent mesenchyme regulate the emergence of the ureteric bud. Loss of genes, such as *Slit2* and *Robo2*, result in multiple ureteric buds and an expanded domain of *Gdnf* expression (26). Since *Gdnf* is expressed in the metanephric mesenchyme and both an important mediator of ureteric bud development and a PAX2 target (107), we tested whether the caudally positioned ureteric bud in *Pax2*$^{1Neu+/-}$ mice was associated with a shift in *Gdnf* gene expression. Recent publications have examined the domain of *Gdnf* by *in situ* hybridization and described its expression relative to the position of the hindlimb (26). We obtained measurements of the anterior and posterior limits of gene expression, the total length of gene expression, and the total area of gene expression. Although some mutant embryos appeared to have smaller domains of *Gdnf* expression, no significant differences were noted between them and wildtype embryos ($p>0.05$, Student's t-test, Figure 2.4 & Table 2.1). *Robo2* is a second metanephric mesenchyme marker whose loss leads to an expanded domain of *Gdnf* expression and supernumerary ureteric buds (26). No differences in *Robo2* expression were able to account for the caudally positioned ureteric buds or the duplex urinary tracts observed in *Pax2*$^{1Neu+/-}$ embryos ($p>0.05$, Student's t-test, Figure 2.4 & Table 2.1). *Bmp4* expression was also examined and no gross changes were noted (data not shown).

2.4.5 *Pax2*$^{1Neu+/-}$ mice exhibit a delay in ureter maturation but this is not due to a difference in common nephric duct apoptosis

We determined whether the altered site of ureteric budding was due to a delay in development of the urinary tract. *Pax2*$^{1Neu+/-}$ mice were crossed with *Hoxb7/GFP*$^{+/-}$ mice to visualize the developing kidney and urinary tract (Figure 2.5A). No differences were observed in the mesonephric duct of wildtype and mutant mice prior to E10. At E10, a slight swelling of the posterior region of the mesonephric duct, the site of the future ureteric bud, was apparent in both *Pax2*$^{1Neu+/-}$ (n=14) and wildtype (n=7) embryos. GFP was used as a marker to follow the emergence of the ureteric bud at E10.25 using the same methodology as in figure 2.3: *Pax2*$^{1Neu+/-}$ embryos had more caudally positioned ureteric buds and some buds had irregular contours compared to their wildtype

counterparts (n=10, $p<0.05$, data not shown). Although the common nephric duct appeared longer in *Pax2*$^{1Neu+/-}$ embryos (0.199 mm ± 0.019, n=10) than in wildtype embryos (0.188 mm ± 0.026, n=5) at E11.25, the difference was not statistically significant ($p>0.05$, Student's t-test). However, by E12.25, 70% (21/30) of wildtype ureters had begun to separate from their corresponding mesonephric ducts compared to only 12.5% (1/8) of *Pax2*$^{1Neu+/-}$ ureters ($p<0.05$, chi squared=8.57). The delay in ureter separation from the mesonephric duct was even more apparent at E14: 25% (6/24) of *Pax2*$^{1Neu+/-}$ ureters remained attached to the mesonephric duct compared to 6.25% (2/32) of wildtype ureters ($p<0.05$, chi squared=3.94). At E17, all *Pax2*$^{1Neu+/-}$ ureters had independent openings into the bladder, but their entry was at a less oblique angle compared to wildtype ureters. An oblique angle of entry was defined as a ureter that had a curved entry into the bladder. Sixty-nine % (9/13) of wildtype embryos had ureters that entered the bladder at an oblique angle compared to only 18% (2/11) of mutant embryos ($p<0.05$, chi squared=6.25). We compared the crown-rump lengths of *Pax2*$^{1Neu+/-}$ and wildtype mice at these same embryonic stages to determine if a global delay in somatic growth was responsible for the delay in kidney and ureter development. No differences in crown-rump lengths were observed between *Pax2*$^{1Neu+/-}$ and wildtype embryos ($p>0.05$, Table 2.2), suggesting that the observed delay was urinary tract-specific.

Apoptosis in the common nephric duct is involved in the separation of the ureter from the mesonephric duct (83). To investigate whether a change in apoptosis was responsible for the delay in urinary tract development, sections were obtained at the level of the common nephric duct at E11, prior to the onset of the delay. We observed similar levels of activated caspase-3 protein in both wildtype and *Pax2*$^{1Neu+/-}$ embryos (Figure 2.5B-D), and the majority of the signal was detected within the lumen of the common nephric duct, the mesonephric duct, and the ureter. The delay in urinary tract development was thus not due to a change in apoptosis in the common nephric duct or the surrounding tissues.

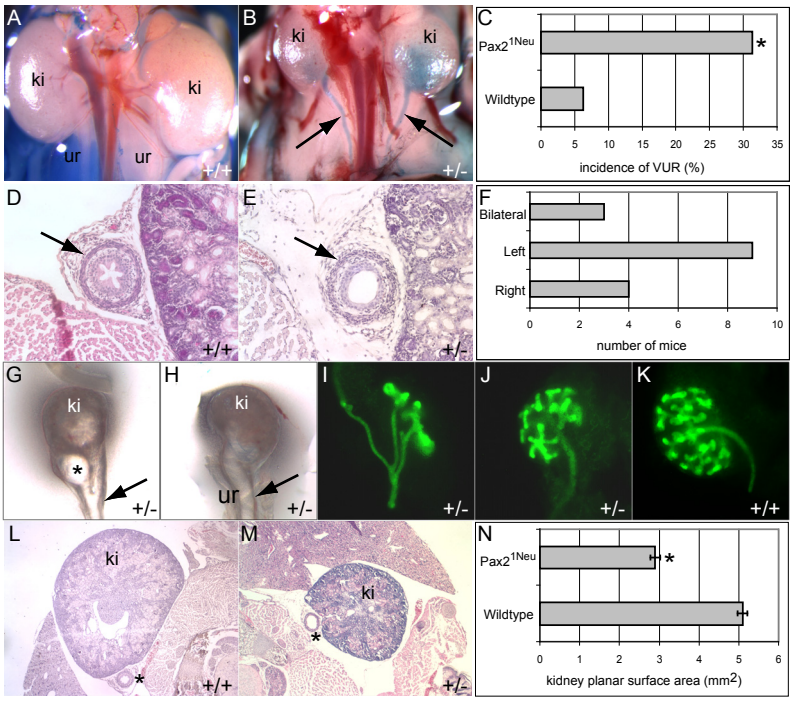

Figure 2.1: *Pax2$^{1Neu+/-}$* mice have VUR, dilated ureters, and duplex systems **(A)** Wildtype kidneys (ki) are normal in size and no reflux is seen at P1. **(B)** *Pax2$^{1Neu+/-}$* kidneys are smaller and bilateral VUR (arrows) is seen extending to the renal pelvis. **(C)** Graphical representation of the incidence of VUR in wildtype (6.25%), and *Pax2$^{1Neu+/-}$* mice (31.37%). **(D-E)** Kidneys and ureters (ur) from newborn mice were paraffin-embedded and transverse sections were obtained through the ureter at the level of the kidney. **(D)** A transverse section of the ureter at the level of the kidney shows a wildtype ureter has a normal transitional epithelium surrounded by smooth muscle layers (arrow). **(E)** The *Pax2$^{1Neu+/-}$* ureter is dilated, but histologically normal (arrow). **(F)** Graphical representation showing the number of *Pax2$^{1Neu+/-}$* mice with bilateral VUR or unilateral VUR. **(G)** A *Pax2$^{1Neu+/-}$* bifid ureter (arrow) with an abnormal cystic lower renal pole (asterisk) at P1. **(H)** An example of a *Pax2$^{1Neu+/-}$* kidney with a dilated ureter (arrow) at P1. **(I)** A *Pax2$^{1Neu+/-}$/Hoxb7/GFP* kidney with a duplex collecting system and abnormal ureteric bud branching is shown at E11.25. **(J)** A *Pax2$^{1Neu+/-}$* kidney with reduced branching compared to a wildtype littermate **(K)** shown at E13. **(L-M)** Transverse sections through kidneys and corresponding ureters (asterisk) at P1 demonstrate the *Pax2$^{1Neu+/-}$* kidney **(M)** is significantly smaller and has a grossly dilated ureter (asterisk) compared with a wildtype **(L)** kidney. **(N)** Graphical representation of kidney planar surface area demonstrates the size difference between wildtype and *Pax2$^{1Neu+/-}$* kidneys at P1.

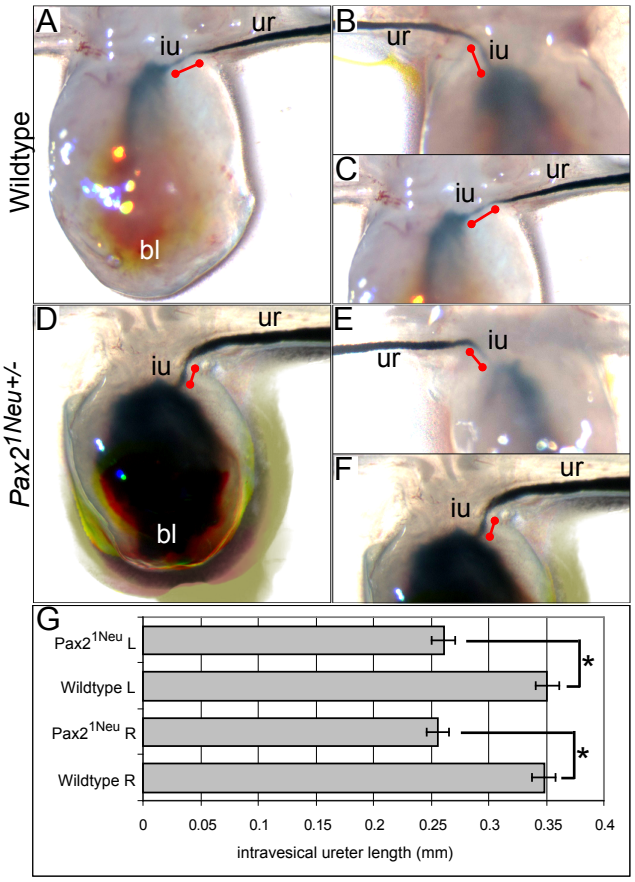

Figure 2.2: *Pax2*$^{1Neu+/-}$ mice have short intravesical ureters

The distance between the extravesical ureter (ur) (site of the bladder (bl) periphery) and the ureteral orifice (site of dye exit) was defined as the intravesical ureter (iu) length (demarcated by line). **(A-C)** Representative images from a wildtype mouse showing left **(A, C)** and right **(B)** intravesical ureters. **(D-F)** Representative images from a *Pax2*$^{1Neu+/-}$ mouse showing left **(D, F)** and right **(E)** intravesical ureters. **(G)** Graphical representation of intravesical ureter lengths in wildtype and *Pax2*$^{1Neu+/-}$ mice.

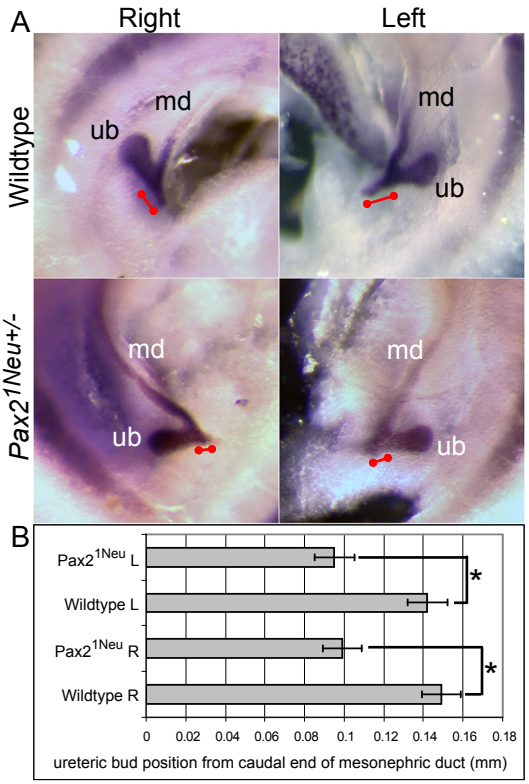

Figure 2.3: *Pax2*$^{1Neu+/-}$ embryos have caudally positioned ureteric buds
(A) Representative images of *in situ* hybridizations show *Ret* expression in the mesonephric duct (md) and ureteric bud (ub) of E10.25 embryos. The site of ureteric budding is measured from the caudal end of the mesonephric duct to the proximal edge of the site of ureteric budding (demarcated by line). **(B)** Graphical representation of the position of ureteric budding shows that *Pax2*$^{1Neu+/-}$ embryos have more caudally positioned ureteric buds.

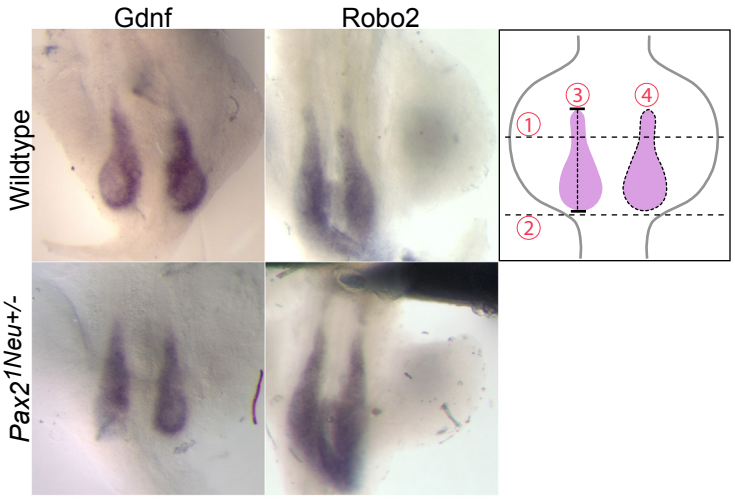

Figure 2.4: *Pax2*$^{1Neu+/-}$ embryos do not exhibit altered *Gdnf* or *Robo2* gene expression

Representative images of in situ hybridizations for *Gdnf* and *Robo2* in E10.25 timed embryos. Embryos were placed ventral side up to expose flanking hindlimbs and the following measurements were obtained: gene expression relative to the midline of the hindlimb (1), gene expression relative to the caudal edge of the hindlimb (2), the total length of gene expression (3), and the total area of gene expression (4). No significant differences in gene expression were detected between wildtype and *Pax2*$^{1Neu+/-}$ embryos for either *Robo2* or *Gdnf*.

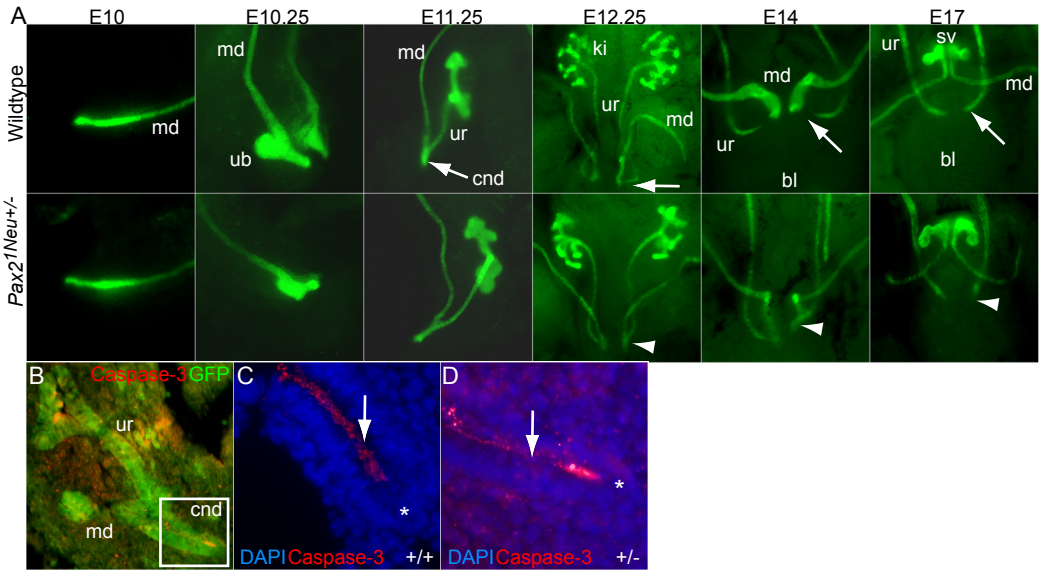

Figure 2.5: *Pax2*$^{1Neu+/-}$ mice exhibit a delay in ureter maturation but this is not due to a difference in common nephric duct apoptosis

(A) *Pax2*$^{1Neu+/-}$ mice were crossed with *Hoxb7/GFP*$^{+/-}$ mice and embryos were dissected at various stages to visualize kidney (ki) and urinary tract development. E10: similar swelling of the posterior end of the mesonephric duct (md) is apparent in both *Pax2*$^{1Neu+/-}$ and wildtype embryos. E10.25: a more caudal ureteric bud (ub) is seen emerging from *Pax2*$^{1Neu+/-}$ mesonephric ducts. E11.25: the ureteric bud has bifurcated once and the common nephric duct (cnd) is seen connecting the ureter (ur) and the mesonephric duct. No differences in the length of the common nephric duct were observed. E12.25: wildtype ureters are beginning to separate from their corresponding mesonephric ducts (arrow) while *Pax2*$^{1Neu+/-}$ ureters appear delayed and remain attached to the mesonephric duct (arrowhead). E14: the wildtype ureter is seen with an independent opening into the bladder (bl) (arrow) while the mutant ureter remains attached to the mesonephric duct (arrowhead). E17: wildtype embryos have ureters that insert into the bladder wall at an oblique angle (arrow) while *Pax2*$^{1Neu+/-}$ embryos have ureters that enter less obliquely (arrowhead). **(B)** Activated caspase-3 protein was detected within the lumen of the common nephric duct (inset) of both wildtype **(C)** and mutant **(D)** embryos. The epithelial layer (asterisk) is labeled with DAPI (blue) and surrounds the lumen (arrow). Similar levels of apoptosis (red) were observed in both wildtype and *Pax2*$^{1Neu+/-}$ embryos.

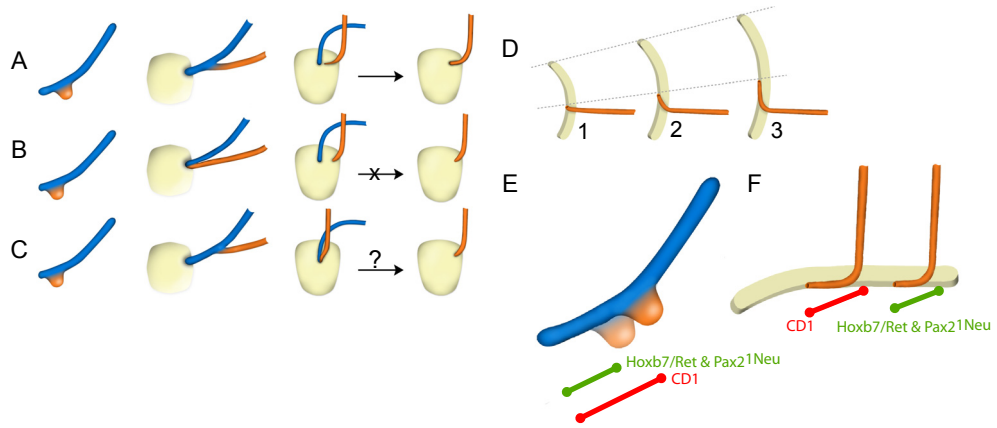

Figure 2.6: The current and revised model of caudal ureteric budding
(A-C) From left to right the images depict two lateral and two posterior views. **(A)** The normally positioned ureteric bud emerges from the mesonephric duct. Vertical displacement of the ureter leads to separation of the ureter (orange) from the mesonephric duct (blue) within the urogenital sinus. Once the ureter has achieved an independent opening into the bladder, the length of the intravesical ureter and its angle of entry into the bladder wall prevent against VUR. **(B)** The old model of ureteric budding predicts that a caudal ureteric bud will cause early separation of the ureter from the mesonephric duct and increased lateral migration of the ureter within the bladder wall, which results in a short intravesical ureter that refluxes. Our data does not support this model. **(C)** Our revised model of ureteric budding shows that a caudal ureteric bud leads to delayed union of the ureter with the urogenital sinus and delayed separation of the ureter from the mesonephric duct. These events lead to the development of a short intravesical ureter that has lost its oblique angle of entry into the bladder and a refluxing ureter. **(D)** Ureteral insertion is likely influenced by bladder development. As the bladder grows (steps 1-3), the intravesical ureter lengthens and enters the bladder wall at an oblique angle (step 3). Delayed separation of the ureter from the mesonephric duct could impair ureteral maturation and bladder growth such that the intravesical ureter resembles that shown in step 2. **(E)** In the *Hoxb7/Ret*$^{+/-}$ and *Pax2*$^{1Neu+/-}$ refluxing mice, we have found the ureteric bud is shifted by approximately 40% when compared to wildtype littermates. **(F)** At birth, the intravesical ureter is shortened by approximately 20% in these two refluxing mouse strains when compared to wildtype mice.

Table 2.1: Measurements of *Robo2* and *Gdnf* gene expression in *Pax2$^{1Neu+/-}$* and wildtype embryos

Gdnf	*Pax2$^{1Neu+/-}$*	wildtype	*P*
1	0.040 ± 0.019 (n=24)	0.052 ± 0.024 (n=20)	0.69
2	0.032 ± 0.010 (n=24)	0.024 ± 0.015 (n=22)	0.68
3	0.534 ± 0.022 (n=24)	0.482 ± 0.016 (n=20)	0.07
4	0.068 ± 0.004 (n=24)	0.068 ± 0.004 (n=22)	0.95
Robo2	*Pax2$^{1Neu+/-}$*	wildtype	*P*
1	0.090 ± 0.017 (n=12)	0.049 ± 0.024 (n=8)	0.18
2	0.032 ± 0.028 (n=12)	0.048 ± 0.034 (n=11)	0.31
3	0.702 ± 0.042 (n=14)	0.614 ± 0.046 (n=11)	0.17
4	0.098 ± 0.008 (n=14)	0.091 ± 0.009 (n=11)	0.56

Values are means (mm) ± SE. n, number of embryos. Student's t-test

1: gene expression relative to the midline of the hindlimb
2: gene expression relative to the caudal edge of the hindlimb
3: total length of gene expression
4: total area of gene expression

Table 2.2: Mean crown-rump lengths in *Pax2$^{1Neu+/-}$* and wildtype embryos

Age	*Pax2$^{1Neu+/-}$*	wildtype	P
E10	4.078 ± 0.117 (n=5)	4.301 ± 0.235 (n=9)	0.41
E10.25	5.522 ± 0.177 (n=13)	5.705 ± 0.111 (n=23)	0.39
E10.5	6.807 ± 0.084 (n=11)	6.719 ± 0.139 (n=14)	0.59
E11	7.196 ± 0.071 (n=30)	7.288 ± 0.112 (n=22)	0.49
E12	8.341 ± 0.300 (n=3)	8.898 ± 0.474 (n=3)	0.39
E12.25	9.901 ± 0.240 (n=4)	9.857 ± 0.151 (n=12)	0.88
E13	10.530 ± 0.088 (n=19)	10.537 ± 0.069 (n=25)	0.95
E14	12.369 ± 0.201 (n=11)	12.034 ± 0.151 (n=9)	0.20

Values are means (mm) ± SE. n, number of embryos. Student's t-test.

2.5 DISCUSSION

We have identified a new mouse model of vesico-ureteric reflux, the *Pax2*$^{1Neu+/-}$ mouse, which directly parallels a human disorder, RCS. Approximately 26% of RCS patients develop VUR in addition to optic colobomas and kidney malformations (233). Our results suggest that the urinary tract defect arises early during embryogenesis from an alteration in the site of ureteric budding that is followed by a delay in ureter development. These events lead to a shortened intravesical ureter that has lost its oblique angle of entry into the bladder, predisposing affected mice to VUR.

2.5.1 Using the *Pax2*$^{1Neu+/-}$ mouse to understand urinary tract development and VUR

The ureteric bud theory proposes that a caudal ureteric bud results in a refluxing ureter (21). Such positioning of the ureteric bud would lead to a shortened common nephric duct, resulting in the early union of the ureter with the urogenital sinus, accelerated separation of the ureter from the mesonephric duct, and lateral displacement of the ureter within the bladder wall (23, 156). The mesenchyme adjacent to the abnormally positioned ureteric bud would be incompetent to respond to inductive signals, resulting in malformed kidneys. While this theory fails to account for all of the features of the refluxing urinary tract, it presents a hypothesis to explain the clinical association of VUR with small or malformed kidneys (437).

VUR spontaneously disappears in as many as 71% of affected children, indicating that this condition can resolve over time (167). This observation supports an alternative theory that VUR is due to a delay in ureter development. In children in whom the condition resolves, it is presumed that the ureter has grown and formed a more competent uretero-vesical junction (169). We observed that *Pax2*$^{1Neu+/-}$ embryos had more caudal ureteric buds, and by E12.25, they showed a delay in ureter maturation. These findings suggest that aspects of both theories may be true.

To characterize the delay in urinary tract development, we examined the onset of ureteric bud formation between E10 and E11. At E10, the mesonephric duct begins to swell and a single ureteric bud emerges by E10.25. No differences between wildtype and mutant mice were observed in the timing of the onset of mesonephric duct swelling, the emergence of the ureteric bud, or the first ureteric bud bifurcation. Thus, the ureteric bud

forms *de novo* from a predetermined location along the duct and does not migrate along the duct to reach its final location. In the *Pax2*$^{1Neu+/-}$ mouse, the caudal ureteric bud arises from a physical displacement in the position of budding and is not due to a delay in ureteric bud formation. This is likely the initial event that leads to the urinary tract malformation. Although bifid and duplicated ureters were observed, double ureteric buds were never seen, suggesting that the duplicated urinary tracts arose after formation of the ureteric bud. The ureteric bud theory proposes that the cranial or rostral ureter in a duplicated urinary system will be obstructed. We rarely observed complete duplications in the newborn period; therefore we were unable to test this aspect of the theory. When duplicated systems were tested for reflux in the newborn period, there were cases in which both ureters freely refluxed suggesting no obstruction at the level uretero-vesical junction in those mice.

To investigate the molecular basis for a caudally positioned ureteric bud, we examined gene expression during its formation. The ligand GDNF is secreted from the surrounding metanephric mesenchyme and interacts with RET, a receptor tyrosine kinase, and GFRα1, a co-receptor, both of which are expressed by the ureteric bud. This signaling event initiates the emergence of the ureteric bud from the mesonephric duct (64). *Gdnf* is a known target of PAX2 (107), and a shift in the domain of *Gdnf* expression has been associated with the emergence of ectopic ureteric buds in a number of mutant mice (26, 28). Although no abnormality was noted in the *Gdnf* expression pattern of *Pax2*$^{1Neu+/-}$embryos, we cannot exclude the possibility that there may be important quantitative differences in expression between wildtype and mutant embryos. The expression of *Gdnf* in the mesenchyme is in the shape of a teardrop, which may represent an increasing concentration gradient along the anterior-posterior axis (67). Therefore, a 50% reduction of GDNF in *Pax2*$^{1Neu+/-}$ embryos could lead to a more caudally positioned ureteric bud as the bottom edge of the teardrop would be relatively more abundant in GDNF.

Both *Pax2* and another one of its targets*, Ret,* are critical for ureteric bud development as homozygous mutants for either gene fail to form ureteric buds (60, 107). In addition, kidneys from *Pax2*$^{+/-}$ mice have been shown to have reduced *Ret* expression by quantitative RT-PCR (258). Our work suggests that alterations in the domain of *Ret*

expression are also important for the position of ureteric budding. As shown in Figure 2.3, *Ret* transcripts are detected in the mesonephric duct and the ureteric bud in both wildtype and *Pax2*$^{1Neu+/-}$ mice. However, the site of ureteric budding as marked by *Ret* is caudally shifted in the mutant mice compared to the wildtype mice. From these results, we cannot address whether the alteration in *Ret* expression is the primary event that leads to the caudally shifted ureteric bud or whether the ureteric bud is caudally shifted and secondarily the domain of *Ret* expression is altered. In a different mouse model in which *Ret* is overexpressed as a transgene driven by the *Hoxb7* promoter, we also noted that the position of the ureteric bud was caudally shifted (24). Taken together, these two models suggest that the domain of *Ret* expression is critical to the site of ureteric budding. In the *Pax2*$^{1Neu+/-}$ mouse, we propose that either the decreased amount of PAX2 or its effect on target genes, such as *Gdnf, Ret,* and *Gata3*, contribute to the caudally shifted ureteric bud.

In addition to genes that promote the emergence of the ureteric bud, there are genes that are inhibitory. In mouse models, the loss of inhibitors leads to an expanded domain of *Gdnf* expression and supernumerary ureteric buds (26, 28). We examined the repressor *Robo2*, however no gross differences in its expression were able to account for the caudally positioned ureteric buds or the duplex urinary tracts observed in *Pax2*$^{1Neu+/-}$ embryos. BMP4 is a growth factor known to inhibit ectopic ureteric budding (25). Although an alteration in *Bmp4* expression could have contributed to the caudally shifted ureteric buds, its diffuse expression throughout the mesenchyme adjacent to the mesonephric duct made it difficult to discern a clear domain of expression for comparative analysis by whole mount *in situ* hybridization. We analyzed two markers of the metanephric mesenchyme, *Robo2* and *Gdnf*, and found that the metanephric mesenchyme was normally located in mutant embryos. We speculate that the kidney and urinary tract defects in the *Pax2*$^{1Neu+/-}$ mouse are initiated when the caudally shifted ureteric bud contacts the lower end of the metanephric mesenchyme that is not able to sustain normal kidney or urinary tract development due to a change in the local environment of growth factors and transcription factors.

Beginning at E12.25, there was a quarter of a day delay, and by E14, there was a day and a half delay in *Pax2*$^{1Neu+/-}$ urinary tract maturation such that the ureters did not separate as rapidly from the mesonephric ducts. Although we cannot track the growth of

a single ureteric bud as it lengthens into a ureter in vivo, our data demonstrates that the caudal ureteric bud arises prior to the onset of the delay in mutant embryos. A delay in urinary tract maturation was observed in all mutant embryos. However, the extent of the delay was variable, therefore it was not surprising that only 31% of the mutant mice had vesico-ureteric reflux. Phenotypic variability in the extent of the delay and its impact on the competence of the uretero-vesical junction at P1 was likely caused by PAX2 haploinsufficiency and/or because the mice were bred on an outbred CD1 background (115, 248).

Normally at E11, the common nephric duct undergoes apoptosis to allow the ureter to separate from the mesonephric duct (83). We examined embryos at E11 to determine if a change in common nephric duct apoptosis was mediating the urinary tract delay. Although no differences were noted, this may not have been completely unexpected. Firstly, the *Pax2*$^{1Neu+/-}$ mouse has intact ureters and uretero-vesical junctions, therefore a major change in apoptosis is unlikely. Secondly, the role of PAX2 in cell survival may not be of primary importance in the developing urinary tract as reported in the kidney (42, 438): its functions in cellular differentiation and tissue remodeling may be more critical. Taken together, the most plausible explanation for the urinary tract defect is that there is a combination of a physical displacement in the position of ureteric budding and a developmental delay.

2.5.2 *Pax2* targets and their roles in urinary tract development

True haploinsufficiency is rare and usually occurs when the protein of interest must interact or compete with other gene products as part of a developmental switch or complex pathway (115). In *Pax2*$^{1Neu+/-}$ mice, kidney and urinary tract development are sensitive to gene dosage: a 50% reduction in the amount of PAX2 protein results in a shifted ureteric bud, a decrease in ureteric bud branching, and a delay in ureter maturation.

While a number of genes regulated by PAX2 are functionally important in the developing kidney, their roles in the urinary tract are not as well defined (101, 234, 257-259, 261). In *Xenopus*, PAX2 acts with WNT4 and WT1, and the transcription factor LIM1 to guide pronephric duct elongation (43). *Gata3* is a target of both PAX2 and

PAX8 (101) and is involved in guidance of the pronephric duct towards the cloaca. In humans, *GATA3* mutations cause renal anomalies and VUR as part of Hypoparathyroidism, deafness and renal dysplasia (HDR) syndrome (439). *Eya1*, *Six1*, *Foxc1,* and *Foxc2* are a group of transcription factors that regulate *Gdnf* (28, 73, 440). A *Pax/Six/Eya* gene network regulates ureteric bud development (108) and mutations in the network are associated with familial renal and urinary tract malformations. Patients with branchio-oto-renal (BOR) syndrome have heterozygous mutations in either *EYA1* and *SIX1* and can develop urinary tract defects including VUR (351).

The evidence above suggests that many of the guidance and/or directional cues that are necessary for pronephric and mesonephric duct development are also important for the steps of ureter maturation. Because the $Pax2^{1Neu+/-}$ mouse is haploinsufficient, it is difficult to demonstrate differences in gene expression using qualitative methods like *in situ* hybridization to explain the caudal emergence of the ureteric bud or the delay in urinary tract maturation. However, we speculate that important quantitative differences in either targets of *Pax2* or genes within the *Pax/Six/Eya* network are most likely responsible for the urinary tract defects we observe. Future work will need to identify the specific targets of *Pax2* and its regulatory networks within the developing urinary tract.

2.5.3 Genetics of VUR and mouse models

VUR most frequently occurs as primary VUR, in which there is an isolated urinary tract malformation with or without a kidney defect. It can also present as syndromic VUR, in which there are other system defects as in RCS, HDR, or BOR. From studies of primary VUR in multi-generational families demonstrate that the condition is genetically heterogeneous (330). Thus far, RCS-causing mutations have all been identified at the 5'end of the *PAX2* gene. Although one family study failed to identified *PAX2* mutations in primary VUR (342), it is possible that mutations or polymorphisms at the 3' end that affect the transactivation potential of PAX2 are associated with this condition (115, 441).

Based on the five mouse models of VUR thus far described (24, 46, 93, 94, 216), genes expressed in the mesonephric duct, the ureteric bud, or surrounding metanephric mesenchyme, are all potential candidates to consider in human studies of primary VUR.

Deletion of the mesenchymally-expressed *Agtr2* gene leads to urinary tract duplications, VUR, and double ureteric buds. Mice lacking *Upk2* or *Upk3*, genes that are expressed by the urothelium, have VUR although it is as yet unknown if this is due to a defect during urinary tract formation. *Lim1*$^{-/-}$ conditional knockout mice have VUR and defects in mesonephric duct elongation, but abnormalities in the position of ureteric budding have not been reported. In addition to malformed kidneys (217), our laboratory has identified that overexpression of *Ret* in the *Hoxb7/Ret*$^{+/-}$ mouse leads to VUR (24). Importantly, both the *Hoxb7/Ret*$^{+/-}$ mouse and the *Pax2*$^{1Neu+/-}$ mouse have ureteric buds that are approximately 37% closer to the end of the mesonephric duct and intravesical ureters that are approximately 20% shorter. These two models therefore suggest that VUR with renal malformation in humans is a developmental field defect that originates from a single caudally shifted ureteric bud (17). These results have implications in the clinical care of patients with VUR in that the malformed urinary tract may be accompanied by severe or subtle defects in nephrogenesis.

2.5.4 Model and conclusions

Our model of the relationship between the position of ureteric budding along the mesonephric duct and the development of urinary tract defects differs from the original ureteric bud theory (Figure 2.6). As proposed, we find that the ureteric bud in *Pax2*$^{1Neu+/-}$ mice exits from a more caudal location along the mesonephric duct and is likely the initial step responsible for the combined kidney and urinary tract defects. However, in contrast to this theory, our results suggest that this event is subsequently followed by a significant delay in the separation of the ureter from the mesonephric duct. This delay results in a shorter intravesical ureter that has lost its oblique angle of entry into the bladder leading to an incompetent uretero-vesical junction that refluxes. The steps by which the intravesical ureter tunnels through the bladder wall are not well described. Tunneling may begin once the ureter has completely separated from the mesonephric duct. If true, then slower separation of the ureter from the duct could reduce the length of time for ureteral growth into the bladder. Growth of the bladder around the separating ureter also needs to be considered as this may affect ureteral migration within the bladder wall as originally proposed by Frazer (442). These questions will be better answered once

there are means to fluorescently label the developing trigone in relation to the intravesical ureter.

2.6 ACKNOWLEDGEMENTS

We thank AK Ryan, L Jerome-Majewska, CG Goodyer, and CL Mendelsohn for critical reading of the manuscript and discussions; F Costantini for providing the *Hoxb7/GFP*$^{+/-}$ mice and the ISH probes for *Gdnf* and *Ret*; U Grieshammer and G Martin for providing the ISH probe for *Robo2*. This work was supported by an operating grant from the Kidney Foundation of Canada. IRG is a recipient of an FRSQ chercheur-boursier clinicien salary award. IJM is a recipient of an FRSQ doctoral award.

Connecting text for Chapters II and III

It is known that VUR and renal malformations can co-occur in humans; however, it is still unknown whether the malformed kidney represents acquired damage from the reflux of infected urine (as part of reflux nephropathy), or whether it represents a congenitally small kidney that is hypo/dysplastic with fewer nephrons (15, 203, 262). The six mouse models of VUR all have congenital renal and urinary tract defects that arise from mutations in genes that are important for kidney and urinary tract development, suggesting that the latter hypothesis can be true (24, 46, 68, 93, 94, 216). However, these mouse models do not represent the large number of patients with VUR (20-67%) that have normal kidneys on ultrasound or DMSA scan (202-205). Therefore, one of the goals of my thesis was to understand the association between VUR and the renal phenotype. This relationship is described in the following chapter of my thesis.

The story for this chapter actually began while I was studying the incidence of VUR in the *Pax2*$^{1Neu+/-}$ mouse. Both a previous graduate student in the lab and myself observed that the genetic background of the mouse strain had a significant impact on the incidence of VUR. Initially, the *Pax2*^{1Neu} mutation was on a C3H/HeN (mouse supplier Charles River) background and both *Pax2*$^{1Neu+/-}$ mice and wildtype C3H/HeN mice exhibited a high incidence of VUR (almost 100%). Because both the mutant and wildtype mice refluxed, we hypothesized that a gene(s) in the C3H/HeN mouse was causing it to reflux. We therefore bred the *Pax2*^{1Neu} mutation onto a CD1 outbred background, which is relatively resistant to VUR and only exhibits a 6% incidence of VUR. Because I observed a low incidence of VUR in CD1 mice and a high incidence of VUR in C3H/HeN mice (93.3%, n=30), we were interested to determine the incidence of VUR in different inbred mouse strains. We therefore examined eleven different inbred mouse strains for VUR and kidney size (mouse supplier Jackson Laboratories) to identify new genetic models of VUR with and without a renal malformation.

During this screen, we identified four inbred mouse strains that were susceptible to VUR, including the C3H/HeJ strain (these data are presented in Chapter IV). The eleven inbred strains also exhibited differences in kidney size. The C3H/HeJ mouse is genetically similar to the C3H/HeN mouse except that it has a mutant toll-like receptor 4 (TLR4) such that it is unable to respond to gram-negative bacteria and is less able to clear

urinary tract infections (443-445). We chose to continue to study the C3H/HeJ strain as it is listed as a priority strain on the Mouse Phenome Database and is better genotypically and phenotypically characterized (http://www.jax.org/phenome).

Like the C3H/HeN mouse, the C3H/HeJ mouse exhibited a 100% incidence of VUR and had small kidneys at birth when compared to the C57BL/6J mouse that had a 0% incidence of VUR and larger kidneys at birth. Interestingly, when C3H/HeJ and C57BL/6J mice were tested for VUR and kidney size at adulthood, C3H/HeJ mice continued to reflux but now had larger kidneys than C57BL/6J mice. These two inbred strains were therefore analyzed in depth because they had the most contrasting renal and urinary tract phenotypes.

We hypothesized that C3H/HeJ mice would have fewer nephrons than C57BL/6J mice and that the increase in kidney size by adulthood was caused by glomerular and renal hypertrophy secondary to a nephron deficit. Nephron counts were obtained from newborn and adult C3H/HeJ and C57BL/6J mice to determine whether this was true. Surprisingly, there was no significant difference in nephron number between the two strains at either timepoint. We therefore explored the relationship between nephron number, kidney size, and body weight in depth in these inbred mouse strains. Although kidney size and body weight did correlate with one another, nephron number did not correlate with kidney size or body weight, suggesting that nephron number is an independent variable in these mouse strains.

CHAPTER III

The relationship between nephron number, kidney size, and body weight in two inbred mouse strains

Inga Murawski, Rita Maina, and Indra Gupta

manuscript to be submitted

3.1 ABSTRACT

While some reports in humans have shown that nephron number is positively correlated with height, body weight or kidney weight, other studies have not reproduced these findings. To understand the impact of genetic and environmental variation on these relationships, we examined whether nephron number correlates with body weight, kidney planar surface area, or kidney weight in two inbred mouse strains with contrasting kidney sizes but no overt renal pathology: C3H/HeJ and C57BL/6J. The C3H/HeJ mouse had smaller kidneys at birth and larger kidneys by adulthood, however there was no significant difference in nephron number between the two strains. Although we did observe a correlation between kidney size and body weight at birth and at adulthood for both strains, there was no relationship between nephron number and body weight or between nephron number and kidney size. From the human data, it appears that a greater than 2-fold variation is required in each of these parameters in order to ascertain these relationships, suggesting they are highly dependent on scale. Our results are therefore not surprising since there was a less than 2-fold variation in each of the parameters examined. In summary, the relationship between nephron number and body or kidney size is most likely to be demonstrated when there is greater phenotypic variation either from genetic and/or environmental factors.

3.2 INTRODUCTION

The vertebrate kidney functions as an excretory system that regulates body homeostasis and hormone secretion. The functional unit of the kidney is the nephron: a structure that contains vascular loops of the glomerulus at the site of blood filtration and a tubular segment that reabsorbs and excretes solutes and connects to the collecting duct system. Based on autopsy specimens from individuals representing various ethnic groups, a large variation in nephron number exists in the "normal" adult human kidney, such that each kidney contains anywhere from 200,000 to over 1.8 million nephrons (269, 274, 275). Recent interest in nephron number has aimed to understand whether individuals with a congenital defect in nephron formation are at an increased risk of developing diseases like hypertension and chronic renal failure.

Nephrogenesis ends by 36 weeks of gestation in humans, such that the final number of nephrons in each kidney is established at birth (273). Infants below the 10^{th} percentile in birth weight have smaller kidneys with fewer nephrons, suggesting that there is a relationship between body weight and kidney size, as well as between body weight and nephron number (267, 269, 272, 277). In addition to its relationship with birth weight, nephron number has been shown to correlate with other factors, including adult height and body surface area (267), kidney weight or volume (274), and glomerular volume (269). These surrogates of nephron number have also been found to be associated with susceptibility to developing diseases like hypertension and chronic renal failure (276, 282, 283).

To test the hypothesis that low nephron number contributes to hypertension, the number of nephrons was examined in kidneys obtained from autopsies of hypertensive and normotensive Caucasians. Although there was no difference in kidney weight between the two groups, hypertensive adults had significantly fewer nephrons that showed evidence of glomerular hypertrophy compared to normotensive adults (266). Because the kidney is unable to regenerate nephrons, the remaining glomeruli undergo hypertrophy to compensate for a reduction in filtration surface area (266, 267, 269, 275, 317). Individuals with or at risk for chronic renal failure, marked by decreased renal function and proteinuria, also have fewer nephrons that may be due to a defect in nephron formation and/or loss through disease (267, 317).

While the aforementioned studies suggest that there is a relationship between nephron number and kidney size and between nephron number and susceptibility to hypertension or chronic renal failure, other studies have not confirmed these relationships (275, 281, 283). These latter results could arise if these parameters are each independent variables, or alternatively, if the relationship is obscured due to excessive genetic and environmental variation.

In contrast to humans in whom nephrogenesis ends prenatally, nephron formation continues postnatally in rodents: up to day 5-7 in mice and up to day 7-10 in rats (355). Rodent models have revealed that both genetic and environmental factors can influence nephron number and kidney size. The disruption of genes involved in kidney development can lead to a spectrum of renal phenotypes, from renal agenesis to small kidneys with a nephron deficit (292, 300-302). In several of the latter models, while no differences in body weight were observed, the nephron deficit was associated with glomerular hypertrophy, hypertension, and reduced renal function (301, 302). Intrauterine growth retardation caused by disruption of fetal blood supply and/or dietary restrictions can also affect kidney growth and nephron formation (105, 287). These rodent models demonstrate that when nephrogenesis is perturbed, whole organ growth is affected and fewer nephrons develop. However, these studies have not looked directly at the relationship between nephron number and kidney size or nephron number and body weight.

We examined the relationship between nephron number and kidney or body size in inbred mouse strains. Inbred mice are genetically homogeneous and are exposed to uniform environmental conditions, making them an ideal model to study these relationships (417). We hypothesized that the heritable differences in kidney size observed between inbred strains would be accompanied by a difference in nephron number (446). We identified two inbred mouse strains, C3H/HeJ and C57BL/6J, that differed significantly in their kidney size, measured as planar surface area and as weight. Nephron number counts and body weights were therefore obtained in the newborn period and at adulthood to determine if there is a relationship between nephron number, body weight, or kidney size in these mouse strains.

3.3 MATERIALS AND METHODS

3.3.1 Sample collection, paraffin sections, and hematoxylin and eosin staining

C3H/HeJ, C57BL/6J (Jackson Laboratories), and CD1 (Charles River Laboratories) kidneys were collected at postnatal day 1 (P1) for the newborn studies. C3H/HeJ and C57BL/6J kidneys were collected at 8 weeks of age (P56) for the adult studies. Body weights and kidney weights were obtained for all mice studied. Whole-mount kidney planar surface areas were measured using SPOT (v.3.5.9) to assess kidney size, as previously described (434). Surface areas and weight measurements were normalized for body weight to account for any differences in gestational age in the newborn mice, and to account for any differences in body size in the adult mice (447). Kidneys were fixed in 4% PFA, processed for paraffin-embedding and cut into 7μm serial sections. Hematoxylin and eosin staining was performed according to standard protocol. Animal studies were performed in accordance with the rules and regulations of the Canadian Council of Animal Care (CCAC) and animal protocols were approved by the McGill University UACC.

3.3.2 Absolute nephron number counts in newborn kidneys

An absolute nephron number count was obtained from newborn C3H/HeJ, C57BL/6J, and CD1 kidneys. Male and female mice as well as left and right kidneys were sampled. Images of each section were taken using a Canon PowerShot S50 attached to a Zeiss Axiophot by a Leica adaptor. The serial sections were printed and 'write-on' transparency films were applied to each image. Glomeruli were identified by the presence of a glomerular tuft, circled on each transparency, and numbered in ascending order. The transparency was then compared to the adjacent section. Overlapping glomeruli were assigned the same number while all new glomeruli were assigned a new number, ensuring that glomeruli that appeared in multiple sections were only counted once. All glomeruli in a newborn kidney were tracked, and an absolute nephron number count was obtained. The same kidneys were used to estimate nephron number using the disector/fractionator method (311, 315). The following formula was used: $Nglom=f\times0.5\times NN$. Where f is the fraction of the kidney sampled, 0.5 corrects for the use of adjacent section pairs, and NN is the total number of nephrons counted from the

sampling. A new estimation counting method was derived from the absolute counts that avoided the use of adjacent section pairs. The following formula was derived: Nglom=f×0.4×NN. Where f is the fraction of the kidney sampled, 0.4 is a constant derived from the absolute counts that corrects for overlapping glomeruli when all glomeruli on one section are counted, and NN is the total number of nephrons counted from the sampling. For the newborn studies, 10% of each kidney was sampled and sections were chosen at least 70μm apart to avoid the possibility of double-counting glomeruli.

3.3.3 Estimated nephron number counts in adult kidneys

Serial sections from adult C3H/HeJ and C57BL/6J kidneys were imaged using a Canon PowerShot S50 attached to a Zeiss Axiophot by a Leica adaptor. Whole kidney sections were imaged in parts and merged using Adobe Photoshop CS. Adult kidneys were analyzed using Image J (v1.36b) and individual glomeruli, defined by the presence of a glomerular tuft, were counted using the point selection tool with auto measure. Our counting method was used to estimate nephron number using the formula Nglom=f×0.4×NN. Two independent counts were obtained for each kidney and the average nephron count is reported. Glomerular tuft sizes, measured as planar surface area, were obtained using SPOT (v.3.5.9) as previously described (255). To obtain cortex and medulla planar surface area measurements, the section with the largest surface area was identified, and the surface area from six adjacent sections was measured and used to obtain an average. Student's t-test and regression analysis was used for statistical analysis of the data.

3.4 RESULTS

3.4.1 B6 and C3H mice have contrasting kidney sizes at birth and at 8 weeks

Kidney weight varies between inbred mouse strains and has been previously demonstrated to be heritable (446). We therefore assessed the variation in kidney size in two inbred mouse strains, C3H/HeJ (C3H) and C57BL/6J (B6) at birth (postnatal day P1). C3H mice had significantly smaller kidneys than B6 mice measured as planar surface area ($P=2x10^{-7}$, Fig 1A) or weight ($P=5x10^{-7}$, data not shown). We also examined kidney size in adult mice at 8 weeks of age (P56), when both nephrogenesis and kidney

growth is completed. Unexpectedly, there was a change in kidney size between the two strains: C3H kidneys had significantly larger planar surface areas ($P=1.8x10^{-7}$, Fig 1B) and weights ($P=3.4x10^{-5}$, data not shown) than B6 kidneys. When males and females were compared individually, C3H females and males had larger kidney surface areas and weights (data not shown) than their B6 counterparts (planar surface area for C3H vs. B6 females: P=0.007, n=12 and C3H vs. B6 males: $P= 1x10^{-5}$, n=12, data not shown).

Birth weights between C3H and B6 mice did not differ (mean ± SE): 1.36 ± 0.05g, n=14, for C3H vs. 1.32 ± 0.04g, n=14, for B6 (P=0.55), demonstrating that while C3H mice had smaller kidneys at birth, there was no difference in their body weight when compared to B6 mice. Similarly, there was no difference in body weight at adulthood when both strains were compared (mean ± SE): 18.8 ± 0.6g, n=12, for C3H vs. 18.6 ± 0.7g, n=12, for B6 (P=0.79), or when males and females were examined separately (C3H vs. B6 females, P=0.08, n=12 and C3H vs. B6 males, P=0.69, n=12, data not shown).

We hypothesized that the change in kidney size between birth and adulthood could be from a nephron deficit with subsequent compensatory hypertrophy of the remaining glomeruli to maintain renal function. To determine if a nephron deficit in the C3H mouse was responsible for the observed kidney phenotype, newborn and adult kidneys from C3H and B6 mice were examined to assess nephron number.

3.4.2 Development of a new method to estimate nephron number

A number of methods have been used to count glomeruli and to estimate total nephron number, including acid maceration and the disector/fractionator method (277, 311). The latter is an unbiased method that uses two projecting microscopes to compare adjacent section pairs so that glomeruli that appear on one of the sections, but not the other, are counted (311). We adapted this method such that one microscope and individual sections would be sufficient to estimate total nephron number in mouse kidneys. Serial sections from newborn kidneys were collected and used to obtain an absolute count of nephron number. From this absolute count, we developed and validated our counting method.

Absolute nephron counts were obtained from nine kidneys sampled from C3H, B6, and CD1 mice, including left and right kidneys, and kidneys from males and females. All sections were collected and each glomerulus was tracked throughout each kidney to obtain an absolute nephron count (Figure 3.2). From this absolute count, a new counting method was derived. A fraction of the kidney was sampled using multiple sections such that all glomeruli on a given section were counted and nephron number was estimated using the following formula: $Nglom=f\times0.4\times NN$ where f is the fraction of the kidney sampled, 0.4 is a correction factor derived from the absolute counts that accounts for overlapping glomeruli in adjacent sections, and NN is the total number of glomeruli counted from all of the sections sampled.

The absolute nephron counts were compared to the estimated counts using both the disector/fractionator and our counting method. The absolute counts, the estimated counts, and the average error between the two estimation methods, when 10%, 5%, and 2.5% of the kidney was sampled, are shown in Table 3.1. The error rates for the two estimation methods were comparable, suggesting that our counting method is as efficient in estimating nephron number as the disector/fractionator method. Our counting method was therefore used for the subsequent studies.

3.4.3 The relationship between nephron number, kidney size, and birth weight

The relationships between nephron number, kidney size, and body weight were examined in newborn C3H and B6 mice. Kidney weight positively correlated with kidney surface area when data from both strains was combined ($P=4x10^{-9}$, Fig 3A) and when each strain was examined individually ($P<0.05$ for each, supplementary Table 1), suggesting that these measurements are interchangeable. When kidney weight was compared to birth weight, a positive correlation was seen when both strains were combined ($P=1.2x10^{-4}$, Fig 3B) and when each strain was examined separately ($P<0.05$ for each, supplementary Table 1), suggesting that mice with a lower birth weights are born with smaller kidneys. The same correlation was observed when kidney surface area was compared to birth weight when both strains were combined ($R^2=0.385$, $P=2.0x10^{-4}$, $n=28$) and when each strain was examined separately ($P<0.05$ for each, supplementary Table 1).

Despite the significant difference in kidney size between the two strains, there was no difference in nephron number. C3H (mean ± SE): 2208 ± 188 nephrons (n=5) vs. B6: 1994 ± 238 nephrons (n=4, P=0.5). The nephron counts were obtained from newborn mice representing the extreme and the mean values obtained for kidney sizes and body weights for these two inbred mouse strains. Importantly, nephron number did not correlate with body weight (P=0.46, Fig 3C), with kidney surface area (R^2=0.0256, P=0.63, n=9), or with kidney weight (P=0.67, Fig 3D). Similarly, no correlation was found between nephron number and kidney size when either strain was examined separately (P>0.05 for each, supplementary Table 1). These results demonstrate that kidney size correlates with birth weight, but nephron number does not correlate with birth weight or kidney size.

3.4.4 The relationship between nephron number and glomerular size

Nephrogenesis continues postnatally in mice, therefore, we examined nephron number in C3H and B6 mice at 8 weeks, when both nephrogenesis and kidney growth have ended. The number of nephrons was estimated in 12 mice from C3H and B6 strains using our counting method (n=48 kidneys, 6 males and 6 females from each strain). When males and females were pooled together, there was no significant difference in nephron number between C3H and B6 kidneys (P=0.4, Fig 4A). When males and females were examined separately, C3H females and both C3H and B6 males had, on average, 13% fewer nephrons when compared to B6 females (P=0.05, Fig 4B).

Studies in humans and mice have shown that as the number of nephrons decreases, glomerular volume and size increases (281, 292, 317). To examine whether the decrease in nephron number in C3H females and C3H and B6 males was accompanied by an increase in glomerular size, glomerular tuft planar surface areas were measured (35 glomeruli were sampled for each of the 48 kidneys) (255). C3H mice had significantly larger glomerular tufts than B6 mice (P=0.002, Fig 4C). When males and females were examined separately, C3H females and C3H and B6 males had glomerular tufts that were on average 12% larger when compared to B6 females (P=0.003, Fig 4D). However, no relationship was observed between glomerular size and nephron number when all groups were pooled together (R2=0.0032, P=0.7, n=48, data not shown).

3.4.5 Nephron number does not correlate with kidney size or body weight in adult C3H and B6 mice

Postnatal renal growth differs between C3H and B6 mice, such that C3H mice are born with smaller kidneys that become larger by adulthood compared with B6 mice (Figure 5A). To characterize this growth response, we measured the planar surface area of the cortex and medulla from serial kidney sections. A larger medulla and a larger cortex were observed in C3H adult kidneys compared with B6 kidneys (mean ± SE): for the medulla, C3H: 11.17 ± 0.19 mm^2, n=24, vs. B6 9.95 ± 0.18 mm^2, n=24, ($P=4x10^{-6}$), and for the cortex: C3H 27.72 ± 0.51 mm^2, n=24, vs. B6 21.46 ± 0.31 mm^2, n=24, ($P=4x10^{-21}$). The same relationship was true when males and females were examined separately (Fig 5B). These results suggest that the kidney architecture differs between different inbred mouse strains and that a larger cortex is not associated with an increase in nephron number.

From studies of adults, nephron number correlates with body weight, body surface area, height, and kidney weight (267, 269, 274, 277). Kidney weight correlated with kidney surface area in adult C3H and B6 mice ($R^2=0.9088$, $P=1.5x10^{-25}$, n=48). Importantly, as in the newborn period, kidney weight correlated with body weight ($R^2=0.551$, $P=1.6x10^{-9}$, n=48). However, we found no relationship between nephron number and body weight (P=0.97, Fig 5C). We also did not find a relationship between nephron number and kidney weight (P=0.58, Fig 5D) or between nephron number and kidney surface area ($R^2=9x10^{-5}$, P=0.95, n=48) in adult C3H and B6 mice. Similarly, we did not find any correlations between nephron number and body weight or kidney size when either strain was examined separately (P>0.05 for each, supplementary Table 1). When data from females and males was examined separately, there was still no correlation between nephron number and kidney size or between nephron number and body weight (P>0.05 for each, supplementary Table 1). These results suggest that differences in nephron number cannot be predicted by a change in kidney size or body weight and that nephron number is an independent variable in these mouse strains.

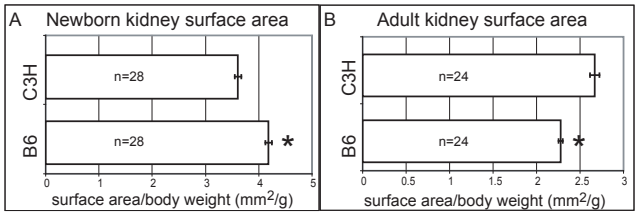

Figure 3.1: C3H and B6 mice have contrasting kidney sizes at birth and at adulthood

(A) Two inbred mouse strains were identified as having contrasting kidney phenotypes at birth. C3H mice have significantly smaller kidneys when compared to B6 mice. C3H: 3.61 ± 0.06 mm^2/g compared to B6: 4.18 ± 0.08 mm^2/g (measured as planar surface area corrected for body weight ± SE, *$P=2x10^{-7}$). **(B)** By adulthood, C3H kidneys are larger than B6 kidneys. C3H: 2.67 ± 0.05 mm^2/g compared to B6: 2.27 ± 0.02 mm^2/g (measured as planar surface area corrected for body weight ± SE,*P=1.8x10-7).

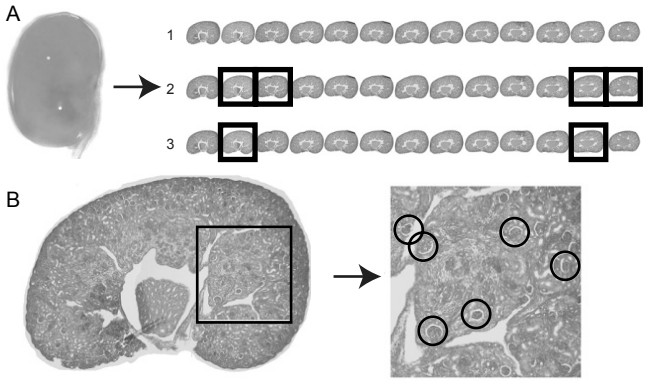

Figure 3.2: Development of a new method to estimate nephron number in mouse kidneys

(A) Serial sections were obtained from newborn kidneys. (1) The absolute nephron number count was obtained such that all glomeruli on a section were counted and compared to the adjacent section to ensure that overlapping glomeruli were not double-counted. (2) The disector/fractionator method of estimating nephron number in newborn kidneys. A fraction of the kidney was sampled and adjacent sections were compared (squares) and glomeruli that appeared in one section and not the other were counted. (3) A new method of estimating nephron number was developed based on the absolute counts obtained from (1). This new method is similar to the disector/fractionator method in that a fraction of the kidney is sampled except that adjacent sections are not compared and all glomeruli that appear on one section are counted. **(B)** The lower panel shows a section through a newborn kidney. Representative glomeruli are shown in the boxed region and are defined by the morphological appearance of the glomerular tuft. Glomeruli to be counted are circled.

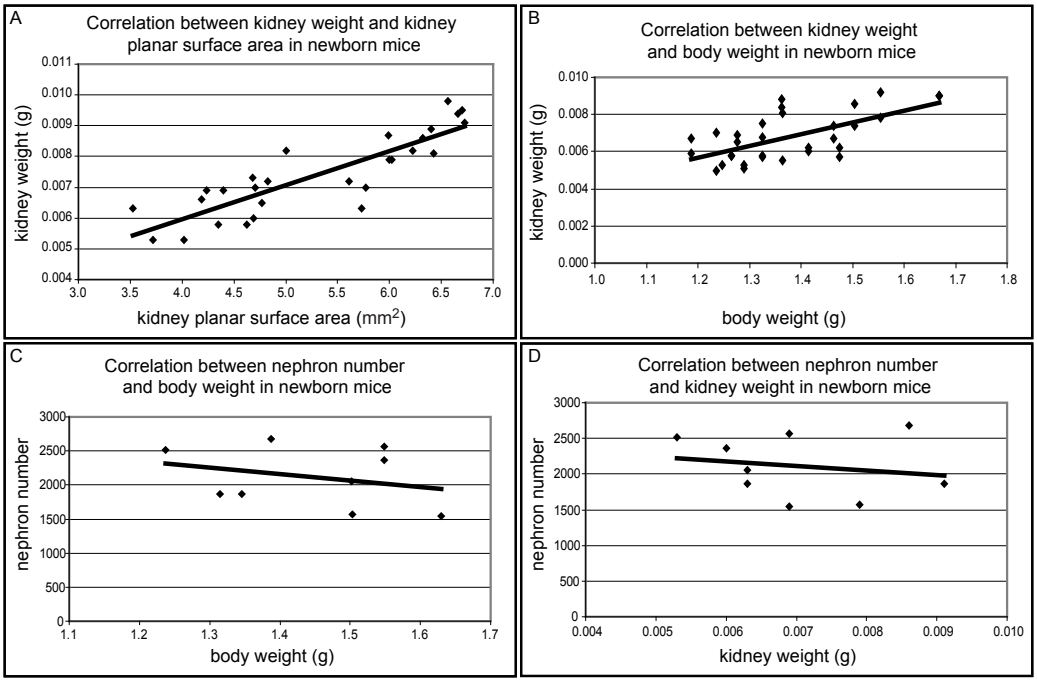

Figure 3.3: Relationship between nephron number, kidney size, and birth weight in newborn mice

(A) A positive correlation between kidney weight and kidney planar surface area is seen in the newborn period when combining data from C3H and B6 mice (R^2=0.7412, P=4x10^{-9}, n=28). **(B)** A positive correlation is observed between kidney weight and birth weight in newborn C3H and B6 mice (R^2=0.406, P=1.2x10^{-4}, n=28). **(C)** Nephron number does not correlate with birth weight (R^2=0.0814, P=0.46, n=9). **(D)** Similarly, nephron number does not correlate with kidney weight (R^2=0.0359, P=0.67, n=9).

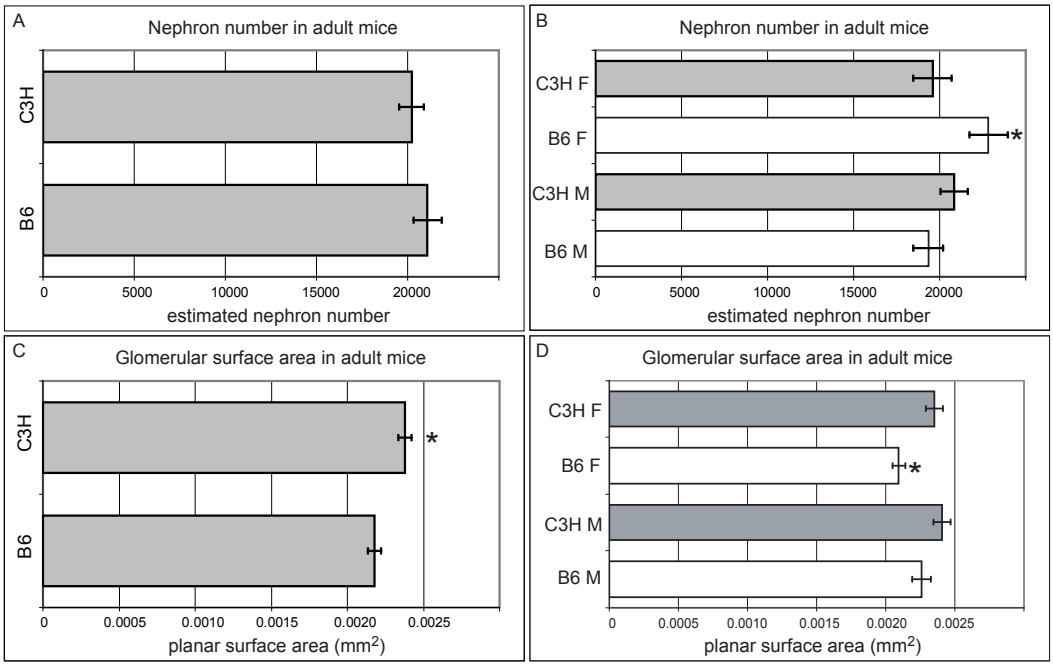

Figure 3.4: The relationship between nephron number and glomerular size **(A)** Estimated nephron number in all C3H and B6 adult kidneys are shown. C3H kidneys do not have significantly fewer nephrons than B6 kidneys (mean ± SE). C3H: 20220 ± 684 nephrons (n=24) vs. B6: 21085 ± 779 nephrons (n=24) (P=0.4). **(B)** Estimated nephron number in males (M) and females (F) are shown (mean ± SE): C3H F (n=12): 19591 ± 1116; B6 F (n=12): 22830 ± 1117; C3H M (n=12): 20848 ± 799; B6 M (n=12): 19341 ± 859. Kidneys from B6 females have, on average, 13% more nephrons than all other groups (*P=0.05). **(C)** Glomerular tuft sizes are shown for all C3H and B6 adult kidneys (mean ± SE). C3H mice: 0.002380 ± 0.000043 mm^2 vs. B6 mice: 0.002178 ± 0.000044 mm^2 (*P=0.002). **(D)** Glomerular surface area in B6 and C3H males (M) and females (F) are shown (mean ± SE). C3H F: 0.002353 ± 0.000061 mm^2; B6 F: 0.002094 ± 0.000045 mm^2; C3H M: 0.002408 ± 0.000062 mm^2; B6 M: 0.00226 2 ± 0.000068 mm^2. B6 females have glomerular tufts that are, on average, 12% smaller than those seen in all other groups (*P=0.003).

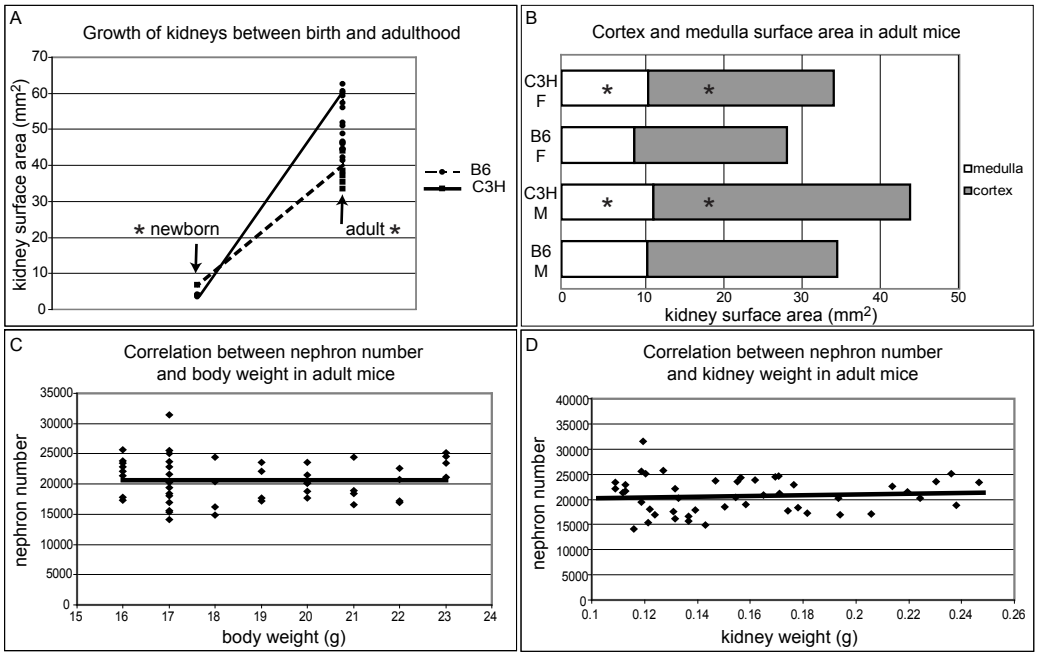

Figure 3.5: Nephron number does not correlate with kidney size or body weight in adult C3H and B6 mice

(A) The rate of postnatal renal growth differs between C3H and B6 mice. At birth, C3H kidneys (n=14, solid line) are smaller than B6 kidneys (n=14, dashed line) and show accelerated postnatal growth such that by adulthood C3H kidneys are larger (n=24) than B6 kidneys (n=24). **(B)** At adulthood, the size of the cortex and the medulla is larger in C3H female and males than B6 females and males. The medulla measurements show (mean ± SE): C3H female 10.85 ± 0.24 mm^2 vs. B6 female 9.17 ± 0.22 mm^2 (*P=$7.8x10^{-7}$), C3H male 11.50 ± 0.28 mm^2 vs. B6 male 10.74 ± 0.26 mm^2 (*P=0.04), while the cortex measurements show: C3H female 23.23 ± 0.35 mm^2 vs. B6 female 19.12 ± 0.23 mm^2 (*P=$4.9x10^{-17}$), C3H male 32.21 ± 0.61 mm^2 vs. B6 male 23.83 ± 0.44 mm^2 (*P=$9.9x10^{-21}$) (n=12 for each group). **(C)** Nephron number does not correlate with body weight in adult C3H and B6 mice (R^2=$3x10^{-5}$, P=0.97, n=48). **(D)** Nephron number does not correlate with kidney weight in adult C3H and B6 mice (R^2=0.0068, P=0.58, n=48).

Table 3.1: Absolute nephron counts for the nine newborn kidneys and estimated nephron counts using the two methods when 10%, 5%, and 2.5% of each kidney is sampled

strain	absolute count	disector/fractionator method			our counting method		
		10%	5%	2.5%	10%	5%	2.5%
C3H	1 544	1 229	1 172	1 032	1 713	1 549	1 299
C3H	2 566	2 649	2 817	2 265	2 551	2 332	2 416
C3H	2 052	2 120	2 099	1 577	2 316	2 474	2 108
B6	1 868	1 630	1 569	1 388	1 805	1 926	1 934
B6	2 675	2 341	2 600	2 076	2 880	2 659	2 475
B6	1 595	1 404	1 643	1 822	1 656	1 639	1 555
CD1	2 281	2 389	2 518	2 220	1 919	1 975	1 893
CD1	1 644	1 577	1 621	1 477	1 560	1 499	1 543
CD1	1 860	1 970	2 058	1 785	1 788	1 858	1 485
average % error		9.2%	8.9%	16.3%	7.1%	6.5%	9.1%

% error = (estimated count absolute count)/absolute count X 100

-

Supplementary Table 1

Correlation examined	R^2	P	n
kidney weight and kidney surface area in C3H mice at P1	0.36	0.02	14
kidney weight and kidney surface area in B6 mice at P1	0.78	2.7×10^{-5}	14
kidney weight and birth weight in C3H mice at P1	0.71	2.8×10^{-11}	14
kidney weight and birth weight in B6 mice at P1	0.69	5.0×10^{-18}	14
kidney surface area and birth weight in C3H mice at P1	0.71	2.6×10^{-11}	14
kidney surface area and birth weight in B6 mice at P1	0.33	3.5×10^{-7}	14
nephron number and kidney weight in C3H mice at P1	0.22	0.42	5
nephron number and kidney weight in B6 mice at P1	0.09	0.69	4
nephron number and kidney surface area in C3H mice at P1	0.05	0.70	5
nephron number and kidney surface area in B6 mice at P1	0.06	0.74	4
nephron number and body weight in C3H mice at P56	0.08	0.16	24
nephron number and body weight in B6 mice at P56	0.04	0.37	24
nephron number and kidney weight in C3H mice at P56	0.17	0.09	24
nephron number and kidney weight in B6 mice at P56	0.02	0.52	24
nephron number and kidney surface area in C3H mice at P56	0.02	0.47	24
nephron number and kidney surface area in B6 mice at P56	0.02	0.50	24
nephron number and body weight in female mice at P56	0.01	0.71	24
nephron number and body weight in male mice at P56	0.22	0.08	24
nephron number and kidney weight in female mice at P56	0.00	0.94	24
nephron number and kidney weight in male mice at P56	0.25	0.07	24
nephron number and kidney surface area in female mice at P56	0.01	0.63	24
nephron number and kidney surface area in male mice at P56	0.20	0.10	24

3.5 DISCUSSION

There is great interest in nephron number, its correlation with body and kidney size, and its association with disease susceptibility in humans (266, 267, 274, 317). To understand the impact of genetic and environmental variation on these relationships, we examined the relationship between kidney size and body size and between nephron number and kidney or body size in two inbred mouse strains with contrasting kidneys sizes. We determined that kidney size does correlate with body weight in the newborn and the adult period in either the C3H or B6 mouse strains. However, nephron number at birth and at adulthood did not correlate with kidney size or body weight. At birth, C3H kidneys were 10% smaller than B6 kidneys, although there were no significant differences in nephron number between the two strains. At adulthood, C3H kidneys were 17% larger than B6 kidneys, and there was still no significant difference in nephron number. These results suggest that kidney size is either independent of nephron number in these inbred mouse strains, or alternatively, we may not have been able to discern a relationship between nephron number and kidney or body size because of the lack of variation in these parameters.

Our estimated nephron counts for adult mouse kidneys were slightly higher than those reported in the literature using the disector/fractionator estimation method, but consistent with estimated counts obtained using the maceration technique (313). To determine if the higher counts were due to the new estimation method, we also estimated nephron number using the disector/fractionator method and obtained similar counts (data not shown). We are therefore confident that our counting method, which was validated in the newborn period using absolute counts, is sufficient in estimating nephron number in mice. We believe that our counts may be higher because of variability in the definition of a glomerulus when comparing studies that rely on the morphological appearance of a glomerulus as seen by the human eye. When we re-counted adult kidney sections and included only glomeruli that had a visible Bowman's space, in addition to a glomerular tuft, the estimated nephron counts dropped by 2-fold (data not shown) and were closer to some reports in the literature (302, 448).

This is the first study to examine the relationship between nephron number and kidney size or body weight in inbred mouse strains. Much of our understanding of these

relationships has come from studies on rats with naturally occurring low birth weight, and different results have emerged (289, 449). One study showed that Wistar rats with naturally occurring low birth weight had normal sized kidneys, a 20% reduction in nephron number, and an increase in glomerular volume (289), while another study showed that Sprague-Dawley rats with naturally occurring low birth weight did not have a decrease in kidney weight or in nephron number (449). This latter study also reported no relationship between nephron number and birth weight (449). Although body weight did correlate with kidney size in C3H and B6 mice, it was not an accurate predictor of nephron number. We also did not observe a relationship between nephron number and kidney size. The C3H mouse is normotensive, does not develop microalbuminuria, and has normal renal function (447, 450, 451). Similarly, the B6 mouse is resistant to renal disease (309, 452). In contrast, other inbred strains, SWR/J and DBA/2J, have been shown to be susceptible to hypertension and chronic kidney disease, respectively (425, 450, 453). It is possible that inbred mouse strains that are susceptible to renal disease may exhibit differences in nephron number that correlate with kidney size and body weight, but this was not examined in the current study.

Nephron number in mice may be influenced not only by strain but also by gender. Gender differences have been observed in humans: females generally have smaller kidneys with fewer nephrons than males (275, 281). Another study identified a correlation between nephron number and birth weight in males, but not in females (269). We separated our data by gender because we hypothesized that gender might affect nephron number and nephron formation. Although C3H females had fewer nephrons than C3H males, the inverse relationship was seen in B6 mice in which females had more nephrons than males. Therefore, the impact of gender on nephron number in these strains remains unclear.

Our results demonstrate that at adulthood, C3H females and C3H and B6 males had a 13% decrease in nephron number that was accompanied by a proportional 12% increase in glomerular tuft size when compared to B6 females. Although a 30% decrease in nephron number in Australian Aboriginals has been associated with a 27% increase in glomerular volume (267), the relationship between nephron loss and glomerular hypertrophy is poorly understood. It appears that the kidney is able to adapt to maintain

an adequate filtration surface area, such that when nephron number decreases, glomerular size increases proportionally.

To determine whether the relationship between nephron number and kidney or body size is an issue of scale, we examined the fold variation in kidney size, body weight, and nephron number reported in the literature. In the studies that showed a positive correlation between nephron number and kidney size, at least a 5.6-fold (range 3.5-8.7) variation in nephron number correlated with a 3-fold (range 2.4-3.4) variation in kidney size (267, 274, 275). In one study that identified a correlation between nephron number and birth weight, there was an 8-fold variation in nephron number and a 2-fold variation in birth weight (269). In the studies that did not show a correlation, there was an average 2.9-fold (range 2.6-3.2) variation in nephron number and an average 1.9-fold (range 1.7-2.2) variation in kidney size (266, 281). In our study, there was a 1.9-fold variation in nephron number, a 2-fold variation in kidney size, and a 1.4-fold variation in body weight at birth and at adulthood. We therefore suspect that large variations in these parameters, greater than 2-fold, may be required before a correlation can be observed between nephron number and kidney or body size.

In summary, while kidney size appears to be tightly correlated with body weight at birth and at adulthood, nephron number does not correlate with kidney size or body weight in C3H and B6 inbred mice. Our results suggest that within the normal, relatively small, range of kidney and body size seen in these inbred mouse strains, these parameters are independent of nephron number. However, we speculate that positive correlations between nephron number and kidney or body size may be observed when there are large differences, greater than 2-fold in these variables. This is most likely to be seen when there is a greater range of phenotypic variability either from a developmental insult or from an acquired disease. Future studies clearly need to continue to examine the relationship between nephron number, kidney size, body weight, and disease susceptibility to determine if these predictions in regards to the issue of scale are correct.

3.6 ACKNOWLEDGEMENTS

We thank CG Goodyer and N Haddad for critical reading of the manuscript and discussions; X He for assistance with the paraffin sections; and X Zhang for help with

statistical analysis. This work was supported by an operating grant from the Kidney Foundation of Canada. IRG is a recipient of an FRSQ chercheur-boursier clinicien salary award. IJM is a recipient of an FRSQ doctoral award.

Connecting text for Chapters III and IV

Whole genome studies on humans with VUR have identified over 10 different loci that are associated with VUR; however, the underlying causative genes associated with these loci have not been identified (32). Approximately 14 genes have been associated with VUR, and most of these have been identified from mouse studies and/or studies on humans with rare syndromes and/or chromosomal abnormalities (32). The majority of studies using the mouse as a model have relied on reverse genetics, which is a technique that determines a gene's function by mutating it and identifying the outcome. All of the six mouse models of VUR are examples of reverse genetics in that the specific gene perturbations were subsequently found to be associated with kidney and urinary tract defects (24, 46, 68, 93, 94, 216). Because of our observation that certain inbred mouse strains are susceptible to VUR while others are resistant, we chose to study the VUR phenotype using forward genetics, which starts with a mutant phenotype and then works towards identifying the underlying genetic cause. We hypothesized that inbred mice, which are genetically homogeneous, would be a good model system in which to identify and study VUR-causing genes.

We screened eleven inbred mouse strains for VUR and for kidney size, and identified four strains that were susceptible to VUR: AKR/J, DBA/2J, CBA/J, and C3H/HeJ. Interestingly, the AKR/J, DBA/2J, and CBA/J strains exhibited incidences of VUR that were similar to those reported for both the transgenic *Hoxb7/Ret*$^{+/-}$ and mutant *Pax2*$^{1Neu+/-}$ reflux mouse models (incidences of VUR range from 28-55%). However, the C3H/HeJ mouse is the only mouse described that exhibited a 100% incidence of VUR at birth. When compared to non-refluxing C57BL/6J mice, C3H/HeJ mice had normal kidneys, caudal ureteric buds, short intravesical ureters, and a delay in urinary tract development. Because of this observation, we hypothesized that the C3H/HeJ mouse would be an ideal strain in which to identify genes that are associated with VUR without a renal malformation.

To identify the VUR-causing locus in the C3H/HeJ mouse, backcross and intercross progeny were bred and tested for VUR. A whole-genome scan using single nucleotide polymorphisms was performed on the backcross and intercross progeny and identified a locus on chromosome 12 that is significantly associated with the VUR

phenotype. This is the first study that uses a mapping strategy in inbred mice to identify novel VUR-causing loci. The large homologies between the mouse and the human genome suggest that the gene(s) that is responsible for VUR in C3H/HeJ mice could also be involved in human VUR. We speculate that this gene(s) may be important in the development of VUR in the subset of humans that have VUR without a renal malformation.

CHAPTER IV

The C3H/HeJ inbred mouse is a model of vesico-ureteric reflux and has a susceptibility locus on chromosome 12

Inga Murawski, Rita Maina, and Indra Gupta

manuscript to be submitted

4.1 ABSTRACT

Vesico-ureteric reflux is a major cause of end-stage renal disease in children and is characterized by a defective uretero-vesical junction that allows urine to flow retrogradely from the bladder towards the kidneys. VUR can have a genetic origin and the discovery of genetic factors that are associated with this disorder is a powerful approach to understand disease outcome in patients with VUR. We screened eleven inbred mouse strains for vesico-ureteric reflux and identified one strain, C3H/HeJ, which has a 100% incidence of vesico-ureteric reflux. C3H/HeJ mice are predisposed to vesico-ureteric reflux as a result of a defective uretero-vesical junction characterized by a short intravesical ureter. The defect appears to arise from a delay in urinary tract development initially manifested by a ureteric bud that arises from a more caudal location along the mesonephric duct. In contrast, C57BL/6J mice are resistant to reflux, have long intravesical ureters, normally positioned ureteric buds, and no delay in urinary tract development. Whole-genome mapping of backcross and intercross mice derived from a C3H/HeJ and C57BL/6J cross was performed and identified a reflux-causing locus spanning the first 24Mb of chromosome 12, VUR1 (LOD=7.4, $P<0.0001$). This region is homologous to human chromosome 2p24-25 and is a novel locus as it does not correlate with any of the genes or loci thus far reported from human studies.

4.2 INTRODUCTION

Vesico-ureteric reflux (VUR) is a congenital urinary tract defect of the uretero-vesical junction in which urine flows retrogradely from the bladder to the ureters and the kidney (3-5). It affects up to 1% of the population and is associated with recurrent urinary tract infections, renal malformations, hypertension, and end-stage renal disease (6-8, 149, 150). The uretero-vesical junction is composed of the intravesical ureter and the surrounding bladder musculature, and is compressed during bladder filling to prevent the reflux of urine (10, 96, 97). Specific defects in the uretero-vesical junction have been observed in patients with VUR, including a short intravesical ureter, an abnormal ureteric orifice, and a poorly muscularized ureter and/or bladder (10, 12, 13). However, it is still unclear whether these defects are primary or secondary manifestations of an abnormal uretero-vesical junction.

Treatment of VUR includes antibiotic prophylaxis to prevent recurrent urinary tract infections that may lead to renal damage and/or surgical treatment to remodel the uretero-vesical junction (208, 209, 212). In spite of these therapies, the incidence of end-stage renal disease secondary to VUR, so-called reflux nephropathy, has not decreased over the past 40 years (208, 212). This strongly suggests that the pathophysiology of VUR and its associated complications need to be re-examined to understand which patients may benefit from treatment.

VUR can have a genetic origin and the discovery of the genetic factors associated with this disorder may be the best approach to characterize and assess outcome in patients with VUR. From twin and family studies, VUR is highly heritable (29, 324, 330). Genetic analysis of patients with VUR has shown that the condition is heterogeneous such that a number of different genes and loci are associated with VUR (29-31, 330). However, the association of specific genes with VUR has not been consistently demonstrated and few of the loci have been replicated in independent cohorts. This suggests that a variety of strategies will be required to identify the underlying genes associated with VUR, and to understand the relationship between these gene candidates and disease progression.

We previously identified two mouse models of VUR with kidney malformations, the *Pax2*$^{1Neu+/-}$ and *Hoxb7/Ret*$^{+/-}$ mice (24, 68). From our work on these models, we have

shown that the position of the ureteric bud, the primordial structure that develops into both the kidney and the ureter, is abnormally positioned along the mesonephric duct, and that the intravesical ureters are shorter compared to non-refluxing mice (24, 68). These models validate the use of the mouse to study VUR, since the associated genes, *Pax2* and *Ret*, have also been found to be important in humans affected with VUR (221, 246, 249).

Most children with VUR have normally formed kidneys (204, 206). Therefore, in the present study, our objective was to identify mouse models of VUR without a renal malformation. Eleven inbred mouse strains were screened for VUR and kidney morphology and from this, we identified the C3H/HeJ (C3H) mouse as a model of VUR without a kidney malformation. Urinary tract development and formation of the uretero-vesical junction was characterized in C3H mice that are extremely susceptible to VUR and compared to C57BL/6J (B6) mice that are resistant to VUR. We then performed linkage analysis on backcross and intercross mice from an initial C3H and B6 cross and identified a reflux-causing locus in the C3H mouse, the VUR1 locus. This is the first report using a whole-genome mapping approach to identify VUR-causing loci in the mouse.

4.3 MATERIALS AND METHODS

4.3.1 Animal breeding: inbred mouse strains

The following eleven inbred mouse strains were purchased from Jackson Laboratories between the ages of 6 to 8 weeks: A/J, BALB/cJ, C57BL/6J, SJL/J, 129S1/Svlmj, FVB/J, SM/J, AKR/J, DBA/2J, CBA/J, C3H/HeJ. We generated F1 hybrids by intercrossing C3H/HeJ and C57BL/6J parental strains. We also generated backcross (N2) [(C3H X B6)F1 X C3H] and intercross (F2) [(C3H X B6)F1 X (C3H X B6)F1] progeny following standard breeding schemes. For all animal experiments, multiple litters from each strain or cross were examined. All animal studies were performed in accordance with the rules and regulations of the Canadian Council of Animal Care (CCAC). Animal protocols were approved by the McGill University Health Center Animal Care Committee (UACC) and Ethics Committee.

4.3.2 Vesico-ureteric reflux and intravesical ureter lengths

Eleven inbred strains were tested for the presence of vesico-ureteric reflux (VUR) at postnatal (P) day 1 as previously described (24). C3H and B6 mice were tested for VUR at 8 weeks in the same manner. VUR was identified by the retrograde passage of methylene blue into the ureters or renal pelvis. During injection, the syringe was raised vertically from 30 to 150 cm by 30 cm every 10 seconds. The hydrostatic pressure was recorded for each ureter and represented the height of the column of methylene blue in relation to the level of the mouse when reflux was first noted. Body weights and kidney weights were obtained for all samples collected. Kidney sizes were measured as whole-mount planar surface areas using SPOT (v.3.5.9), as previously described (68, 434). The length of the intravesical ureter was measured as previously described (68). The dye was photographed moving through the ureters into the bladder and the distance between the bladder periphery and the site of dye exit was defined as the intravesical ureter length and measured using SPOT (v.3.5.9). All measurements were taken by one observer who was blinded to the strain of the embryonic tissue.

4.3.3 *In situ* hybridization

Embryos were generated by performing timed two-hour early-morning matings. The visualization of a vaginal plug was recorded as embryonic (E) day 0 and embryos were collected at E11 for *in situ* hybridization. Embryos were staged using Theiler's criteria and crown-rump lengths were measured such that embryos with similar morphological features and of similar size were used for analysis. Whole-mount *in situ* hybridization was performed as previously described (68, 435). A DIG-labelled UTP (Roche) *c-Ret* probe was used to visualize the mesonephric duct and the ureteric bud. The position of the ureteric bud was determined by measuring the distance between the caudal edge of the mesonephric duct and the start of the ureteric bud (24, 68). All measurements were taken by one observer who was blinded to the strain of the embryonic tissue.

4.3.4 Animal breeding: C3H/GFP and B6/GFP mice

To examine kidney and urinary tract development in C3H and B6 mice, both strains were crossed to *Hoxb7/GFP*$^{+/-}$ transgenic mice that express green fluorescent protein throughout the mesonephric duct and its derivatives (432). After 10 generations of backcrossing the GFP transgene onto the two inbred backgrounds, embryos from timed matings were collected between E11 and E15. Embryos were staged in the same manner as for the *in situ* experiments. Embryos were dissected using fluorescent microscopy and the developing mesonephric ducts, ureteric buds, ureters, and kidneys were imaged.

4.3.5 Genotyping and linkage analysis

An initial genome-wide screen was performed on N2 animals using the Illumina mouse low density linkage panel that contains 268 informative single nucleotide polymorphisms (SNPs) between the C3H and B6 mouse strains. Linkage analysis was performed by comparing the proportion of C3H homozygous alleles compared to recombinant alleles in both VUR-affected and VUR-unaffected offspring at each SNP. A chi-square test statistic (1 d.f.) of independence was used for statistical analysis and LOD scores were calculated manually: $LOD=X^2/2(\log_e 10)$ (454). Based on criteria established by Lander and Kruglyak (454), significant linkage was defined as a LOD=3.3 and $P=1.0\times10^{-4}$, while suggestive linkage was defined as a LOD=1.9 and $P=3.4\times10^{-3}$. Genotyping data were

analyzed with J/qtl (http://research.jax.org/faculty/ churchill/software/Jqtl), which is a JAVA-enabled version of the R/QTL package (455). One thousand permutation tests were performed for the analysis to reduce the probability of finding false associations and to determine a threshold of significance for linkage findings. In addition to performing linkage analysis using VUR as a binary trait (present or absent), the following phenotypes were examined as quantitative traits using non-parametric analysis: pressure when reflux occurred, kidney planar surface area, and kidney weight. To confirm the results identified in the first genome-wide screen, four additional informative microsatellite markers were used to genotype all of the N2 and F2 progeny: D12Mit37, D12Mit215, D12Mit240, and D12Mit105, at positions 5.4Mb, 7.6Mb, 11.2Mb, and 25.6Mb, respectively. PCR conditions were 95C for 3 min, followed by 35 cycles of 94C for 30 sec, 55C for 30sec, 72C for 1 min, followed by a final incubation at 72C for 7 min. PCR products were electrophoresed on 4% agarose gels (Wisent). Results were analyzed in the same manner as for the first genome-wide screen.

4.3.6 Animal breeding: recombinant inbred mouse strains

Ten recombinant inbred BXH (B6 X C3H) strains were purchased from Jackson Laboratories: BXH2, BXH4, BXH6, BXH7, BXH8, BXH9, BXH10, BXH11, BXH14, BXH19 and tested for VUR. Kidney sizes and the length of the intravesical ureters were measured as described above from multiple litters. SNP genotype data for the ten BXH strains was obtained from the Mouse Phenome Database (http://www.jax.org/phenome) and genotype-phenotype correlations were made.

4.3.7 *In silico* haplotype mapping, RT-PCR and sequencing of *Rdh14* and *Osr1*

SNP genotype data was obtained from the Mouse Phenome Database (http://www.jax.org/phenome) for the eleven inbred mouse strains tested for VUR. Mice were labelled as either VUR-affected or VUR-unaffected and genotype-phenotype correlations were made. RT-PCR was performed on kidneys with their ureters that were microdissected at E14 using primers designed for *Rdh14*: forward 5'GGTGCCCAGACTTCCATCTA reverse 5'CCCACAGTTTTCTTGCCACT, and for *Osr1:* forward 5'CATCCCTGCAGCTTACCAAT reverse

5’ATGAAGAGCGCTGAAACCAT. Primers designed for RT-PCR on the remaining 18 candidate genes within VUR1 are available upon request. RNA was extracted from embryonic kidneys using the RNeasy Mini Kit (Qiagen) as per manufacturer’s instructions. DNase treatment was performed on all extracted RNA to remove any DNA contamination using TURBO DNA-free (Ambion) as per manufacturer’s instructions. Positive and negative controls for the RT-PCR were performed using β-actin primers. For sequencing, oligonucleotides were designed to the coding regions of *Rdh14* and *Osr1* based on transcript maps obtained from Ensembl (www.ensembl.org). Oligonucleotides used for PCR amplification are available upon request. DNA was extracted from mouse tail-clips following standard protocol and PCR products were sequenced at the McGill University and Genome Québec Innovation Centre (www.genomequebecplatforms.com/mcgill). Transcription factor binding sites were predicted using TFSEARCH program (456).

4.4 RESULTS

4.4.1 The C3H mouse is a model of VUR without a renal malformation

To identify mouse models with VUR, we screened eleven inbred mouse strains for the presence of VUR at birth. Four strains were susceptible to VUR: AKR, DBA, CBA, and C3H (Figure 4.1A-B), while the remaining seven strains were resistant. In addition to testing for VUR, we assessed kidney size, measured as planar surface area and as kidney weight, for all of the strains (434) (Figure 4.1D). Two strains, C3H and B6, showed contrasting phenotypes and were analyzed in depth for the remainder of the studies (Figure 4.1B-C). B6 mice had no VUR and larger kidneys (measured as planar surface area corrected for body weight ± SE): 4.18 ± 0.08 mm^2/g when compared to C3H mice that had a 100% incidence of VUR and significantly smaller kidneys: 3.61 ± 0.06 mm^2/g ($P=2x10^{-7}$). The same results were obtained when kidney weights were compared (data not shown). C3H mice exhibited both bilateral and unilateral VUR (bilateral: 61% (11/18) vs. unilateral: 39% (7/18), $X^2=1.8$, P=0.18). In the cases of unilateral VUR, right-sided VUR was more common (right-sided VUR: 71%, (5/7) vs. left-sided VUR: 29% (2/7), $X^2=2.57$, P=0.1). Among the C3H and B6 litters, there was an equal proportion of males and females with no skewing of the sex ratio. C3H and B6 mice were tested for VUR at 8 weeks of age to determine if VUR resolved. C3H mice continued to reflux (incidence: 92% (11/12)), while B6 mice continued to be resistant with only one mouse showing mild unilateral reflux that did not reach the renal pelvis (incidence: 8% (1/12)).

C3H mice had smaller kidneys at birth compared to B6 mice; we therefore hypothesized that they might have fewer nephrons. As part of another study, nephron counts were obtained at adulthood and no differences in nephron number were noted between the two strains (Murawski, unpublished). The C3H mouse is therefore a model of VUR without a kidney malformation, and thus it reproduces the phenotype seen in most children with VUR who have normally formed kidneys (204, 436).

4.4.2 C3H mice have short intravesical ureters and caudal ureteric buds

The intravesical ureter must be of sufficient length to prevent the backflow of urine from the bladder into the ureters (10, 12, 13, 179). Intravesical ureter lengths were measured at birth and C3H mice had significantly shorter intravesical ureters than B6

mice, for both the left and the right ureters (Figure 4.2A-D). Length of the left intravesical ureter (mean ± SE) was 0.203 ± 0.012 mm, n=6, in C3H mice, and 0.344 ± 0.043 mm, n=8, in B6 mice ($P=5.5x10^{-3}$). Length of the right intravesical ureter (mean ± SE) was 0.215 ± 0.016 mm, n=8, in C3H mice, and 0.314 ± 0.003 mm, n=8, in B6 mice ($P=1.7x10^{-3}$). When the intravesical ureter lengths were plotted for each strain, the data formed a continuous distribution suggesting that intravesical ureter length is a quantitative trait that is determined by more than one gene (Figure 4.2D).

The position from which the ureteric bud emerges along the mesonephric duct has been shown to be important for normal kidney and urinary tract development and was assessed at embryonic day (E) 11 (21, 24, 68). C3H embryos had ureteric buds that developed more caudally, closer to the end of the mesonephric duct, while B6 embryos had ureteric buds that developed more cranially, further from the end of the mesonephric duct (Figure 4.2E-H). Position of the ureteric bud relative to the end of the mesonephric duct on the left was (mean ± SE) 0.089 ± 0.007 mm, n=3, in C3H embryos and 0.156 ± 0.005 mm, n=3, in B6 embryos ($P=6.3x10^{-6}$). Position of the ureteric bud relative to the end of the mesonephric duct on the right was (mean ± SE) 0.077 ± 0.005 mm, n=3, in C3H embryos and 0.138 ± 0.011 mm, n=3, in B6 embryos ($P=6.7x10^{-4}$). When the position of the ureteric bud was plotted for each strain, the data was also continuously distributed suggesting that ureteric bud position, like intravesical ureter length, is a quantitative trait (Figure 4.2H).

4.4.3 C3H mice exhibit a delay in urinary tract development

We have previously shown that a caudal ureteric bud is associated with a delay in urinary tract development and VUR; therefore, we speculated that the caudal ureteric bud in C3H embryos might also represent a delay (68). Kidney and urinary tract development was compared in detail in C3H and B6 embryos by crossing the *Hoxb7/GFP* transgene onto both a C3H and B6 background (432). Embryos were collected between E11 and E15 and were carefully staged so that only those with similar morphological features were compared. Between E11 and E13, no gross differences in kidney and urinary tract morphology were noted between the two strains (data not shown and Figure 4.3A). At E13, the ureter had reached the developing bladder and remained attached to the

mesonephric duct in both C3H and B6 embryos (C3H n=5, B6 n=5, Figure 4.3A). However, at E14, 50% (3/6) of B6 embryos had ureters that had separated from their mesonephric ducts, while none (0/5) of the C3H embryos had ureters that had separated (X^2=3.4, P=0.06, Figure 4.3B). The delay was even more apparent at E15, when 100% (4/4) of B6 embryos had ureters that had separated from their mesonephric ducts, while only 17% (1/6) of C3H embryos had complete separation of the ureter from the mesonephric duct (X^2=6.67, P=0.001, Figure 4.3C-D). By birth, all C3H mice had ureters that had separated from their mesonephric ducts, although the intravesical ureter lengths were shortened. We therefore speculate that the delay in ureter separation disrupts the spatial and temporal growth of the ureter into the bladder leading to a short intravesical ureter that refluxes.

4.4.4 N2 mice have a high incidence of VUR

Inbred mouse strains are powerful tools for dissecting the underlying genetic causes of diseases (412). Analysis of 54 F1 (C3H X B6), 303 N2 (F1 X C3H), and 116 F2 (F1 X F1) progeny suggested that the VUR phenotype segregates as a recessive trait since the majority of F1 animals did not exhibit reflux (Figure 4.4A). The VUR assay that was developed can be scored both qualitatively as a binary trait, by the presence/absence of VUR, but also quantitatively as a quantitative trait, by documenting the pressure required for VUR to occur in a ureter (24, 68). If a ureter refluxes at a lower pressure, this suggests a more severe uretero-vesical junction defect. Analysis of the segregation of the VUR phenotype as a binary trait in the N2 and F2 progeny is consistent with the effect of a major gene with incomplete penetrance; however, the analysis of both qualitative and quantitative evaluation of VUR may underlie a more complex mode of inheritance. Most of the VUR observed in C3H mice occurred at low pressures, below 90cm (88% (22/25 ureters) VUR ≤ 90cm vs. 12% (3/25 ureters) VUR ≥ 120cm, X^2=29, P=$8x10^{-8}$, Figure 4.4B). For the two F1 mice that refluxed (2/54), reflux occurred at the highest pressure, suggesting that these mice had a mild form of VUR. In the N2 mice, 46% (140/303) had VUR, and of these, 66.5% (93/140) had unilateral VUR with no left or right-sided predominance (left: 50.5% (47/93) vs. right: 49.5% (46/93), X^2=0.02, P=0.88). Consistent with the results from the parental C3H strain, there was no gender effect: N2

males and females were equally affected with VUR (females: 49% vs. males: 51%, X^2=0.06, P=0.81). The pressure at which each ureter refluxed is represented in Figure 4.4C, in which half of the ureters in N2 progeny showed VUR below 90cm. In the F2 mice, 16% (19/116) had VUR, and most of these were unilateral (unilateral: 68% (13/19) vs. bilateral 32% (6/19), X^2=5.2, P=0.02) with a slight predominance of left-sided VUR, although this was not statistically significant (left: 62% (8/13) vs. right: 38% (5/13), X^2=1.4, P=0.2). The majority of ureters in F2 progeny showed VUR below 90cm (68% VUR ≤ 90cm vs. 32% VUR ≥ 120cm, X^2=6.5, P=0.01, data not shown).

Given that C3H mice had smaller kidneys than B6 mice in the newborn period, and kidney sizes have been shown to be heritable in the mouse (446), we examined kidney sizes in F1, N2, and F2 progeny. Kidney planar surface areas corrected for body weight were examined and there were no significant differences (mean ± SE) when C3H mice (3.60 ± 0.06 mm^2/g, n=38) were compared to F1 (3.41 ± 0.06 mm^2/g, n=114) or to F2 mice (3.47 ± 0.05 mm^2/g, n=232, ANOVA P=0.3). However, N2 mice had significantly smaller kidneys (3.24 ± 0.01g, n=606) than C3H, B6, F1, and F2 mice (P<0.05 for each, Figure 4.4D). The same findings were observed when kidney weights were used in the analysis (data not shown). Importantly, refluxing N2 mice did not have significantly smaller kidneys than non-refluxing N2 mice. Kidney planar surface areas corrected for body weight (mean ± SE) for N2 mice with VUR: 3.24 ± 0.03 mm^2/g, n=140 and for N2 mice without VUR: 3.24 ± 0.02 mm^2/g, n=163, (P=0.9). These results demonstrate that VUR and a smaller kidney size do not segregate together as phenotypes.

4.4.5 A locus on mouse chromosome 12, VUR1, is associated with VUR in the C3H mouse

To map VUR-causing loci in C3H mice, a genome-wide scan of 172 affected and unaffected N2 animals was performed. Linkage analysis was initially performed by comparing the proportion of C3H homozygous alleles to recombinant alleles in both VUR-affected and VUR-unaffected offspring at each SNP (457). The C3H genotype was over-represented at four consecutive markers at the proximal end of chromosome 12 in refluxing mice, with a peak LOD score at marker rs3709002 (LOD=3.5, X^2=16.2, P=5.68x10^{-5}). This genomic region is hereafter called the VUR1 locus. On chromosome

2, marker rs13476573 reached suggestive linkage (LOD=1.9, X^2=8.6, P=3.4x10^{-3}) and the allele-effect plot showed an over-representation of the homozygous C3H genotype suggesting the presence of another susceptibility locus. On chromosome 6, marker rs13478728 approached suggestive linkage (LOD=1.5, X^2=6.8, P=9.3x10^{-3}), and the allele-effect plot shown an over-representation of the heterozygous genotype suggesting the presence of a locus that confers resistance to VUR.

The linkage analysis was redone using J/qtl and revealed the same VUR1 locus on chromosome 12 and the two suggestive peaks on chromosomes 2 and 6 described above. When VUR was scored as a binary trait, the LOD score was 3.5 (genome-wide significance P=0.014), and the VUR1 locus accounted for 8.9% of the phenotypic variance. When VUR was scored as a quantitative trait (non-parametric analysis), the LOD score increased to 5.0 (genome-wide significance, P=0.008, Figure 4.5A), and the VUR1 locus now accounted for 12.5% of the phenotypic variance. The 1.5-LOD support interval (95% confidence interval) for VUR1 suggests that the locus spans the first 24Mb of chromosome 12 (458).

To confirm the association between chromosome 12 and VUR1, additional genotyping was performed on a larger sample of N2 (n=303) and F2 (n=116) progeny using microsatellite markers spanning the VUR1 locus. For the N2 progeny, a peak LOD score of 6.6 (binary trait) and 7.4 (quantitative trait) was observed at marker D12Mit240 (11.2Mb) (genome-wide significance P<0.0001 for each, Figure 4.5B). For the F2 progeny, a peak LOD score of 4.1 (binary trait) and 4.3 new data (quantitative trait) was observed at the same marker (genome-wide significance, P<0.0001 for both). The linkage analysis supports the results found in the segregation analysis: VUR in the C3H mouse appears to be a complex recessive trait likely caused by the interaction of several genes with a major gene contained within VUR1.

Linkage analysis was also performed on the N2 progeny to determine if kidney size (kidney weight or kidney planar surface area) segregated with particular genotypes. Three loci were associated with kidney weight and kidney planar surface area on chromosomes 1 (LOD 1.6), 11 (LOD 1.5), and 12 (LOD 1.2). Although the locus on chromosome 12 overlaps with the VUR1 locus, all three loci only approached suggestive linkage. These results support our phenotype observations and suggest that the gene(s)

that confers susceptibility to VUR does not segregate together with the gene(s) that regulates kidney size.

4.4.6 BXH mice with VUR have short intravesical ureters

To prioritize the genomic regions within the VUR1 locus, ten recombinant inbred BXH lines were screened for VUR and intravesical ureter length. Kidney size was also assessed. Based on the incidence of VUR in other mouse models of VUR (24, 68), five of the 10 BXH lines exhibited significant VUR (defined as incidence of VUR > 20%): BXH14, BXH7, BXH4, BXH11, BXH19 (Figure 4.6A). Consistently, the BXH lines that refluxed had shorter intravesical ureters than the non-VUR lines (mean length ± SE), demonstrating that the length of the intravesical ureter is a strong determinant of VUR. Intravesical ureter length in refluxing BXH lines was: 0.21 ± 0.1 mm, n=105, vs. non-refluxing BXH lines: 0.30 ± 0.1 mm, n=126, $P=8x10^{-5}$, Figure 4.6B. Left and right intravesical ureter lengths were pooled as there was no significant difference when left and right intravesical ureters were examined separately for each of the lines (data not shown). When kidney size was assessed, refluxing BXH strains did not have smaller kidneys than non-refluxing BXH strains. Kidney size (kidney planar surface area corrected for body weight ± SE) in refluxing BXH lines was: 3.24 ± 0.05 mm^2/g, n=262, vs. non-refluxing BXH lines: 3.33 ± 0.05 mm^2/g, n=302, P=0.3, Figure 4.6C. These results suggest that VUR and short intravesical ureters, but not kidney size, segregate together as phenotypes, which is consistent with the findings in the N2 progeny.

The BXH10 line has no VUR, a long intravesical ureter, and it is homozygous C3H for the first 9.5Mb of chromosome 12, after which it is homozygous B6 until 36Mb. While this data does not definitively rule-out or rule-in a particular genomic region, it does suggest that within the VUR1 locus, the region between 9.5 and 24Mb should be prioritized for further study. Three BXH lines showed phenotypes contrary to what was expected based on their genotypes on chromosome 12. BXH9 and BXH6 mice are homozygous C3H within the VUR1 locus, however they have long intravesical ureters and only a 10-12.5% incidence of VUR. BXH 4 mice are homozygous B6 within the VUR1 locus, however they have short intravesical ureters and a 57.7% incidence of VUR. These results suggest that in BXH mice, VUR represents a continuous distribution

and that resampling of the B6 and C3H genome has an impact on the expression of the phenotype.

4.4.7 *In silico* mapping and candidate gene analysis in the VUR1 locus

The C3H mouse has a 100% incidence of VUR, short intravesical ureters, a caudally shifted ureteric bud, and a delay in urinary tract development. We therefore hypothesized that the VUR1 candidate gene(s) would be expressed and function during urinary tract and possibly kidney development. The VUR1 locus has 198 gene candidates (NCBI Build 37.1). To prioritize genomic regions and candidate genes, *in silico* mapping was used (409). We compared haplotypes in the refluxing and non-refluxing strains identified in the initial mouse screen (Figure 4.7A). Regions within VUR1 that contained SNPs that were common between VUR-affected strains, and different from VUR-unaffected strains, were considered as priority regions for assessment of gene candidates. Many of these haplotypes contained ribosomal proteins and pseudogenes of unknown significance; therefore, haplotypes that contained genes with more obvious developmental roles were prioritized for further study. Based on literature searches, approximately 20 genes within VUR1 were chosen for analysis because of their apparent role during development. RT-PCR confirmed the expression of these genes in the developing kidney and ureter (Figure 4.7B).

Using the above described *in silico* approach, and the data from the BXH strains, two promising candidate genes were identified: retinol dehydrogenase 14 (*Rdh14*) and odd skipped related 1 (*Osr1*). RT-PCR was performed on microdissected kidneys with their attached ureters from C3H embryos at E14 to confirm the expression of *Rdh14* and *Osr1* in the developing kidney and urinary tract (Figure 4.7B). Sequencing for the coding, 5' flanking, and 3'UTR regions of *Rdh14* and *Osr1* was performed using DNA extracted from C3H and B6 mice. There were no differences in the *Osr1* sequence between the 2 strains; however, a number of polymorphisms were identified in the *Rdh14* sequence obtained from C3H DNA (Figure 4.7C). In addition to polymorphisms in the 3'UTR of *Rdh14* that are hypothesized to affect mRNA stability (459, 460), a CCTT-TCTG polymorphism was identified in the 5' splice junction of exon 2 that is predicted to affect

the binding of transcription factors to this site (456). These results suggest that *Rdh14* is a strong candidate gene for VUR1.

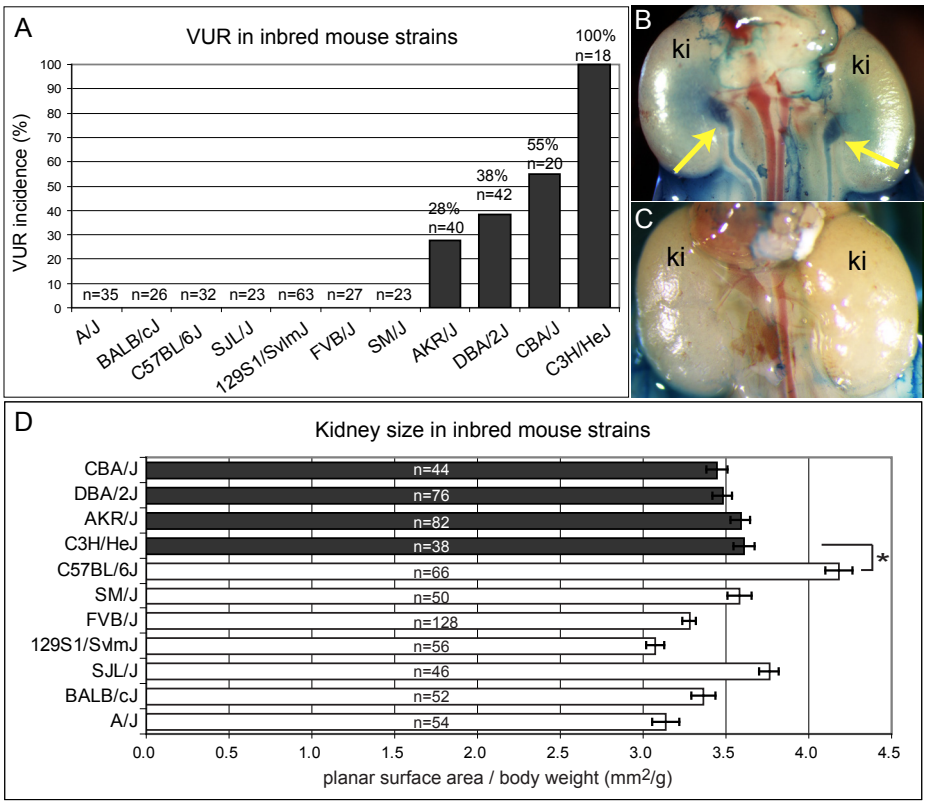

Figure 4.1: C3H mice have a 100% incidence of VUR at birth

(A) Eleven inbred mouse strains were screened for VUR at birth. The majority of these inbred mouse strains are resistant to VUR. Four mouse strains are susceptible and show varying incidences of VUR: AKR/J, DBA/2J, CBA/J, C3H/HeJ. **(B)** VUR is observed when the retrograde passage of dye is observed flowing from the bladder into the ureters and pelvis of the kidneys. The C3H strain is the most susceptible to VUR and has a 100% incidence of VUR and smaller kidneys (ki) at birth when compared to the B6 strain. The C3H mouse shown has bilateral VUR (arrows). **(C)** The B6 strain is resistant to VUR and has larger kidneys at birth when compared to the C3H strain. **(D)** Kidney planar surface areas corrected for body weight are shown for the eleven inbred strains at birth (mean ± SE). C3H and B6 mice have contrasting kidney sizes (*P=2x10-7). The first four inbred mouse strains shown in black are those that are susceptible to VUR.

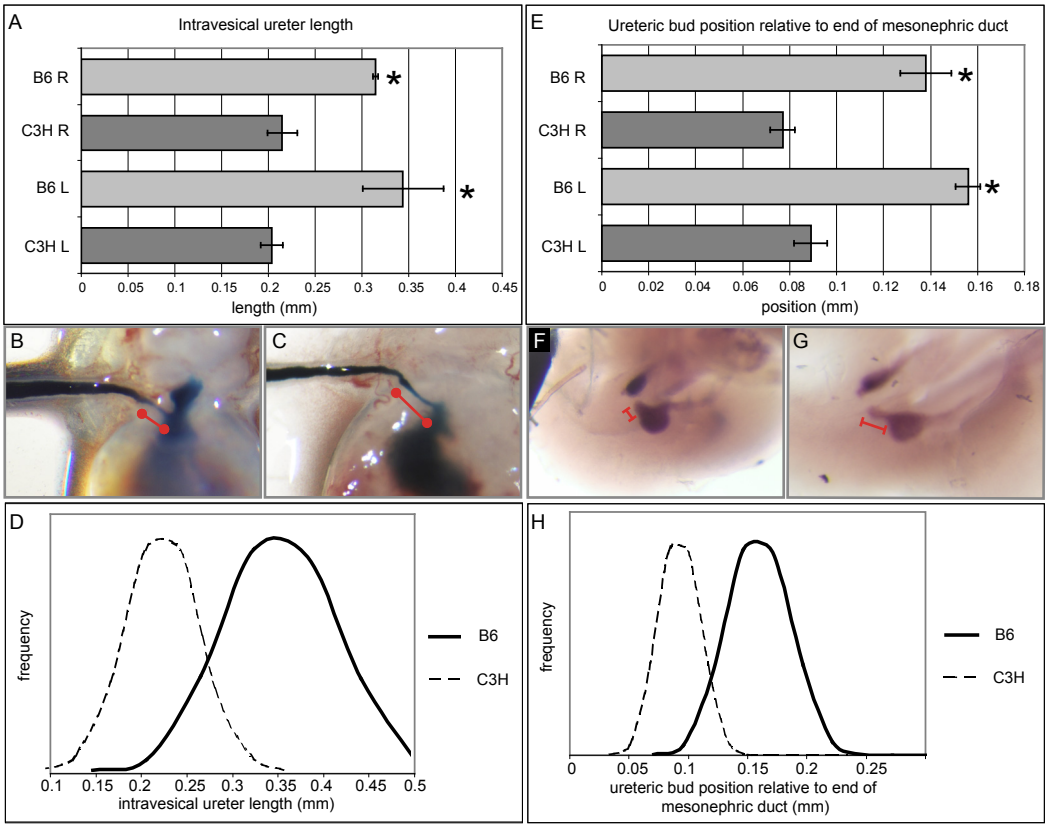

Figure 4.2: C3H mice have short intravesical ureters and caudal ureteric buds **(A)** Bar graph representing the length of the intravesical ureter in B6 and C3H mice at birth. C3H mice have significantly shorter intravesical ureters than B6 mice on both the left and the right sides (*P<0.05). **(B)** The intravesical ureter is measured as the length of the ureter within the bladder wall (red line). A short right-sided intravesical ureter from a C3H mouse is shown. **(C)** A long right-sided intravesical ureter from a B6 mouse. **(D)** Normal distribution of intravesical ureter lengths in B6 (solid line) and C3H (dashed line) mice. The mean intravesical ureter length is significantly shorter in C3H mice (P=0.0004). **(E)** Bar graph representing the position of the ureteric bud relative to the end of the mesonephric duct in E11 embryos. C3H embryos have ureteric buds that emerge significantly closer to the end of the mesonephric duct than in B6 embryos on both the left and right sides (*P<0.05). **(F)** A ureteric bud from a C3H embryo is seen emerging caudally, closer to the end of the mesonephric duct (red line). **(G)** A ureteric bud from a B6 embryo is seen emerging more cranially, further from the end of the mesonephric duct. **(H)** Normal distribution of ureteric bud positions in B6 (solid line) and C3H (dashed line) embryos. The ureteric bud is caudally shifted in C3H embryos ($P=4x10^{-8}$).

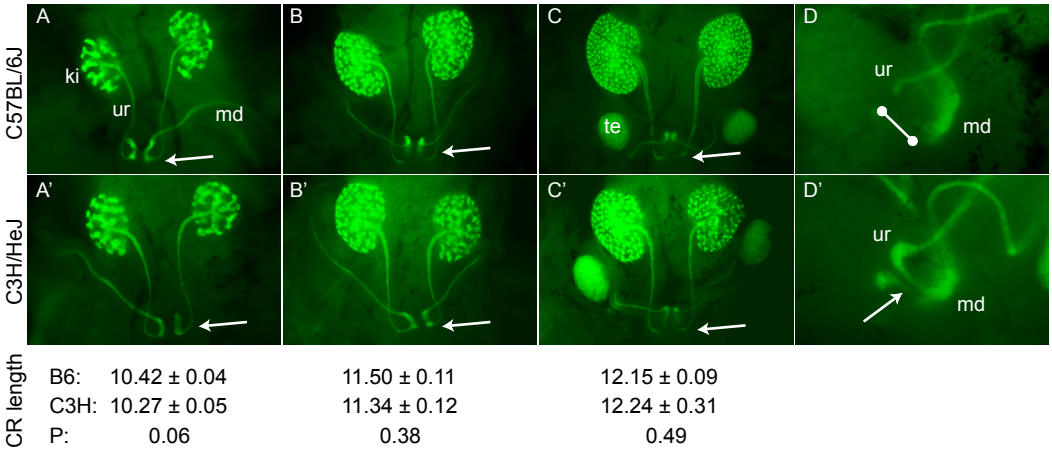

Figure 4.3: C3H mice exhibit a delay in urinary tract development
Hoxb7/GFP mice were bred onto either a B6 **(A-D)** or C3H **(A'-D')** background and dissected at various stages during embryonic development to expose the developing kidney (ki) and urinary tract. The average crown rump length (mean ± SE in millimeters) for each embryonic stage is shown for each strain. **(A-A')** Ventral view of E13 kidneys and urinary tracts. The kidney has undergone several branching events. The mesonephric duct (md) is still attached to the ureter (ur) (arrow) in both B6 and C3H embryos. **(B-B')** Ventral view of E14 kidneys and urinary tracts. **(B)** The kidneys have grown larger and the ureters in B6 embryos have separated from the mesonephric duct and have achieved their own independent insertion into the bladder (arrow). **(B')** The kidneys have grown in C3H mice as well, however, the ureters remain attached to their respective mesonephric ducts (arrow). **(C-C')** Ventral view of E15 kidneys and urinary tracts. **(C)** By this stage, B6 ureters have their own independent insertion into the bladder (arrow). A male mouse with testes (te) is shown. **(C')** In contrast, ureters from a C3H male remain fused to their mesonephric ducts (arrow). **(D)** Lateral view of the left B6 ureter shown in C that has separated from the mesonephric duct (line). **(D')** Lateral view of the left C3H ureter shown in C' that has not yet separated from its mesonephric duct (arrow).

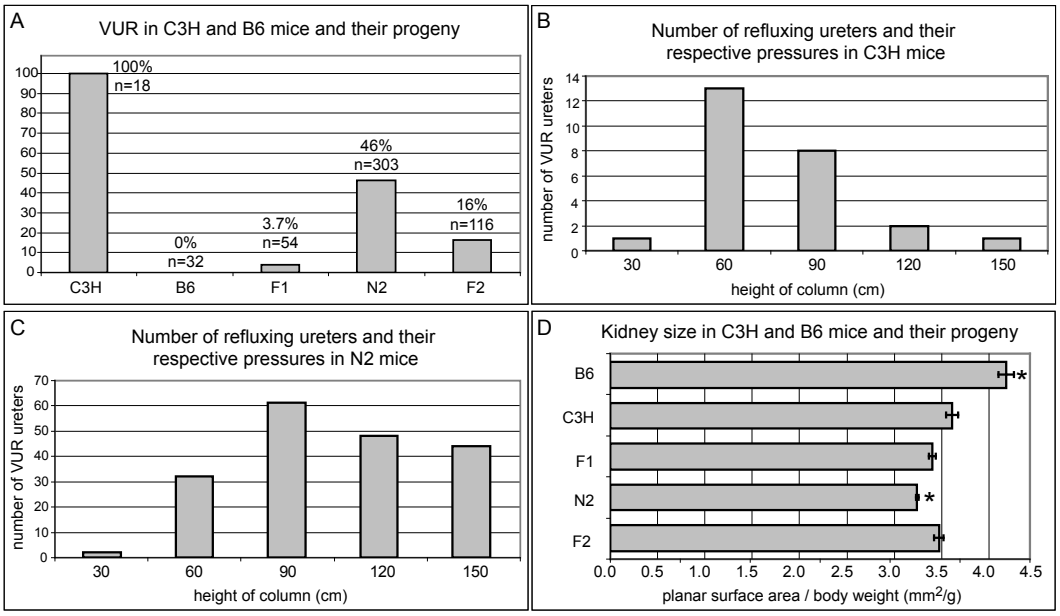

Figure 4.4: N2 mice have a high incidence of VUR

(A) Incidence of VUR in C3H, B6, F1, N2, and F2 mice at birth. C3H and B6 mice were crossed to create F1 hybrids. F1 hybrids have a 3.7% incidence of VUR. N2 backcross progeny from a (C3H X B6)F1 x C3H cross have a 46% incidence of VUR. F2 intercross progeny from a (C3H X B6)F1 X (C3H X B6)F1 cross have a 16% incidence of VUR. **(B)** VUR can be scored as a binary trait, as either present or absent, or as a quantitative trait in which the pressure at which reflux occurs is noted. VUR at lower pressures is considered to be more severe than VUR that occurs at higher pressures. The pressures at which ureters reflux are shown for C3H mice. Note that the majority of ureters reflux below 90cm. **(C)** The pressures at which ureters reflux are shown for N2 mice. **(D)** Kidney surface areas corrected for body weight are shown for B6, C3H, F1, N2 and F2 mice at birth. B6 mice have the largest kidneys while N2 mice have the smallest (*$P<0.05$). C3H mice have kidneys that are similar in size to F1 and F2 mice ($P>0.05$).

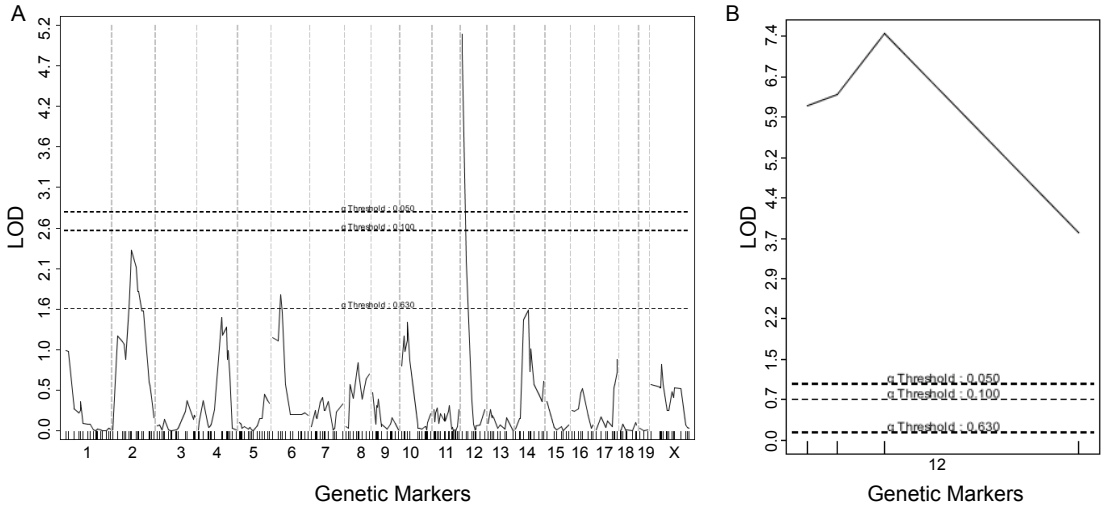

Figure 4.5: A locus on chromosome 12 is associated with VUR in C3H mice **(A)** Genome-wide scan for loci affecting VUR in backcross progeny from a (C3H X B6)F1 X C3H cross. The X axis displays the SNP markers across the 19 autosomes and X chromosome. The Y axis displays the LOD score. The three horizontal lines, from lowest to highest, show genome-wide significance thresholds estimated by permutations tests: α 0.630, α 0.100, α 0.050. Linkage analysis identified a genomic region associated with the VUR phenotype on chromosome 12, called VUR1, when VUR was scored as a quantitative trait. LOD score=5.0, genome-wide significance P<0.008. **(B)** Additional mapping of the VUR1 locus on chromosome 12 using microsatellite markers on all N2 progeny to confirm the association of the VUR1 locus with the VUR phenotype. A peak LOD score of 7.4 was observed at marker D12Mit240 (11.2Mb), genome-wide significance P<0.001.

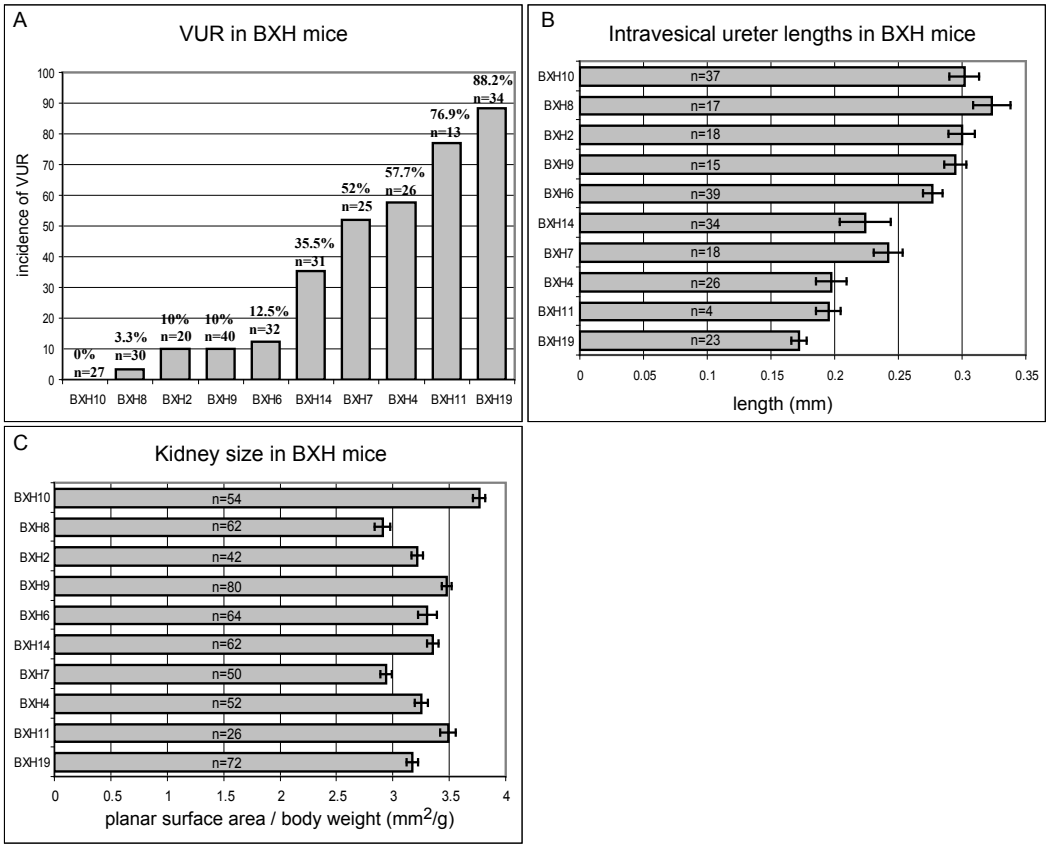

Figure 4.6: BXH mice that reflux have short intravesical ureters

(A) Ten BXH recombinant inbred strains were tested for VUR at birth. Shown in ascending order, the BXH10 strain is resistant to VUR, while BXH8, BXH2, BXH9, and BXH6 show a low incidence of VUR. The remaining five strains show higher incidences of VUR, and BXH19 mice have the highest incidence of VUR (88%). **(B)** Shown in the same order as in A, the BXH strains that show a low incidence of VUR have the longest intravesical ureters at birth, while the strains that are most susceptible to VUR have short intravesical ureters ($P=8x10^{-5}$). **(C)** Kidney planar surface areas corrected for body weight for the 10 BXH recombinant inbred strains are shown. When kidney size was assessed at birth, refluxing BXH strains did not have smaller kidneys than non-refluxing BXH strains (P=0.3).

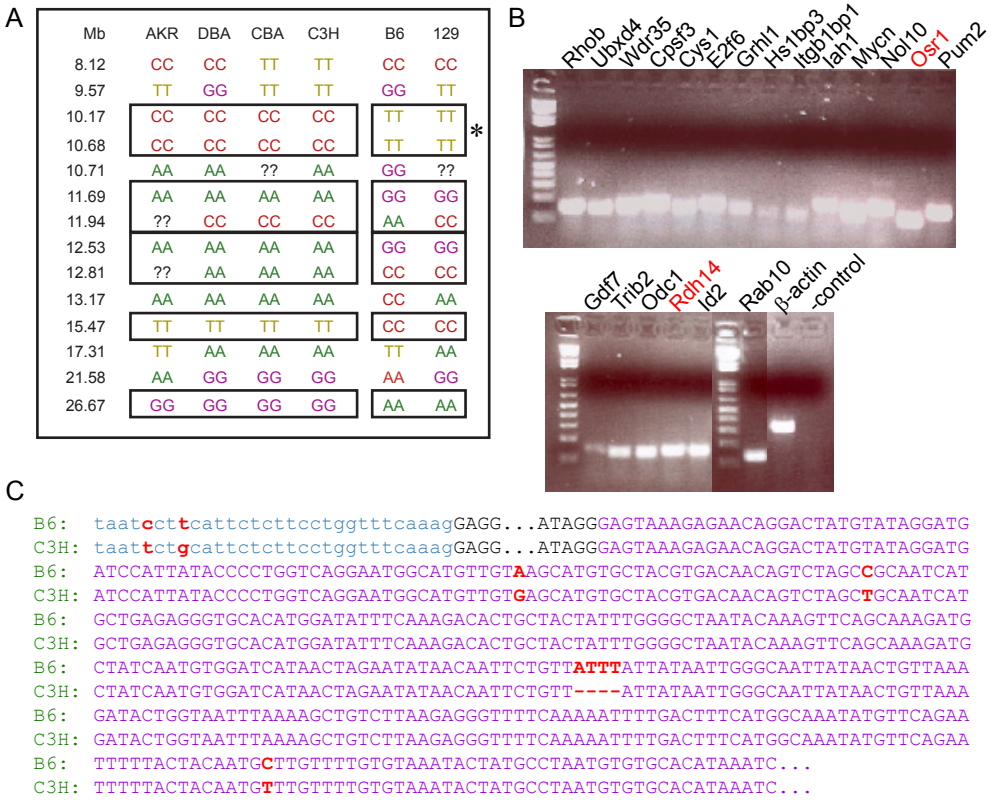

Figure 4.7: *Rdh14* and *Osr1* are candidate genes within the VUR1 locus
(A) SNP genotype data was obtained for the four inbred mouse strains that are susceptible to VUR (AKR, DBA, CBA, C3H) and was compared to SNP data from inbred mouse strains that are resistant to VUR (only B6 and 129 are shown). Selective SNPs within VUR1 are shown. Haplotypes that are common to the refluxing inbred strains and different from the non-refluxing strains are shown in boxes. One haplotype contained two potential candidate genes: *Osr1* and *Rdh14* (star). **(B)** Genes within VUR1 that are known to have a role during development were evaluated by RT-PCR on RNA extracted from E14 kidneys and ureters. Importantly, *Osr1* and *Rdh14*, shown in red, are both expressed in E14 kidneys and ureters during development. **(C)** Sequencing results for *Rdh14* from C3H and B6 genomic DNA identified some polymorphisms. The sequence for *Rdh14* exon 2 and flanking sequences is shown. The intron is shown in blue, the exon in black, and the 3'UTR (untranslated region) in purple. Polymorphisms identified are shown in red. The CCTT-TCTG polymorphism in the intron is predicted to affect the binding of transcription factors to this site. Polymorphisms in the 3'UTR may affect mRNA stability.

4.5 DISCUSSION

In this study, we identified four inbred mouse strains with a susceptibility to VUR. Of these, the C3H mouse has a 100% incidence of VUR and normally formed kidneys. Therefore, its phenotype reproduces that observed in the vast majority of children with VUR who do not have a renal malformation (204, 206). We showed that the C3H mouse has caudally shifted ureteric buds, short intravesical ureters, and a delay in urinary tract development, three phenotypes that have previously been associated with a refluxing urinary tract (24, 68). By crossing the C3H refluxing strain to the B6 non-refluxing strain, we ascertained that the VUR trait is inherited in a complex recessive pattern with 46% of the backcross and 16% of the intercross mice demonstrating VUR. Genome-wide mapping and linkage analysis was used to identify a susceptibility locus, called VUR1, on chromosome 12 that spans the first 24Mb of the chromosome. This region is homologous to human chromosome 2p24-25 and is a novel locus, as it does not correlate with any of the genes or loci thus far reported from human studies.

Our results in the C3H mouse and in the BXH lines clearly demonstrate the importance of the length of the intravesical ureter. From the BXH lines, it is evident that a shorter intravesical ureter correlates with a higher incidence of VUR, while a longer intravesical ureter is protective and prevents VUR. We have previously shown that there is a normal distribution of intravesical ureter length in outbred and mutant mouse strains; this finding was also observed in the C3H and B6 mice examined in this study (32). These results suggest that the length of the intravesical, in addition to the position of the ureteric bud along the mesonephric duct, is determined by a number of genes. This is in agreement with our findings in the C3H mouse that VUR is inherited in a complex recessive pattern. We therefore speculate that there is one major gene and several additional genes that affect the maturation of the intravesical ureter and susceptibility to VUR.

The C3H mouse resembles other mouse models of VUR, like the *Pax2*$^{1Neu+/-}$ and the *Hoxb7/Ret*$^{+/-}$ mice, as it has a caudally shifted ureteric bud during development (24, 68). However, the two latter models are associated with severe kidney malformations, while the C3H mouse has a normal kidney phenotype. While all of these models have abnormally positioned ureteric buds, the gene defects in *Pax2*$^{1Neu+/-}$ and *Hoxb7/Ret*$^{+/-}$

mice also affect later stages of kidney development that ultimately lead to a malformed kidney. We speculate that the protein encoded by the VUR1 locus exerts an effect during formation of the ureteric bud, but either it does not have a role during later stages of kidney development, or alternatively, there are other genes that can replace its function such that no kidney defect arises.

The caudally shifted ureteric bud in C3H embryos is associated with a delay in urinary tract development, a short intravesical ureter, and VUR. However, the mechanism by which a shifted ureteric bud leads to a refluxing urinary tract is unknown. We speculate that the caudally shifted ureteric bud could interact with a population of mesenchymal cells that are unable to support normal growth and maturation of the ureter. Alternatively, a caudally shifted ureteric bud is in closer proximity to the future bladder, and is exposed to a new domain of signals released from the bladder that impact normal ureter separation. Furthermore, a delay in ureter maturation might disrupt bladder growth such that less bladder surrounds the uretero-vesical junction, or alternatively, it might prevent the ureter from migrating to its final position within the bladder wall, leading to a shorter intravesical ureter. By identifying the developmental mechanisms that lead to VUR, we will gain a better understanding of the genetic and cellular events that lead to uretero-vesical junction defects.

Within the VUR1 locus, there are 198 positional candidates. After analyzing both the BXH mice and haplotypes that are common within refluxing inbred mouse strains, we identified two potential gene candidates: *Osr1* and *Rdh14*. *Osr1* is the earliest known marker of the intermediate mesoderm, which gives rise to the mesonephric duct and ureteric bud (45). Knockout $Osr1^{-/-}$ mice fail to develop the mesenchyme that surrounds the ureteric bud and have a thin mesonephric duct (44). We did not identify any coding mutations in *Osr1* between C3H and B6 mice, however we cannot exclude the possibility that there may be differences in upstream or intronic regulatory sequences that might lead to expression differences between these strains. Preliminary results suggest that there are no expression level differences for *Osr1* between C3H and B6 embryonic kidney and urinary tracts.

Rdh14 encodes for an enzyme involved in the oxidation of retinol into retinaldehyde, which is a precursor involved in the synthesis of retinoic acid. The vitamin

A pathway and its metabolite, retinoic acid, are critical for kidney and urinary tract development and direct many aspects of morphogenesis (18, 83). Mutations in retinoic acid receptors, *Rar*α and *Rar*β*2*, or in *Raldh2*, an enzyme involved in the oxidation of retinaldehyde into retinoic acid, disrupt both kidney and urinary tract development: the kidneys are hypoplastic with a decrease in branching morphogenesis and the ureters fail to separate from their respective mesonephric ducts (18, 83). We identified a number of polymorphisms in the 5' splice junction and 3'UTR of *Rdh14* that may affect transcription factor binding or mRNA stability. Preliminary results suggest that there are no expression level differences for *Rdh14* between C3H and B6 embryonic kidneys and ureters. It is plausible that *Rdh14*, like other members of the Vitamin A pathway, may be important for early ureteric bud development and may have a role in ureter maturation and uretero-vesical junction formation.

From clinical studies in humans with VUR, there is clearly a need to re-examine the development of the urinary tract and its relationship with VUR to better understand the pathophysiology of the condition. Whole-genome mapping studies in humans have identified multiple loci associated with VUR, but the underlying genes have yet to be identified (29-31). We have expanded these genetic studies to include inbred mice, and have identified a novel VUR1 locus on mouse chromosome 12 that is not homologous to any of the loci thus far identified from human studies. By identifying the gene(s) responsible for VUR in the C3H mouse, we will gain new knowledge about the biology of urinary tract defects in humans.

4.6 ACKNOWLEDGEMENTS

We thank D Malo, M Fujiwara, and K Morgan for critical reading of the manuscript and discussions; F Costantini for the *Hoxb7/GFP*$^{+/-}$ mice. This work was supported by an operating grant from the Kidney Foundation of Canada. IRG is a recipient of an FRSQ chercheur-boursier clinicien salary award. IJM is a recipient of an FRSQ doctoral award.

CHAPTER V

DISCUSSION

5.1 Overview of project and aims

During kidney development, the ureteric bud gives rise to the collecting ducts of the kidney, induces nephrogenesis in the adjacent metanephric mesenchyme, and elongates into the ureter. The ureter must connect with the bladder to form a proper connection at the level of the UVJ in order to have a functional urinary system. Abnormalities in the formation and development of the ureteric bud have been hypothesized to give rise to abnormalities of the kidney and the urinary tract, as described in the ureteric bud theory (21-23). When a ureteric bud develops from an abnormal location along the mesonephric duct, it is hypothesized to give rise to a malformed kidney with fewer nephrons and a ureter that fails to connect properly with the bladder. Such abnormalities of the ureter include a ureter that is either obstructed, which may be caused by a ureteric bud that emerges more cranially along the mesonephric duct, or a ureter that refluxes, which may be caused by a ureteric bud that emerges more caudally along the mesonephric duct. Although the ureteric bud theory has prevailed in the literature for many years, it has never been formally tested. We therefore hypothesized that mutations in genes expressed in the ureteric bud or the surrounding metanephric mesenchyme could lead to a caudally positioned ureteric bud along the mesonephric duct, which would then develop into a malformed kidney and a refluxing urinary tract.

We identified two novel mouse models of VUR that we examined in depth: the mutant *Pax2*$^{1Neu+/-}$ mouse and the inbred C3H/HeJ (C3H) mouse. The *Pax2*$^{1Neu+/-}$ mouse was previously identified for its renal and ocular malformations and is a model of human RCS (114). Because *Pax2* is expressed in the developing mesonephric duct and ureteric bud (51), we hypothesized that the *Pax2*$^{1Neu+/-}$ mouse would be a model of VUR and malformed kidneys. We showed that *Pax2*$^{1Neu+/-}$ mice had a 31.4% incidence of VUR and small malformed kidneys at birth. The C3H model of VUR was identified after we screened different inbred mouse strains for VUR and kidney size with the objective to identify new models of VUR with or without renal malformations. We demonstrated that C3H mice had a 100% incidence of VUR and normal kidneys and therefore are a model of VUR without renal malformations.

When we examined the position of the ureteric bud along the mesonephric duct in *Pax2*$^{1Neu+/-}$ and C3H embryos, we observed that the ureteric buds emerged from a more

caudal location along the mesonephric duct when compared to control mice (CD1 and B6, respectively). These observations confirmed our hypothesis and the ureteric bud theory that a caudal ureteric bud is associated with VUR. Furthermore, refluxing *Pax2*$^{1Neu+/-}$ and C3H mice had shorter intravesical ureters than CD1 and B6 mice, providing evidence that the UVJ is abnormal and predisposes to VUR.

The *Pax2*$^{1Neu+/-}$, C3H, and B6 mice were crossed to the transgenic *Hoxb7/GFP* mouse that expresses green fluorescent protein throughout the epithelial structures of the kidney and urinary tract (432). This allowed for detailed visualization of the kidney and the urinary tract throughout development. Based on human observations of duplex kidneys, it was hypothesized that a caudal ureteric bud gives rise to a ureter that separates from the mesonephric duct prematurely, thus giving rise to a defective UVJ that refluxes (21-23). However, we demonstrated that this hypothesis is incorrect. Although both *Pax2*$^{1Neu+/-}$ and C3H embryos had caudal ureteric buds, their urinary tracts were severely delayed in their separation from the mesonephric duct. In summary, we demonstrate that haploinsufficiency of *Pax2*, and the yet to be characterized gene(s) defect in the C3H mouse, is sufficient to cause a caudally shifted ureteric bud. This caudal ureteric bud is associated with delayed formation of the UVJ, which in turn leads to the development of a short intravesical ureter that refluxes.

The *Pax2*$^{1Neu+/-}$ mouse has been shown to have malformed kidneys with fewer nephrons due to a defect in branching morphogenesis (230, 254). We further demonstrate that a caudal ureteric bud is associated with both VUR and malformed kidneys in these mice. Interestingly, patients with VUR can exhibit a range of renal phenotypes. In addition to having malformed kidneys that are small and dysplastic (263, 461), some patients have small kidneys with a nephron deficit (hypoplasia), while others have completely normal kidneys (154, 202-205, 263, 265). It is not known if this last category of "normal" kidneys has a subtle-nephron deficit or not; however, it is presumed that each of these kidney phenotypes is at risk of acquiring VUR-related renal damage (7, 8, 265). Because the C3H mouse had smaller kidneys at birth compared to the B6 mouse, we hypothesized that the C3H mouse would have a nephron deficit and represent the renal hypoplasia phenotype.

When we tested adult C3H and B6 mice for VUR, C3H mice continued to reflux, but now had larger kidneys than non-refluxing B6 mice. We therefore hypothesized that a congenital nephron deficit in C3H mice was responsible for the increase in kidney size observed by adulthood. However, we demonstrated that C3H mice did not have fewer nephrons than B6 mice at birth or at adulthood, despite the significant difference in kidney size. What was even more interesting was that nephron number did not correlate with kidney size or body weight in either mouse strain. These results suggest that the mechanisms that determine nephron number differ from those that establish kidney size or growth. These results also demonstrate that the C3H mouse is a model of VUR and normal kidneys, which is the phenotype most commonly seen in humans.

There is a great interest in the genetic predisposition to VUR. Evidence from human and mouse studies demonstrates that 14 genes and at least 10 potentially interesting loci are associated with VUR, indicating that VUR is an extremely genetically heterogeneous trait (32). The high incidence of VUR in the C3H mouse and the resistance of the B6 mouse to VUR led us to cross these strains and identify the underlying gene(s) that is associated with the caudal ureteric bud, the short intravesical ureter, and the refluxing urinary tract in the C3H mouse. Linkage analysis was performed on DNA extracted from backcross and intercross mice and we identified a novel locus on chromosome 12, VUR1, which is significantly associated with the reflux phenotype. Within VUR1, we identified a promising candidate, *Rdh14*, which is involved in Vitamin A metabolism. We predict that the candidate gene(s) in VUR1 will be expressed in the ureteric bud or the surrounding metanephric mesenchyme and anticipate that the identification of this gene(s) will provide new mechanistic insights into the development of VUR.

5.2 The role of *Pax2* during urinary tract development

5.2.1 *Pax2* haploinsufficiency causes urinary tract defects

Our studies on the $Pax2^{1Neu+/-}$ mouse confirmed our hypothesis that mutations in genes important for ureteric bud development can lead to a caudally shifted ureteric bud, a malformed kidney, and VUR (68). The $Pax2^{1Neu+/-}$ mouse is the first mouse model of VUR that illustrates that VUR may actually arise from a delay in urinary tract maturation.

We believe that the delayed separation of the ureter from the mesonephric duct impairs the normal formation of the UVJ such that the intravesical ureter is shorter and does not acquire its oblique angle of entry into the bladder, thus predisposing to VUR. The delayed maturation of the ureter is interesting because it may explain why VUR resolves with time in some patients (167). Eventual maturation of the intravesical ureter after birth, such that it increases in length and acquires a more oblique angle of insertion into the bladder could allow for the UVJ to become more competent with time such that VUR resolves in some patients (169).

The UVJ consists of several components that work together to prevent VUR, including a sufficient length of the intravesical ureter, an oblique angle of entry of the ureter into the bladder wall, a well-formed trigone that compresses the ureteral orifices during voiding, and correctly positioned ureteric orifices within the trigone (14). Of the other mouse models with VUR (*Hoxb7/Ret*$^{+/-}$, *Lim1*$^{-/-}$, *Upk2*$^{-/-}$, *Upk3*$^{-/-}$, and *Agtr2*$^{-/-}$) (24, 46, 93, 94, 216), only *Hoxb7/Ret*$^{+/-}$ mice were screened for intravesical ureter lengths and they were found to have short intravesical ureters. It is unclear whether a defective UVJ is responsible for VUR in the remaining VUR mouse models. Scanning electron microscopy of *Upk3*$^{-/-}$ mouse bladders demonstrates the mutant mice have enlarged ureteric orifices. However, it is not clear whether the dilated ureteric orifice is a primary or a secondary manifestation of an abnormal UVJ.

Pax2$^{1Neu+/-}$ mice exhibited unilateral left-sided VUR more frequently than right-sided VUR, even though the lengths of the left and right intravesical ureters were not significantly different. In humans with unilateral VUR, left-sided VUR is reported to be more common than right-sided VUR (170). The mechanism to explain why left-sided VUR is more common remains unknown. One possibility is that the different anatomical positions of the right and left kidneys may affect the anatomical position of the ureter within the bladder wall. In the mice that we tested for VUR, the left kidney is consistently higher in the body cavity, has a larger planar surface area, but weighs less compared to the right kidney. It has been suggested that surrounding organs, like the liver that develops on the right side of the embryo, might influence kidney morphology and explain why the right kidney is lower than the left (40). Although the left intravesical ureter is the same length as the right intravesical ureter, other components of the UVJ might be

defective in *Pax2*$^{1Neu+/-}$ mice. The position of the ureter within the bladder trigone and/or the angle of intravesical ureter entry into the bladder might be different on the left compared to the right side and this might influence the propensity of one side to reflux more often than the other.

The higher incidence of left-sided VUR in *Pax2*$^{1Neu+/-}$ mice and in humans may be further explained at a molecular level. One group examined *Osr1*$^{-/-}$ mutant embryos that lack expression of the transcription factor OSR1 in the developing intermediate mesoderm, and observed that formation of the mesonephric duct was always more severely impaired on the left side (44). These results suggest that gene expression differences between the left and the right sides of the embryo may have an impact on the timing of kidney and urinary tract development. However, it is important to mention that *Hoxb7/Ret*$^{+/-}$ and C3H mice exhibit right-sided VUR more often than left-sided VUR (although this only approached statistical significance for C3H mice), suggesting that there are genetic and environmental factors that favor right-sided VUR in these mice.

5.2.2 The role of *Pax2* during urinary tract maturation

Apoptosis plays an important role in the normal development of the kidney and the urinary tract (83, 255, 462). During kidney development, mesenchymal cells that do not receive appropriate survival and inductive signals from the ureteric bud undergo apoptosis (462, 463). PAX2 has been shown to protect the ureteric bud cell population from apoptosis (255). Haploinsufficiency of *Pax2* in *Pax2*$^{1Neu+/-}$ mice leads to an increase in collecting duct apoptosis and to a defect in ureteric bud branching, which results in renal hypoplasia and a reduction in nephron number (230, 255). To confirm that PAX2 has a role in preventing ureteric bud cell apoptosis, a transgenic mouse expressing an anti-apoptotic gene in the developing ureteric bud was created (300). When this transgenic mouse is crossed with *Pax2*$^{1Neu+/-}$ mice, it is able to rescue the renal hypoplasia and nephron deficit (300).

Apoptosis also plays a critical role in the maturation of the ureter at the level of the bladder. The common nephric duct connects the mesonephric duct and the ureter during development. Apoptosis of the common nephric duct is required for the ureter to separate from the mesonephric duct and achieve its own independent insertion into the

bladder (83). Mice that are deficient in *Raldh2*, a retinaldehyde dehydrogenase enzyme critical for retinoic acid synthesis, do not exhibit apoptosis of the common nephric duct at E11 (83). This results in ureters that cannot separate from the mesonephric ducts and connect to the bladder, resulting in a malformed UVJ that is obstructed. Because *Pax2* has a role in preventing apoptosis in the kidney, we hypothesized that *Pax2* would also regulate apoptosis in the common nephric duct. Increased apoptosis in the common nephric duct of $Pax2^{1Neu+/-}$ embryos could influence the maturation of the ureter and result in a shorter intravesical ureter. However, when we examined E11 $Pax2^{1Neu+/-}$ embryos, the time at which apoptosis of the common nephric duct first begins, no differences in common nephric duct apoptosis were observed between mutant and wildtype embryos.

Although we did not detect any differences in common nephric duct apoptosis at E11, we cannot exclude the possibility that there may be differences in apoptosis at later stages of ureter maturation. A change in common nephric duct apoptosis that occurs between E12 and E14 could explain why $Pax2^{1Neu+/-}$ embryos exhibited a delay in urinary tract development. Unfortunately, we cannot answer this question because if differences in common nephric duct apoptosis are observed, they may merely be a reflection of the delay in development between mutant and wildtype embryos and not actual differences in levels of apoptosis. Furthermore, PAX2 is described as having an anti-apoptotic effect (255). We would therefore expect that reducing *Pax2* gene dosage would increase apoptosis in the common nephric duct and cause precocious separation of the ureter from the mesonephric duct. However, this phenotype was not observed. To answer the question whether apoptosis is truly involved in the urinary tract delay observed, $Pax2^{1Neu+/-}$ mice could be rescued with the same anti-apoptotic transgene used to rescue the renal hypoplasia and nephron deficit (300). If common nephric duct apoptosis after E11 is involved in the formation of a refluxing ureter, then progeny from this cross should not reflux.

In addition to preventing apoptosis, PAX2 is a transcription factor that has a number of downstream targets that are important for kidney development, including *Gdnf*, *Sfrp2*, *Ret*, *Wt1*, *Gata3*, *Wnt4*, and *Naip* (101, 107, 257-261). *Pax2* haploinsufficiency may be sufficient to disrupt ureter maturation by directly affecting the

transcriptional regulation of these downstream targets. Although the roles of most these genes during urinary tract development are not well described, there are two interesting candidates: *Ret* and *Gata3*. *Ret* is critical for the formation of the ureteric bud and we have shown that misexpression of *Ret* in *Hoxb7/Ret*$^{+/-}$ mice leads to a caudal ureteric bud and an abnormal UVJ that refluxes (24). In addition, *Ret*$^{-/-}$ embryos have ureters that fail to separate from the mesonephric duct resulting in obstruction (18). We speculate that *Pax2* haploinsufficiency could decrease *Ret* expression in the common nephric duct such that cell migration and differentiation during remodelling of the ureter is impaired, resulting in a short intravesical ureter that refluxes. Another transcriptional target of PAX2 is *Gata3*, which is expressed in the mesonephric duct and ureteric bud and is important for the extension of the duct towards the cloaca (101). Humans with *GATA3* mutations develop renal anomalies and VUR as part of HDR syndrome (354, 385). *Pax2* haploinsufficiency could decrease *Gata3* expression and in turn disrupt important guidance cues that are required for the ureter to insert into the bladder. These studies demonstrate that the transcriptional regulation of *Ret* and *Gata3* by PAX2 could provide a molecular explanation as to why urinary tract defects are observed in *Pax2*$^{1Neu+/-}$ mice and patients with RCS.

In conclusion, the *Pax2*$^{1Neu+/-}$ mouse has been an important mouse model for studying the development of VUR. It has revealed that mutations in genes important for ureteric bud formation can cause combined kidney and urinary tract defects. It has also demonstrated that VUR is a congenital defect of the UVJ that can arise from a delay in urinary tract maturation.

5.3 Variation in nephron number and kidney/body size in inbred mice

5.3.1 The C3H mouse is a model of VUR and normal kidneys

The *Pax2*$^{1Neu+/-}$ mouse is a model of VUR and malformed kidneys with a nephron deficit (68, 230), while the C3H mouse does not have malformed kidneys. We assessed the kidney phenotype in C3H mice by measuring kidney planar surface area, kidney weight, and by counting the number of nephrons. Interestingly, our results demonstrated that C3H newborn mice did not have fewer nephrons than B6 mice despite the significant

difference in kidney size at birth and at adulthood. However, adult C3H females did have a small nephron deficit compared to B6 females, which was accompanied by significant glomerular hypertrophy. Because both C3H females and males exhibited an increase in the size of the medulla and the cortex, we suspect that kidney growth and size in these inbred mice is independent of nephron formation and glomerular hypertrophy. From these results, the C3H mouse is a model of VUR with normal kidneys. If we compare the C3H mouse to humans with VUR, up to 2/3^{rds} of children with VUR have normal kidneys (167, 202-205, 262-264).

There are three renal phenotypes associated with VUR. The first is the group of patients with VUR, dysplastic kidneys, and a severe nephron deficit (4, 7, 189). The second is the group of patients with VUR, hypoplastic kidneys, and a variable nephron deficit from mild to severe (265, 436). The third is the group of patients with VUR, normal kidneys, with no nephron deficit (204, 206). However, all three groups appear to be at risk of developing hypertension and end-stage renal disease (189, 266-268, 464, 465). The risk of acquiring these complications may be due to the congenital nephron deficit from renal hypo/dysplasia, to an acquired nephron loss from renal scars from sustained exposure to VUR and/or exposure to urinary tract infections, or it might be a combination of both.

Although the C3H mouse has normal renal function and is normotensive, we cannot rule out the possibility that another gene, in addition to the one that confers susceptibility to VUR, protects it from hypertension and renal failure. The refluxing DBA/2J strain might be an interesting model to study because in addition to having VUR, it is susceptible to developing proteinuria and chronic kidney disease (425, 447, 450, 451). DBA/2J kidneys could be examined to determine if a nephron deficit in these mice is associated with VUR and the development of chronic kidney disease.

5.3.2 The relationship between nephron number and kidney size/body weight

Nephron number is correlated with kidney weight or volume, birth weight, adult height, and glomerular volume (267, 269, 274, 277). However, other studies have not identified these correlations (281, 283). Because these studies examined individuals of different ages and ethnicities, it is possible that excessive genetic and environmental

variation could obscure the detection of these correlations. We also speculate that these relationships might depend on scale. We therefore hypothesized that if there is insufficient variation in nephron number, kidney size, and body weight, the detection of correlations between these factors could be further masked.

To understand the role of genetic and environmental variation on these relationships, we chose to study nephron number in inbred mice because they are genetically homogeneous and are exposed to uniform environmental conditions, unlike the human population. However, despite the significant difference in kidney size between C3H and B6 mice at birth and at adulthood, nephron number did not correlate with kidney size or body weight at either time point. These results suggest that nephron number is independent of kidney size. One limitation of our study is that we chose to compare the C3H and B6 strains because of their contrasting kidney and urinary tract phenotypes. Future studies could compare the B6 strain to either the 129 or the A/J strains, which have even smaller kidneys at birth and no VUR. The larger difference in kidney size between these inbred strains might be correlated with differences in nephron number.

To determine if these relationships could actually depend on scale, we examined the fold variations in nephron number, kidney size, and birth weight reported in the human literature. We were interested in knowing whether the positive studies had larger fold-variations than those that showed negative correlations. Taken together, the results suggest that large differences in kidney size and in birth weight (over 2-fold) are positively correlated with differences in nephron number. Conversely, smaller fold-differences in kidney weight are not correlated with differences in nephron number. This then raises the issue whether counting nephrons is necessary, as a decrease in nephron number can only be detected when there is a corresponding large decrease in kidney size or birth weight.

In our study, there was a 2-fold variation for kidney size and 1.4-fold variation for body weight between the two strains at birth and at adulthood. Since there is little genetic variability in inbred strains and environmental variability is minimized in mouse studies (417), we hypothesized that this would be favorable to demonstrate a positive correlation between nephron number and kidney size/body weight. Clearly, while too much

variability may be problematic, some is required to see these correlations. In addition, the method of estimating nephron number itself may not be sufficiently sensitive to detect subtle nephron deficits. When our estimated counts (using either the disector/fractionator method or our counting method) were compared to the absolute nephron counts in the newborn kidneys, the error rates for the two estimation methods were between 6.5% and 16.3%. This suggests that subtle nephron deficits may not be accurately detected with current estimation methods and may explain why we did not see a positive correlation between nephron number and kidney size.

Although current estimation methods for nephron number may not detect subtle nephron deficits, such deficits appear to be clinically important. In a study on newborn infants in Montreal, a 10% reduction in kidney volume was associated with a 9% increase in serum Cystatin C, a marker for impaired renal function and glomerular filtration (466, 467). When DNA was genotyped from these infants, those with reduced kidney volumes and reduced renal function exhibited SNPs in either *RET* or *PAX2* (466, 467). The SNPs identified in both genes were common gene variants. Interestingly, in the infants that had both *RET* and *PAX2* allele variants, renal volume was decreased even further by 23%, suggesting that these two genes interact synergystically to determine kidney size (467). This group hypothesized that the reduced renal size and function represented a reduction in nephron number. The results show that polymorphisms in these genes can cause subtle differences in kidney size that may be of clinical importance.

5.3.3 The relationship between nephron number and glomerular size

Despite the lack of a relationship between nephron number and kidney size in C3H and B6 mice, we did show that a decrease in nephron number (by 13%) in adult mice was associated with a proportional increase in glomerular size (by 12%). These are interesting results as the relationship between nephron number and glomerular size is poorly understood. We still do not know how many nephrons a kidney must lose before a renal or glomerular hypertrophic response is detected. Infants with unilateral renal agenesis show evidence of renal hypertrophy that can be detected *in utero* (126, 127). Rats with uni-nephrectomy have an increase in glomerular size of 41% and rat models of $5/6^{th}$ nephrectomy have an increase in glomerular size and glomerulosclerosis (291, 293).

Our results demonstrate that the lower nephron number in C3H mice and B6 males compared to B6 females is accompanied by an increase in glomerular size, which may occur to maintain an adequate filtration surface area.

Even though studies in humans do not always show positive correlations between nephron number and kidney size, there appears to be a strong inverse correlation between nephron number and glomerular size (266, 269, 275, 280, 281). One study on patients with reflux nephropathy demonstrated that although nephron number, estimated from biopsy, did correlate with the extent of renal scarring, renal function, and proteinuria, the strongest correlation was between nephron number and glomerular hypertrophy (317). These results are important because they demonstrate that glomerular size or volume is a stronger correlate of nephron number than kidney size. However, when we pooled all adult mice, there was no correlation between nephron number and glomerular size, suggesting this may further be an issue of scale in our data set.

5.3.4 Nephron number and VUR

When we started this study, we were interested in the association between VUR and kidney size. We thought the C3H mouse would be a good model of small kidneys that are not malformed and would represent the subset of patients with renal hypoplasia. One study has examined nephron number in patients with reflux nephropathy, and found that those patients with fewer nephrons had worse renal function (317). It has also been shown that patients with reflux nephropathy have glomerular hypertrophy, implying that patients with reflux nephropathy may have a nephron deficit (214). However, it is not known if the nephron deficit is congenital or acquired in these patients. Nevertheless, these are important observations because reductions in nephron number in patients with VUR may have an impact on susceptibility to hypertension and end-stage renal disease.

Studies that focus on determining the relationship between nephron number, kidney size, and glomerular hypertrophy in patients with VUR or reflux nephropathy may help identify the subset of patients that are at risk of developing hypertension and end-stage renal disease later in life. With our work on the C3H mouse, we now know that it is a model of VUR with normal kidneys and normal nephron counts. The C3H mouse is also normotensive, it does not develop proteinuria, and it has normal renal function (447,

450, 451, 453). We therefore speculate that the C3H mouse is a model that represents the subset of patients that have VUR and normal kidneys, but who do not develop hypertension and renal failure.

5.4 VUR in the inbred C3H/HeJ mouse

5.4.1 Characterizing the urinary tract defect in C3H/HeJ mice

The C3H mouse is a unique mouse model of VUR in that it had a very high incidence of VUR but normal kidneys. We demonstrated that C3H mice had caudal ureteric buds, a delay in urinary tract development, and short intravesical ureters, suggesting that similar developmental mechanisms contribute to VUR in these mice as in *Hoxb7/Ret*$^{+/-}$ and *Pax2*$^{1Neu+/-}$ (24, 68).

If we compare the positions of ureteric buds along the mesonephric duct and the lengths of intravesical ureters from all the mice that were tested for VUR, including *Hoxb7/Ret*$^{+/-}$, *Pax2*$^{1Neu+/-}$, C3H, B6 and CD1 mice, the mice that reflux consistently have more caudal ureteric buds and shorter intravesical ureters than non-refluxing CD1 and B6 mice (24, 68). Interestingly, C3H mice have the most caudal ureteric buds and the shortest intravesical ureters when compared to *Hoxb7/Ret*$^{+/-}$ and *Pax2*$^{1Neu+/-}$ mice (24, 68). These results suggest that a higher incidence of VUR is associated with a more caudal ureteric bud and a shorter intravesical ureter.

The ureteric bud theory predicts that the more abnormally positioned the ureteric bud is, the more severe the kidney and urinary tract phenotype will be (21). In contrast to this theory, our results suggest that a caudal ureteric bud can give rise to an abnormal urinary tract, but it can also develop into a normal kidney. One study that misexpressed *Gdnf* using the *Hoxb7* promoter in *Gdnf*$^{-/-}$ knockout mice observed a similar outcome (468). The mesonephric ducts in these mice formed ectopic ureteric buds, but some of the ectopic ureteric buds developed into normal well-patterned kidneys, demonstrating that an abnormally positioned ureteric bud can develop into a normal kidney (468).

While obtaining the intravesical ureter measurements, we noticed that C3H bladders appeared smaller in size compared to B6 bladders. This raised the issue as to whether the shortened intravesical ureter was a true shortening of the ureter or whether it was secondary to a thinner bladder wall. Since we obtain our intravesical ureter

measurements as the distance between the bladder periphery and the site of dye exit, a thinner bladder wall could make the intravesical ureter appear shorter. When we prepare urinary tracts for the intravesical ureter measurements, the posterior end of the bladder is removed to allow the dye to flow freely out of the bladder so that the ureteral orifice can be better visualized. We therefore paraffin-sectioned through intact C3H and B6 bladders, and preliminary data suggest that while C3H bladders are smaller, the bladder wall is comparable in thickness to B6 bladders, appears normal in morphology, and has a thick smooth muscle layer and urothelium. Smooth muscle staining of the bladder would determine whether a reduction in the smooth muscle layer at the UVJ, in addition to the reduced length of the intravesical ureter, could affect the competence of the UVJ.

In addition, when testing for VUR or measuring the length of the intravesical ureter, some C3H ureters appeared dilated. This raised another question: is the dilation because of the backflow of urine, or is there an intrinsic smooth muscle defect in the ureter that impairs normal peristalsis of urine? Although preliminary data from sections through C3H and B6 ureters suggest that C3H ureters appear normal in morphology, future studies on C3H and B6 mice could examine the expression of smooth muscle within the ureter to determine whether a subtle smooth muscle deficiency may be associated with a refluxing urinary tract.

5.4.2 CAKUT is a spectrum of kidney and urinary tract defects

If we compare C3H embryos to *Pax2*$^{1Neu+/-}$ embryos, the latter exhibited a range of kidney and urinary tract phenotypes very much in keeping with CAKUT, including double ureteric buds that developed into duplex systems, normal-looking kidneys, small malformed kidneys, and renal agenesis (either from the absence of ureteric bud formation or from apoptosis of a small rudimentary kidney) (68). However, C3H embryos never exhibited duplex systems or renal agenesis. We suspect that this difference may be caused by two possibilities. The first possibility is that the effect of *Pax2* haploinsufficiency and the mis-regulation of any of its downstream targets has an effect not only on the position and the number of the ureteric buds, but also on the regulation of ureteric branching such that some kidneys branch more than others. The second possibility is that modifier genes on the CD1 outbred background of the *Pax2*$^{1Neu+/-}$

mouse could influence development and give rise to the range of phenotypes observed in these embryos. The absence of phenotypic variation in C3H embryos might be due to the nature of the genetic mutation in the C3H mouse that has less of an influence on ureteric bud number and branching but more of an effect on urinary tract maturation. In addition, C3H mice are inbred such that genetic modifiers will have less of an effect.

In addition to the nature of the genetic mutation, the spectrum of defects associated with CAKUT could also arise because of the impact of an abnormally positioned ureteric bud on the spatial and temporal regulation of ureter maturation. Because of our observation in *Pax2*$^{1Neu+/-}$ and C3H embryos that a caudal ureteric bud is associated with a delay in urinary tract maturation but not necessarily a renal malformation, we speculate that the timing of urinary tract maturation could also explain why a spectrum of defects arises, even between the left and the right urinary tracts. Differences in the timing of urinary tract development in regards to bladder development could explain why some ureters show obstruction (because they never reach the bladder wall) while others show unilateral or bilateral reflux (because they never form a proper UVJ).

5.4.3 Characterizing the urinary tract defect in BXH mice

A study that examined the length of the intravesical ureter in children with VUR concluded that those children with the shortest intravesical ureters had more severe forms of VUR (469). A similar relationship was identified in the BXH lines: the BXH lines that refluxed had shorter intravesical ureters than those that did not reflux. Similarly, the extremely short intravesical ureter in C3H mice might explain why VUR did not resolve by adulthood in these mice. We hypothesize that there is a certain threshold length of the intravesical ureter that is necessary to prevent VUR, and ureters that are shorter are at increased risk of developing VUR. We also suspect that the gene(s) that determines susceptibility to VUR in the C3H mouse will also determine intravesical ureter length.

While assessing the different BXH lines for VUR, we noticed that 36% of BXH14 mice that refluxed either had duplex systems or bifid ureters. This is the first example of duplex systems occurring in an inbred mouse strain. All other examples of duplex systems are of mice that develop supernumerary ureteric buds and have ureters that fail to

separate from the mesonephric duct, and most of these mice die soon after birth from kidney failure (26-28). We are currently crossing the *Hoxb7/GFP* transgene (432) onto the BXH14 background so that kidney and urinary tract development in BXH14 embryos can be monitored. We will determine if the duplex systems follow the Weigert-Meyer Principle; which states that the upper renal pole usually drains into the bladder through an orifice that is lower than normal within the bladder wall (closer to the urethra), while the lower renal pole usually drains into the bladder through an orifice that is higher than normal (4). Ureteric buds will also be examined to determine if two ureteric buds develop or whether a single ureteric bud splits into two ureters and kidneys. We will also examine the expression domain of *Gdnf* in BXH14 embryos to determine if it is expanded within the metanephric mesenchyme. As in the mouse models of supernumerary ureteric buds, an expanded *Gdnf* expression domain is associated with ectopic ureteric budding (26-28). These studies on the BXH14 mouse will help us to understand how the position of the ureteric bud influences the final position of the ureter within the bladder wall and the formation of the UVJ.

Future studies on the BXH14 line will also concentrate on identifying the genetic mutation responsible for the duplex systems. Sequencing of genes known to cause duplex systems, like *Spry1*, *Foxd1/Foxc1*, *Slit*, and *Robo2* (26-28) in BXH14, C3H, and B6 mice could identify a possible mutation in these genes. If these genes do not show any mutations, then a genetic approach similar to the one we used to identify the VUR-causing gene in C3H mice could be used. Intercross or backcross progeny from an initial cross between susceptible BXH14 mice and resistant B6 mice can be genotyped for SNPs across the genome. Regions of the genome that segregate with the duplex kidney phenotype will lead to the identification of a locus that harbors a gene that is associated with the formation of duplex systems.

5.4.4 Candidate gene analysis within the VUR1 locus

Finding the genes that are associated with VUR is the first step to explaining the biology and the pathogenesis of VUR. From our studies on the C3H refluxing mouse, we have identified a 24Mb genomic region on chromosome 12, called VUR1, which is associated with the VUR phenotype in C3H mice. Our results also demonstrate that the

mechanisms that control VUR development differ from those that control kidney growth. To help prioritize gene candidates within VUR1 for sequencing, we used a number of different *in silico* approaches.

The first *in silico* approach we used was to search online databases for known functional SNPs between C3H and B6 mice. We refined our search to identify SNPs that occur within coding regions of genes and SNPs that are predicted to change an amino acid in the protein (non-synonymous SNPs). We hypothesized that genes that have documented non-synonymous SNPs would be good gene candidates because the polymorphism could impact protein function. Five genes within our VUR1 locus have known coding non-synonymous polymorphisms between C3H and B6: *Asxl2* (additional sex-combs like 2), *Pomc1* (pro-opiomelanocortin-alpha), *Atad2b* (ATPase family), *ApoB* (apolipoprotein B), and *Nt5c1B* (5'-nucleotidase, cytosolic IB). However, of these 5 genes, a literature search revealed that none of these genes appear to be critical or specific for kidney development; therefore, they were not given top priority in the initial analysis.

The second *in silico* approach we used to prioritize candidates within the VUR1 locus was haplotype analysis, which was described in Chapter IV. Using haplotype analysis, combined with the genotype-phenotype analysis from the BXH strains, we compiled a new list of candidate genes. Many of these candidate genes are not yet annotated or encode ribosomal proteins. Although we cannot rule out the possibility that these genes may be our reflux-causing gene, two genes within this list appear to have a role in kidney and urinary tract development and were therefore examined in depth: *Rdh14* (retinol dehydrogenase 14) and *Osr1* (odd skipped related 1).

Osr1 is an interesting candidate because it encodes a transcription factor that is expressed in the metanephric mesenchyme and $Osr1^{-/-}$ mice never form a ureteric bud and fail to develop kidneys (44, 45). To determine if *Osr1* is our candidate gene, complementation analysis could be performed. If offspring from an $Osr1^{+/-}$ and C3H cross reflux then the *Osr1* gene is likely responsible for VUR in C3H mice. *Rdh14* is our top candidate for VUR1 because it demonstrates a number of polymorphisms in the 5' splice junction of exon 2 and in the 3'UTR that may affect transcription factor binding or mRNA stability. Furthermore, studies on mice and rats have shown that the Vitamin A pathway is critical for normal kidney and urinary tract development, and mice

homozygous mutant for genes in this pathway develop CAKUT (18, 83). Expression studies on E11 embryos will determine if *Rdh14* is expressed in the ureteric bud or the surrounding mesenchyme, and expression studies on older embryos will determine if *Rdh14* is expressed at the level of the UVJ.

The VUR1 gene(s), whether it is *Osr1*, *Rdh14*, or another gene, shows complex recessive inheritance in C3H mice. This is in contrast to most findings in humans in which a single dominant gene with incomplete penetrance is largely responsible for VUR (29, 150). Recessive inheritance has been described in one consanguineous family with VUR and urinary tract malformations (128) and one genome-wide study of VUR in the Hasidic Jewish population (333). This latter study identified a novel VUR locus that maps to chromosome 12p11-q13, a 22MB region with 161 positional candidates, with over 100 of them expressed in the urinary tract (333). This group is currently sequencing the most interesting candidates, but thus far no coding polymorphisms have been identified. Interestingly, two retinol dehydrogenase genes map to this region, *RDH5* and *RDH16*, in addition to the retinoic acid receptor gamma, *RARγ*.

Although VUR in the C3H mouse shows recessive inheritance, we cannot rule out the possibility that a mutation in the same gene or pathway in humans could show either dominant or recessive inheritance. There are examples of mice that demonstrate recessive inheritance of Hirschsprung's disease but the same gene mutation in humans shows dominant inheritance (470). In addition, the nature of the mutation may impact whether dominant or recessive inheritance is observed. A point mutation may require two copies of the mutation to affect protein activity, while a truncation mutation may be sufficient to abrogate protein activity and therefore demonstrate autosomal dominant inheritance.

5.4.5 Narrowing the VUR1 locus

One approach we will use to narrow the VUR1 locus will be to create congenic mice so that the VUR1 locus will be captured on a different genetic background (399, 405). Two separate congenic lines will be created: one in which VUR1 from C3H is introgressed onto a B6 background (B6.C3H^{VUR1}), and the other in which VUR1 from B6 is introgressed onto a C3H background as a control (C3H.B6^{VUR1}). Phenotypic characterization of these mice will provide insight into the contribution of the VUR1

locus to the VUR phenotype, as the effect of the original background will be eliminated (405). If one major recessive gene is responsible for the VUR1 phenotype, then 100% of homozygous B6.C3H^{VUR1} congenic mice are expected to reflux, and none of the C3H.B6^{VUR1} congenic mice are expected to reflux. However, we predict VUR1 is a complex recessive trait, therefore we expect that less than 100% of our B6.C3H^{VUR1} congenic mice will reflux, and a small percentage of the C3H.B6^{VUR1} will reflux. These congenic strains will be invaluable tools because they are genetically identical to each other and can be studied indefinitely. Genotyping DNA markers flanking the VUR1 locus in these congenic mice will reveal the size of the VUR1 locus and therefore help to refine the original 24Mb region (405).

Crosses between refluxing and non-refluxing inbred strains, other than C3H and B6, will also help narrow the VUR1 locus. Genotyping of the N2 or F2 progeny from this cross will identify regions of the genome that are linked with the VUR phenotype, as we have done in the C3H mouse. For example, genotyping of backcross progeny from a DBA/2J (refluxing) and A/J (non-refluxing) cross will determine if the VUR1 locus, or another locus, is responsible for the VUR phenotype in DBA/2J mice. If the VUR1 locus is responsible for VUR in DBA/2J mice, then where the linkage peaks overlap will help narrow the VUR1 locus. Similarly, we can perform complementation analysis between refluxing strains: if the same locus is responsible for VUR in the two strains, then F1 hybrids should be susceptible. For example, if F1 hybrids from a DBA/2J and C3H/HeJ cross reflux, then VUR1 is responsible for the refluxing phenotype in both of these inbred mouse strains. If a founder mutation is responsible for reflux in the different inbred mouse strains, then we can perform detailed haplotype analysis and identify the ancestral haplotype for the VUR phenotype (471).

5.4.6 The future of genetic studies on VUR

Of the four inbred mouse strains that are susceptible to VUR (AKR/J, DBA/2J, CBA/J, and C3H/HeJ), the C3H mouse has the highest incidence of VUR. We therefore hypothesized that the C3H mouse would be an ideal strain in which to identify genes that are associated with VUR. Genetic studies on AKR/J, DBA/2J, and CBA/J mice may identify the same or a new gene(s) associated with VUR.

Linkage studies performed on families with VUR have shown that VUR is extremely genetically heterogeneous and that different families likely have mutations in different genes (29-31). One limitation of these studies is that they have limited power in being able to detect genes that have a small effect on a trait (472-474). This is why many groups have used association studies to determine if a candidate gene is actually associated with a trait (393, 473, 475, 476). The one disadvantage of association studies is that prior knowledge of the candidate gene is required since the test determines the association of a specific genotype with a specific phenotypic trait (475).

Despite the limitation of association studies, they have already proven successful in patients with VUR. These studies have identified associations between polymorphisms in *RET*, *AGTR2*, *UPK2*, and *UPK3* with VUR (216, 222, 223, 360). In one study, a common SNP in *RET*, rs1799939:G>A, was found to be associated with VUR in the French-Canadian population (221). This polymorphism was predicted to affect the kinase activity of the RET receptor suggesting that decreased RET activity is associated with VUR (221). Interestingly, another polymorphism in the *RET* gene that is predicted to decrease the normal mRNA levels of *RET* is associated with reduced kidney size in newborn infants in Montreal (467). In the latter study, the infants were not tested for VUR, but these studies together suggest that common polymorphisms in *RET* are associated with kidney and urinary tract defects in humans. We must keep in mind that VUR is extremely genetically heterogeneous and that while these genes are associated with VUR, they are likely only responsible for VUR in a subset of these patients. We hypothesize that candidate genes identified through mouse genetics, including the gene(s) responsible for VUR in the C3H mouse, can be used in association studies to determine if SNPs in these genes are associated with VUR in humans (472, 474).

It is possible that in many patients with VUR, there is a combination of polymorphisms and/or mutations that are responsible for VUR and its associated phenotypes. This may explain why some patients develop reflux nephropathy, hypertension, and end-stage renal disease, while others do not. An example of this was identified in the European ESCAPE study that aimed to assess the genetic and molecular mechanisms that lead to renal failure in patients with renal hypoplasia or dysplasia (477). As part of the study, a number of genes, including *PAX2*, *EYA1*, *SIX1*, and *SALLI*, were

sequenced in over 400 patients and 17% of these patients had sequence variants in these genes. In one of the families, Renal-coloboma syndrome was identified in a father and his two children (477). The father had moderate chronic renal insufficiency, while the two children had a more severe RCS phenotype and early-onset chronic renal insufficiency. Sequencing identified *PAX2* mutations in the father and his children; however, both children inherited a *SIX1* heterozygous sequence variant from their mother (477). These results suggest that the renal phenotype in the children is worse because of the *SIX1* polymorphism in addition to the *PAX2* mutation. The same study identified Branchio-oto-renal syndrome in a mother and her children; however, only her children had renal abnormalities normally associated with BOR. It was found that the children inherited an *EYA1* mutation from their mother, but also had *GDNF* and *RET* sequence variants. These results suggest that many of the diseases we study, including VUR, may be caused by polymorphisms in multiple genes at the same time (i.e. oligogenic) and the severity of the disease will be influenced by which polymorphisms are present.

The future of VUR genetic research may not only include whole-genome linkage studies, but may also include large-scale genome-wide association studies. These genome-wide association studies are currently being used to study many complex human diseases including diabetes and are believed to be able to identify both common and rare variants that are associated with a disease (396, 478). The advantage of these studies is that hundreds of thousands of SNPs that are known to capture a large fraction of the common variation in the human genome are genotyped in a large number of cases and controls. The genetic variants that co-occur with VUR can then be identified and genetic variants that are frequently missed in linkage studies may be identified. Unfortunately, the high cost associated with whole-genome genotyping technologies currently limits the feasibility of this approach to most investigators. Furthermore, this approach requires the recruitment and the phenotyping of thousands of cases and controls. Nonetheless, the future of genetic research for patients with VUR appears to be promising as the identification of genes that predispose to VUR are being identified and this is providing new insight about the biology of urinary tract defects.

We anticipate that our research on the C3H mouse will be important to understand the link between gene mutation and disease susceptibility. Not only are VUR and its

complications a major health burden, but also treatment of VUR and its complications are extremely costly (176, 479-481). The ultimate goal of genetic research on VUR is to improve treatment of VUR and to facilitate early diagnosis and identification of those patients that are at risk of developing reflux nephropathy, hypertension, and end-stage renal disease. It is equally important that patients with VUR that are not at risk of these complications do not receive unnecessary treatments. We hypothesize that the VUR1 gene(s) in the C3H mouse is associated with the development of VUR without these complications, and may be an important reflux-causing gene in patients with this same phenotype.

5.5 Summary

Our work on the *Pax2*$^{1Neu+/-}$ and C3H mouse has contributed to the understanding of the pathogenesis of VUR. Results from the *Pax2*$^{1Neu+/-}$ mouse demonstrate that genes that are expressed during ureteric bud formation are also involved in determining the position of the ureteric bud along the mesonephric duct. Results from both the *Pax2*$^{1Neu+/-}$ and C3H mouse models demonstrate that when the ureteric bud emerges from a more caudal location along the mesonephric duct, the development of the urinary tract becomes affected such that the ureter is delayed in its separation from the mesonephric duct. This event subsequently leads to the formation of a shortened intravesical ureter and an incompetent UVJ that refluxes.

Our data suggest that VUR is a part of a spectrum of defects that have a similar developmental origin: maldevelopment of the ureteric bud that subsequently impacts kidney and/or urinary tract development. The *Pax2*$^{1Neu+/-}$ mouse exhibits a range of CAKUT phenotypes, including malformed kidneys and duplex systems. In contrast, the C3H mouse is a model of normal kidneys without a nephron deficit, which is a phenotype commonly seen in humans with VUR. We speculate that the degree of the renal malformation is not only influenced by the position of the ureteric bud, but is also affected by the nature of the genetic mutation. *Pax2* is important not only for ureteric bud formation, but also for branching morphogenesis and nephrogenesis, thus drastic changes in kidney morphology and nephron number are not entirely unexpected in the *Pax2*$^{1Neu+/-}$ mouse. The gene defect in the C3H mouse may not have as critical of a role in the

patterning of the kidney, but may have a more important role during the spatial and temporal regulation of ureter maturation, such that a caudally shifted ureteric bud results in a refluxing ureter and a normal kidney.

In summary, *Rdh14* is a strong candidate for VUR in the C3H mouse. The causative gene(s) within the VUR1 locus is expected to be involved in ureteric bud development and will likely highlight an important molecular network that is critical for subsequent ureter maturation and UVJ formation. We hypothesize that the gene(s) in our VUR1 locus will be a candidate to consider in human studies of VUR.

5.6 Original Contributions

The following are original contributions to the knowledge of the development and the genetics of VUR.

Chapter II: *Pax2*$^{1Neu+/-}$ mice have VUR and short intravesical ureters. I developed a standardized technique to detect the presence of VUR, to measure the length of the intravesical ureter in newborn mice, and to measure the position of the ureteric bud along the mesonephric duct. My work on the *Pax2*$^{1Neu+/-}$ mouse confirmed that a caudal ureteric bud is associated with a malformed kidney and a refluxing urinary tract. We are the first to demonstrate that VUR may actually be caused by a delay in urinary tract development.

Chapter III: Different inbred mouse strains demonstrate different kidney sizes at birth. I developed and validated a new counting method that estimates nephron number in mouse kidneys. I further validated the gold-standard disector/fractionator estimation method. The C3H mouse has normal kidneys without a nephron deficit. From our studies on inbred mouse strains with contrasting kidney sizes, I observed that nephron number is not correlated with kidney size or body weight in mice, suggesting that kidney size may not be an adequate surrogate for nephron number.

Chapter III: Different inbred mouse strains have different susceptibilities to VUR and kidney size. We are the first to map a VUR-causing locus using inbred mice. The C3H mouse is a model of VUR without renal malformations. We demonstrate that a caudal ureteric bud is associated with the development of normal kidneys, VUR, short intravesical ureters, and a delay in urinary tract development.

BIBLIOGRAPHY

1. Editorial, Vesicoureteral reflux and its familial distribution. *Br Med J* 1975; 4 (5999): 726.

2. Scott JE and Renwick M, Antenatal diagnosis of congenital abnormalities in the urinary tract. Results from the Northern Region Fetal Abnormality Survey. *Br J Urol* 1988; 62 (4): 295-300.

3. Johnston JH, Vesico-ureteric reflux: its anatomical mechanism, causation, effects and treatment in the child. *Ann R Coll Surg Engl* 1962; 30: 324-341.

4. Campbell M, Walsh, P and Retik, A (eds) *Campbell's Urology*. 8 ed. Saunders Harcourt Publishing: Philadelphia, 2002.

5. McGovern JH, Marshall, V.F., Paquin, A.J., Vesicoureteral Regurgitation in Children. *J Urol* 1960; 83 (2): 122-149.

6. Hodson CJ and Edwards D, Chronic pyelonephritis and vesico-ureteric reflux. *Clin Radiol* 1960; 11: 219-231.

7. Wolfish NM, Delbrouck NF, Shanon A, *et al.*, Prevalence of hypertension in children with primary vesicoureteral reflux. *J Pediatr* 1993; 123 (4): 559-563.

8. Bailey RR and Lynn KL, End-stage reflux nephropathy. *Contrib Nephrol* 1984; 39: 102-110.

9. Stephens FD, Urologic aspects of recurrent urinary tract infection in children. *J Pediatr* 1972; 80 (5): 725-737.

10. Paquin AJ, Jr., Ureterovesical anastomosis: the description and evaluation of a technique. *J Urol* 1959; 82: 573-583.

11. Tanagho EA, Guthrie TH, and Lyon RP, The intravesical ureter in primary reflux. *J Urol* 1969; 101 (6): 824-832.

12. Vermillion CD and Heale WF, Position and configuration of the ureteral orifice and its relationship to renal scarring in adults. *J Urol* 1973; 109 (4): 579-584.

13. Lyon RP, Marshall S, and Tanagho EA, The ureteral orifice: its configuration and competency. *J Urol* 1969; 102 (4): 504-509.

14. Tanagho EA and Pugh RC, The anatomy and function of the ureterovesical junction. *Br J Urol* 1963; 35: 151-165.

15. Risdon RA, Yeung CK, and Ransley PG, Reflux nephropathy in children submitted to unilateral nephrectomy: a clinicopathological study. *Clin Nephrol* 1993; 40 (6): 308-314.

16. Vize, PD, Woolf, AS, and Bard, JB (eds) *The Kidney From Normal Development to Congenital Disease*. Elsevir Science: San Diego, 2003.

17. Murawski IJ and Gupta IR, Vesicoureteric reflux and renal malformations: a developmental problem. *Clin Genet* 2006; 69 (2): 105-117.

18. Batourina E, Choi C, Paragas N, *et al.*, Distal ureter morphogenesis depends on epithelial cell remodeling mediated by vitamin A and Ret. *Nat Genet* 2002; 32 (1): 109-115.

19. Watanabe T and Costantini F, Real-time analysis of ureteric bud branching morphogenesis in vitro. *Dev Biol* 2004; 271 (1): 98-108.

20. Saxen L, (eds) *Organogenesis of the Kidney*. Cambridge University Press: Cambridge, 1987.

21. Mackie GG and Stephens FD, Duplex kidneys: a correlation of renal dysplasia with position of the ureteral orifice. *J Urol* 1975; 114 (2): 274-280.

22. Tanagho EA, Embryologic basis for lower ureteral anomalies: a hypothesis. *Urology* 1976; 7 (5): 451-464.

23. Weiss JP, Embryogenesis of ureteral anomalies: a unifying theory. *Aust N Z J Surg* 1988; 58 (8): 631-638.

24. Yu OH, Murawski IJ, Myburgh DB, *et al.*, Overexpression of RET leads to vesicoureteric reflux in mice. *Am J Physiol Renal Physiol* 2004; 287 (6): F1123-1130.

25. Miyazaki Y, Oshima K, Fogo A, *et al.*, Bone morphogenetic protein 4 regulates the budding site and elongation of the mouse ureter. *J Clin Invest* 2000; 105 (7): 863-873.

26. Grieshammer U, Le M, Plump AS, *et al.*, SLIT2-mediated ROBO2 signaling restricts kidney induction to a single site. *Dev Cell* 2004; 6 (5): 709-717.

27. Basson MA, Akbulut S, Watson-Johnson J, *et al.*, Sprouty1 is a critical regulator of GDNF/RET-mediated kidney induction. *Dev Cell* 2005; 8 (2): 229-239.

28. Kume T, Deng K, and Hogan BL, Murine forkhead/winged helix genes Foxc1 (Mf1) and Foxc2 (Mfh1) are required for the early organogenesis of the kidney and urinary tract. *Development* 2000; 127 (7): 1387-1395.

29. Feather SA, Malcolm S, Woolf AS, *et al.*, Primary, nonsyndromic vesicoureteric reflux and its nephropathy is genetically heterogeneous, with a locus on chromosome 1. *Am J Hum Genet* 2000; 66 (4): 1420-1425.

30. Kelly H, Molony CM, Darlow JM, *et al.*, A genome-wide scan for genes involved in primary vesicoureteric reflux. *J Med Genet* 2007; 44 (11): 710-717.

31. Conte ML, Bertoli-Avella AM, de Graaf BM, *et al.*, A genome search for primary vesicoureteral reflux shows further evidence for genetic heterogeneity. *Pediatr Nephrol* 2008; 23 (4): 587-595.

32. Murawski IJ and Gupta IR, Gene Discovery and Vesicoureteric Reflux. *Pediatr Nephrol* 2008; 23 (7): 1021-1027.

33. Gilbert, SF (eds) *Developmental Biology*. Sinauer Associates, Inc.: Sunderland, MA, 2000.

34. Langman's Medical Embryology.

35. Bard JB, McConnell JE, and Davies JA, Towards a genetic basis for kidney development. *Mech Dev* 1994; 48 (1): 3-11.

36. Dressler GR, The Cellular Basis of Kidney Development. *Annu Rev Cell Dev Biol* 2006.

37. Brandli AW, Towards a molecular anatomy of the Xenopus pronephric kidney. *Int J Dev Biol* 1999; 43 (5): 381-395.

38. Obara-Ishihara T, Kuhlman J, Niswander L*, et al.*, The surface ectoderm is essential for nephric duct formation in intermediate mesoderm. *Development* 1999; 126 (6): 1103-1108.

39. Cuckow PM, Nyirady P, and Winyard PJ, Normal and abnormal development of the urogenital tract. *Prenat Diagn* 2001; 21 (11): 908-916.

40. Young B and Heath JW, (eds) *Wheater's Functional Histology*. 3rd ed. Harcourt Publishers: Edinburgh, 2000.

41. Clark AT and Bertram JF, Molecular regulation of nephron endowment. *Am J Physiol* 1999; 276 (4 Pt 2): F485-497.

42. Bouchard M, Souabni A, Mandler M*, et al.*, Nephric lineage specification by Pax2 and Pax8. *Genes Dev* 2002; 16 (22): 2958-2970.

43. Carroll TJ, Wallingford JB, and Vize PD, Dynamic patterns of gene expression in the developing pronephros of Xenopus laevis. *Dev Genet* 1999; 24 (3-4): 199-207.

44. Wang Q, Lan Y, Cho ES*, et al.*, Odd-skipped related 1 (Odd 1) is an essential regulator of heart and urogenital development. *Dev Biol* 2005; 288 (2): 582-594.

45. James RG, Kamei CN, Wang Q*, et al.*, Odd-skipped related 1 is required for development of the metanephric kidney and regulates formation and differentiation of kidney precursor cells. *Development* 2006; 133 (15): 2995-3004.

46. Pedersen A, Skjong C, and Shawlot W, Lim 1 is required for nephric duct extension and ureteric bud morphogenesis. *Dev Biol* 2005; 288 (2): 571-581.

47. Kreidberg JA, Sariola H, Loring JM*, et al.*, WT-1 is required for early kidney development. *Cell* 1993; 74 (4): 679-691.

48. Sainio K, Hellstedt P, Kreidberg JA*, et al.*, Differential regulation of two sets of mesonephric tubules by WT-1. *Development* 1997; 124 (7): 1293-1299.

49. Joseph A, Yao H, and Hinton BT, Development and morphogenesis of the Wolffian/epididymal duct, more twists and turns. *Dev Biol* 2009; 325 (1): 6-14.

50. Plachov D, Chowdhury K, Walther C*, et al.*, Pax8, a murine paired box gene expressed in the developing excretory system and thyroid gland*. Development* 1990; 110 (2): 643-651.

51. Dressler GR, Deutsch U, Chowdhury K*, et al.*, Pax2, a new murine paired-box-containing gene and its expression in the developing excretory system*. Development* 1990; 109 (4): 787-795.

52. Torres M, Gomez-Pardo E, Dressler GR*, et al.*, Pax-2 controls multiple steps of urogenital development*. Development* 1995; 121 (12): 4057-4065.

53. Eccles MR, The role of PAX2 in normal and abnormal development of the urinary tract*. Pediatr Nephrol* 1998; 12 (9): 712-720.

54. Hu MC and Rosenblum ND, Genetic regulation of branching morphogenesis: lessons learned from loss-of-function phenotypes*. Pediatr Res* 2003; 54 (4): 433-438.

55. Grobstein C, Inductive epitheliomesenchymal interaction in cultured organ rudiments of the mouse*. Science* 1953; 118 (3054): 52-55.

56. Bard JB, Growth and death in the developing mammalian kidney: signals, receptors and conversations*. Bioessays* 2002; 24 (1): 72-82.

57. Davies J. *The Kidney Development Database*. 2008 [cited; Available from: http://golgi.ana.ed.ac.uk/kidhome.html.

58. Durbec P, Marcos-Gutierrez CV, Kilkenny C*, et al.*, GDNF signalling through the Ret receptor tyrosine kinase*. Nature* 1996; 381 (6585): 789-793.

59. Cacalano G, Farinas I, Wang LC*, et al.*, GFRalpha1 is an essential receptor component for GDNF in the developing nervous system and kidney. *Neuron* 1998; 21 (1): 53-62.

60. Schuchardt A, D'Agati V, Pachnis V*, et al.*, Renal agenesis and hypodysplasia in ret-k-mutant mice result from defects in ureteric bud development*. Development* 1996; 122 (6): 1919-1929.

61. Enomoto H, Araki T, Jackman A*, et al.*, GFR alpha1-deficient mice have deficits in the enteric nervous system and kidneys*. Neuron* 1998; 21 (2): 317-324.

62. Tang MJ, Cai Y, Tsai SJ*, et al.*, Ureteric bud outgrowth in response to RET activation is mediated by phosphatidylinositol 3-kinase*. Dev Biol* 2002; 243 (1): 128-136.

63. Pachnis V, Mankoo B, and Costantini F, Expression of the c-ret proto-oncogene during mouse embryogenesis*. Development* 1993; 119 (4): 1005-1017.

64. Sainio K, Suvanto P, Davies J*, et al.*, Glial-cell-line-derived neurotrophic factor is required for bud initiation from ureteric epithelium*. Development* 1997; 124 (20): 4077-4087.

65. Pepicelli CV, Kispert A, Rowitch DH*, et al.*, GDNF induces branching and increased cell proliferation in the ureter of the mouse*. Dev Biol* 1997; 192 (1): 193-198.

66. Tang MJ, Worley D, Sanicola M*, et al.*, The RET-glial cell-derived neurotrophic factor (GDNF) pathway stimulates migration and chemoattraction of epithelial cells*. J Cell Biol* 1998; 142 (5): 1337-1345.

67. Drawbridge J, Meighan CM, and Mitchell EA, GDNF and GFRalpha-1 are components of the axolotl pronephric duct guidance system*. Dev Biol* 2000; 228 (1): 116-124.

68. Murawski IJ, Myburgh DB, Favor J*, et al.*, Vesico-ureteric reflux and urinary tract development in the Pax21Neu+/- mouse*. Am J Physiol Renal Physiol* 2007; 293 (5): F1736-1745.

69. Moore MW, Klein RD, Farinas I*, et al.*, Renal and neuronal abnormalities in mice lacking GDNF. *Nature* 1996; 382 (6586): 76-79.

70. Pichel JG, Shen L, Sheng HZ*, et al.*, Defects in enteric innervation and kidney development in mice lacking GDNF. *Nature* 1996; 382 (6586): 73-76.

71. Schedl A, Renal abnormalities and their developmental origin*. Nat Rev Genet* 2007; 8 (10): 791-802.

72. Self M, Lagutin OV, Bowling B*, et al.*, Six2 is required for suppression of nephrogenesis and progenitor renewal in the developing kidney. *Embo J* 2006; 25 (21): 5214-5228.

73. Xu PX, Adams J, Peters H*, et al.*, Eya1-deficient mice lack ears and kidneys and show abnormal apoptosis of organ primordia*. Nat Genet* 1999; 23 (1): 113-117.

74. Yang J, Blum A, Novak T*, et al.*, An epithelial precursor is regulated by the ureteric bud and by the renal stroma*. Dev Biol* 2002; 246 (2): 296-310.

75. Cui S, Schwartz L, and Quaggin SE, Pod1 is required in stromal cells for glomerulogenesis*. Dev Dyn* 2003; 226 (3): 512-522.

76. Cebrian C, Borodo K, Charles N*, et al.*, Morphometric index of the developing murine kidney. *Dev Dyn* 2004; 231 (3): 601-608.

77. Dressler G, Tubulogenesis in the developing mammalian kidney. *Trends Cell Biol* 2002; 12 (8): 390-395.

78. Koeppen BM and Stanton BA, (eds) *Renal Physiology*. 3 ed. Mosby: St. Louis, 2001.

79. Kispert A, Vainio S, and McMahon AP, Wnt-4 is a mesenchymal signal for epithelial transformation of metanephric mesenchyme in the developing kidney. *Development* 1998; 125 (21): 4225-4234.

80. Stark K, Vainio S, Vassileva G*, et al.*, Epithelial transformation of metanephric mesenchyme in the developing kidney regulated by Wnt-4*. Nature* 1994; 372 (6507): 679-683.

81. Carroll TJ, Park JS, Hayashi S*, et al.*, Wnt9b plays a central role in the regulation of mesenchymal to epithelial transitions underlying organogenesis of the mammalian urogenital system*. Dev Cell* 2005; 9 (2): 283-292.

82. Yu J, Carroll TJ, and McMahon AP, Sonic hedgehog regulates proliferation and differentiation of mesenchymal cells in the mouse metanephric kidney. *Development* 2002; 129 (22): 5301-5312.

83. Batourina E, Tsai S, Lambert S*, et al.*, Apoptosis induced by vitamin A signaling is crucial for connecting the ureters to the bladder. *Nat Genet* 2005; 37 (10): 1082-1089.

84. Airik R and Kispert A, Down the tube of obstructive nephropathies: The importance of tissue interactions during ureter development. *Kidney Int* 2007; 72 (12): 1459-1467.

85. Mahoney ZX, Sammut B, Xavier RJ*, et al.*, Discs-large homolog 1 regulates smooth muscle orientation in the mouse ureter. *Proc Natl Acad Sci U S A* 2006; 103 (52): 19872-19877.

86. Iizuka-Kogo A, Ishidao T, Akiyama T*, et al.*, Abnormal development of urogenital organs in Dlgh1-deficient mice. *Development* 2007; 134 (9): 1799-1807.

87. Airik R, Bussen M, Singh MK*, et al.*, Tbx18 regulates the development of the ureteral mesenchyme. *J Clin Invest* 2006; 116 (3): 663-674.

88. Thomas JC, DeMarco RT, and Pope JCt, Molecular biology of ureteral bud and trigonal development. *Curr Urol Rep* 2005; 6 (2): 146-151.

89. Viana R, Batourina E, Huang H*, et al.*, The development of the bladder trigone, the center of the anti-reflux mechanism. *Development* 2007; 134 (20): 3763-3769.

90. Brown MC, An Analysis of the Developing Metanephros in Mouse Embryos With Abnormal Kidneys. *American Journal of Anatomy* 1931; 47 (1): 117-171.

91. Avni EF, Gallety E, Rypens F*, et al.*, A hypothesis for the higher incidence of vesico-ureteral reflux and primary megaureters in male babies. *Pediatr Radiol* 1992; 22 (1): 1-4.

92. Haraguchi R, Motoyama J, Sasaki H*, et al.*, Molecular analysis of coordinated bladder and urogenital organ formation by Hedgehog signaling. *Development* 2007; 134 (3): 525-533.

93. Hu P, Deng FM, Liang FX*, et al.*, Ablation of uroplakin III gene results in small urothelial plaques, urothelial leakage, and vesicoureteral reflux. *J Cell Biol* 2000; 151 (5): 961-972.

94. Kong XT, Deng FM, Hu P*, et al.*, Roles of uroplakins in plaque formation, umbrella cell enlargement, and urinary tract diseases. *J Cell Biol* 2004; 167 (6): 1195-1204.

95. Schultheiss D, Grunewald V, and Jonas U, Urodynamics in the anatomical work of Leonardo da Vinci (1452-1519). *World J Urol* 1999; 17 (3): 137-143.

96. Tanagho EA, Meyers FH, and Smith DR, The trigone: anatomical and physiological considerations. I. In relation to the ureterovesical junction. *J Urol* 1968; 100 (5): 623-632.

97. Tanagho EA and Hutch JA, Primary Reflux. *J Urol* 1965; 93: 158-164.

98. Wesson MB, Anatomical, Embryological and Physiological Studies of the Trigone and Neck of the Bladder. *J Urol* 1920; 4: 279-315.

99. Trupp M, Raynoschek C, Belluardo N*, et al.*, Multiple GPI-anchored receptors control GDNF-dependent and independent activation of the c-Ret receptor tyrosine kinase. *Mol Cell Neurosci* 1998; 11 (1-2): 47-63.

100. Lim KC, Lakshmanan G, Crawford SE*, et al.*, Gata3 loss leads to embryonic lethality due to noradrenaline deficiency of the sympathetic nervous system. *Nat Genet* 2000; 25 (2): 209-212.

101. Grote D, Souabni A, Busslinger M*, et al.*, Pax 2/8-regulated Gata 3 expression is necessary for morphogenesis and guidance of the nephric duct in the developing kidney. *Development* 2006; 133 (1): 53-61.

102. Batourina E, Gim S, Bello N*, et al.*, Vitamin A controls epithelial/mesenchymal interactions through Ret expression. *Nat Genet* 2001; 27 (1): 74-78.

103. Napoli JL, Interactions of retinoid binding proteins and enzymes in retinoid metabolism. *Biochim Biophys Acta* 1999; 1440 (2-3): 139-162.

104. Mendelsohn C, Batourina E, Fung S*, et al.*, Stromal cells mediate retinoid-dependent functions essential for renal development. *Development* 1999; 126 (6): 1139-1148.

105. Lelievre-Pegorier M, Vilar J, Ferrier ML*, et al.*, Mild vitamin A deficiency leads to inborn nephron deficit in the rat. *Kidney Int* 1998; 54 (5): 1455-1462.

106. Goodyer P, Kurpad A, Rekha S*, et al.*, Effects of maternal vitamin A status on kidney development: a pilot study. *Pediatr Nephrol* 2007; 22 (2): 209-214.

107. Brophy PD, Ostrom L, Lang KM*, et al.*, Regulation of ureteric bud outgrowth by Pax2-dependent activation of the glial derived neurotrophic factor gene. *Development* 2001; 128 (23): 4747-4756.

108. Brodbeck S and Englert C, Genetic determination of nephrogenesis: the Pax/Eya/Six gene network. *Pediatr Nephrol* 2004; 19 (3): 249-255.

109. Sajithlal G, Zou D, Silvius D*, et al.*, Eya 1 acts as a critical regulator for specifying the metanephric mesenchyme. *Dev Biol* 2005; 284 (2): 323-336.

110. Xu PX, Zheng W, Huang L*, et al.*, Six1 is required for the early organogenesis of mammalian kidney. *Development* 2003; 130 (14): 3085-3094.

111. Yu J, McMahon AP, and Valerius MT, Recent genetic studies of mouse kidney development. *Curr Opin Genet Dev* 2004; 14 (5): 550-557.

112. Patterson LT, Pembaur M, and Potter SS, Hoxa11 and Hoxd11 regulate branching morphogenesis of the ureteric bud in the developing kidney. *Development* 2001; 128 (11): 2153-2161.

113. Wellik DM, Hawkes PJ, and Capecchi MR, Hox11 paralogous genes are essential for metanephric kidney induction. *Genes Dev* 2002; 16 (11): 1423-1432.

114. Favor J, Sandulache R, Neuhauser-Klaus A, *et al.*, The mouse Pax2(1Neu) mutation is identical to a human PAX2 mutation in a family with renal-coloboma syndrome and results in developmental defects of the brain, ear, eye, and kidney. *Proc Natl Acad Sci U S A* 1996; 93 (24): 13870-13875.

115. Schedl A, Ross A, Lee M, *et al.*, Influence of PAX6 gene dosage on development: overexpression causes severe eye abnormalities. *Cell* 1996; 86 (1): 71-82.

116. Gross I, Morrison DJ, Hyink DP, *et al.*, The receptor tyrosine kinase regulator Sprouty1 is a target of the tumor suppressor WT1 and important for kidney development. *J Biol Chem* 2003; 278 (42): 41420-41430.

117. Yerkes E, Nishimura H, Miyazaki Y, *et al.*, Role of angiotensin in the congenital anomalies of the kidney and urinary tract in the mouse and the human. *Kidney Int Suppl* 1998; 67: S75-77.

118. Oshima K, Miyazaki Y, Brock JW, 3rd, *et al.*, Angiotensin type II receptor expression and ureteral budding. *J Urol* 2001; 166 (5): 1848-1852.

119. Torres VE and Scheinman SJ, Genetic Diseases of the Kidney. *Nephrol Self-Assessment Program* 2004; 3 (1): 5-11.

120. NAPRTCS Annual Report, 2008 [Internet] Website:. *http://spitfire.emmes.com/study/ped/annlrept/Annual%20Report%20-2008.pdf*.

121. Atiyeh B, Husmann D, and Baum M, Contralateral renal abnormalities in patients with renal agenesis and noncystic renal dysplasia. *Pediatrics* 1993; 91 (4): 812-815.

122. Robson WL, Rogers RC, and Leung AK, Renal agenesis, multicystic dysplasia, and uretero-pelvic junction obstruction--a common pathogenesis? *Am J Med Genet* 1994; 53 (3): 302.

123. Potter EL, (eds) *Normal and abnormal development of the kidney*. Year Book Medical Publishers: Chicago, 1972.

124. Song JT, Ritchey ML, Zerin JM, *et al.*, Incidence of vesicoureteral reflux in children with unilateral renal agenesis. *J Urol* 1995; 153 (4): 1249-1251.

125. Woolf AS and Winyard PJ, Advances in the cell biology and genetics of human kidney malformations. *J Am Soc Nephrol* 1998; 9 (6): 1114-1125.

126. Mei-Zahav M, Korzets Z, Cohen I, *et al.*, Ambulatory blood pressure monitoring in children with a solitary kidney - a comparison between unilateral renal agenesis and uninephrectomy. *Blood Press Monit* 2001; 6 (5): 263-267.

127. Hill LM, Nowak A, Hartle R, *et al.*, Fetal compensatory renal hypertrophy with a unilateral functioning kidney. *Ultrasound Obstet Gynecol* 2000; 15 (3): 191-193.

128. Pasch A, Hoefele J, Grimminger H*, et al.*, Multiple urinary tract malformations with likely recessive inheritance in a large Somalian kindred. *Nephrol Dial Transplant* 2004; 19 (12): 3172-3175.

129. Moerman P, Fryns JP, Sastrowijoto SH*, et al.*, Hereditary renal adysplasia: new observations and hypotheses. *Pediatr Pathol* 1994; 14 (3): 405-410.

130. Burger RH and Burger SE, Genetic determinants of urologic disease. *Urol Clin North Am* 1974; 1 (3): 419-440.

131. Devriendt K, Moerman P, Van Schoubroeck D*, et al.*, Chromosome 22q11 deletion presenting as the Potter sequence. *J Med Genet* 1997; 34 (5): 423-425.

132. Pierides AM, Athanasiou Y, Demetriou K*, et al.*, A family with the branchio-oto-renal syndrome: clinical and genetic correlations. *Nephrol Dial Transplant* 2002; 17 (6): 1014-1018.

133. Zenteno JC, Mendez JP, Maya-Nunez G*, et al.*, Renal abnormalities in patients with Kallmann syndrome. *BJU Int* 1999; 83 (4): 383-386.

134. McPherson E, Carey J, Kramer A*, et al.*, Dominantly inherited renal adysplasia. *Am J Med Genet* 1987; 26 (4): 863-872.

135. Sanna-Cherchi S, Caridi G, Weng PL*, et al.*, Localization of a gene for nonsyndromic renal hypodysplasia to chromosome 1p32-33. *Am J Hum Genet* 2007; 80 (3): 539-549.

136. Bialestock D, Renal Malformations And Pyelonephritis. The Role Of Vesico-Ureteral Reflux. *Aust N Z J Surg* 1963; 33: 114-127.

137. Royer P, Habib R, Broyer M*, et al.*, Segmental hypoplasia of the kidney in children. *Adv Nephrol Necker Hosp* 1971; 1: 145-159.

138. Heptinstall RH, Jennette, JC (eds). Heptinstall's Pathology of the Kidney 5th edition. Lippincott-Raven: Philadelphia, 1998.

139. Buscemi M, Shanske A, Mallet E*, et al.*, Dominantly inherited ureteropelvic junction obstruction. *Urology* 1985; 26 (6): 568-571.

140. Horton CE, Jr., Davisson MT, Jacobs JB*, et al.*, Congenital progressive hydronephrosis in mice: a new recessive mutation. *J Urol* 1988; 140 (5 Pt 2): 1310-1315.

141. Reynard J, Brewster S, and Biers S, (eds) *Oxford Handbook of Urology*. 1st ed. Oxford University Press: USA, 2005.

142. Uetani N, Bertozzi K, Chagnon MJ*, et al.*, Maturation of ureter-bladder connection in mice is controlled by LAR family receptor protein tyrosine phosphatases. *J Clin Invest* 2009.

143. Simpson JL and German J, Familial urinary tract anomalies. *Jama* 1970; 212 (13): 2264-2265.

144. van Eerde AM, Koeleman BP, van de Kamp JM*, et al.*, Linkage study of 14 candidate genes and loci in four large Dutch families with vesico-ureteral reflux. *Pediatr Nephrol* 2007; 22 (8): 1129-1133.

145. Atwell JD, Cook PL, Howell CJ*, et al.*, Familial incidence of bifid and double ureters. *Arch Dis Child* 1974; 49 (5): 390-393.

146. Practice parameter: the diagnosis, treatment, and evaluation of the initial urinary tract infection in febrile infants and young children. American Academy of Pediatrics. Committee on Quality Improvement. Subcommittee on Urinary Tract Infection. *Pediatrics* 1999; 103 (4 Pt 1): 843-852.

147. Siomou E, Papadopoulou F, Kollios KD*, et al.*, Duplex collecting system diagnosed during the first 6 years of life after a first urinary tract infection: a study of 63 children. *J Urol* 2006; 175 (2): 678-681; discussion 681-672.

148. Guarino N, Tadini B, Camardi P*, et al.*, The incidence of associated urological abnormalities in children with renal ectopia. *J Urol* 2004; 172 (4 Pt 2): 1757-1759; discussion 1759.

149. Burger RH and Smith C, Hereditary and familial vesicoureteral reflux. *J Urol* 1971; 106 (6): 845-851.

150. Chapman CJ, Bailey RR, Janus ED*, et al.*, Vesicoureteric reflux: segregation analysis. *Am J Med Genet* 1985; 20 (4): 577-584.

151. Bois E, Feingold J, Benmaiz H*, et al.*, Congenital urinary tract malformations: epidemiologic and genetic aspects. *Clin Genet* 1975; 8 (1): 37-47.

152. Amar AD, Familial vesicoureteral reflux. *J Urol* 1972; 108 (6): 969-971.

153. Cascio S, Paran S, and Puri P, Associated urological anomalies in children with unilateral renal agenesis. *J Urol* 1999; 162 (3 Pt 2): 1081-1083.

154. Polito C, La Manna A, Rambaldi PF*, et al.*, High incidence of a generally small kidney and primary vesicoureteral reflux. *J Urol* 2000; 164 (2): 479-482.

155. Smellie JM, Normand IC, and Katz G, Children with urinary infection: a comparison of those with and those without vesicoureteric reflux. *Kidney Int* 1981; 20 (6): 717-722.

156. Mackie GG, Abnormalities of the ureteral bud. *Urol Clin North Am* 1978; 5 (1): 161-174.

157. Schwarz RD, Stephens FD, and Cussen LJ, The pathogenesis of renal dysplasia. II. The significance of lateral and medial ectopy of the ureteric orifice. *Invest Urol* 1981; 19 (2): 97-100.

158. King LR, Kazmi SO, and Belman AB, Natural history of vesicoureteral reflux. Outcome of a trial of nonoperative therapy. *Urol Clin North Am* 1974; 1 (3): 441-455.

159. Gruber CM, A comparative study of the intra-vesical ureters (uretero-vesical valves) in man and in experimental animals. *J Urol* 1929; 21 (5): 567-581.

160. Stephens FD and Lenaghan D, The anatomical basis and dynamics of vesicoureteral reflux. *J Urol* 1962; 87: 669-680.

161. Williams G, Fletcher JT, Alexander SI*, et al.*, Vesicoureteral reflux. *J Am Soc Nephrol* 2008; 19 (5): 847-862.

162. Hodson EM, Wheeler DM, Vimalchandra D*, et al.*, Interventions for primary vesicoureteric reflux. *Cochrane Database Syst Rev* 2007; (3): CD001532.

163. Amar AD and Singer B, Vesicoureteral reflux: a 10-year study of 280 patients. *J Urol* 1973; 109 (6): 999-1001.

164. Sengar DP, Rashid A, and Wolfish NM, Familial urinary tract anomalies: association with the major histocompatibility complex in man. *J Urol* 1979; 121 (2): 194-197.

165. Medical versus surgical treatment of primary vesicoureteral reflux: report of the International Reflux Study Committee. *Pediatrics* 1981; 67 (3): 392-400.

166. Connolly LP, Treves ST, Zurakowski D*, et al.*, Natural history of vesicoureteral reflux in siblings. *J Urol* 1996; 156 (5): 1805-1807.

167. Edwards D, Normand IC, Prescod N*, et al.*, Disappearance of vesicoureteric reflux during long-term prophylaxis of urinary tract infection in children. *Br Med J* 1977; 2 (6082): 285-288.

168. Schwab CW, Jr., Wu HY, Selman H*, et al.*, Spontaneous resolution of vesicoureteral reflux: a 15-year perspective. *J Urol* 2002; 168 (6): 2594-2599.

169. Hutch JA, Theory of maturation of the intravesical ureter. *J Urol* 1961; 86: 534-538.

170. McLorie GA, McKenna PH, Jumper BM*, et al.*, High grade vesicoureteral reflux: analysis of observational therapy. *J Urol* 1990; 144 (2 Pt 2): 537-540; discussion 545.

171. Marra G, Oppezzo C, Ardissino G*, et al.*, Severe vesicoureteral reflux and chronic renal failure: a condition peculiar to male gender? Data from the ItalKid Project. *J Pediatr* 2004; 144 (5): 677-681.

172. Ekman H, Jacobsson B, Kock NG*, et al.*, High diuresis, a factor in preventing vesicoureteral reflux. *J Urol* 1966; 95 (4): 511-515.

173. Zerati Filho M, Calado AA, Barroso U, Jr.*, et al.*, Spontaneous resolution rates of vesicoureteral reflux in Brazilian children: a 30-year experience. *Int Braz J Urol* 2007; 33 (2): 204-212; discussion 213-205.

174. el-Khatib MT, Becker GJ, and Kincaid-Smith PS, Reflux nephropathy and primary vesicoureteric reflux in adults. *Q J Med* 1990; 77 (284): 1241-1253.

175. Cleper R, Krause I, Eisenstein B*, et al.*, Prevalence of vesicoureteral reflux in neonatal urinary tract infection. *Clin Pediatr (Phila)* 2004; 43 (7): 619-625.

176. Cohen AL, Rivara FP, Davis R*, et al.*, Compliance with guidelines for the medical care of first urinary tract infections in infants: a population-based study. *Pediatrics* 2005; 115 (6): 1474-1478.

177. Ransley PG, Vesicoureteric reflux: continuing surgical dilemma. *Urology* 1978; 12 (3): 246-255.

178. Murawski IJ and Gupta IR, Genetic heterogeneity of vesicoureteric reflux: insights from mouse models. *Paediatriki* 2007; 70 (6): 428-435.

179. Gordon AC, Thomas DF, Arthur RJ*, et al.*, Prenatally diagnosed reflux: a follow-up study. *Br J Urol* 1990; 65 (4): 407-412.

180. Najmaldin A, Burge DM, and Atwell JD, Fetal vesicoureteric reflux. *Br J Urol* 1990; 65 (4): 403-406.

181. Chertin B and Puri P, Familial vesicoureteral reflux. *J Urol* 2003; 169 (5): 1804-1808.

182. de Vargas A, Evans K, Ransley P*, et al.*, A family study of vesicoureteric reflux. *J Med Genet* 1978; 15 (2): 85-96.

183. Noe HN, The long-term results of prospective sibling reflux screening. *J Urol* 1992; 148 (5 Pt 2): 1739-1742.

184. Jerkins GR and Noe HN, Familial vesicoureteral reflux: a prospective study. *J Urol* 1982; 128 (4): 774-778.

185. Wan J, Greenfield SP, Ng M*, et al.*, Sibling reflux: a dual center retrospective study. *J Urol* 1996; 156 (2 Pt 2): 677-679.

186. Anderson NG, Wright S, Abbott GD*, et al.*, Fetal renal pelvic dilatation--poor predictor of familial vesicoureteral reflux. *Pediatr Nephrol* 2003; 18 (9): 902-905.

187. Van den Abbeele AD, Treves ST, Lebowitz RL*, et al.*, Vesicoureteral reflux in asymptomatic siblings of patients with known reflux: radionuclide cystography. *Pediatrics* 1987; 79 (1): 147-153.

188. Ardissino G, Avolio L, Dacco V*, et al.*, Long-term outcome of vesicoureteral reflux associated chronic renal failure in children. Data from the ItalKid Project. *J Urol* 2004; 172 (1): 305-310.

189. Bailey RR, Vesico-ureteric reflux and reflux nephropathy. *Kidney Int Suppl* 1993; 42: S80-85.

190. Goonasekera CD and Dillon MJ, Reflux nephropathy and hypertension. *J Hum Hypertens* 1998; 12 (8): 497-504.

191. Chertin B, Farkas A, and Puri P, Insulin-like growth factor-1 expression in reflux nephropathy. *Pediatr Surg Int* 2004; 20 (4): 283-289.

192. Risdon RA, The small scarred kidney in childhood. *Pediatr Nephrol* 1993; 7 (4): 361-364.

193. Hodson J, Maling TM, McManamon PJ*, et al.*, Reflux nephropathy. *Kidney Int Suppl* 1975; 4: S50-58.

194. Hodson CJ, Maling TM, McManamon PJ*, et al.*, The pathogenesis of reflux nephropathy (chronic atrophic pyelonephritis). *Br J Radiol* 1975; Suppl 13: 1-26.

195. Silva JM, Diniz JS, Oliveira EA*, et al.*, Features of primary vesicoureteral reflux and renal damage in children at a single institution in Brazil from 1969 to 1999. *Int Urol Nephrol* 2003; 35 (2): 161-168.

196. Lama G, Russo M, De Rosa E*, et al.*, Primary vesicoureteric reflux and renal damage in the first year of life. *Pediatr Nephrol* 2000; 15 (3-4): 205-210.

197. Stutley JE and Gordon I, Vesico-ureteric reflux in the damaged non-scarred kidney. *Pediatr Nephrol* 1992; 6 (1): 25-29.

198. Lee JH, Son CH, Lee MS*, et al.*, Vesicoureteral reflux increases the risk of renal scars: a study of unilateral reflux. *Pediatr Nephrol* 2006; 21 (9): 1281-1284.

199. Bailey RR, Long-term follow-up of infants with gross vesico-ureteric reflux. *Contrib Nephrol* 1984; 39: 146-151.

200. Assael BM, Guez S, Marra G*, et al.*, Congenital reflux nephropathy: a follow-up of 108 cases diagnosed perinatally. *Br J Urol* 1998; 82 (2): 252-257.

201. Bailey RR, End-stage reflux nephropathy. *Nephron* 1981; 27 (6): 302-306.

202. Redman JF, Scriber LJ, and Bissada NK, Apparent failure of renal growth secondary to vesicoureteral reflux. *Urology* 1974; 3 (6): 704-707.

203. Gordon I, Vesico-ureteric reflux, urinary-tract infection, and renal damage in children. *Lancet* 1995; 346 (8973): 489-490.

204. Sargent MA, What is the normal prevalence of vesicoureteral reflux? *Pediatr Radiol* 2000; 30 (9): 587-593.

205. Willscher MK, Bauer SB, Zammuto PJ*, et al.*, Renal growth and urinary infection following antireflux surgery in infants and children. *J Urol* 1976; 115 (6): 722-725.

206. Muensterer OJ, Comprehensive ultrasound versus voiding cysturethrography in the diagnosis of vesicoureteral reflux. *Eur J Pediatr* 2002; 161 (8): 435-437.

207. Lahdes-Vasama T, Niskanen K, and Ronnholm K, Outcome of kidneys in patients treated for vesicoureteral reflux (VUR) during childhood. *Nephrol Dial Transplant* 2006; 21 (9): 2491-2497.

208. Bundy DG, Vesicoureteral reflux. *Pediatr Rev* 2007; 28 (2): e6-8; discussion e8.

209. Smellie J, Edwards D, Hunter N*, et al.*, Vesico-ureteric reflux and renal scarring. *Kidney Int Suppl* 1975; 4: S65-72.

210. O'Donnell B and Puri P, Treatment of vesicoureteric reflux by endoscopic injection of Teflon. *Br Med J (Clin Res Ed)* 1984; 289 (6436): 7-9.

211. Medical versus surgical treatment of primary vesicoureteral reflux: a prospective international reflux study in children. *J Urol* 1981; 125 (3): 277-283.

212. Craig JC, Irwig LM, Knight JF, *et al.*, Does treatment of vesicoureteric reflux in childhood prevent end-stage renal disease attributable to reflux nephropathy? *Pediatrics* 2000; 105 (6): 1236-1241.

213. Babcock JR, Keats GK, and King LR, Renal changes after an uncomplicated antireflux operation. *J Urol* 1976; 115 (6): 720-721.

214. Torres VE, Velosa JA, Holley KE, *et al.*, The progression of vesicoureteral reflux nephropathy. *Ann Intern Med* 1980; 92 (6): 776-784.

215. Sjostrom S, Sillen U, Bachelard M, *et al.*, Spontaneous resolution of high grade infantile vesicoureteral reflux. *J Urol* 2004; 172 (2): 694-698; discussion 699.

216. Nishimura H, Yerkes E, Hohenfellner K, *et al.*, Role of the angiotensin type 2 receptor gene in congenital anomalies of the kidney and urinary tract, CAKUT, of mice and men. *Mol Cell* 1999; 3 (1): 1-10.

217. Srinivas S, Wu Z, Chen CM, *et al.*, Dominant effects of RET receptor misexpression and ligand-independent RET signaling on ureteric bud development. *Development* 1999; 126 (7): 1375-1386.

218. Vogels R, Charite J, de Graaff W, *et al.*, Proximal cis-acting elements cooperate to set Hoxb-7 (Hox-2.3) expression boundaries in transgenic mice. *Development* 1993; 118 (1): 71-82.

219. Kress C, Vogels R, De Graaff W, *et al.*, Hox-2.3 upstream sequences mediate lacZ expression in intermediate mesoderm derivatives of transgenic mice. *Development* 1990; 109 (4): 775-786.

220. Dressler GR, Transcription factors in renal development: the WT1 and Pax-2 story. *Semin Nephrol* 1995; 15 (4): 263-271.

221. Yang Y, Letendre J, Houle A, *et al.*, RET Gly691Ser mutation is associated with primary vesicoureteral reflux in the French-Canadian population from Quebec. *Hum Mutat* 2008; 29 (5): 695-702.

222. Jenkins D, Bitner-Glindzicz M, Malcolm S, *et al.*, Mutation analyses of Uroplakin II in children with renal tract malformations. *Nephrol Dial Transplant* 2006; 21 (12): 3415-3421.

223. Jenkins D, Bitner-Glindzicz M, Malcolm S, *et al.*, De novo uroplakin 111a heterozygous mutations cause renal adysplasia leading to severe kidney failure. *JASN* 2005; 16 (7): 2141-2149.

224. Mansouri A, Hallonet M, and Gruss P, Pax genes and their roles in cell differentiation and development. *Curr Opin Cell Biol* 1996; 8 (6): 851-857.

225. Oefelein M, Grapey D, Schaeffer T*, et al.*, Pax-2: a developmental gene constitutively expressed in the mouse epididymis and ductus deferens. *J Urol* 1996; 156 (3): 1204-1207.

226. Burton Q, Cole LK, Mulheisen M*, et al.*, The role of Pax2 in mouse inner ear development. *Dev Biol* 2004; 272 (1): 161-175.

227. Pfeffer PL, Bouchard M, and Busslinger M, Pax2 and homeodomain proteins cooperatively regulate a 435 bp enhancer of the mouse Pax5 gene at the midbrain-hindbrain boundary. *Development* 2000; 127 (5): 1017-1028.

228. Dressler GR and Douglass EC, Pax-2 is a DNA-binding protein expressed in embryonic kidney and Wilms tumor. *Proc Natl Acad Sci U S A* 1992; 89 (4): 1179-1183.

229. Patel SR and Dressler GR, Expression of Pax2 in the intermediate mesoderm is regulated by YY1. *Dev Biol* 2004; 267 (2): 505-516.

230. Porteous S, Torban E, Cho NP*, et al.*, Primary renal hypoplasia in humans and mice with PAX2 mutations: evidence of increased apoptosis in fetal kidneys of Pax2(1Neu) +/- mutant mice. *Hum Mol Genet* 2000; 9 (1): 1-11.

231. Sanyanusin P, Norrish JH, Ward TA*, et al.*, Genomic structure of the human PAX2 gene. *Genomics* 1996; 35 (1): 258-261.

232. Chi N and Epstein JA, Getting your Pax straight: Pax proteins in development and disease. *Trends Genet* 2002; 18 (1): 41-47.

233. Eccles MR and Schimmenti LA, Renal-coloboma syndrome: a multi-system developmental disorder caused by PAX2 mutations. *Clin Genet* 1999; 56 (1): 1-9.

234. Bouchard M, Grote D, Craven SE*, et al.*, Identification of Pax2-regulated genes by expression profiling of the mid-hindbrain organizer region. *Development* 2005; 132 (11): 2633-2643.

235. Pfeffer PL, Gerster T, Lun K*, et al.*, Characterization of three novel members of the zebrafish Pax2/5/8 family: dependency of Pax5 and Pax8 expression on the Pax2.1 (noi) function. *Development* 1998; 125 (16): 3063-3074.

236. Chang CP, McDill BW, Neilson JR*, et al.*, Calcineurin is required in urinary tract mesenchyme for the development of the pyeloureteral peristaltic machinery. *J Clin Invest* 2004; 113 (7): 1051-1058.

237. Hueber PA, Fukuzawa R, El-Kares R*, et al.*, PAX3 is expressed in the stromal compartment of the developing kidney and in Wilms Tumors with myogenic phenotype. *Pediatr Dev Pathol* 2008: 1.

238. Schimmenti LA, Manligas GS, and Sieving PA, Optic nerve dysplasia and renal insufficiency in a family with a novel PAX2 mutation, Arg115X: further ophthalmologic delineation of the renal-coloboma syndrome. *Ophthalmic Genet* 2003; 24 (4): 191-202.

239. Hoth CF, Milunsky A, Lipsky N, *et al.*, Mutations in the paired domain of the human PAX3 gene cause Klein-Waardenburg syndrome (WS-III) as well as Waardenburg syndrome type I (WS-I). *Am J Hum Genet* 1993; 52 (3): 455-462.

240. Baldwin CT, Lipsky NR, Hoth CF, *et al.*, Mutations in PAX3 associated with Waardenburg syndrome type I. *Hum Mutat* 1994; 3 (3): 205-211.

241. Epstein DJ, Vekemans M, and Gros P, Splotch (Sp2H), a mutation affecting development of the mouse neural tube, shows a deletion within the paired homeodomain of Pax-3. *Cell* 1991; 67 (4): 767-774.

242. Glaser T, Jepeal L, Edwards JG, *et al.*, PAX6 gene dosage effect in a family with congenital cataracts, aniridia, anophthalmia and central nervous system defects. *Nat Genet* 1994; 7 (4): 463-471.

243. Macdonald R, Barth KA, Xu Q, *et al.*, Midline signalling is required for Pax gene regulation and patterning of the eyes. *Development* 1995; 121 (10): 3267-3278.

244. Macchia PE, Lapi P, Krude H, *et al.*, PAX8 mutations associated with congenital hypothyroidism caused by thyroid dysgenesis. *Nat Genet* 1998; 19 (1): 83-86.

245. Stockton DW, Das P, Goldenberg M, *et al.*, Mutation of PAX9 is associated with oligodontia. *Nat Genet* 2000; 24 (1): 18-19.

246. Sanyanusin P, Schimmenti LA, McNoe LA, *et al.*, Mutation of the PAX2 gene in a family with optic nerve colobomas, renal anomalies and vesicoureteral reflux. *Nat Genet* 1995; 9 (4): 358-364.

247. Sanyanusin P, McNoe LA, Sullivan MJ, *et al.*, Mutation of PAX2 in two siblings with renal-coloboma syndrome. *Hum Mol Genet* 1995; 4 (11): 2183-2184.

248. Schimmenti LA, Cunliffe HE, McNoe LA, *et al.*, Further delineation of renal-coloboma syndrome in patients with extreme variability of phenotype and identical PAX2 mutations. *Am J Hum Genet* 1997; 60 (4): 869-878.

249. Schimmenti LA, Pierpont ME, Carpenter BL, *et al.*, Autosomal dominant optic nerve colobomas, vesicoureteral reflux, and renal anomalies. *Am J Med Genet* 1995; 59 (2): 204-208.

250. Fletcher J, Hu M, Berman Y, *et al.*, Multicystic dysplastic kidney and variable phenotype in a family with a novel deletion mutation of PAX2. *J Am Soc Nephrol* 2005; 16 (9): 2754-2761.

251. *Human PAX2 Allelic Variant Database*. [cited 2008 October]; Available from: https://lsdb.hgu.mrc.ac.uk/.

252. Cunliffe HE, McNoe LA, Ward TA*, et al.*, The prevalence of PAX2 mutations in patients with isolated colobomas or colobomas associated with urogenital anomalies. *J Med Genet* 1998; 35 (10): 806-812.

253. Keller SA, Jones JM, Boyle A*, et al.*, Kidney and retinal defects (Krd), a transgene-induced mutation with a deletion of mouse chromosome 19 that includes the Pax2 locus. *Genomics* 1994; 23 (2): 309-320.

254. Torban E, Eccles MR, Favor J*, et al.*, PAX2 suppresses apoptosis in renal collecting duct cells. *Am J Pathol* 2000; 157 (3): 833-842.

255. Dziarmaga A, Clark P, Stayner C*, et al.*, Ureteric bud apoptosis and renal hypoplasia in transgenic PAX2-Bax fetal mice mimics the renal-coloboma syndrome. *J Am Soc Nephrol* 2003; 14 (11): 2767-2774.

256. Dressler GR, Wilkinson JE, Rothenpieler UW*, et al.*, Deregulation of Pax-2 expression in transgenic mice generates severe kidney abnormalities. *Nature* 1993; 362 (6415): 65-67.

257. Brophy PD, Lang KM, and Dressler GR, The secreted frizzled related protein 2 (SFRP2) gene is a target of the Pax2 transcription factor. *J Biol Chem* 2003; 278 (52): 52401-52405.

258. Clarke JC, Patel SR, Raymond RM, Jr.*, et al.*, Regulation of c-Ret in the developing kidney is responsive to Pax2 gene dosage. *Hum Mol Genet* 2006; 15 (23): 3420-3428.

259. Dehbi M, Ghahremani M, Lechner M*, et al.*, The paired-box transcription factor, PAX2, positively modulates expression of the Wilms' tumor suppressor gene (WT1). *Oncogene* 1996; 13 (3): 447-453.

260. Dziarmaga A, Hueber PA, Iglesias D*, et al.*, Neuronal apoptosis inhibitory protein is expressed in developing kidney and is regulated by PAX2. *Am J Physiol Renal Physiol* 2006; 291 (4): F913-920.

261. Torban E, Dziarmaga A, Iglesias D*, et al.*, PAX2 activates WNT4 expression during mammalian kidney development. *J Biol Chem* 2006; 281 (18): 12705-12712.

262. Caione P, Ciofetta G, Collura G*, et al.*, Renal damage in vesico-ureteric reflux. *BJU Int* 2004; 93 (4): 591-595.

263. Godley ML, Desai D, Yeung CK*, et al.*, The relationship between early renal status, and the resolution of vesico-ureteric reflux and bladder function at 16 months. *BJU Int* 2001; 87 (6): 457-462.

264. Yeung CK, Godley ML, Dhillon HK*, et al.*, The characteristics of primary vesico-ureteric reflux in male and female infants with pre-natal hydronephrosis. *Br J Urol* 1997; 80 (2): 319-327.

265. Hinchliffe SA, Chan YF, Jones H*, et al.*, Renal hypoplasia and postnatally acquired cortical loss in children with vesicoureteral reflux. *Pediatr Nephrol* 1992; 6 (5): 439-444.

266. Keller G, Zimmer G, Mall G*, et al.*, Nephron number in patients with primary hypertension. *N Engl J Med* 2003; 348 (2): 101-108.

267. Hoy WE, Hughson MD, Singh GR*, et al.*, Reduced nephron number and glomerulomegaly in Australian Aborigines: a group at high risk for renal disease and hypertension. *Kidney Int* 2006; 70 (1): 104-110.

268. Brenner BM, Garcia DL, and Anderson S, Glomeruli and blood pressure. Less of one, more the other? *Am J Hypertens* 1988; 1 (4 Pt 1): 335-347.

269. Hughson M, Farris AB, 3rd, Douglas-Denton R*, et al.*, Glomerular number and size in autopsy kidneys: the relationship to birth weight. *Kidney Int* 2003; 63 (6): 2113-2122.

270. Samuel T, Hoy WE, Douglas-Denton R*, et al.*, Determinants of glomerular volume in different cortical zones of the human kidney. *J Am Soc Nephrol* 2005; 16 (10): 3102-3109.

271. Douglas-Denton RN, McNamara BJ, Hoy WE*, et al.*, Does nephron number matter in the development of kidney disease? *Ethn Dis* 2006; 16 (2 Suppl 2): S2-40-45.

272. Spencer J, Wang Z, and Hoy W, Low birth weight and reduced renal volume in Aboriginal children. *Am J Kidney Dis* 2001; 37 (5): 915-920.

273. Hinchliffe SA, Sargent PH, Howard CV*, et al.*, Human intrauterine renal growth expressed in absolute number of glomeruli assessed by the disector method and Cavalieri principle. *Lab Invest* 1991; 64 (6): 777-784.

274. Nyengaard JR and Bendtsen TF, Glomerular number and size in relation to age, kidney weight, and body surface in normal man. *Anat Rec* 1992; 232 (2): 194-201.

275. Hoy WE, Douglas-Denton RN, Hughson MD*, et al.*, A stereological study of glomerular number and volume: preliminary findings in a multiracial study of kidneys at autopsy. *Kidney Int Suppl* 2003; (83): S31-37.

276. Barker DJ, Osmond C, Golding J*, et al.*, Growth in utero, blood pressure in childhood and adult life, and mortality from cardiovascular disease. *Bmj* 1989; 298 (6673): 564-567.

277. Merlet-Benichou C, Gilbert T, Vilar J*, et al.*, Nephron number: variability is the rule. Causes and consequences. *Lab Invest* 1999; 79 (5): 515-527.

278. Taal MW, Tilney NL, Brenner BM*, et al.*, Renal Mass: An Improrant Determinant of Late Allograft Outcome. *Transplantation Reviews* 1998; 12 (2): 74-84.

279. Luyckx VA and Brenner BM, Low birth weight, nephron number, and kidney disease. *Kidney Int Suppl* 2005; (97): S68-77.

280. Manalich R, Reyes L, Herrera M*, et al.*, Relationship between weight at birth and the number and size of renal glomeruli in humans: a histomorphometric study. *Kidney Int* 2000; 58 (2): 770-773.

281. McNamara BJ, Diouf B, Hughson MD*, et al.*, Renal pathology, glomerular number and volume in a West African urban community. *Nephrol Dial Transplant* 2008; 23 (8): 2576-2585.

282. Barker DJ, Bull AR, Osmond C*, et al.*, Fetal and placental size and risk of hypertension in adult life. *Bmj* 1990; 301 (6746): 259-262.

283. Hughson MD, Douglas-Denton R, Bertram JF*, et al.*, Hypertension, glomerular number, and birth weight in African Americans and white subjects in the southeastern United States. *Kidney Int* 2006; 69 (4): 671-678.

284. Moritz KM, Dodic M, and Wintour EM, Kidney development and the fetal programming of adult disease. *Bioessays* 2003; 25 (3): 212-220.

285. Hinchliffe SA, Lynch MR, Sargent PH*, et al.*, The effect of intrauterine growth retardation on the development of renal nephrons. *Br J Obstet Gynaecol* 1992; 99 (4): 296-301.

286. Vilar J, Gilbert T, Moreau E*, et al.*, Metanephros organogenesis is highly stimulated by vitamin A derivatives in organ culture. *Kidney Int* 1996; 49 (5): 1478-1487.

287. Merlet-Benichou C, Gilbert T, Muffat-Joly M*, et al.*, Intrauterine growth retardation leads to a permanent nephron deficit in the rat. *Pediatr Nephrol* 1994; 8 (2): 175-180.

288. Kittelson JA, The postnatal growth of the kidney of the albino rat, with observations on an adult human kidney. *Anat Rec* 1917; 13: 385-408.

289. Schreuder MF, Nyengaard JR, Fodor M*, et al.*, Glomerular number and function are influenced by spontaneous and induced low birth weight in rats. *J Am Soc Nephrol* 2005; 16 (10): 2913-2919.

290. Sakurai H and Nigam SK, In vitro branching tubulogenesis: implications for developmental and cystic disorders, nephron number, renal repair, and nephron engineering. *Kidney Int* 1998; 54 (1): 14-26.

291. Shimamura T and Morrison AB, A progressive glomerulosclerosis occurring in partial five-sixths nephrectomized rats. *Am J Pathol* 1975; 79 (1): 95-106.

292. Cullen-McEwen LA, Kett MM, Dowling J*, et al.*, Nephron number, renal function, and arterial pressure in aged GDNF heterozygous mice. *Hypertension* 2003; 41 (2): 335-340.

293. Woods LL, Weeks DA, and Rasch R, Hypertension after neonatal uninephrectomy in rats precedes glomerular damage. *Hypertension* 2001; 38 (3): 337-342.

294. Skov K, Nyengaard JR, Korsgaard N*, et al.*, Number and size of renal glomeruli in spontaneously hypertensive rats. *J Hypertens* 1994; 12 (12): 1373-1376.

295. Black MJ, Briscoe TA, Constantinou M*, et al.*, Is there an association between level of adult blood pressure and nephron number or renal filtration surface area? *Kidney Int* 2004; 65 (2): 582-588.

296. Fassi A, Sangalli F, Maffi R*, et al.*, Progressive glomerular injury in the MWF rat is predicted by inborn nephron deficit*. J Am Soc Nephrol* 1998; 9 (8): 1399-1406.

297. Schulz A, Weiss J, Schlesener M*, et al.*, Development of overt proteinuria in the Munich Wistar Fromter rat is suppressed by replacement of chromosome 6 in a consomic rat strain*. J Am Soc Nephrol* 2007; 18 (1): 113-121.

298. Schulz A, Standke D, Kovacevic L*, et al.*, A major gene locus links early onset albuminuria with renal interstitial fibrosis in the MWF rat with polygenetic albuminuria*. J Am Soc Nephrol* 2003; 14 (12): 3081-3089.

299. Schulz A, Hansch J, Kuhn K*, et al.*, Nephron deficit is not required for progressive proteinuria development in the Munich Wistar Fromter rat*. Physiol Genomics* 2008; 35 (1): 30-35.

300. Dziarmaga A, Eccles M, and Goodyer P, Suppression of ureteric bud apoptosis rescues nephron endowment and adult renal function in Pax2 mutant mice*. J Am Soc Nephrol* 2006; 17 (6): 1568-1575.

301. Zhao H, Kegg H, Grady S*, et al.*, Role of fibroblast growth factor receptors 1 and 2 in the ureteric bud*. Dev Biol* 2004; 276 (2): 403-415.

302. Cullen-McEwen LA, Drago J, and Bertram JF, Nephron endowment in glial cell line-derived neurotrophic factor (GDNF) heterozygous mice*. Kidney Int* 2001; 60 (1): 31-36.

303. Poladia DP, Kish K, Kutay B*, et al.*, Link between reduced nephron number and hypertension: studies in a mutant mouse model*. Pediatr Res* 2006; 59 (4 Pt 1): 489-493.

304. Moreau E, Vilar J, Lelievre-Pegorier M*, et al.*, Regulation of c-ret expression by retinoic acid in rat metanephros: implication in nephron mass control*. Am J Physiol* 1998; 275 (6 Pt 2): F938-945.

305. Schwedler SB, Gilbert T, Moreau E*, et al.*, Nephrotoxin exposure in utero reduces glomerular number in sclerosis-prone but not sclerosis-resistant mice*. Kidney Int* 1999; 56 (5): 1683-1690.

306. Vehaskari VM, Aviles DH, and Manning J, Prenatal programming of adult hypertension in the rat*. Kidney Int* 2001; 59 (1): 238-245.

307. Hoppe CC, Evans RG, Bertram JF*, et al.*, Effects of dietary protein restriction on nephron number in the mouse*. Am J Physiol Regul Integr Comp Physiol* 2007; 292 (5): R1768-1774.

308. Knight BS, Pennell CE, Shah R*, et al.*, Strain differences in the impact of dietary restriction on fetal growth and pregnancy in mice*. Reprod Sci* 2007; 14 (1): 81-90.

309. He C, Esposito C, Phillips C*, et al.*, Dissociation of glomerular hypertrophy, cell proliferation, and glomerulosclerosis in mouse strains heterozygous for a mutation (Os) which induces a 50% reduction in nephron number. *J Clin Invest* 1996; 97 (5): 1242-1249.

310. Esposito C, He CJ, Striker GE*, et al.*, Nature and severity of the glomerular response to nephron reduction is strain-dependent in mice*. Am J Pathol* 1999; 154 (3): 891-897.

311. Bendtsen TF and Nyengaard JR, Unbiased estimation of particle number using sections--an historical perspective with special reference to the stereology of glomeruli*. J Microsc* 1989; 153 (Pt 1): 93-102.

312. Bertram JF, Analyzing renal glomeruli with the new stereology*. Int Rev Cytol* 1995; 161: 111-172.

313. Takemoto M, Asker N, Gerhardt H*, et al.*, A new method for large scale isolation of kidney glomeruli from mice*. Am J Pathol* 2002; 161 (3): 799-805.

314. Murawski IJ, Myburgh D, Maina R*, et al. The use of inbred mice to study vesico-ureteric reflux and kidney hypoplasia*. in *American Society of Pediatric Nephrology*. 2007. Toronto, Canada, publication 7918.13.

315. Sterio DC, The unbiased estimation of number and sizes of arbitrary particles using the disector*. J Microsc* 1984; 134 (Pt 2): 127-136.

316. Barai S, Bandopadhayaya GP, Bhowmik D*, et al.*, Prevalence of vesicoureteral reflux in patients with incidentally diagnosed adult hypertension*. Urology* 2004; 63 (6): 1045-1048; discussion 1048-1049.

317. Matsuoka H, Nakashima Y, and Oshima K, Prognostic significance of the number of renal glomeruli in reflux nephropathy*. BJU Int* 2006; 98 (1): 172-176.

318. Prospective trial of operative versus non-operative treatment of severe vesicoureteric reflux in children: five years' observation. Birmingham Reflux Study Group*. Br Med J (Clin Res Ed)* 1987; 295 (6592): 237-241.

319. Stephens FD, Joske RA, and Simmons RT, Megaureter with vesico-ureteric reflux in twins*. Aust N Z J Surg* 1955; 24 (3): 192-194.

320. Redman JF, Vesicoureteral reflux in identical twins*. J Urol* 1976; 116 (6): 792-793.

321. Mebust WK and Foret JD, Vesicoureteral reflux in identical twins*. J Urol* 1972; 108 (4): 635-636.

322. Hampel N, Levin DR, and Gersh I, Bilateral vesico-ureteral reflux with pyelonephritis in identical twins*. Br J Urol* 1975; 47 (5): 535-537.

323. Kiruluta GH, Afridi SK, and Winsor GM, Familial reflux in monozygotic twins*. Urology* 1983; 21 (3): 298-299.

324. Kaefer M, Curran M, Treves ST*, et al.*, Sibling vesicoureteral reflux in multiple gestation births*. Pediatrics* 2000; 105 (4 Pt 1): 800-804.

325. King LR, Vesicoureteral reflux: a radiographic sign common to multiple diseases*. Jama* 1972; 220 (6): 854.

326. Tobenkin MI, Hereditary Vesicoureteral Reflux*. South Med J* 1964; 57: 139-147.

327. Burger RH, Familial and hereditary vesicouretral reflux. *Jama* 1971; 216 (4): 680-681.

328. Miller HC and Caspari EW, Ureteral reflux as genetic trait. *Jama* 1972; 220 (6): 842-843.

329. Schmidt JD, Hawtrey CE, Flocks RH, *et al.*, Vesicoureteral reflux. An inherited lesion. *Jama* 1972; 220 (6): 821-824.

330. Sanna-Cherchi S, Reese A, Hensle T, *et al.*, Familial Vesicoureteral Reflux: Testing Replication of Linkage in Seven New Multigenerational Kindreds. *J Am Soc Nephrol* 2005.

331. Devriendt K, Groenen P, Van Esch H, *et al.*, Vesico-ureteral reflux: a genetic condition? *Eur J Pediatr* 1998; 157 (4): 265-271.

332. Middleton GW, Howards SS, and Gillenwater JY, Sex-linked familial reflux. *J Urol* 1975; 114 (1): 36-39.

333. Weng PL, Sanna-Cherchi S, Hensle T, *et al.*, A Common Gene Predisposing to Vesicoureteral Reflux Is Located on Chromosome 12p11-q13. *American Society of Nephrology, Philadelphia* 2008: [F-FC256].

334. Uehling DT, Vlach RE, Pauli RM, *et al.*, Vesicoureteric reflux in sibships. *Br J Urol* 1992; 69 (5): 534-537.

335. Vesicoureteric reflux: all in the genes? Report of a meeting of physicians at the Hospital for Sick Children, Great Ormond Street, London. *Lancet* 1996; 348 (9029): 725-728.

336. Strachan R and Read AP, (eds) *Human Molecular Genetics 2*. BIOS Scientific Publishers: UK, 1999.

337. Atwell JD, Familial pelviureteric junction hydronephrosis and its association with a duplex pelvicaliceal system and vesicoureteric reflux. A family study. *Br J Urol* 1985; 57 (4): 365-369.

338. Cussen LJ, Vesicoureteral reflux in children. Frequency and associated urologic abnormalities. *Invest Urol* 1971; 8 (6): 640-644.

339. Ambrose SS, Parrott TS, Woodard JR, *et al.*, Observations on the small kidney associated with vesicoureteral reflux. *J Urol* 1980; 123 (3): 349-351.

340. Baker RM, W.; Maylath, J.; Shuman, I., Relation of age, sex and infection to reflux: data indicating high spontaneous cure rate in pediatric patients. *J Urol* 1966; 95: 27-32

341. Jiang S, Gitlin J, Deng FM, *et al.*, Lack of major involvement of human uroplakin genes in vesicoureteral reflux: implications for disease heterogeneity. *Kidney Int* 2004; 66 (1): 10-19.

342. Choi KL, McNoe LA, French MC, *et al.*, Absence of PAX2 gene mutations in patients with primary familial vesicoureteric reflux. *J Med Genet* 1998; 35 (4): 338-339.

343. Torres VE, Moore SB, Kurtz SB, *et al.*, In search of marker for genetic susceptibility to reflux nephropathy. *Clin Nephrol* 1980; 14 (5): 217-222.

344. Shefelbine SE, Khorana S, Schultz PN, *et al.*, Mutational analysis of the GDNF/RET-GDNFR alpha signaling complex in a kindred with vesicoureteral reflux. *Hum Genet* 1998; 102 (4): 474-478.

345. Yim HE, Bae IS, Yoo KH, *et al.*, Genetic control of VEGF and TGF-beta1 gene polymorphisms in childhood urinary tract infection and vesicoureteral reflux. *Pediatr Res* 2007; 62 (2): 183-187.

346. Bertoli-Avella AM, Conte ML, Punzo F, *et al.*, ROBO2 Gene Variants Are Associated with Familial Vesicoureteral Reflux. *J Am Soc Nephrol* 2008; 19 (4): 825-831.

347. Ogata T, Muroya K, Sasagawa I, *et al.*, Genetic evidence for a novel gene(s) involved in urogenital development on 10q26. *Kidney Int* 2000; 58 (6): 2281-2290.

348. Anderson NG, Abbott GD, Mogridge N, *et al.*, Vesicoureteric reflux in the newborn: relationship to fetal renal pelvic diameter. *Pediatr Nephrol* 1997; 11 (5): 610-616.

349. Vats KR, Ishwad C, Singla I, *et al.*, A locus for renal malformations including vesico-ureteric reflux on chromosome 13q33-34. *J Am Soc Nephrol* 2006; 17 (4): 1158-1167.

350. Lu W, van Eerde AM, Fan X, *et al.*, Disruption of ROBO2 is associated with urinary tract anomalies and confers risk of vesicoureteral reflux. *Am J Hum Genet* 2007; 80 (4): 616-632.

351. Ruf RG, Xu PX, Silvius D, *et al.*, SIX1 mutations cause branchio-oto-renal syndrome by disruption of EYA1-SIX1-DNA complexes. *Proc Natl Acad Sci U S A* 2004; 101 (21): 8090-8095.

352. Heimler A and Lieber E, Branchio-oto-renal syndrome: reduced penetrance and variable expressivity in four generations of a large kindred. *Am J Med Genet* 1986; 25 (1): 15-27.

353. Engels S, Kohlhase J, and McGaughran J, A SALL1 mutation causes a branchio-oto-renal syndrome-like phenotype. *J Med Genet* 2000; 37 (6): 458-460.

354. Van Esch H, Groenen P, Nesbit MA, *et al.*, GATA3 haplo-insufficiency causes human HDR syndrome. *Nature* 2000; 406 (6794): 419-422.

355. Guron G and Friberg P, An intact renin-angiotensin system is a prerequisite for normal renal development. *J Hypertens* 2000; 18 (2): 123-137.

356. Carpenter C, Honkanen AA, Mashimo H, *et al.*, Renal abnormalities in mutant mice. *Nature* 1996; 380 (6572): 292.

357. Liu KP, Lin CY, Chen HJ, *et al.*, Renin-angiotensin system polymorphisms in Taiwanese primary vesicoureteral reflux. *Pediatr Nephrol* 2004; 19 (6): 594-601.

358. Esther CR, Jr., Howard TE, Marino EM*, et al.*, Mice lacking angiotensin-converting enzyme have low blood pressure, renal pathology, and reduced male fertility. *Lab Invest* 1996; 74 (5): 953-965.

359. Ohtomo Y, Nagaoka R, Kaneko K*, et al.*, Angiotensin converting enzyme gene polymorphism in primary vesicoureteral reflux. *Pediatr Nephrol* 2001; 16 (8): 648-652.

360. Rigoli L, Chimenz R, di Bella C*, et al.*, Angiotensin-converting enzyme and angiotensin type 2 receptor gene genotype distributions in Italian children with congenital uropathies. *Pediatr Res* 2004; 56 (6): 988-993.

361. Yoneda A, Oue T, and Puri P, Angiotensin-converting enzyme genotype distribution in familial vesicoureteral reflux. *Pediatr Surg Int* 2001; 17 (4): 308-311.

362. Park HW, Koo JW, Kim JS*, et al.*, Association of angiotensin I converting enzyme gene polymorphism with reflux nephropathy in children. *Nephron* 2000; 86 (1): 52-55.

363. Hohenfellner K, Hunley TE, Yerkes E*, et al.*, Angiotensin II, type 2 receptor in the development of vesico-ureteric reflux. *BJU Int* 1999; 83 (3): 318-322.

364. Yoneda A, Cascio S, Green A*, et al.*, Angiotensin II type 2 receptor gene is not responsible for familial vesicoureteral reflux. *J Urol* 2002; 168 (3): 1138-1141.

365. Hiraoka M, Taniguchi T, Nakai H*, et al.*, No evidence for AT2R gene derangement in human urinary tract anomalies. *Kidney Int* 2001; 59 (4): 1244-1249.

366. Natarajan D, Marcos-Gutierrez C, Pachnis V*, et al.*, Requirement of signalling by receptor tyrosine kinase RET for the directed migration of enteric nervous system progenitor cells during mammalian embryogenesis. *Development* 2002; 129 (22): 5151-5160.

367. Takahashi M, Iwashita T, Santoro M*, et al.*, Co-segregation of MEN2 and Hirschsprung's disease: the same mutation of RET with both gain and loss-of-function? *Hum Mutat* 1999; 13 (4): 331-336.

368. Lore F, Talidis F, Di Cairano G*, et al.*, Multiple endocrine neoplasia type 2 syndromes may be associated with renal malformations. *J Intern Med* 2001; 250 (1): 37-42.

369. Enomoto H, Crawford PA, Gorodinsky A*, et al.*, RET signaling is essential for migration, axonal growth and axon guidance of developing sympathetic neurons. *Development* 2001; 128 (20): 3963-3974.

370. Pini Prato A, Musso M, Ceccherini I*, et al.*, Hirschsprung disease and congenital anomalies of the kidney and urinary tract (CAKUT): a novel syndromic association. *Medicine (Baltimore)* 2009; 88 (2): 83-90.

371. Skinner MA, Safford SD, Reeves JG*, et al.*, Renal aplasia in humans is associated with RET mutations. *Am J Hum Genet* 2008; 82 (2): 344-351.

372. Kelly H, Ennis S, Yoneda A*, et al.*, Uroplakin III is not a major candidate gene for primary vesicoureteral reflux. *Eur J Hum Genet* 2005; 13 (4): 500-502.

373. Giltay JC, van de Meerakker J, van Amstel HK*, et al.*, No pathogenic mutations in the uroplakin III gene of 25 patients with primary vesicoureteral reflux. *J Urol* 2004; 171 (2 Pt 1): 931-932.

374. Schonfelder EM, Knuppel T, Tasic V*, et al.*, Mutations in Uroplakin IIIA are a rare cause of renal hypodysplasia in humans. *Am J Kidney Dis* 2006; 47 (6): 1004-1012.

375. Bailey RR, The relationship of vesico-ureteric reflux to urinary tract infection and chronic pyelonephritis-reflux nephropathy. *Clin Nephrol* 1973; 1 (3): 132-141.

376. Sengar DP, McLeish WA, Rashid A*, et al.*, Histocompatibility antigens in urinary tract infection and vesicoureteral reflux: a preliminary communication. *Clin Nephrol* 1978; 10 (4): 166-169.

377. Mackintosh P, Almarhoos G, and Heath DA, HLA linkage with familial vesicoureteral reflux and familial pelvi-ureteric junction obstruction. *Tissue Antigens* 1989; 34 (3): 185-189.

378. Konda R, Sato H, Sakai K*, et al.*, Urinary excretion of vascular endothelial growth factor is increased in children with reflux nephropathy. *Nephron Clin Pract* 2004; 98 (3): c73-78.

379. Yamamoto T, Noble NA, Miller DE*, et al.*, Sustained expression of TGF-beta 1 underlies development of progressive kidney fibrosis. *Kidney Int* 1994; 45 (3): 916-927.

380. Gorinati M, Zamboni G, Padoin N*, et al.*, Terminal deletion of the long arm of chromosome 10: case report and review of the literature. *Am J Med Genet* 1989; 33 (4): 502-504.

381. Devriendt K, Swillen A, Fryns JP*, et al.*, Renal and urological tract malformations caused by a 22q11 deletion. *J Med Genet* 1996; 33 (4): 349.

382. Lipson AH, Yuille D, Angel M*, et al.*, Velocardiofacial (Shprintzen) syndrome: an important syndrome for the dysmorphologist to recognise. *J Med Genet* 1991; 28 (9): 596-604.

383. Guay-Woodford LM and Torres VE, Genetic Diseases of the Kidney. *Nephrol Self-Assessment Program* 2005; 4 (4): 166-175.

384. Murer L, Benetti E, and Artifoni L, Embryology and genetics of primary vesico-ureteric reflux and associated renal dysplasia. *Pediatr Nephrol* 2007; 22 (6): 788-797.

385. Muroya K, Hasegawa T, Ito Y*, et al.*, GATA3 abnormalities and the phenotypic spectrum of HDR syndrome. *J Med Genet* 2001; 38 (6): 374-380.

386. Lichtner P, Konig R, Hasegawa T*, et al.*, An HDR (hypoparathyroidism, deafness, renal dysplasia) syndrome locus maps distal to the DiGeorge syndrome region on 10p13/14. *J Med Genet* 2000; 37 (1): 33-37.

387. Mino Y, Kuwahara T, Mannami T*, et al.*, Identification of a novel insertion mutation in GATA3 with HDR syndrome. *Clin Exp Nephrol* 2005; 9 (1): 58-61.

388. Nesbit MA, Bowl MR, Harding B*, et al.*, Characterization of GATA3 mutations in the hypoparathyroidism, deafness, and renal dysplasia (HDR) syndrome. *J Biol Chem* 2004; 279 (21): 22624-22634.

389. Zahirieh A, Nesbit MA, Ali A*, et al.*, Functional analysis of a novel GATA3 mutation in a family with the hypoparathyroidism, deafness, and renal dysplasia syndrome. *J Clin Endocrinol Metab* 2005; 90 (4): 2445-2450.

390. Nishinakamura R and Takasato M, Essential roles of Sall1 in kidney development. *Kidney Int* 2005; 68 (5): 1948-1950.

391. Kim HG, Herrick SR, Lemyre E*, et al.*, Hypogonadotropic hypogonadism and cleft lip and palate caused by a balanced translocation producing haploinsufficiency for FGFR1. *J Med Genet* 2005; 42 (8): 666-672.

392. Duke V, Quinton R, Gordon I*, et al.*, Proteinuria, hypertension and chronic renal failure in X-linked Kallmann's syndrome, a defined genetic cause of solitary functioning kidney. *Nephrol Dial Transplant* 1998; 13 (8): 1998-2003.

393. Lander ES and Schork NJ, Genetic dissection of complex traits. *Science* 1994; 265 (5181): 2037-2048.

394. McPeek MS, From mouse to human: fine mapping of quantitative trait loci in a model organism. *Proc Natl Acad Sci U S A* 2000; 97 (23): 12389-12390.

395. Motulsky AG, Genetics of complex diseases. *J Zhejiang Univ Sci B* 2006; 7 (2): 167-168.

396. Polychronakos C, Common and rare alleles as causes of complex phenotypes. *Curr Atheroscler Rep* 2008; 10 (3): 194-200.

397. Korstanje R and Paigen B, From QTL to gene: the harvest begins. *Nat Genet* 2002; 31 (3): 235-236.

398. Korstanje R and DiPetrillo K, Unraveling the genetics of chronic kidney disease using animal models. *Am J Physiol Renal Physiol* 2004; 287 (3): F347-352.

399. Flint J, Valdar W, Shifman S*, et al.*, Strategies for mapping and cloning quantitative trait genes in rodents. *Nat Rev Genet* 2005; 6 (4): 271-286.

400. Moore KJ and Nagle DL, Complex trait analysis in the mouse: The strengths, the limitations and the promise yet to come. *Annu Rev Genet* 2000; 34: 653-686.

401. Risch N, Burchard E, Ziv E*, et al.*, Categorization of humans in biomedical research: genes, race and disease. *Genome Biol* 2002; 3 (7): comment2007.

402. Copeland NG, Jenkins NA, Gilbert DJ*, et al.*, A genetic linkage map of the mouse: current applications and future prospects. *Science* 1993; 262 (5130): 57-66.

403. Waterston RH, Lindblad-Toh K, Birney E*, et al.*, Initial sequencing and comparative analysis of the mouse genome. *Nature* 2002; 420 (6915): 520-562.

404. Peters LL, Robledo RF, Bult CJ, *et al.*, The mouse as a model for human biology: a resource guide for complex trait analysis. *Nat Rev Genet* 2007; 8 (1): 58-69.

405. Silver LM, (eds) *Mouse Genetics: Concepts and Applications*. Oxford University Press: New York, 1995.

406. Tokuda M, An Eighteenth Century Japanese Guide-Book on Mouse-Breeding. *Journal of Heredity* 1935; 26 (12): 481-484.

407. Beck JA, Lloyd S, Hafezparast M, *et al.*, Genealogies of mouse inbred strains. *Nat Genet* 2000; 24 (1): 23-25.

408. Wade CM and Daly MJ, Genetic variation in laboratory mice. *Nat Genet* 2005; 37 (11): 1175-1180.

409. DiPetrillo K, Wang X, Stylianou IM, *et al.*, Bioinformatics toolbox for narrowing rodent quantitative trait loci. *Trends Genet* 2005; 21 (12): 683-692.

410. Tsang S, Sun Z, Luke B, *et al.*, A comprehensive SNP-based genetic analysis of inbred mouse strains. *Mamm Genome* 2005; 16 (7): 476-480.

411. Moen C and Hofker M, Mouse Genetics as a Research Tool. *Encyclopedia of Life Sciences* 2006; DOI: 10.1038/npg.els.0005681.

412. Silver J, Confidence limits for estimates of gene linkage based on analysis of recombinant inbred strains. *J Hered* 1985; 76 (6): 436-440.

413. Svenson KL, Von Smith R, Magnani PA, *et al.*, Multiple trait measurements in 43 inbred mouse strains capture the phenotypic diversity characteristic of human populations. *J Appl Physiol* 2007; 102 (6): 2369-2378.

414. Boyd Y, Genetic mapping of the mouse genome. *Methods* 1998; 14 (2): 120-134.

415. Petkov PM, Ding Y, Cassell MA, *et al.*, An efficient SNP system for mouse genome scanning and elucidating strain relationships. *Genome Res* 2004; 14 (9): 1806-1811.

416. Rice MC and O'Brien SJ, Genetic variance of laboratory outbred Swiss mice. *Nature* 1980; 283 (5743): 157-161.

417. Chia R, Achilli F, Festing MF, *et al.*, The origins and uses of mouse outbred stocks. *Nat Genet* 2005; 37 (11): 1181-1186.

418. Mannen H, Tsuji S, and Goto N, Incomplete protection mechanism against vesico-ureteral reflux and hydronephrosis in the inbred mouse strain DDD. *Lab Anim* 1991; 25 (2): 156-161.

419. Mannen H, Tsuji S, and Goto N, Influence of chronic oestrogen treatment on severity of hydronephrosis in inbred DDD mice. *Lab Anim* 1993; 27 (2): 124-130.

420. Kruglyak L and Lander ES, A nonparametric approach for mapping quantitative trait loci. *Genetics* 1995; 139 (3): 1421-1428.

421. Avner P, Complex traits and polygenic inheritance in the mouse. *Methods* 1998; 14 (2): 191-198.

422. Demant P and Hart AA, Recombinant congenic strains--a new tool for analyzing genetic traits determined by more than one gene. *Immunogenetics* 1986; 24 (6): 416-422.

423. Sancho-Shimizu V and Malo D, Sequencing, expression, and functional analyses support the candidacy of Ncf2 in susceptibility to Salmonella typhimurium infection in wild-derived mice. *J Immunol* 2006; 176 (11): 6954-6961.

424. Nadeau JH, Singer JB, Matin A, *et al.*, Analysing complex genetic traits with chromosome substitution strains. *Nat Genet* 2000; 24 (3): 221-225.

425. Sheehan S, Tsaih SW, King BL, *et al.*, Genetic analysis of albuminuria in a cross between C57BL/6J and DBA/2J mice. *Am J Physiol Renal Physiol* 2007; 293 (5): F1649-1656.

426. Park YG, Clifford R, Buetow KH, *et al.*, Multiple cross and inbred strain haplotype mapping of complex-trait candidate genes. *Genome Res* 2003; 13 (1): 118-121.

427. Reuveni E, Ramensky VE, and Gross C, Mouse SNP Miner: an annotated database of mouse functional single nucleotide polymorphisms. *BMC Genomics* 2007; 8: 24.

428. Kuschert S, Rowitch DH, Haenig B, *et al.*, Characterization of Pax-2 regulatory sequences that direct transgene expression in the Wolffian duct and its derivatives. *Dev Biol* 2001; 229 (1): 128-140.

429. Mak RH and Kuo HJ, Primary ureteral reflux: emerging insights from molecular and genetic studies. *Curr Opin Pediatr* 2003; 15 (2): 181-185.

430. Roshani H, Dabhoiwala NF, Verbeek FJ, *et al.*, Functional anatomy of the human ureterovesical junction. *Anat Rec* 1996; 245 (4): 645-651.

431. Sampson JA, Ascending renal infection; with special reference to the reflux of urine from the bladder into the ureters as an etiological factor in its causation and maintenance. *Johns Hopkins Hospital Bulletin* 1903; 14: 334-352.

432. Srinivas S, Goldberg MR, Watanabe T, *et al.*, Expression of green fluorescent protein in the ureteric bud of transgenic mice: a new tool for the analysis of ureteric bud morphogenesis. *Dev Genet* 1999; 24 (3-4): 241-251.

433. Clark P, Dziarmaga A, Eccles M, *et al.*, Rescue of defective branching nephrogenesis in renal-coloboma syndrome by the caspase inhibitor, Z-VAD-fmk. *J Am Soc Nephrol* 2004; 15 (2): 299-305.

434. Gupta IR, Lapointe M, and Yu OH, Morphogenesis during mouse embryonic kidney explant culture. *Kidney Int* 2003; 63 (1): 365-376.

435. Vrljicak P, Myburgh D, Ryan AK, *et al.*, Smad expression during kidney development. *Am J Physiol Renal Physiol* 2004; 286 (4): F625-633.

436. Hiraoka M, Hori C, Tsukahara H*, et al.*, Congenitally small kidneys with reflux as a common cause of nephropathy in boys. *Kidney Int* 1997; 52 (3): 811-816.

437. Marra G, Barbieri G, Dell'Agnola CA*, et al.*, Congenital renal damage associated with primary vesicoureteral reflux detected prenatally in male infants. *J Pediatr* 1994; 124 (5 Pt 1): 726-730.

438. Majumdar A, Lun K, Brand M*, et al.*, Zebrafish no isthmus reveals a role for pax2.1 in tubule differentiation and patterning events in the pronephric primordia. *Development* 2000; 127 (10): 2089-2098.

439. Van Esch H and Devriendt K, Transcription factor GATA3 and the human HDR syndrome. *Cell Mol Life Sci* 2001; 58 (9): 1296-1300.

440. Brodbeck S, Besenbeck B, and Englert C, The transcription factor Six2 activates expression of the Gdnf gene as well as its own promoter. *Mech Dev* 2004; 121 (10): 1211-1222.

441. Nishimoto K, Iijima K, Shirakawa T*, et al.*, PAX2 gene mutation in a family with isolated renal hypoplasia. *J Am Soc Nephrol* 2001; 12 (8): 1769-1772.

442. Frazer JE, The terminal part of the wolffian duct. *J Anat* 1935; 69: 455-468.

443. Totemeyer S, Foster N, Kaiser P*, et al.*, Toll-like receptor expression in C3H/HeN and C3H/HeJ mice during Salmonella enterica serovar Typhimurium infection. *Infect Immun* 2003; 71 (11): 6653-6657.

444. Nowicki B, Singhal J, Fang L*, et al.*, Inverse relationship between severity of experimental pyelonephritis and nitric oxide production in C3H/HeJ mice. *Infect Immun* 1999; 67 (5): 2421-2427.

445. Hopkins WJ, Elkahwaji JE, Heisey DM*, et al.*, Inheritance of susceptibility to induced Escherichia coli bladder and kidney infections in female C3H/HeJ mice. *J Infect Dis* 2003; 187 (3): 418-423.

446. Schlager G, Kidney weight in mice: strain differences and genetic determination. *J Hered* 1968; 59 (3): 171-174.

447. Deschepper CF, Olson JL, Otis M*, et al.*, Characterization of blood pressure and morphological traits in cardiovascular-related organs in 13 different inbred mouse strains. *J Appl Physiol* 2004; 97 (1): 369-376.

448. Takemoto M, He L, Norlin J*, et al.*, Large-scale identification of genes implicated in kidney glomerulus development and function. *Embo J* 2006; 25 (5): 1160-1174.

449. Jones SE, Nyengaard JR, Flyvbjerg A*, et al.*, Birth weight has no influence on glomerular number and volume. *Pediatr Nephrol* 2001; 16 (4): 340-345.

450. Tsukahara C, Sugiyama F, Paigen B*, et al.*, Blood pressure in 15 inbred mouse strains and its lack of relation with obesity and insulin resistance in the progeny of an NZO/HILtJ x C3H/HeJ intercross. *Mamm Genome* 2004; 15 (12): 943-950.

451. Korstanje R. *Aging study: Urine albumin and creatinine. MDP:297.* [cited The Jackson Laboratory, Bar Harbor, Maine USA. October 2008]; Available from: http://www.jax.org/phenome.

452. Qi Z, Fujita H, Jin J*, et al.*, Characterization of susceptibility of inbred mouse strains to diabetic nephropathy. *Diabetes* 2005; 54 (9): 2628-2637.

453. DiPetrillo K, Tsaih S, Sheehan S*, et al.*, Genetic analysis of blood pressure in C3H/HeJ and SWR/J mice. *Physiol Genomics* 2004; 17 (2): 215-220.

454. Lander E and Kruglyak L, Genetic dissection of complex traits: guidelines for interpreting and reporting linkage results. *Nat Genet* 1995; 11 (3): 241-247.

455. Broman KW, Wu H, Sen S*, et al.*, R/qtl: QTL mapping in experimental crosses. *Bioinformatics* 2003; 19 (7): 889-890.

456. Heinemeyer T, Wingender E, Reuter I*, et al.*, Databases on transcriptional regulation: TRANSFAC, TRRD and COMPEL. *Nucleic Acids Res* 1998; 26 (1): 362-367.

457. Zheng Z, Schmidt-Ott KM, Chua S*, et al.*, A Mendelian locus on chromosome 16 determines susceptibility to doxorubicin nephropathy in the mouse. *Proc Natl Acad Sci U S A* 2005; 102 (7): 2502-2507.

458. Dupuis J and Siegmund D, Statistical methods for mapping quantitative trait loci from a dense set of markers. *Genetics* 1999; 151 (1): 373-386.

459. Chen JM, Ferec C, and Cooper DN, A systematic analysis of disease-associated variants in the 3' regulatory regions of human protein-coding genes II: the importance of mRNA secondary structure in assessing the functionality of 3' UTR variants. *Hum Genet* 2006; 120 (3): 301-333.

460. Chen JM, Ferec C, and Cooper DN, A systematic analysis of disease-associated variants in the 3' regulatory regions of human protein-coding genes I: general principles and overview. *Hum Genet* 2006; 120 (1): 1-21.

461. Stecker JF, Jr., Rose JG, and Gillenwater JY, Dysplastic kidneys associated with vesicoureteral reflux. *J Urol* 1973; 110 (3): 341-343.

462. Cole LK and Ross LS, Apoptosis in the developing zebrafish embryo. *Dev Biol* 2001; 240 (1): 123-142.

463. Coles HS, Burne JF, and Raff MC, Large-scale normal cell death in the developing rat kidney and its reduction by epidermal growth factor. *Development* 1993; 118 (3): 777-784.

464. Blank E and Girdany BR, Prognosis with vesicoureteral reflux. *Pediatrics* 1971; 48 (5): 782-787.

465. Simoes e Silva AC, Silva JM, Diniz JS*, et al.*, Risk of hypertension in primary vesicoureteral reflux. *Pediatr Nephrol* 2007; 22 (3): 459-462.

466. Quinlan J, Lemire M, Hudson T*, et al.*, A common variant of the PAX2 gene is associated with reduced newborn kidney size. *J Am Soc Nephrol* 2007; 18 (6): 1915-1921.

467. Zhang Z, Quinlan J, Hoy W*, et al.*, A common RET variant is associated with reduced newborn kidney size and function. *J Am Soc Nephrol* 2008; 19 (10): 2027-2034.

468. Hogan B, Deconstructing the genesis of animal form. *Development* 2004; 131 (11): 2515-2520.

469. King LR, The development of the management of vesico-ureteric reflux in the USA. *BJU Int* 2003; 92 Suppl 1: 4-6.

470. Roberts RR, Bornstein JC, Bergner AJ*, et al.*, Disturbances of colonic motility in mouse models of Hirschsprung's disease. *Am J Physiol Gastrointest Liver Physiol* 2008; 294 (4): G996-G1008.

471. Zheng Z, Pavlidis P, Chua S*, et al.*, An ancestral haplotype defines susceptibility to doxorubicin nephropathy in the laboratory mouse. *J Am Soc Nephrol* 2006; 17 (7): 1796-1800.

472. Gray IC, Campbell DA, and Spurr NK, Single nucleotide polymorphisms as tools in human genetics. *Hum Mol Genet* 2000; 9 (16): 2403-2408.

473. Cordell HJ and Clayton DG, Genetic association studies. *Lancet* 2005; 366 (9491): 1121-1131.

474. Risch N and Merikangas K, The future of genetic studies of complex human diseases. *Science* 1996; 273 (5281): 1516-1517.

475. Purcell S, Cherny SS, and Sham PC, Genetic Power Calculator: design of linkage and association genetic mapping studies of complex traits. *Bioinformatics* 2003; 19 (1): 149-150.

476. Burton PR, Tobin MD, and Hopper JL, Key concepts in genetic epidemiology. *Lancet* 2005; 366 (9489): 941-951.

477. Weber S, Moriniere V, Knuppel T*, et al.*, Prevalence of Mutations in Renal Developmental Genes in Children with Renal Hypodysplasia: Results of the ESCAPE Study. *J Am Soc Nephrol* 2006; 17 (10): 2864-2870.

478. Hakonarson H, Grant SF, Bradfield JP*, et al.*, A genome-wide association study identifies KIAA0350 as a type 1 diabetes gene. *Nature* 2007; 448 (7153): 591-594.

479. Elder JS, Peters CA, Arant BS, Jr.*, et al.*, Pediatric Vesicoureteral Reflux Guidelines Panel summary report on the management of primary vesicoureteral reflux in children. *J Urol* 1997; 157 (5): 1846-1851.

480. Walsh TJ, Hsieh S, Grady R*, et al.*, Antenatal hydronephrosis and the risk of pyelonephritis hospitalization during the first year of life. *Urology* 2007; 69 (5): 970-974.

481. Foxman B, Epidemiology of urinary tract infections: incidence, morbidity, and economic costs. *Am J Med* 2002; 113 Suppl 1A: 5S-13S.

APPENDIX A: List of publications

Peer-Reviewed Publications

Murawski IJ, Maina R, Gupta IR. The C3H/HeJ inbred mouse is a model of primary vesico-ureteric reflux and has a susceptibility locus on chromosome 12. (manuscript in preparation)

Murawski IJ, Maina R, Gupta IR. The relationship between nephron number, kidney size, and body weight in two inbred mouse strains. (manuscript in preparation).

Murawski IJ, Gupta IR. Gene discovery and vesicoureteric reflux. Ped Neph 2008: 23(7): 1021-27.

Murawski IJ, Gupta IR. Genetic heterogeneity of vesicoureteric reflux: insights from mouse models. Paediatriki 2007: 70(6): 428-435.

Murawski IJ, Myburgh DB, Favor J, Gupta IR. The *Pax2*^{1Neu} mouse: an experimental model of vesico-ureteric reflux. Am J Physiol Renal Physiol 2007: 293(5): F1736-45.

Murawski IJ, Gupta IR. Vesicoureteric reflux and renal malformations: a developmental problem. Clinical Genetics 2006: 69: 105-117.

Yu OH, **Murawski IJ**, Myburgh DB, Gupta IR. Overexpression of RET leads to vesico-ureteric reflux in mice. Am J Physiol Renal Physiol. 2004: 287(6): F1123-1130.

Oral Presentations at Scientific Meetings

Murawski IJ, Maina R. and Gupta IR. Pediatric Academic Society, Baltimore, MD, USA (May 2009) Recombinant inbred BXH mice have vesico-ureteric reflux and can develop duplex kidneys and bifid ureters.

Murawski IJ, Maina R. and Gupta IR. 7th Annual Meeting of the Complex Trait Consortium, Montreal, QC, Canada (June 2008) A novel locus on mouse chromosome 12 is associated with urinary tract defects in mice. *Prize for Best Oral Presentation*

Murawski IJ and Gupta IR. Pediatric Academic Society, Honolulu, HI, USA (May 2008) Using the mouse to understand vesico-ureteric reflux.

Murawski, IJ, Myburgh DB, Favor J, Gupta IR. XIX International Symposium of Morphological Sciences, Budapest, Hungary (August 19-24, 2007). A delay in urinary tract maturation causes vesicoureteral reflux in the *Pax2*$^{1Neu+/-}$ mouse. *Awarded Young Scientist Award*

Murawski IJ, Myburgh DB, Gupta IR. Research Institute of the Montreal Children's Hospital, McGill University Health Centre, Montreal, QC, Canada (May 2005) Vesico-ureteric reflux and the roles of the genes *Ret* and *Pax2* in the development of urinary tract defects. *Awarded First Prize*

Murawski IJ, Myburgh DB, Gupta IR. McGill 15th Urology Research Day, Montreal, QC, Canada (April 2005). Three experimental mouse models of vesico-ureteric reflux. *Awarded First Prize*

Murawski IJ, Myburgh DB, Gupta IR. Research Institute of the Montreal Children's Hospital, McGill University Health Centre, Montreal, QC, Canada (May 2004) Vesico-ureteric reflux and kidney defects in the mouse.

Murawski IJ, Myburgh DB, Gupta IR. McGill Department of Human Genetics Graduate Student Research Day, Montreal, QC, Canada (May 2004) Vesico-ureteric reflux and kidney defects in the mouse.

Poster Presentations at Scientific Meetings

Murawski IJ, Maina R. and Gupta IR. Canadian Society of Nephrology, Edmonton, AB, Canada (May 2009) The relationship between nephron number, kidney size, and body weight in inbred mouse strains.

Murawski IJ, Maina R, and Gupta IR. American Society of Nephrology ASN Renal Week (November 2008) Recombinant inbred BXH mice have variable incidences of VUR and are being used to identify a vesico-ureteric reflux-causing locus.

Murawski IJ, Maina R, and Gupta IR. Human Reproduction and Development Axis Research Day, Montreal, QC, Canada (October 2008) Recombinant inbred mice derived from the C3H/HeJ and C57BL/6J inbred strains have variable incidences of vesico-ureteric reflux, a common pediatric urinary tract defect, and are being used to narrow a reflux-causing locus.

Murawski IJ, Maina R, and Gupta IR. Pediatric Academic Society, Honolulu, HI, USA (May 2008) A novel locus on mouse chromosome 12 is associated with vesico-ureteric reflux.

Murawski IJ, Maina R, and Gupta IR. 1st Annual Canadian Human Genetics Conference, St-Sauveur, QC, Canada (April 2008) A novel locus on mouse chromosome 12 is associated with vesico-ureteric reflux, a common urinary tract defect.

Murawski IJ, Maina R, and Gupta IR. 8th Annual McGill Biomedical Graduate Conference, Montreal, QC, Canada (February 2008) Nephron number and its correlation with kidney size in mice: new implications in how we understand the kidney.

Murawski IJ, Maina R, Myburgh DB, Gupta IR. American Society of Nephrology, San-Francisco, CA, USA (November 2007) Searching for Vesico-Ureteric Reflux Causing Genes in the Mouse.

Murawski IJ, Myburgh DB, Favor J, Gupta IR. 10th International Workshop on Developmental Nephrology, Pécs, Hungary (August 28-30, 2007). Vesico-ureteric reflux is caused by a delay in urinary tract maturation in the *Pax2*$^{1Neu+/-}$ mouse, a model of Renal-Coloboma Syndrome.

Murawski IJ, Myburgh DB, Maina R, Gupta IR. Pediatric Academic Society, Toronto, ON, Canada (May 2007) The use of inbred mice to study vesico-ureteric reflux and kidney hypoplasia.

Murawski IJ, Maina R, Myburgh DB, Gupta IR. 7th Annual McGill Biomedical Graduate Conference, Montreal, QC, Canada (February 2007) The association of vesicoureteral reflux and kidney hypoplasia in inbred mice. *Awarded First Prize*

Murawski IJ, Myburgh, DB, Favor, J, Gupta IR. Canadian Society of Nephrology, Quebec-City, QC, Canada (May 2006) *Pax2* haploinsufficiency in the *Pax2*^{1Neu} mouse causes vesicoureteral reflux, a urinary tract defect present in renal coloboma syndrome.

Murawski IJ, Myburgh DB, Gupta IR. 3rd Canadian Developmental Biology Conference, Mont-Tremblant, QC, Canada (April 2006) The Position of Ureteric Budding During Kidney Development is Associated with Combined Kidney and Urinary Tract Defects in Mice.

Murawski IJ, Myburgh DB, Guay-Woodford L, Gupta IR. American Society of Nephrology, Philadelphia, PA, USA (November 2005) Ureteric Bud Position Is Associated with Vesicoureteral Reflux and Renal Malformations in Mice.

Murawski IJ, Myburgh DB, Gupta IR. Society for Developmental Biology - Northeast Regional Developmental Biology Conference, Woods Hole, MA, USA (April 2005) Vesico-ureteric reflux and urinary tract defects in the mouse.

Murawski IJ, Myburgh DB, Gupta IR. Human Reproduction and Developmental Axis Research Day, McGill University Health Center, Montreal, QC, Canada (April 2005). Defects in the urinary tract lead to vesico-ureteric reflux in three experimental mouse models.

Murawski IJ, Myburgh DB, Gupta IR. 5th Annual McGill Biomedical Graduate Conference, Montreal, QC, Canada (February 2005) The presence of vesico-ureteric reflux in the *Pax2*^{1Neu} mouse makes it a good model for studying urinary tract defects.

Murawski IJ, Myburgh DB, Gupta IR. Montreal Children's Hospital Open House, Montreal, QC, Canada (December 2004) Vesico-ureteric reflux and urinary tract defects in the mouse.